UNESP - Universidade Estadual Paulista

“Júlio de Mesquita Filho”

Faculdade de Odontologia de Araraquara

Jáder Camilo Pinto

Aplicação de diferentes métodos de análise de imagens para pesquisa em Endodontia: tomografia computadorizada de feixe cônico, micro-CT e nano-CT

Araraquara

2022

UNESP - Universidade Estadual Paulista
“Júlio de Mesquita Filho”
Faculdade de Odontologia de Araraquara

Jáder Camilo Pinto

Aplicação de diferentes métodos de análise de imagens para pesquisa em Endodontia: tomografia computadorizada de feixe cônico, micro-CT e nano-CT

Tese apresentada à Universidade Estadual Paulista (UNESP), Faculdade de Odontologia de Araraquara para obtenção do título de Doutor em Odontologia, na Área de Endodontia.

Orientador: Prof. Dr. Mario Tanomaru Filho

Araraquara

2022

P659a

Pinto, Jáder Camilo

Aplicação de diferentes métodos de análise de imagens para pesquisa em Endodontia: tomografia computadorizada de feixe cônico, micro-CT e nano-CT / Jáder Camilo Pinto. -- Araraquara, 2022

210 p. : il., tabs., fotos

Tese (doutorado) - Universidade Estadual Paulista (Unesp), Faculdade de Odontologia, Araraquara

Orientador: Mario Tanomaru Filho

1. Endodontia. 2. Dentina. 3. Preparo de canal radicular. 4. Cavidade Pulpar. 5. Microtomografia por Raio-X. I. Título.

Sistema de geração automática de fichas catalográficas da Unesp. Biblioteca da Faculdade de Odontologia, Araraquara. Dados fornecidos pelo autor(a).

Essa ficha não pode ser modificada.

Jáder Camilo Pinto

Aplicação de diferentes métodos de análise de imagens para pesquisa em Endodontia: tomografia computadorizada de feixe cônico, micro-CT e nano-CT

Comissão julgadora

Qualificação para obtenção do grau de Doutor em Odontologia

Presidente e orientador: Prof. Dr. Mario Tanomaru-Filho

2º Examinador: Prof. Dr. André Ferreira Leite

3º Examinador: Prof. Dr. Bruno Cavalini Cavenago

4° Examinador: Prof. Dr. Giulio Gavini

Araraquara 21 de março de 2022

DADOS CURRICULARES

Jáder Camilo Pinto

NASCIMENTO: 16/10/1984, Resende Costa, MG.

FILIAÇÃO: Marieta Dalva de Mendonça Pinto

Vanderlei Camilo Pinto

2004 – 2007 - Graduação em Odontologia no Centro Universitário de Lavras, UNILAVRAS, Brasil.

2009 – 2011 - Especialização em Endodontia no Centro Universitário de Lavras, UNILAVRAS, Brasil.

2016 – 2018 - Pós-graduação em Odontologia, Área de Endodontia, nível Mestrado, na Faculdade de Odontologia de Araraquara, Universidade Estadual Paulista – UNESP.

2020 - 2021 - Período Sanduíche Doutorado - Faculdade de Medicina, Universidade Católica de Leuven – KU Leuven, Bélgica

2018 – 2022 - Pós-graduação em Odontologia, Área de Endodontia, nível Doutorado, na Faculdade de Odontologia de Araraquara, Universidade Estadual Paulista – UNESP.

À minha esposa Paula pelo carinho, amor e apoio!

AGRADECIMENTOS

Foram quatro anos de dedicação e muito estudo para a obtenção do título de Doutor em Odontologia, ênfase em Endodontia, pela Faculdade de Odontologia de Araraquara, UNESP. Durante esse período, circulei por três instituições onde fui acolhido e encontrei pessoas que me ajudaram bastante. Correndo o risco de omitir alguém, gostaria de listar nomes de pessoas e instituições que me deram suporte e deixar registrado meu mais sincero agradecimento por tudo que fizeram por mim

Em primeiro lugar, gostaria de agradecer a meu orientador Prof. Dr. Mário Tanomaru Filho. Não tenho palavras para expressar minha gratidão e admiração pelo meu orientador. Sua dedicação a pesquisa, a presença e o constante estímulo deixaram marcas nesta tese e na minha formação. Para mim, foi uma honra tê-lo como orientador. Muito do meu rigor científico foi adquirido pelo seu exemplo de como executar um experimento, analisar os dados e desenvolver um adequado raciocínio na escrita. E por tudo isso, eu só tenho a agradecer: muito obrigado Professor Mário!

Gostaria de agradecer aos membros da banca de defesa de doutorado, Prof. Dr. André Ferreira Leite, Prof. Dr. Bruno Cavalini Cavenago, e Prof. Dr. Giulio Gavini pela leitura criteriosa da tese e suas contribuições para as melhorias no trabalho. Destaco o agradecimento especial ao Prof. Dr. André Ferreira Leite, que além da leitura, contribuiu significativamente com o desenvolvimento dos experimentos e escrita de vários artigos desta tese. Agradeço também os membros suplentes da banca, Profª. Drª. Karla de faria Vasconcelos, Prof. Dr. Daniel Almeida Decurcio e Prof. Dr. Marco Antonio Hungaro Duarte pelo pronto aceite da leitura da tese. Devo um agradecimento especial à Profª. Drª. Karla de faria Vasconcelos, que ainda contribuiu significativamente tanto na metodologia, quanto na escrita de várias publicações desta tese.

Agradeço à Faculdade de Medicina, Universidade Católica de Leuven (KU Leuven), Bélgica, pela acolhida e pela experiência incrível de viver um ano fora do Brasil. Agradeço à Profª Drª. Reinhilde Jacobs por me aceitar no estágio e pela amabilidade com que sempre me ensinou e supervisionou meus trabalhos. Agradeço a todos os amigos que lá me receberam, dividindo muito conhecimento e ótimos momentos. Volto a destacar meus grandes amigos Profª. Drª. Karla de Faria Vasconcelos e ao Prof· Dr. André Ferreira Leite que fizeram muito por mim na

Bélgica e, depois, no Brasil. Vocês me acolheram como família e palavras me faltam para explicar e agradecer o sentimento de amizade que me envolve. Estendo este agradecimento ao Kristof e Lucas e à Gabriela, Mariana e Gabriel. Muito obrigado, meus amigos! Ainda da Bélgica para o Brasil e Hungria, um agradecimento especial aos amigos da "Abrolhos gang", Maurício Gerhardt e Artúr Kesztyűs, sempre companheiros nos trabalhos científicos e nos momentos de descontração dos finais de semana.

Ao Instituto de Física, Universidade de São Paulo (IFSC-USP) agradeço a parceria no desenvolvimento deste trabalho. Um agradecimento especial ao Prof. Dr. Tito José Bonagamba e Dr. Everton Lucas Oliveira pela valiosa colaboração no desenvolvimento deste trabalho.

À Profª. Drª. Juliane Maria Guerreiro Tanomaru agradeço por todo apoio e ensinamentos despendidos a mim desde o início do mestrado. Aos meus professores da Foar-Unesp à Profª. Drª Gisele Faria e aos professores doutores Idomeo Bonetti Filho, Fábio Berbet e Renato Leonardo as palavras de incentivo e os ensinamentos passados a mim nestes seis anos de instituição.

Gostaria de deixar registrado minha gratidão aos meus professores do UNILAVRAS, Dr. Marcone Reis Luis e Ms. Nemam Jorge Murad pela formação e o incentivo à prática da endodontia, assim como o apoio para que eu seguisse nesta nova etapa da minha vida.

Aos meus amigos Karina e Airton pelo companheirismo durante estes últimos quatro anos, à Fernanda pela amizade e valiosas contribuições neste trabalho e aos meus amigos, que em algum momento compartilharam comigo esta jornada da Pós-Graduação, Bernardo, Índia, Gissele, Carlos, Victor, Cristiane e Hernán. Não posso deixar de mencionar Alejandro, grande amigo da época de mestrado.

Em especial, gostaria de agradecer à minha esposa Paula, pelo amor, companheirismo e apoio incondicional sem o qual eu não poderia fazer esta pós-graduação.

Agradeço aos meus pais Vanderlei e Dalva, por tudo que me proporcionaram para que pudesse chegar até aqui.

Aos meus sogros Maria Lúcia e Jorge, que sempre me apoiaram e me incentivaram muito.

Agradecimento especial à Denita, pela torcida e oração constantes.

Agradeço ao Programa de Pós-Graduação em Odontologia da Foar-Unesp a acolhida.

Por fim, agradeço à FAPESP – Fundação de Amparo à Pesquisa do Estado de São Paulo (Processo nº 2018/19665-6 e 2019/22885-0), pelas bolsas de estudos concedida durante todo o Doutorado, cujo apoio financeiro foi essencial para o desenvolvimento desta pesquisa.

“Dê-me, Senhor, agudeza para entender, capacidade para reter, método e faculdade para aprender, sutileza para interpretar, graça e abundância para falar, acerto ao começar, direção ao progredir e perfeição ao concluir. ”

São Tomás de Aquino

Pinto JC. Aplicação de diferentes métodos de análise de imagens para pesquisa em Endodontia: tomografia computadorizada de feixe cônico, micro-CT e nano-CT. [tese de doutorado]. Araraquara: Faculdade de Odontologia da UNESP; 2022.

RESUMO

Imagens tridimensionais são amplamente utilizadas na endodontia para avaliação de técnicas e materiais endodônticos, além de diagnóstico, planejamento e proservação. O objetivo deste estudo foi avaliar diferentes etapas do tratamento endodôntico usando microtomografia computadorizada (micro-CT) e nanotomografia computadorizada (nano-CT), além da avaliação de estruturas endodônticas pequenas por meio de diferentes aparelhos de tomografia computadorizada de feixe cônico (TCFC). Publicação 1 – Avaliou a influência do tamanho do voxel em análise do preparo do canal radicular por micro-CT. Imagens de micro-CT usando diferentes tamanhos de voxel não influenciaram os resultados de aumento de volume e avaliação de debris. Porém, as imagens a 5 µm mostraram maior acurácia para avaliar a porcentagem de superfícies não instrumentadas. Publicação 2 – Avaliou a influência do tamanho do voxel do micro-CT na detecção de microtrincas dentinárias. Diferentes tamanhos de voxel influenciam a análise de microtrincas por micro-CT. Análises a 5 µm mostraram que o preparo do canal radicular com HyFlex EDM aumentou a presença de microtrincas no terço médio. Publicação 3 – Avaliou a influência do tamanho do voxel de micro-CT na avaliação de debris. Os tamanhos dos voxels avaliados não tiveram impacto significativo na análise de debris. Publicação 4 –Investigou a capacidade de preenchimento de Bio-C Sealer em comparação com AH Plus usando diferentes métodos de segmentação e tamanhos de voxel em imagens de micro-CT. Bio-C Sealer mostrou capacidade de preenchimento similar ao AH Plus. Segmentação visual e automática podem ser aplicadas a imagens de micro-TC com tamanhos de voxel de 5 a 20 µm para análise do preenchimento de cimentos com radiopacidade adequada. Publicação 5 - Avaliou a influência do cimento endodôntico na remoção do material obturador, bem como a eficácia do XP-endo Finisher e PDL 50/.01 como protocolo de retratamento complementar. A remoção do AH Plus foi menor do que no Bio-C. PDL 50/.01 e XP-endo Finisher proporcionaram maior remoção de materiais obturadores no terço apical após o retratamento. Publicação 6 - Investigou a influência do tamanho do voxel na avaliação por micro-CT da remoção de material obturador remanescente. Os tamanhos dos voxel utilizados não influenciaram nas análises de material obturador residual. Publicação 7 – Classificou dez dispositivos de TCFC de acordo com a detecção de estruturas endodônticas finas. As tarefas endodônticas avaliadas foram dependentes do dispositivo de TCFC, e sua detecção foi influenciada pela presença de metal. Publicação 8 - Avaliou a influência dos protocolos de TCFC e a presença de metal na visualização de trincas radiculares e estruturas anatômicas endodônticas pequenas. A capacidade das imagens de TCFC para análise de trincas é altamente limitada e restrita. Estruturas anatômicas endodônticas pequenas são melhor visualizadas com um protocolo com FOV pequeno e alta resolução, desde que não haja objetos de alta densidade na região de interesse. Publicação 9 - Avaliou a influência do alargamento foraminal na formação de microtrincas e transporte apical em canais radiculares com curvatura apical. O alargamento foraminal promoveu novas microtrincas, não observadas no grupo controle. Maior transporte apical foi observado quando o alargamento foraminal foi realizado.

Palavras-chave: Endodontia. Dentina. Preparo de canal radicular. Cavidade pulpar. Microtomografia por Raio-X.

Pinto JC. Application of different methods of image analysis for research in Endodontics: cone beam computed tomography, micro-CT and nano-CT. [tese de doutorado]. Araraquara: Faculdade de Odontologia da UNESP; 2021.

ABSTRACT

Three-dimensional images are widely used in endodontics, both in the evaluation of endodontic techniques and materials and in diagnosis, planning and prognosis. The aims of this study was to evaluate different steps of endodontic treatment using computed microtomography (micro-CT) and computed nanotomography (nano-CT). Additionally to verify the capacity of 10 cone beam computed tomography (CBCT) devices to visualize small endodontic structures. Publication 1 – Assessed the influence of micro-computed tomography (micro-CT) voxel size on evaluation of the root canal preparation. Micro-CT images using different voxel sizes did not influence the results of volume increase and debris evaluation. However, images at 5 µm showed greater accuracy to evaluate the percentage of uninstrumented surfaces. Publication 2 - Assessed the influence of micro-CT voxel size on dentinal microcrack detection. The voxel size may influence the detection of dentinal microcracks. HyFlex EDM caused even more microcracks to develop in the middle third, detectable only by visualization of images made at 5 µm voxel size. Publication 3 – Assessed the influence of micro-CT voxel size on the evaluation of debris accumulation. The voxel sizes evaluated did not have a significant impact on the analysis of accumulated debris. Publication 4 – Investigated the filling ability of Bio- C Sealer in comparison with AH Plus using different segmentation methods and voxel sizes in micro-CT images. Bio-C Sealer had appropriate filling ability. Visual and automatic segmentation can be applied to micro-CT images with voxel sizes from 5 to 20 µm to evaluate the filling of sealers with adequate radiopacity. Publication 5 - Assessed the influence of root canal sealers on filling material removal during endodontic retreatment, as well as to compare the efficacy of XP-endo Finisher and ProDesign Logic 50/.01 as supplementary retreatment protocols. The removal of AH Plus was more difficult than in Bio-C. PDL 50/.01 and XP-endo Finisher provided greater removal of filling materials in the apical third after retreatment. Publication 6 - Investigated the influence of micro-CT voxel size on assessment of remaining filling material. The voxels sizes used (5, 10 and 20 µm) did not influence the analyzes of residual filling material in both sealers evaluated. Publication 7 – Classified ten CBCT devices, by using a ranking model, according to the detection of fine endodontic structures. The evaluated endodontic tasks were CBCT device-dependent, and its detection was influenced by the presence of metal. Publication 8 – Assessed the influence of CBCT scanning protocols and the presence of metal on the visualization of root cracks and fine endodontic anatomical structures. The capacity of CBCT images for visualizing cracks is highly limited and restricted to certain devices and protocols in the absence of metal. Fine endodontics structures were better visualized with a small FOV high-resolution protocol as long as there were no high-density objects in the region of interest. Publication 9 - Evaluated the foraminal enlargement and its influence on microcrack formation and apical transportation in root canals with apical curvature. The foraminal enlargement promoted new microcracks, not observed in the control group. Higher apical transportation was observed when foraminal enlargement was performed.

Keywords: Endodontics. Dentin. Root Canal Preparation. Dental Pulp Cavity. X-Ray Microtomography.

SUMÁRIO

1 INTRODUÇÃO

Imagens tridimensionais obtidas por microtomografia computadorizada (micro-CT) são amplamente utilizadas para avaliação de todas as etapas do tratamento endodôntico[1-3]. No entanto, parâmetros adequados para os escaneamentos por micro-CT ainda são estudados. Apesar de imagens com maior resolução, apresentando menor tamanho de voxel, serem mais indicadas para as análises por micro-CT[4], elas demandam maior tempo de escaneamento e maior tempo para o carregamento nos softwares de reconstrução e análise.

Para análise do preparo de canais radiculares, as resoluções de aquisição são variadas[1,3,5-9], podendo trazer resultados diversos nas diferentes comparações[6-8]. Para análise de debris após preparo ou limpeza dos canais radiculares, esta variação de parâmetros também é observada[1,6,10], podendo mostrar limitações para análise destas estruturas[12-14]. Por exemplo, voxels que representam a parede da dentina removida durante a instrumentação e ocupada por detritos de tecido duro podem não ser avaliados com precisão[1,12].

A análise de microtrincas dentinárias por micro-CT também apresenta limitações[15], sobretudo com relação as diferentes resoluções de escaneamento usadas[16-20]. Além disso, o uso de micro-CT para visualizar pequenas trincas mostrou menor acurácia que o microscópio cirúrgico com transiluminação[15]. Assim, para detectar pequenas estruturas ou realizar medições de alta precisão, uma ferramenta de maior precisão é necessária[21]. Os dispositivos de nano tomografia computadorizada (nano-TC) apresentam pequeno ponto focal e aumento da relação sinal-ruído, possibilitando atingir resolução espacial máxima na faixa submicrométrica[22]. Além disso, os dispositivos nano-CT são equipados com detectores de tela plana (FPD) que geram qualidade de imagem superior à dos dispositivos charge-couple (CCD), proporcionando imagens sem distorção, alta sensibilidade a raios-X e excelente resolução de contraste[23].

O preparo biomecânico visa proporcionar limpeza e conformação do canal radicular, por meio da ação mecânica dos instrumentos e atuações física e química das soluções irrigadoras[24]. A desinfecção e completa limpeza do sistema de canais radiculares é um procedimento complexo[25.] Configurações anatômicas desafiadoras, como curvaturas[9], fazem com que o preparo seja ainda mais desafiador[5]. A evolução dos instrumentos endodônticos fabricados com ligas de Níquel e Titânio (NiTi) usando tratamento térmico permitiu maior resistência à fadiga cíclica e maior flexibilidade[26,27] proporcionando preparos centralizados em canais curvos[28].

HyFlex CM (Coltene / Whaledent AG, Altstatten, Suíça) é um Sistema NiTi com tratamento térmico control memory (CM), que proporciona maior resistência à flexão para a liga de NiTi[29,30]. O sistema Hyflex EDM (Coltene / Whaledent AG, Altstatten, Suíça) é composto por instrumentos com tratamento térmico CM, e que são confeccionados por eletro-erosão[30]. Este método proporciona superfície dura e áspera e melhora a ação de corte e propriedades mecânicas do instrumento[31-33]. O Sistema HyFlex EDM é composto de instrumento rotatórios de alargamento cervical 25.12, para Glide Path 10.05, modelagem 25.08 e instrumentos para ampliação apical 40.04, 50.03 e 60.02.

A Easy Equipamentos Odontológicos é uma indústria brasileira que desenvolve instrumentos de NiTi com tratamento térmico CM. ProDesign Logic segue o conceito de lima única em movimento rotatório após glide path com instrumentos para exploração (25.01, 30.01, 35.01 e 40.01). Além dos instrumentos para preparo final dos canais radiculares (conicidades .05 e 06) existem instrumentos intermediários (conicidades .03 e .04), indicados para canais atresiados e curvos. ProDesign Logic apresenta maior resistência à fadiga cíclica que os instrumentos reciprocantes Wave One Gold[34]. Em estudo por micro-CT, ProDesign Logic apresentou menor transporte em raízes mesiais de molares inferiores, quando comparado aos instrumentos ProTaper Gold, ProDesign S, e HyFlex EDM[30]. O sistema Reciproc Blue, (VDW, Munique, Alemanha) é acionado em movimentação reciprocante a esquerda, e apresenta as mesmas dimensões do Reciproc. O tratamento térmico Blue Wire modifica a estrutura molecular dos instrumentos aumentando flexibilidade e resistência à fadiga cíclica[35].

O preparo com adequada conicidade e manutenção do trajeto original do canal radicular favorece a obturação[36,37]. Uma obturação correta pode impedir a reinfecção do sistema de canais radiculares e o desenvolvimento da lesão periapical. Técnicas obturadoras que empregam cone único com tamanho semelhante aos instrumentos mecanizados de NiTi de modelagem, tem como principais vantagens a facilidade de execução, baixo custo e tempo de procedimento curto[38,39]. Todavia, as técnicas de obturação necessitam de cimentos endodônticos para o preenchimento entre a guta percha e a parede do canal[40]. AH Plus é um cimento obturador à base de resina epóxi, considerado padrão ouro devido suas excelentes propriedades físico-químicas[41]. Cimentos endodônticos à base de trissilicato de cálcio apresentam capacidade de induzir diferenciação celular[42,43], além de apresentarem bioatividade, estimulando a mineralização[43,44]. Recentemente foi desenvolvido o cimento biocerâmico Bio-C Sealer (Angelus, Londrina, PR, Brazil), que segundo o fabricante não apresenta material resinoso em sua composição, sendo assim, sua viscosidade é dada por um álcool de cadeia longa, o politilenoglicol, aumentando sua biocompatibilidade. Este material apresenta adequada radiopacidade e escoamento, curto tempo de presa, capacidade de alcalinização[45] e baixo percentual de falhas após imersão em diferentes meios de armazenamento[46]. Desta forma, se justifica a avaliação do preenchimento Bio-C Sealer em canais radiculares, sobretudo em canais curvos que apresentam maior desafio para obturação endodôntica.

Vários estudos utilizaram micro-CT como método de avaliação da capacidade de preenchimento das obturações endodônticas, comparando o volume dos canais preparados e após a obturação com diferentes técnicas obturadoras em diferentes resoluções, dificultando comparações mais precisas[47-50]. As imagens para análise de obturação têm sido obtidas com diferentes parâmetros de resolução[47-49], sendo ainda relatada dificuldade ou até mesmo impossibilidade de observação de determinadas estruturas, como falhas ou gaps[50,51]. Segundo alguns autores a formação de artefatos também pode dificultar a análises de obturação, uma vez que tanto o cimento quanto a guta percha apesentam grande radiopacidade, podendo ocasionar margens borradas e mal definidas[52,53]. Assim, se faz necessário verificar a reprodutibilidade das análises da presença de falhas na obturação endodôntica, usando materiais com radiopacidades diferentes e métodos menos dependentes do avaliador.

Em alguns tratamentos endodônticos, devido à persistência bacteriana já existente ou contaminação do canal radicular posterior ao tratamento, o retratamento endodôntico é indicado[37]. A remoção do material obturador pode ser realizada de diversas maneiras, como uso de instrumentos manuais, instrumentos rotatórios, reciprocantes ou mesmo associações de técnicas. O emprego de técnicas que utilizam instrumentos rotatórios na remoção da massa obturadora do interior do canal radicular permite remoção da guta-percha em direção coronária reduzindo o risco de extravasamento de material obturador[54]. No entanto nenhuma técnica de retratamento é capaz de remover totalmente o material obturador do interior dos canais radiculares[55,56].

O sistema ProDesign Logic RT (Easy Equipamentos Odontológicos, Belo Horizonte, MG, Brasil) foi desenvolvido especificamente para realização de retratamento endodôntico. Este sistema é composto por três instrumentos fabricados com liga de NiTi submetida a tratamento térmico CM, seguindo o conceito de preparo coroa ápice: 30.10 para ser empregada no terço cervical, 25.08 para o terço médio e 20.06 para o terço apical. XP-endo Finisher (XP-F) (FKGDentaire,La Chaux-deFonds, Suíça) é um instrumento de NiTi, que tem forma de C em sua ponta, sendo acionado em movimentação rotatória. Este instrumento é fabricado a partir de uma liga de NíTi com tratamento térmico MaxWire, tem um tamanho de ponta ISO # 25 e não possui conicidade, porém quando ativado, após exposição à temperatura corporal (35° C) se expande em até 6 mm. O instrumento XP-F mostrou bons resultados com relação à remoção de debris na limpeza final[57] e na complementação de limpeza em retratamento de canais radiculares[59].

Análises em micro-CT são eficazes para comparações do retratamento endodôntico, uma vez que fornece uma avaliação quantitativa dos resíduos de materiais obturadores em mm^3 [60,61]. Porém não existe uma padronização com relação ao tamanho de voxel dos escaneamentos e aos parâmetros de aquisição de imagens[55,58-61]. Resultados divergentes entre os estudos têm sido atribuídos à anatomia dos canais radiculares[59], material obturador ou procedimentos de retratamento[62]. Porém as diferentes resoluções empregadas entre as análises devem ser levadas em consideração, uma vez que, dependendo do que se visa avaliar, a utilização de resoluções elevadas permite a análise de estruturas específicas e de tamanhos reduzidos[63,64].

Além de todos os fatores técnicos relacionados as diferentes etapas do tratamento endodôntico, o conhecimento da anatomia radicular é importante para o diagnóstico, tratamento e prognóstico das doenças endodônticas[65-67]. A tomografia computadorizada de feixe cônico (TCFC) é uma tecnologia de TC avançada com ampla aplicação em imagiologia dentomaxilofacial, uma vez que este método permite a análise de pequenas estruturas em três dimensões. As imagens de TCFC permitem um melhor conhecimento da detecção de características endodônticas, impactando diretamente nas decisões clínicas[65-67]

No entanto, a detecção precisa de estruturas anatômicas pequenas como canal estreito, istmo, ramificações e pequenas trincas radiculares em imagens TCFC permanece um desafio[67-69]. Além disso, o diagnóstico baseado em TCFC é dificultado por artefatos decorrentes de materiais de alta densidade, como guta-percha, cimentos endodônticos e pinos metálicos[70-73]. Assim, deve-se ter cuidado ao interpretar os relatórios baseados em TCFC para fins endodônticos[67,74-80]. Ainda, a qualidade da imagem obtida por um aparelho TCFC não podem ser simplesmente extrapolados para outro aparelho de TCFC[81,82] . Embora estudos anteriores tenham mostrado alta sensibilidade e especificidade para imagens de TCFC[67,75], outros estudos não mostraram diferença significativa entre esta modalidade de imagem e imagens 2D para a realização de diferentes tarefas[83-85]. Essa variabilidade pode ser explicada pela grande diversidade de aparelhos de TCFC disponíveis no mercado, com características técnicas distintas e, consequentemente, desempenho clínico diferente[86,87].

A seleção de protocolos de alta resolução em dispositivos de TCFC é fortemente recomendada para visualizar pequenas estruturas do sistema de canais radiculares e do periodonto[88]. Embora alguns autores recomendem uma TCFC com pequeno campo de visão (FOV) e tamanhos pequenos de voxels[89] para aplicações endodônticas, uma revisão sistemática não encontrou qualquer correlação entre tamanhos menores de voxels e melhor precisão diagnóstica de fraturas radiculares em pacientes com dentes não tratados endodonticamente[83]. Além disso, o efeito do tamanho do voxel pode ser dependente do dispositivo devido a outros fatores limitantes para a resolução espacial[90]. Portanto, a influência de diferentes dispositivos de CBCT, bem como do protocolo de aquisição e a presença de metal no campo de visão requerem uma investigação mais aprofundada.

2 PROPOSIÇÃO

Os objetivos do presente estudo foram os que seguem.

2.1 Objetivo Geral

Avaliar diferentes etapas do tratamento endodôntico usando micro-CT e nano-CT e a influência do tamanho do voxel nas análises por micro-CT, além da capacidade de visualização de estruturas anatómicas endodônticas em imagens adquiridas de 10 aparelhos de TCFC.

2.2 Objetivos Específicos

Avaliar a influência do tamanho do voxel nas imagens de micro-CT em análises de aumento do volume, debris e superfície não instrumentada do canal radicular, após instrumentação com ProDesign Logic (PDL) ou HyFlex EDM (HFEDM).

Avaliar a influência do tamanho do voxel do micro-CT na detecção de microtrincas dentinárias após instrumentação com PDL ou HFEDM.

Avaliar por micro-CT o acúmulo de debris após a aplicação de PUI em canais radiculares curvos preparados com PDL ou HEDM, bem como a influência do tamanho do voxel nestas análises.

Avaliar a porcentagem de vazios em canais radiculares curvos preenchidos com Bio-C Sealer, em comparação com o padrão ouro AH Plus, utilizando imagens de micro-CT com diferentes tamanhos de voxel e métodos de segmentação.

Avaliar a influência de um cimento à base de silicato de cálcio pronto para usar em comparação a um cimento à base de resina epóxi na remoção do material obturador durante o retratamento endodôntico, bem como comparar a remoção do material obturador, transporte apical e aumento de volume de canais radiculares mesiais curvos de molar inferior preenchidos com AH Plus ou Bio-C Sealer, após o uso de PDL 50/.01 ou XP-endo Finisher.

Avaliar influência do tamanho de voxel nas imagens de micro-CT em quantificação volumétrica do material obturador remanescente após o retratamento de canal radicular curvo preenchido com AH Plus ou Bio-C Sealer.

Classificar dez dispositivos de TCFC de acordo com a detecção de estruturas endodônticas finas na presença e ausência de pino metálico.

Avaliar 10 dispositivos de TCFC quanto à influência dos protocolos de aquisição e da presença de metal na visualização de trincas radiculares e estruturas anatômicas pequenas, como canais estreitos, istmo e delta apical.

Avaliar a influência do alargamento foraminal na formação de microtrincas e transporte apical em incisivos laterais superiores com curvatura apical por meio de nano-TC.

3 PUBLICAÇÕES

Essa pesquisa resultou nas publicações apresentadas a seguir.

3.1 Publicação 1*

Effect of voxel size of micro-computed tomography on the assessment of root canal preparation

Abstract

Introduction: The aim of this study was to assess the influence of micro-computed tomography (micro-CT) voxel size on evaluation of root canal preparation using rotary heat-treated nickel-titanium files. **Methods:** Curved mesial root canals of mandibular molars were prepared using ProDesign Logic 30/.05 (PDL) or HyFlex EDM 25/.08 (HEDM) (n=12). The specimens were scanned using micro-CT with 5 µm of voxel size before and after root canal preparation. Images with sub-resolution of 10 and 20 µm voxel sizes were obtained. The percentage of volume increase, debris and uninstrumented root canal surface were analyzed in the different voxel sizes. Data were compared using unpaired Student's t-test and ANOVA statistical tests ($\alpha = .05$). **Results:** No differences were observed for percentage of volume increase, debris and instrumented surface between the root canals prepared by PDL and HEDM ($P > .05$). Both systems promoted higher percentage of debris in the apical third compared to the middle third ($P <.05$). After instrumentation using PDL the percentage of uninstrumented surface was higher in the apical third than middle third only when analysis were performed at 5 µm ($P < .05$). When comparing the different voxel sizes (5, 10 or 20 µm), both groups showed different means for the variables, with no significant difference ($P > .05$). **Conclusions**: PDL and HEDM had similar root canal preparation capacity. Micro-CT images using different voxel sizes did not influence the results of volume increase and debris evaluation. However, images at 5 µm showed greater accuracy to evaluate the percentage of uninstrumented surfaces.

Keywords: Endodontics; dentin; root canal preparation; dental pulp cavity; x-ray microtomography

---

* Artigo escrito nas normas do periódico *Journal of Endodontics* para o qual foi submetido.

Introduction

The root canal preparation aims cleaning and shaping the root canal by means of action of instruments and irrigating solutions (1). Disinfection and complete cleaning of the root canal system is a complex procedure (2), and an improper cleaning may result in treatment failure (3). The evolution of endodontic instruments using nickel-titanium alloys (NiTi) and heat treatment allowed greater resistance to cyclic fatigue and greater flexibility (4) providing centralized preparation in curved root canals (5, 6).

ProDesign Logic (PDL) (Easy Equipamentos Odontológicos, Belo Horizonte, MG, Brazil) is a rotary NiTi instrument system (7) glide path file (taper .01) and shaping files (taper .05 or .06) (6). The heat treatment Control Memory (CM) of these files provides flexibility and improves their flexural resistance (4), promoting centralization for curved root canal preparation (5, 6). Hyflex EDM (HEDM) (Coltène / Whaledent, Allstätten, Switzerland) instruments have also CM heat treatment, however, are produced via electro-discharge machining (EDM) (8). This manufacturing process improves the mechanical properties of HEDM (9). These files maintain its integrity after multiple uses, and they are associated with high resistance to cyclic fatigue (10).

Micro-computed tomography (micro-CT) has been used to evaluate root canal preparation using different NiTi instruments (5, 11, 12). However, these analyzes can be influenced by many factors, such as different scan settings, images resolutions and misinterpretation of ring artifacts (13). For analysis of root canal preparation, different micro-CT acquisition parameters are used, with scanning voxel size of 9 µm (6, 14, 15), 14 to 15 µm (5, 16, 17), 16 to 18 µm (11, 12, 18), until 30 µm (19). The different approaches for image acquisition, image evaluation, and reporting of outcomes make difficult the interpretation of reported results and comparation of different studies (13).

Up to now there are no studies that assessed the influence of micro-CT voxel size on root canal preparation evaluation, as well as no study assessed this influence at 5 µm. Therefore, the aim of this study was to assess the influence of micro-CT voxel size on analysis of increase in volume, debris, and uninstrumented root canal surface, after instrumentation with PDL or HEDM. The null hypotheses were that there would be no differences between the voxel sizes, and between the different systems to root canal preparation.

Material and Methods

Sample size calculation

For sample calculation, G* Power 3.1.7 for Windows program (Heinrich-Heine-Universität Dusseldorf, Dusseldorf, Germany) was used. T test for 2 independent groups was used with an alpha-type error of .05 and a beta power of .95 for all the variables. Previous studies that used micro-CT imaging for evaluating root canal preparation with similar morphology were used to determine the specific effect size for volume of root canal, 2.723 (15); debris, 3.432 (14); and untouched surface, 1.451 (20). Twelve specimens per group were indicated as being the ideal size required.

Specimen Selection

All procedures were approved by the Faculty's Ethics Committee (CEP no. 64736116.4.0000.5416). The roots were inspected under a stereomicroscope at ×12 magnification to exclude those with any external dentinal defect and the roots with immature apices.

Human mandibular first and second molars previously stored in 0.1% thymol solution at 5°C were used. The inclusion criteria included two independent mesial root canals according type IV Vertucci's classification (21), angle of curvature between 25° and 35° in accordance with the Schneider method (22) and radius of curvature smaller than 10 mm, following the Pruett's method (23), besides complete apical formation, absence of root fractures, calcifications or internal resorptions. For this purpose, a digital radiographic system (RVG 6100; Kodak Dental Systems, NY) was used to select teeth according to inclusion criteria. Image J program (National Institutes of Health, Bethesda, MD, USA) was used to assess the degree of curvature in radiographic images. All selected teeth were scanned using a micro-CT device (SkyScan 1276; Bruker-micro-CT, Kontich, Belgium) at a low-resolution (35 µm voxel size) under the following settings: copper and aluminum filters, 87-millisecond exposure time, frame averaging of 3, 180° rotation around the vertical axis, rotational step of 0.5° at 80 kV and 300 µA.

The mesial root canals of the specimens were divided into two experimental groups randomly (n = 12), considering the preoperative volume of the root canals. The root length was standardized at 18 mm, with a tolerance of ±1 mm of discrepancy. The specimens were embedded in condensation silicone (Oranwash, Zhermack SpA, Badia Polesine, Italy) to simulate the periodontal ligament.

Root Canal Instrumentation

Conventional access cavities were performed, and the root canals were explored by using a size #10 K-file (Dentsply Sirona Endodontics, Ballaigues, Switzerland). The working length was established 1 mm shorter from the apical foramen of each specimen. In the sequence, a trained operator instrumented all the specimens with the aid of an operating microscope (MC-M1232, DF Vasconcellos, Valença, RJ, Brazil) at 13X magnification, using an endodontic motor (VDW Silver, VDW GmbH, Munich, Germany).

PDL Group: Instrumentation with PDL. The 30/.01 file was used in continuous rotation at 350 rpm speed and 1 Ncm torque, using in-and-out movements up to the working length. Then, the 30/.05 file was used at 600 rpm speed and 4 Ncm torque.

HEDM Group: Instrumentation with HEDM. The 10/.05 file was used in continuous rotation at 300 rpm speed and 1.8 Ncm torque, using in-and-out movements up to the working length. Then, the HEDM 25/.08 file was used at 500 rpm speed and 2.5 Ncm torque.

The root canal irrigation was performed with 5 mL of 2.5% sodium hypochlorite (NaOCl), using a 30G side-vented needle (NaviTip, Ultradent Products, South Jordan, UT) adapted to a 5 mL syringe (Ultradent Products), which was placed 2 mm short of the working length. As final irrigation, 2 mL of 17% EDTA followed by 5 mL of distilled water were used.

Micro-CT analysis

The specimens were rescanned at a high-resolution (5 µm voxel size) before and after instrumentation in a micro-CT device (SkyScan 1272; Bruker-microCT, Kontich, Belgium) under the following settings: copper filter, 180° rotation around the vertical axis and rotational step of 0.2° at 100 kV and 100 µA. The images were reconstructed using NRecon software (V1.6.10.4; Bruker, Belgium), and superimposed with geometric alignment using the DataViewer software (V.1.5.1, Bruker, Belgium). The qualitative analysis was performed using the CTAn software (V.1.14.4, Bruker, Belgium). Images at 5, 10 and 20 µm were used for quantitative analysis (Figure 1). For this purpose, the previously scanned 5 μm images were resized by 2 and 4, respectively using the CTAn software (24-26).

Analyzes were performed in the middle and apical thirds of the roots, being considered 3 mm for each third. Preoperative volume, volume of prepared canal, surface area after preparation and volume of debris after preparation were obtained. Based on these values, the percentage of volumetric increase (% Volumetric increase), percentage of debris (% Debris) and percentage of uninstrumented surface (% Uninstrumented surface) were calculated using the following formulas:

$$\%\ \text{Volumetric increase} = 100 - \frac{\text{Volume of prepared canal} \times 100}{\text{Preoperative volume}}$$

$$\%\ \text{Debris} = \frac{\text{Volume of debris} \times 100}{\text{Volume of prepared canal}}$$

$$\%\ \text{Uninstrumented surface} = \frac{\text{Uninstrumented surface area} \times 100}{\text{Surface area after preparation}}$$

Statistical analysis

The data obtained for each of the parameters evaluated were submitted to the Shapiro-Wilks normality test, and all data presented normal distribution. For analysis between groups and between the middle and apical thirds was use no-paired t-test. For analysis among images with different voxel size was used ANOVA test. The level of significance was set at $P < .05$.

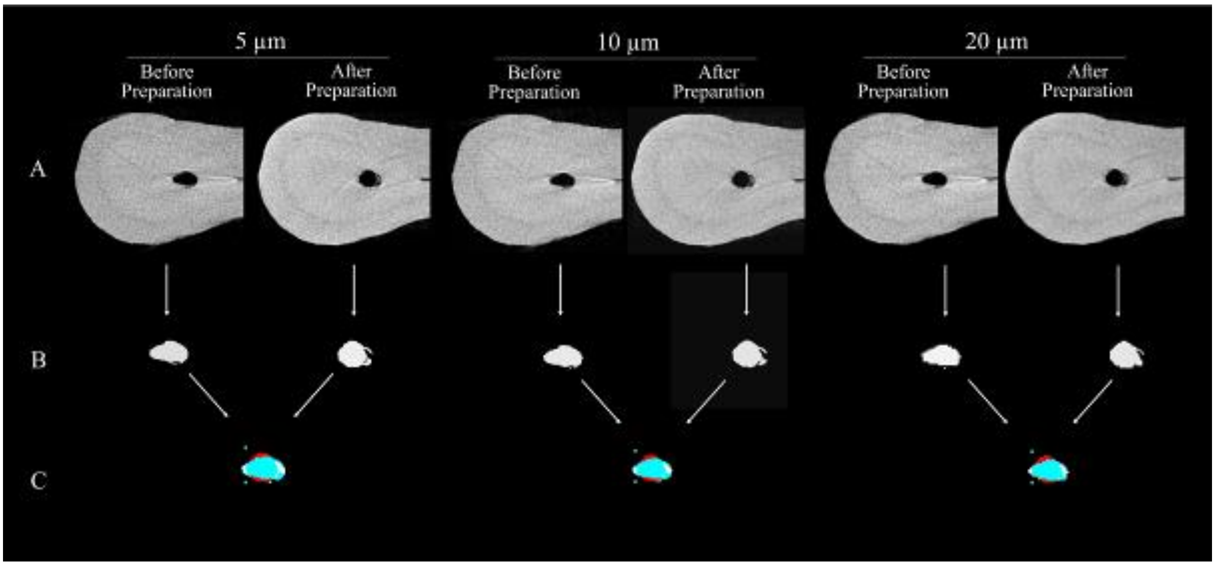

Figure 1 – Representative micro-CT images at different voxel sizes showing original transversal slices of the roots canals (A), segmented root canals (B) and the superposition of the segmented root canal before and after instrumentation for volumetric analyses (C).

Results

No differences were observed for percentage of volume increase, debris and uninstrumented surface between the root canals prepared by PDL and HEDM in the middle and apical thirds at all voxel sizes (5, 10 and 20 µm) ($P > .05$) (Figure 2). Both systems promoted higher percentage of debris in apical third compared with middle third ($P <.05$). The comparison for uninstrumented surface of root canal showed similar results between thirds for both groups at 10 and 20 µm ($P > .05$). However, after instrumentation with PDL the percentage of uninstrumented surface was higher in the apical third than middle third at 5 µm ($P < .05$). When comparing images with different voxel sizes (5, 10 or 20 µm), both groups showed different means for the variables without significant difference ($P > .05$) (Table 1).

Table 1 - Means and standard deviations of volume, volume increase (%), debris (%) and uninstrumented surface (%) of root canals in different voxel sizes after preparation

		ProDesign Logic			HyFlex EDM		
		5 μm	**10 μm**	**20 μm**	**5 μm**	**10 μm**	**20 μm**
Pre-operative canal (mm^3)	**Middle**	0.4 ± 0.1^a	0.4 ± 0.1^a	0.4 ± 0.1^a	0.4 ± 0.1^a	0.3 ± 0.2^a	0.4 ± 0.2^a
	Apical	0.20 ± 0.07^b	0.20 ± 0.07^b	0.19 ± 0.06^b	0.2 ± 0.1^b	0.2 ± 0.1^b	0.2 ± 0.1^b
Prepared canal (mm^3)	**Middle**	0.5 ± 0.1^a	0.5 ± 0.1^a	0.6 ± 0.1^a	0.7 ± 0.2^a	0.7 ± 0.2^a	0.7 ± 0.2^a
	Apical	0.30 ± 0.07^b	0.27 ± 0.05^b	0.27 ± 0.05^b	0.31 ± 0.04^b	0.3 ± 0.2^b	0.3 ± 0.1^b
Volume Increase (%)	**Middle**	60 ± 30^a	60 ± 30^a	60 ± 30^a	90 ± 50^a	80 ± 50^a	90 ± 30^a
	Apical	60 ± 50^a	50 ± 30^a	60 ± 50^a	70 ± 60^a	70 ± 40^a	70 ± 50^a
Debris (%)	**Middle**	3 ± 2^b	3 ± 2^b	2 ± 2^b	4 ± 2^b	3 ± 2^b	3 ± 2^b
	Apical	5 ± 3^a	5 ± 2^a	4 ± 3^a	6 ± 3^a	6 ± 3^a	5 ± 3^a
Uninstrumented surface (%)	**Middle**	30 ± 20^b	30 ± 20^a	30 ± 20^a	40 ± 10^a	30 ± 20^a	30 ± 10^a
	Apical	54 ± 20^a	50 ± 20^a	40 ± 20^a	50 ± 20^a	40 ± 20^a	30 ± 20^a

There was no statistically significant difference among the columns. Different superscript lowercase letters in the same column indicate statistical difference between the thirds of the same preparation (*P* <. 05).

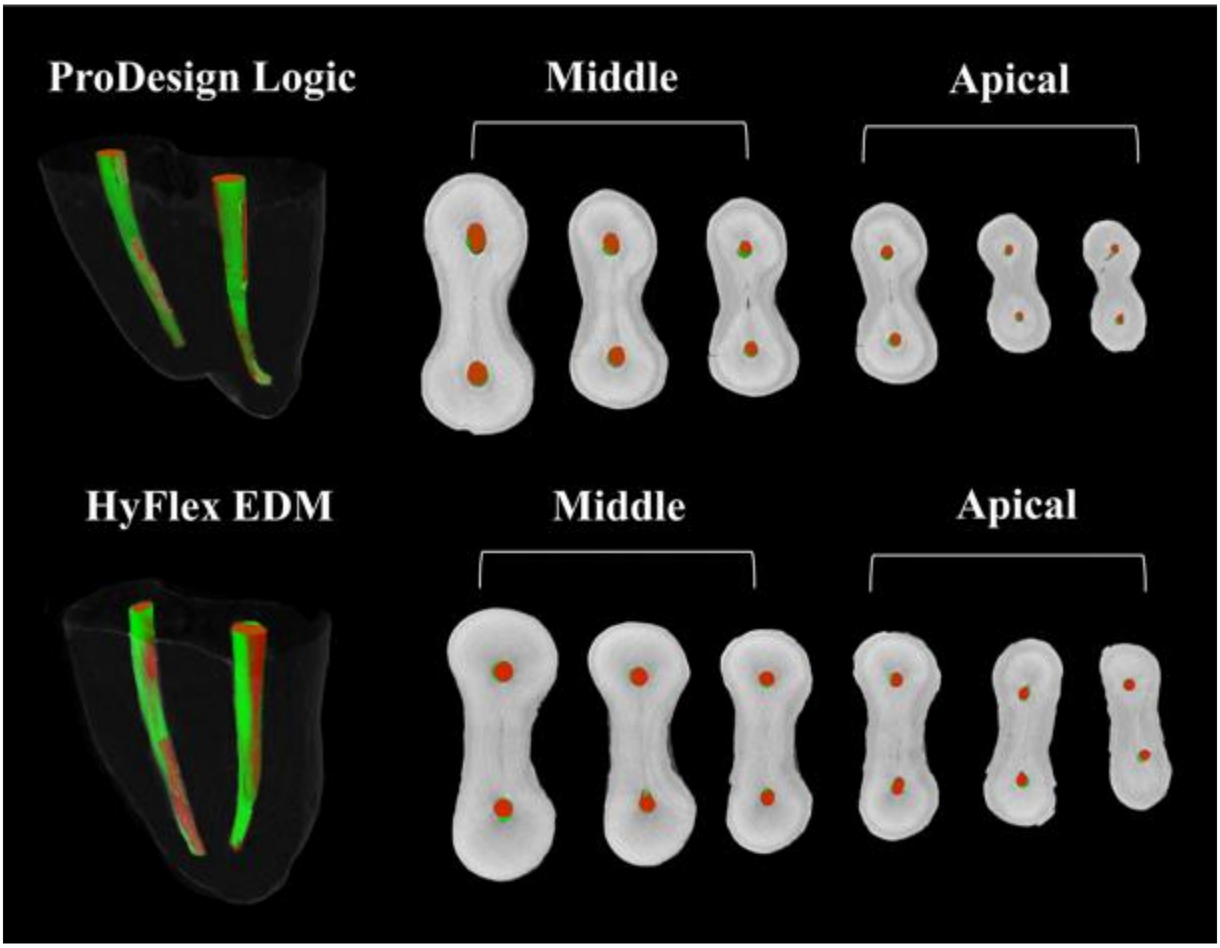

Figure 2 – 3D reconstructions and cross-sectional views of images with 5 µm of voxel size of middle and apical thirds of mesial roots od mandibular molars prepared by ProDesign Logic or HyFlex EDM. Root canal before preparation (red), root canal after preparation (green).

Discussion

Micro-CT is one of the most used analysis tool for root canal preparation assessments (5, 6, 27). Therefore, it is important to know the influence of scanning parameters on the outcomes of each variable associated to the instrumentation capacity. Previous study has reported no influence of voxel size on debris evaluation when analyses was performed between 5 and 20 µm voxel size (25). However, other investigation, assessing the influence of voxel size on microcracks analyses showed higher accuracy for images with lower voxel size (26). Therefore, in agreement with the current literature, our results report that the influence of voxel size on analyses of root canal preparations using micro-CT is variable-dependent. Although, in the present study, the voxel size did not influence the analyses of root canal volume and debris, the root canals prepared by PDL showed higher uninstrumented surface in apical third than middle third only when the evaluation was performed at 5 µm.

A high percentage of uninstrumented surface after root canal preparation have been reported by several investigations. However, their micro-CT images were obtained using different parameters of scanning, varying since 9 to 30 µm of voxel size (6, 11, 12, 16, 18, 19). These studies have showed conflicting results, even using similar size (6, 11, 12, 16, 18) or similar root canal anatomy for root canal preparation (6, 11, 12, 18). In this study a different outcome was observed when the uninstrumented surface analyzes were performed at 5 µm, therefore, the micro-CT voxel size must be taken into account for comparisons between studies. A voxel is the discrete unit of the scan volume that is the result of the tomographic reconstruction representing three dimensions (13). The voxel size seems to be one of the main factors that can affect the quality of the images and consequently the analyzes performed (13, 24). The analysis of trabecular bone structure was significantly affected by micro-CT scanning voxel size (23, 28, 29). A previous study (29), evaluating the presence of voids in filled root canal at different voxel size, detected more voids at smaller voxel sizes (5.2, 8.1 and 11.2 µm) than at 16.73.

The CM heat treatment applicated for PDL and HEDM instruments allows safe preparations in curved canals (5). Moreover, the EDM surface treatment present in HEDM files improve its mechanical properties (10). The greater taper of the first 4 mm for 25/.08 HEDM file, with its progressive taper reduction until to .04 has motivated the use of PDL file with larger tip diameter, size 30/.05 in this study. The constant taper of PDL promotes similar size along the active part between the instruments evaluated. Thus, in the present study, PDL and HEDM presented similar percentage of volumetric increase and uninstrumented surface.

The presence of debris in the root canal make difficult its disinfection (31), and decreases sealer adhesion to dentinal tubules (26). There were no differences for percentage of debris accumulated between the root canals prepared for PDL or HEDM. However, for both instruments evaluated, there was more percentage of debris in apical third than middle third, with means of 5,07 % for PDL and 5,77 for HEDM, in analysis at 5 µm. Previous studies have also observed large amounts of accumulated debris in mesial roots of mandibular molars (6, 14, 26). These studies suggest greater apical enlargement (6) or additional cleaning protocols as passive ultrasonic irrigation (14, 26) or XP-endo Finisher (14) as methods to decrease accumulated root canal debris after root canal preparation using mechanized NiTi files.

Since the influence of voxel size on root canal preparation analyses seems to be depended of the variable evaluated, it is important the planning of study design considering the choice of adequate micro-CT scanning protocol. In addition, taking account that besides voxel size, the final images resolution also depends of other paramenters such as mean absorption of the sample, detector noise, reconstruction algorithm, X-ray focal spot size and shape, detector aperture, and scanner geometry (32), a pilot study is strongly recommended before the scans, instead of using parameters from previous study.

Conclusion

Within the limitations of this ex vivo study, it can be concluded that voxel sizes do not have a significant impact on analysis of volume of root canals and accumulated debris. However, the voxel size should be considered as a potential factor for uninstrumented surface, since it was observed different results for images at 5 µm, in comparation with images of 10 and 20 µm of voxel sizes. Further research is necessary using lower micro-CT voxel size scans.

Acknowledgments

This study was supported by the Coordenação de Aperfeiçoamento de Pessoal de Nível Superior, Brasil (CAPES) Funding Code 001, Conselho Nacional de Desenvolvimento Científico e Tecnológico (CNPq), Brazil, 308076/2018-4 and São Paulo Research Foundation – FAPESP [grant numbers 2018/19665-6-0 and 2019/22885-0].

The authors deny any conflicts of interest related to this study

References

1. Schilder H. Cleaning and shaping the root canal. Dent Clin North Am. 1974;18:269-96.

2. Wu MK, Dummer PM, Wesselink PR. Consequences of and strategies to deal with residual post-treatment root canal infection. Int Endod J. 2006;39:343-56.

3. Azim AA, Griggs JA, Huang GT. The Tennessee study: factors affecting treatment outcome and healing time following nonsurgical root canal treatment. Int Endod J. 2016;49:6-16.

4. Alcalde MP, Duarte MAH, Bramante CM, de Vasconselos BC, Tanomaru-Filho M, Guerreiro-Tanomaru JM, et al. Cyclic fatigue and torsional strength of three different thermally treated reciprocating nickel-titanium instruments. Clin Oral Investig. 2018;22:1865-71.

5. Pinheiro SR, Alcalde MP, Vivacqua-Gomes N, Bramante CM, Vivan RR, Duarte MAH, et al. Evaluation of apical transportation and centring ability of five thermally treated NiTi rotary systems. Int Endod J. 2018;51:705-13.

6. Pinto JC, Pivoto-Joao MMB, Espir CG, Ramos MLG, Guerreiro-Tanomaru JM, Tanomaru-Filho M. Micro-CT evaluation of apical enlargement of molar root canals using rotary or reciprocating heat-treated NiTi instruments. J Appl Oral Sci. 2019;27:e20180689.

7. Rodrigues CT, Duarte MA, de Almeida MM, de Andrade FB, Bernardineli N. Efficacy of CM-Wire, M-Wire, and Nickel-Titanium Instruments for Removing Filling Material from Curved Root Canals: A Micro-Computed Tomography Study. J Endod. 2016;42:1651-5.

8. Pedulla E, Genovesi F, Rapisarda S, La Rosa GR, Grande NM, Plotino G, et al. Effects of 6 Single-File Systems on Dentinal Crack Formation. J Endod. 2017;43:456-61.

9. Iacono F, Pirani C, Generali L, Bolelli G, Sassatelli P, Lusvarghi L, et al. Structural analysis of HyFlex EDM instruments. Int Endod J. 2017;50:303-13.

10. Pirani C, Iacono F, Generali L, Sassatelli P, Nucci C, Lusvarghi L, et al. HyFlex EDM: superficial features, metallurgical analysis and fatigue resistance of innovative electro discharge machined NiTi rotary instruments. Int Endod J. 2016;49:483-93.

11. da Silva Limoeiro AG, Dos Santos AH, De Martin AS, Kato AS, Fontana CE, Gavini G, et al. Micro-Computed Tomographic Evaluation of 2 Nickel-Titanium Instrument Systems in Shaping Root Canals. J Endod. 2016;42:496-9.

12. Stringheta CP, Bueno CES, Kato AS, Freire LG, Iglecias EF, Santos M, et al. Micro-computed tomographic evaluation of the shaping ability of four instrumentation systems in curved root canals. Int Endod J. 2019;52:908-16.

13. Bouxsein ML, Boyd SK, Christiansen BA, Guldberg RE, Jepsen KJ, Muller R. Guidelines for assessment of bone microstructure in rodents using micro-computed tomography. J Bone Miner Res. 2010;25:1468-86.

14. Leoni GB, Versiani MA, Silva-Sousa YT, Bruniera JF, Pecora JD, Sousa-Neto MD. Ex vivo evaluation of four final irrigation protocols on the removal of hard-tissue debris from the mesial root canal system of mandibular first molars. Int Endod J. 2017;50:398-406.

15. Pivoto-João MMB, Tanomaru-Filho M, Pinto JC, Espir CG, Guerreiro-Tanomaru JM. Root Canal Preparation and Enlargement Using Thermally Treated Nickel-Titanium Rotary Systems in Curved Canals. J Endod. 2020;46:1758-65.

16. Zuolo ML, Zaia AA, Belladonna FG, Silva E, Souza EM, Versiani MA, et al. Micro-CT assessment of the shaping ability of four root canal instrumentation systems in oval-shaped canals. Int Endod J. 2018;51:564-71.

17. Zhao Y, Fan W, Xu T, Tay FR, Gutmann JL, Fan B. Evaluation of several instrumentation techniques and irrigation methods on the percentage of untouched canal wall and accumulated dentine debris in C-shaped canals. Int Endod J. 2019;52:1354-65.

18. Siqueira JF, Jr., Alves FR, Versiani MA, Rocas IN, Almeida BM, Neves MA, et al. Correlative bacteriologic and micro-computed tomographic analysis of mandibular molar mesial canals prepared by self-adjusting file, reciproc, and twisted file systems. J Endod. 2013;39:1044-50.

19. Zhao D, Shen Y, Peng B, Haapasalo M. Micro-computed tomography evaluation of the preparation of mesiobuccal root canals in maxillary first molars with Hyflex CM, Twisted Files, and K3 instruments. J Endod. 2013;39:385-8.

20. Peters OA, Arias A, Paqué F. A Micro-computed Tomographic Assessment of Root Canal Preparation with a Novel Instrument, TRUShape, in Mesial Roots of Mandibular Molars. J Endod. 2015; 41:1545-50.

21. Vertucci FJ. Root canal anatomy of the human permanent teeth. Oral Surg Oral Med Oral Pathol. 1984;58:589-99.

22. Schneider SW. A comparison of canal preparations in straight and curved root canals. Oral Surg Oral Med Oral Pathol. 1971;32:271-5.

23. Pruett JP, Clement DJ, Carnes DL, Jr. Cyclic fatigue testing of nickel-titanium endodontic instruments. J Endod. 1997;23:77-85.

24. Isaksson H, Töyräs J, Hakulinen M, Aula AS, Tamminen I, Julkunen P, et al. Structural parameters of normal and osteoporotic human trabecular bone are affected differently by microCT image resolution. Osteoporos Int. 2011;22:167-77.

25. Pinto JC, Torres FFE, Santos Junior AO, Tavares KIMC, Guerreiro-Tanomaru JM, Tanomaru-Filho M. Influence of voxel size on micro-CT analysis of debris after root canal preparation. Braz Oral Res. 2020;13;35:e008.

26. Pinto JC, Coaguila-Llerena H, Torres FFE, Lucas-Oliveira É, Bonagamba TJ, Guerreiro-Tanomaru JM, Tanomaru-Filho M. Influence of voxel size on dentinal microcrack detection by micro-CT after root canal preparation. Braz Oral Res. 2021; 11;35:e074.

27. Freire LG, Iglecias EF, Cunha RS, Dos Santos M, Gavini G. Micro-Computed Tomographic Evaluation of Hard Tissue Debris Removal after Different Irrigation Methods and Its Influence on the Filling of Curved Canals. J Endod. 2015;41:1660-6.

28. Christiansen BA. Effect of micro-computed tomography voxel size and segmentation method on trabecular bone microstructure measures in mice. Bone Rep. 2016;5:136-40.

29. Sode M, Burghardt AJ, Nissenson RA, Majumdar S. Resolution dependence of the non-metric trabecular structure indices. Bone. 2008;42:728-36.

30. Orhan K, Jacobs R, Celikten B, Huang Y, de Faria Vasconcelos K, Nicolielo LFP, et al. Evaluation of Threshold Values for Root Canal Filling Voids in Micro-CT and Nano-CT Images. Scanning. 2018;2018:9437569.

31. Paque F, Laib A, Gautschi H, Zehnder M. Hard-tissue debris accumulation analysis by high-resolution computed tomography scans. J Endod. 2009;35:1044-7.

32. Bouxsein ML, Boyd SK, Christiansen BA, Guldberg RE, Jepsen KJ, Müller R. Guidelines for assessment of bone microstructure in rodents using micro-computed tomography. J Bone Miner Res. 2010;25:1468-86.

3.2 Publicação 2*

Influence of voxel size on dentinal microcrack detection by micro-CT after root canal preparation

Abstract

The aim of this study was to assess the influence of micro-computed tomography (micro-CT) voxel size on dentinal microcrack detection after root canal preparation using rotary heat-treated nickel-titanium files. Curved mesial root canals (n = 24) of mandibular molars were prepared using ProDesign Logic 30/.05 (PDL) or HyFlex EDM 25/.08 (HEDM). The specimens were scanned by micro-CT with a voxel size of 5 μm before and after root canal preparation. The percentage of microcracks was evaluated in images at 5, 10 and 20 μm voxel size, by two examiners at two moments. The Kappa and McNemar tests ($\alpha = 0.05$) were used. The percentage of dentinal microcracks was similar before and after PDL and HEDM preparations, at 10 and 20 μm ($p > 0.05$). HEDM showed a higher percentage of dentinal microcracks in the middle third at 5 μm after preparation ($p < 0.05$). The detection of dentinal microcracks before and after instrumentation using PDL was more accurate at 5 μm than at 20 μm, in all thirds ($p < 0.05$). Within the expected limitations of this *ex vivo* study, it can be concluded that different resolutions influence the micro-CT analysis of microcracks. The voxel size may influence the detection of dentinal microcracks. The highest accuracy to detect microcracks was observed for analyses performed with a voxel size of 5 μm. HyFlex EDM caused even more microcracks to develop in the middle third, detectable only by visualization of images made at 5 μm voxel size.

Keywords: Endodontics; Dentin; Root Canal Preparation; Dental Pulp Cavity; X-Ray Microtomography

---

* Artigo publicado no periódico *Brazilian Oral Research.* (https://doi.org/10.1590/1807-3107bor-2021.vol35.0074).

Introduction

Nickel-titanium (Ni-Ti) files have improved root canal preparations by enabling enlargement and maintenance of the canal trajectory[1,2]. Although mechanized root canal preparation presents several advantages, it has also been reported to cause potential dentinal microcracks[3-6]. The performance of endodontic files during root canal preparation is related to their cross-sectional design, taper, and thermal or surface treatment[7,8]. Heat treatments applied to NiTi files have been associated with lower risk of dentinal microcracks[9]. These microcracks could potentially promote a vertical root fracture[10], especially in roots with reduced dentin thickness[11]. Owing to contrasting information in the literature, there is still no consensus on whether root canal preparation using continuous or reciprocating motion induces the formation of microcracks[4,9,12-14].

High precision tools are required to detect microcracks, such as micro-computed tomography (micro-CT), which allows the defect to be located with great precision[9]. Microcracks can be evaluated for endodontic instrumentation at different resolutions, using scanning voxel sizes of 10 μm[14], 14 μm[15,16], 17.42 to 21 μm[9,12,17], and 30 μm[13,18]. Although most studies using micro-CT have not observed any correlation between root canal preparation with NiTi files and microcrack formation[14-18], some studies have correlated the presence of microcracks with root canal preparation using rotary NiTi files[12,13].

ProDesign Logic - PDL (Easy Equipamentos Odontológicos, Belo Horizonte, MG, Brazil) are Ni-Ti files with control memory (CM)[19]. PDL allow shorter working time associated with resistance to cyclic fatigue[20]. In addition, preparation with these instruments has not been associated with the formation of new dentin defects[17]. Although Hyflex EDM – HEDM files (Coltène / Whaledent, Allstätten, Switzerland) also have CM characteristics, they are manufactured using electrical discharge machining[18,21]. HEDM instruments maintain their integrity after multiple use, and are associated with high resistance to cyclic fatigue[20]. There is contrasting evidence regarding microcracks after HEDM root canal preparation[13,18].

There are no studies that assessed the influence of micro-CT voxel size on microcrack evaluation, much less any assessing this influence at 5 μm. Therefore, this study aimed to evaluate the influence of micro-CT voxel size on microcrack detection after instrumentation with CM files. The null hypotheses were that there would be no difference among the voxel sizes, or between the dentinal macrocracks present after preparation with PDL and HEDM.

Materials and methods

Specimen Selection

The sample size for this study was calculated using a specific software (G * Power 3.1.7 for Windows, Heinrich Heine, Universitat Dusseldorf). The chi-square test was used, with an alpha type error of 0.05, beta power of 0.90, and effect size of 0.93. The ideal sample size was reported to be six specimens per group.

All procedures were approved by the dental school ethics committee (CEP no. 64736116.4.0000.5416). The roots were inspected under a stereomicroscope at 12× magnification to exclude any roots with external dentinal defect or immature apices. The study used human mandibular first and second molars previously stored in 0.1% thymol solution at 5°C. The inclusion criteria required teeth with two independent mesial root canals according to Vertucci's type IV classification[23], angle of curvature between 25° and 35° based on the Schneider method[24], and radius of curvature smaller than 10 mm, following the Pruett method[25], in addition to complete apical formation, and absence of root fractures, calcifications or internal resorptions. Compliance with the criteria required that the specimens be radiographed using a digital system (RVG 6100; Kodak Dental Systems, NY), and scanned with a micro-CT device (SkyScan 1176; Bruker-microCT, Kontich, Belgium). The first scanning was performed at low-resolution (35 µm voxel size) under the following settings: copper and aluminum filters, 87-millisecond exposure time, frame averaging of 3, 180° rotation around the vertical axis, rotational step of 0.5° at 80 kV and 300 µA. After excluding all the teeth that did not comply with the inclusion criteria, 12 mesial roots of mandibular molars were selected, totaling 24 root canals.

The mesial root canals of the specimens were divided into two experimental groups randomly (n = 12), with stratified random sampling, considering the preoperative volume of the root canals. The root length was standardized at 18 mm, with a tolerance of ±1 mm of discrepancy. The specimens were embedded in condensation silicone (Oranwash, Zhermack SpA, Badia Polesine, Italy) to simulate the periodontal ligament.

Root Canal Preparation

Conventional access cavities were performed, and the root canals were explored by using a size #10 K-file (Dentsply Sirona Endodontics, Ballaigues, Switzerland). The working length was established at 1 mm short of the apical foramen of each specimen. Afterwards, a trained operator instrumented all the specimens with an operating microscope (MC-M1232, DF Vasconcellos, Valença, RJ, Brazil) at 13× magnification, using an endodontic motor (VDW Silver, VDW, Munich, Germany).

PDL Preparation: A 30/.01 file was used in continuous rotation at 350 rpm speed and 1 Ncm torque, using in-and-out movements up to the working length. Then, a 30/.05 file was used at 600 rpm speed and 4 Ncm torque.

HEDM Preparation: A 10/.05 file was used in continuous rotation at 300 rpm speed and 1.8 Ncm torque, using in-and-out movements up to the working length. Then, a HEDM 25/.08 file was used at 500 rpm speed and 2.5 Ncm torque.

Root canal irrigation was performed with 5 mL of 2.5% sodium hypochlorite (NaOCl), using a 30G side-vented needle (NaviTip, Ultradent Products, South Jordan, UT) adapted to a 5 mL syringe (Ultradent Products), which was placed 2 mm short of the working length. The final irrigation used 2 mL of 17% EDTA, followed by 5 mL of distilled water, as described above.

Micro-CT Analysis

The micro-CT analysis was performed by scanning the specimens with a voxel size of 5 µm in a micro-CT device (SkyScan 1272. Bruker, Kontich, Belgium), before and after instrumentation, under the following settings: copper filter, 180° rotation around the vertical axis and rotational step of 0.2° at 100 kV and 100 µA. The images were reconstructed using a NRecon software program (NRecon v.1.6.3; Bruker), and superimposed with geometric alignment using a DataViewer software program (Data Viewer v.1.5.1, Bruker). The qualitative analysis was performed using a CTAn software program (CTAn v.1.14.4, Bruker). The original images were resized isotropically to perform analyses with different voxel sizes. Images at 10 and 20 µm were obtained for qualitative analysis. This was achieved by resizing the previously scanned 5 µm images by 2 and 4, respectively, using a CTAn software program, while the dataset previously superimposed in DataViewer software was being loaded.[26] Three dimensional images were made with a CTVox software program (CTVox v.3.2; Bruker).

The analyses were performed in the middle and apical thirds of the roots, considering 3 mm for each third. The microcracks were evaluated by opening the cross-sectional images before and after instrumentation, and evaluating them at the same time. The analyses were performed in three voxel sizes, totaling 14,400 slices of cross-sectional images at 5 μm, 7,200 at 10 μm, and 3,660 at 20 μm, per third in each group. The images were then compared twice by two blinded examiners, at two different times. Microcracks were defined as lines or defects extending from inside the root canal to the dentin, or from the outer root surface into the dentin (Figure 1). The distribution of microcracks was expressed as a percentage of the total cross-sectional images.

Statistical Analysis

The results were expressed as a percentage for each group. Kappa statistics were used to ascertain intra- and extraexaminer agreement. The McNemar test was used to determine significant differences before and after instrumentation, and at different voxel sizes in the same group. The level of significance was set at 5%.

Results

The kappa values were greater than 0.81 for all parameters assessed, thus confirming intraexaminer and extraexaminer agreement. The detection of dentinal microcracks in the PDL group, before and after instrumentation, was more accurate at 5 μm than at 20 μm in all thirds ($p < 0.05$) (Table 1). Figure 2 shows a thinner continuity of microcracks based on different voxel sizes.

No differences were observed in the apical third before or after instrumentation in any of the voxel sizes (5, 10 and 20 μm), in the HEDM group, ($p > 0.05$). The comparison between before and after instrumentation with PDL and HEDM showed that the percentage of dentinal microcracks was similar for both groups at 10 and 20 μm ($p > 0.05$). However, the percentage of dentinal microcracks after instrumentation with HEDM was higher in the middle third at 5 μm ($p < 0.05$) (Table 1). Figure 3 shows cross-sectional images revealing microcracks before and after instrumentation with the PDL and HEDM systems.

Table 2 - Percentage of sections with dentinal microcracks before and after preparation, based on different voxel sizes

		ProDesign Logic 30.05			HyFlex EDM 25.08		
		5 μm	**10 μm**	**20 μm**	**5 μm**	**10 μm**	**20 μm**
Before preparation	Middle	3.04^{a}	2.92^{ab}	1.85^{b}	19.94^{a*}	18.80^{b}	17.32^{b}
	Apical	3.19^{a}	2.35^{b}	2.32^{b}	1.40^{a}	1.13^{a}	1.13^{a}
After preparation	Middle	3.36^{a}	3.02^{a}	2.09^{b}	24.11^{a*}	20.04^{b}	18.16^{b}
	Apical	3.45^{a}	2.44^{ab}	2.38^{b}	1.52^{a}	1.23^{a}	1.20^{a}

Different lowercase letters on the same line indicate statistical difference among the different analysis resolutions of the same group. * represents statistical difference between before and after preparation in same group and third (McNemar test, 5% significance).

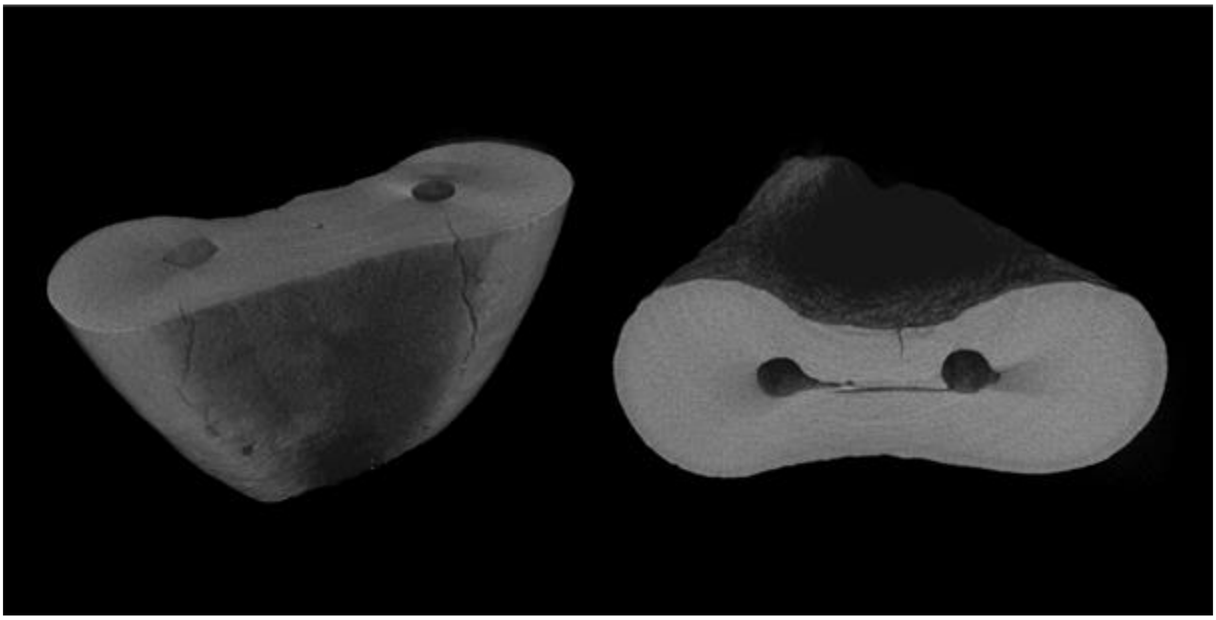

Figure 1 - 3D reconstructions showing microcracks in the mesial roots of mandibular molars.

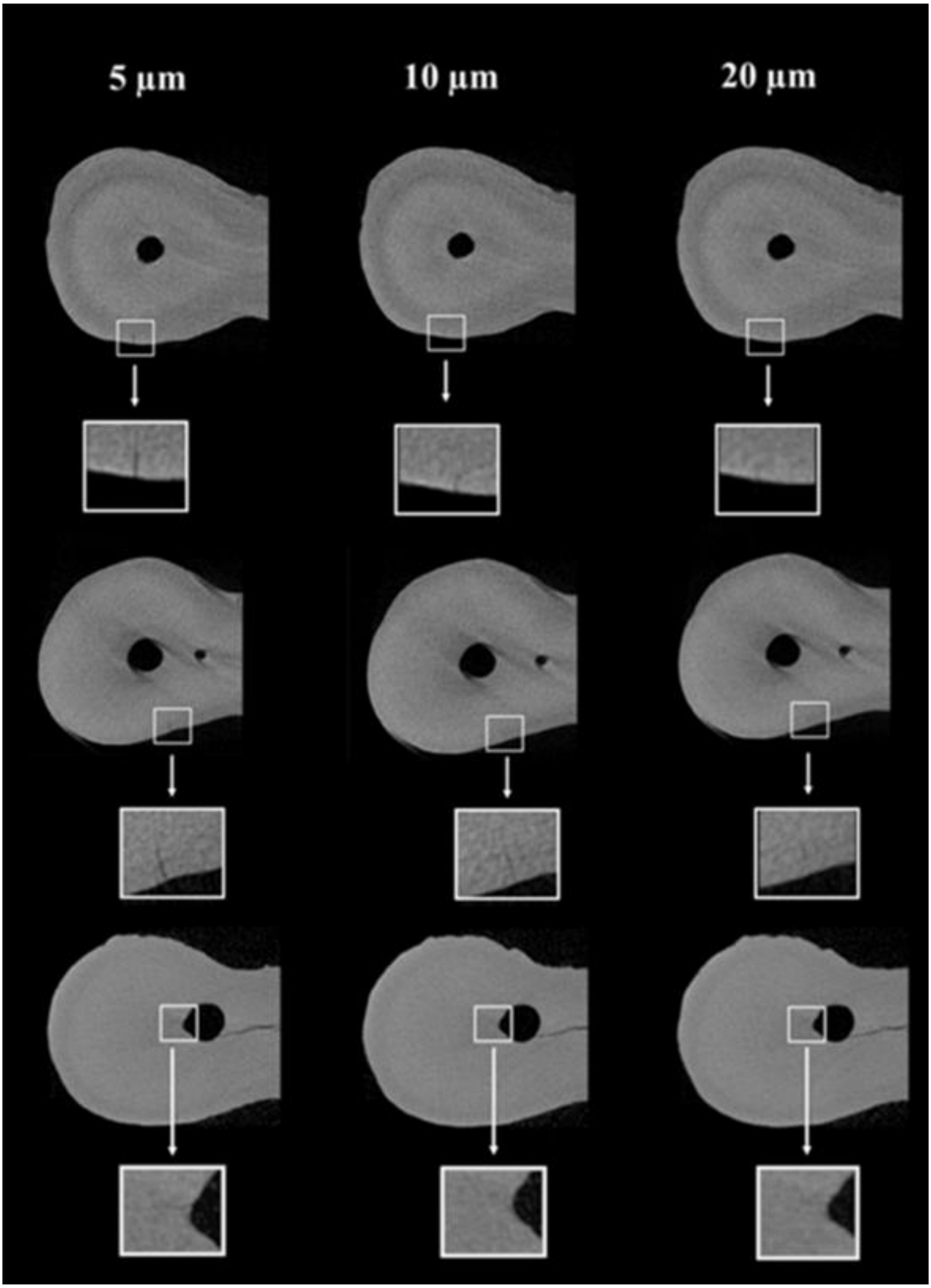

Figure 2 - Representative cross-sectional micro–CT images showing a thinner continuity of microcracks based on different voxel sizes.

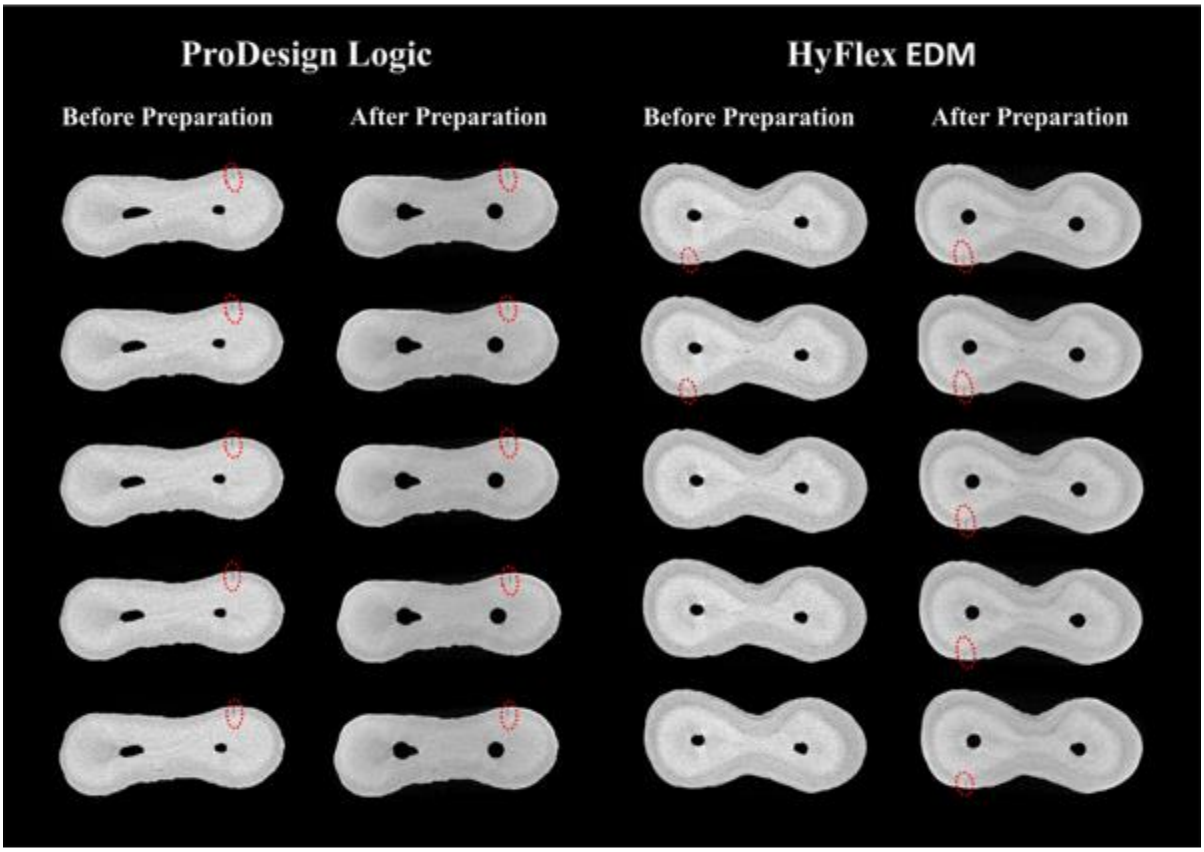

Figure 3 - Representative cross-sectional micro–CT images, at 5 µm voxel size, showing microcrack continuity with a 50 µm interval between slices, before and after instrumentation with the ProDesign Logic and HyFlex EDM systems. Microcracks are circled in red.

Discussion

Tooth fracture is a critical issue in endodontics, owing to its direct relation to long-term survival rates[27]. In the present study, a higher percentage of microcracks was observed at a small voxel size (5 µm). Hence, our first null hypothesis was rejected, considering that microcrack detection was influenced by the voxel size.

Many factors may influence microcrack evaluation, such as different scan settings, number of cross-sectional images, different voxel sizes, and misinterpretation of ring artifacts[18]. The influence of voxel size has been previously assessed for cone beam computed tomography[28,29]. Similarly, previous studies have observed that analysis of trabecular bone structure can be significantly affected due to micro-CT voxel size[26,30,31]. In endodontics, Orhan et al.[32] evaluated the presence of voids in filled root canals, at different voxel sizes. The authors detected more voids at smaller voxel sizes (5.2, 8.1 and 11.2 µm) than at 16.73 µm. In the current study, voxel size was the only variable evaluated, since the samples were scanned at 5 µm, and the reconstructed images were resized to acquire images with 10 and 20 µm voxel size[26]. This method allows the micro-CT images to be resized to higher voxel sizes, which represent an average of the previous voxels[26,33]. Therefore, the smallest voxel size used during the scanning procedure can be considered the gold standard for determining the level of accuracy under limited resolution scenarios [31,34].

The analyses at 10 and 20 µm were similar regarding the presence of microcracks before and after the preparation with HEDM files. However, assessment at 5 µm showed a higher percentage of microcracks in the middle third after instrumentation, partially rejecting the second null hypothesis. The highest number of image slices at 5 µm can be attributed to the ability of micro-CT to detect a thinner continuity of microcracks than images at 10 and 20 µm, based on its high-resolution scans, known to provide more accurate analysis of microstructures[30]. On the other hand, considering that statistical significance is dependent on the sample size[35], and that each cross-sectional image was used for statistical qualitative tests[9,12,14], the larger number of slices observed at the higher resolution (5 µm) may have contributed to the statistical significance observed in the analyses before and after preparation with HEDM performed at 5 um.

In a previous study, HEDM did not cause microcracks in mandibular premolars with straight root canals[18]. However, Mandava et al.[13] showed a higher percentage of microcracks after HEDM instrumentation in mesial curved canals of mandibular molars. The root canal anatomy may have contributed to producing discordant observations between the two studies, since mesial curved canals may favor microcracks formation[13]. The increased percentage of microcracks could be attributed to the taper[7,9], the hard surface induced by the surface treatment[21,36,37], the tip design, the cross-sectional geometry, the variable pitch or the flute form[7,9,27]. Specifically, the greater taper of the first 4 mm of the 25/.08 HEDM file, despite its progressive taper reduction to .04[13,21,38], may have caused a more aggressive instrumentation than the constant taper of the 30/.05 PDL file. The propagation of microcracks in HEDM instrumentation was probably caused by tensions inside the root canal, which were transmitted to the external root surface, thus increasing a preexisting defect. A previous study reported that this effect is caused by the collapse of the dentin bonds around the external root surface[10].

After PDL preparation, no new microcracks were observed, even at 5 μm. Moreover, no correlation was observed between the instrumentation and the formation/propagation of microcracks after preparation with PDL files[17]. Although PDL also has CM heat treatment[19], its reduced taper could influence the differences observed in regard to the HEDM group, even at the similar speed and torque values used in both systems.

In the present study, the images revealed that microcracks were already present in all the groups before instrumentation, thus corroborating previous investigations that used larger voxel sizes[12,15,16,18]. These defects in uninstrumented teeth could be attributed to the forces at play during extraction, excessive occlusal functional loads, tooth age[39] or dentin dehydration[16]. The authors decided to reduce this methodological bias by carefully selecting the specimens, and storing them in 0.1% thymol, as part of our methodology. This resulted in a low percentage of pre-existing microcracks. The majority of microcracks were observed from the external root surface extending to the root canal, corroborating a previous study[9]. In the current study, the preoperative volume of root canals was considered in selecting the sample. The HF-EDM group presented a higher percentage of microcracks than the PDL group. Micro-CT analysis allows visualization of preexisting and post-operative microcracks, thereby allowing each specimen to act as its own control[40]. However, the greater presence of preexisting microcracks may have induced a greater formation of microcracks during the preparation by HF-EDM. Therefore, within the limitations of this *ex vivo* study, it can be concluded that the voxel size should be considered as a potential factor for detecting microcracks when assessing micro-CT images. Further studies are needed to evaluate detection in lower micro-CT voxel size scans.

Conclusions

As expected, the results showed that different resolutions influenced the micro-CT analysis of microcracks. The highest accuracy in detecting microcracks was observed for analyses performed at 5 μm voxel size. HyFlex EDM caused even more microcracks to develop in the middle third, detectable only by visualization of images made at 5 μm voxel size.

Acknowledgments

This study was supported by the Coordenação de Aperfeiçoamento de Pessoal de Nível Superior, Brasil (CAPES) Funding Code 001, and São Paulo Research Foundation – FAPESP [grant numbers 2017/19049-0, 2018/19665-6-0 and 2019/22885-0].

Conflict of interest: The authors declare that they have no conflict of interest.

References

1. Schafer E, Burklein S. Impact of nickel-titanium instrumentation of the root canal on clinical outcomes: a focused review. Odontology. 2012 Jul;100(2):130-6. https://doi.org/10.1007/s10266-012-0066-1

2. Gavini G, Santos MD, Caldeira CL, Machado MEL, Freire LG, Iglecias EF, et al. Nickel-titanium instruments in endodontics: a concise review of the state of the art. Braz Oral Res. 2018 Oct;32(suppl 1):e67. https://doi.org/10.1590/1807-3107bor-2018.vol32.0067

3. Adorno CG, Yoshioka T, Suda H. Crack initiation on the apical root surface caused by three different nickel-titanium rotary files at different working lengths. J Endod. 2011 Apr;37(4):522-5. https://doi.org/10.1016/j.joen.2010.12.002

4. Kfir A, Elkes D, Pawar A, Weissman A, Tsesis I. Incidence of microcracks in maxillary first premolars after instrumentation with three different mechanized file systems: a comparative ex vivo study. Clin Oral Investig. 2017 Jan;21(1):405-11. https://doi.org/10.1007/s00784-016-1806-3

5. Kesim B, Sagsen B, Aslan T. Evaluation of dentinal defects during root canal preparation using thermomechanically processed nickel-titanium files. Eur J Dent. 2017 2017 Apr-Jun;11(2):157-61. https://doi.org/10.4103/ejd.ejd_254_16

6. Ustun Y, Aslan T, Sagsen B, Kesim B. The effects of different nickel-titanium instruments on dentinal microcrack formations during root canal preparation. Eur J Dent. 2015 2015 Jan-Mar;9(1):41-6. https://doi.org/10.4103/1305-7456.149638

7. Elashiry MM, Saber SE, Elashry SH. Comparison of Shaping Ability of Different Single-File Systems Using Microcomputed Tomography. Eur J Dent. 2020 Jan; https://doi.org/10.1055/s-0040-1701393.

8. Sousa-Neto MD, Silva-Sousa YC, Mazzi-Chaves JF, Carvalho KKT, Barbosa AFS, Versiani MA, et al. Root canal preparation using micro-computed tomography analysis: a literature review. Braz Oral Res. 2018 Oct;32(suppl 1):e66. https://doi.org/10.1590/1807-3107bor-2018.vol32.0066
9. Aksoy C, Keris EY, Yaman SD, Ocak M, Geneci F, Celik HH. Evaluation of XP-endo Shaper, Reciproc Blue, and ProTaper Universal NiTi Systems on Dentinal Microcrack Formation Using Micro-Computed Tomography. J Endod. 2019 Mar;45(3):338-42. https://doi.org/10.1016/j.joen.2018.12.005
10. Wilcox LR, Roskelley C, Sutton T. The relationship of root canal enlargement to finger-spreader induced vertical root fracture. J Endod. 1997 Aug;23(8):533-4. https://doi.org/10.1016/S0099-2399(97)80316-0
11. Lertchirakarn V, Palamara JE, Messer HH. Patterns of vertical root fracture: factors affecting stress distribution in the root canal. J Endod. 2003 Aug;29(8):523-8. https://doi.org/10.1097/00004770-200308000-00008
12. Ceyhanli KT, Erdilek N, Tatar I, Celik D. Comparison of ProTaper, RaCe and Safesider instruments in the induction of dentinal microcracks: a micro-CT study. Int Endod J. 2016 Jul;49(7):684-9. https://doi.org/10.1111/iej.12497
13. Mandava J, Yelisela RK, Arikatla SK, Ravi RC. Micro-computed tomographic evaluation of dentinal defects after root canal preparation with hyflex edm and vortex blue rotary systems. J Clin Exp Dent. 2018 Sep;10(9):e844-e51. https://doi.org/10.4317/jced.54853
14. Ugur Aydin Z, Keskin NB, Ozyurek T. Effect of Reciproc blue, XP-endo shaper, and WaveOne gold instruments on dentinal microcrack formation: A micro-computed tomographic evaluation. Microsc Res Tech. 2019 Jun;82(6):856-60. https://doi.org/10.1002/jemt.23227
15. De-Deus G, Belladonna FG, Souza EM, Silva EJ, Neves Ade A, Alves H, et al. Micro-computed Tomographic Assessment on the Effect of ProTaper Next and Twisted File Adaptive Systems on Dentinal Cracks. J Endod. 2015 Jul;41(7):1116-9. https://doi.org/10.1016/j.joen.2015.02.012
16. De-Deus G, Cesar de Azevedo Carvalhal J, Belladonna FG, Silva E, Lopes RT, Moreira Filho RE, et al. Dentinal Microcrack Development after Canal Preparation: A Longitudinal in Situ Micro-computed Tomography Study Using a Cadaver Model. J Endod. 2017 Sep;43(9):1553-8. https://doi.org/10.1016/j.joen.2017.04.027

17. Stringheta CP, Pelegrine RA, Kato AS, Freire LG, Iglecias EF, Gavini G, et al. Micro-computed Tomography versus the Cross-sectioning Method to Evaluate Dentin Defects Induced by Different Mechanized Instrumentation Techniques. J Endod. 2017 Dec;43(12):2102-7. https://doi.org/10.1016/j.joen.2017.07.015

18. Bayram HM, Bayram E, Ocak M, Uzuner MB, Geneci F, Celik HH. Micro-computed Tomographic Evaluation of Dentinal Microcrack Formation after Using New Heat-treated Nickel-titanium Systems. J Endod. 2017 Oct;43(10):1736-9. https://doi.org/10.1016/j.joen.2017.05.024

19. Pinheiro SR, Alcalde MP, Vivacqua-Gomes N, Bramante CM, Vivan RR, Duarte MAH, et al. Evaluation of apical transportation and centring ability of five thermally treated NiTi rotary systems. Int Endod J. 2018 Jun;51(6):705-13. https://doi.org/10.1111/iej.12881

20. de Menezes S, Batista SM, Lira JOP, de Melo Monteiro GQ. Cyclic Fatigue Resistance of WaveOne Gold, ProDesign R and ProDesign Logic Files in Curved Canals In Vitro. Iran Endod J. 2017 Fall;12(4):468-73. https://doi.org/10.22037/iej.v12i4.17494

21. Pedulla E, Genovesi F, Rapisarda S, La Rosa GR, Grande NM, Plotino G, et al. Effects of 6 Single-File Systems on Dentinal Crack Formation. J Endod. 2017 Mar;43(3):456-61. https://doi.org/10.1016/j.joen.2016.10.038

22. Rödig T, Krämer J, Müller C, Wiegand A, Haupt F, Rizk M. Incidence of microcracks after preparation of straight and curved root canals with three different NiTi instrumentation techniques assessed by micro-CT. Aust Endod J. 2019 Dec;45(3):394-9. https://doi.org/10.1111/aej.12339

23. Vertucci FJ. Root canal anatomy of the human permanent teeth. Oral Surg Oral Med Oral Pathol. 1984 Nov;58(5):589-99. https://doi.org/10.1016/0030-4220(84)90085-9

24. Schneider SW. A comparison of canal preparations in straight and curved root canals. Oral Surg Oral Med Oral Pathol. 1971 Aug;32(2):271-5. https://doi.org/10.1016/0030-4220(71)90230-1

25. Pruett JP, Clement DJ, Carnes DL, Jr. Cyclic fatigue testing of nickel-titanium endodontic instruments. J Endod. 1997 Feb;23(2):77-85. https://doi.org/10.1016/S0099-2399(97)80250-6

26. Isaksson H, Töyräs J, Hakulinen M, Aula AS, Tamminen I, Julkunen P, et al. Structural parameters of normal and osteoporotic human trabecular bone are

affected differently by microCT image resolution. Osteoporos Int. 2011 Jan;22(1):167-77. https://doi.org/10.1007/s00198-010-1219-0

27. Yoldas O, Yilmaz S, Atakan G, Kuden C, Kasan Z. Dentinal microcrack formation during root canal preparations by different NiTi rotary instruments and the self-adjusting file. J Endod. 2012 Feb;38(2):232-5. https://doi.org/10.1016/j.joen.2011.10.011

28. Bragatto FP, Iwaki Filho L, Kasuya AV, Chicarelli M, Queiroz AF, Takeshita WM, et al. Accuracy in the diagnosis of vertical root fractures, external root resorptions, and root perforations using cone-beam computed tomography with different voxel sizes of acquisition. J Conserv Dent. 2016 Nov-Dec;19(6):573-7. https://doi.org/10.4103/0972-0707.194029

29. Guo XL, Li G, Zheng JQ, Ma RH, Liu FC, Yuan FS, et al. Accuracy of detecting vertical root fractures in non-root filled teeth using cone beam computed tomography: effect of voxel size and fracture width. Int Endod J. 2019 Jun;52(6):887-98. https://doi.org/10.1111/iej.13076

30. Christiansen BA. Effect of micro-computed tomography voxel size and segmentation method on trabecular bone microstructure measures in mice. Bone Rep. 2016 Dec;5:136-40. https://doi.org/10.1016/j.bonr.2016.05.006

31. Sode M, Burghardt AJ, Nissenson RA, Majumdar S. Resolution dependence of the non-metric trabecular structure indices. Bone. 2008 Apr;42(4):728-36. https://doi.org/10.1016/j.bone.2007.12.004

32. Orhan K, Jacobs R, Celikten B, Huang Y, de Faria Vasconcelos K, Nicolielo LFP, et al. Evaluation of Threshold Values for Root Canal Filling Voids in Micro-CT and Nano-CT Images. Scanning. 2018 2018:9437569. https://doi.org/10.1155/2018/9437569

33. Kim HC, Hwang YJ, Jung DW, You SY, Lee W. Micro-computed tomography and scanning electron microscopy comparisons of two nickel-titanium rotary root canal instruments used with reciprocating motion. Scanning. 2013 2013 Mar-Apr;35(2):112-8. https://doi.org/10.1002/sca.21039

34. Versluis A, Kim HC, Lee W, Kim BM, Lee CJ. Flexural stiffness and stresses in nickel-titanium rotary files for various pitch and cross-sectional geometries. J Endod. 2012 Oct;38(10):1399-403. https://doi.org/10.1016/j.joen.2012.06.008

35. Van Calster B, Steyerberg EW, Collins GS, Smits T. Consequences of relying on statistical significance: Some illustrations. Eur J Clin Invest. 2018 May;48(5):e12912. https://doi.org/10.1111/eci.12912

36. Pirani C, Iacono F, Generali L, Sassatelli P, Nucci C, Lusvarghi L, et al. HyFlex EDM: superficial features, metallurgical analysis and fatigue resistance of innovative electro discharge machined NiTi rotary instruments. Int Endod J. 2016 May;49(5):483-93. https://doi.org/10.1111/iej.12470

37. Iacono F, Pirani C, Generali L, Bolelli G, Sassatelli P, Lusvarghi L, et al. Structural analysis of HyFlex EDM instruments. Int Endod J. 2017 Mar;50(3):303-13. https://doi.org/10.1111/iej.12620

38. Gundogar M, Ozyurek T. Cyclic Fatigue Resistance of OneShape, HyFlex EDM, WaveOne Gold, and Reciproc Blue Nickel-titanium Instruments. J Endod. 2017 Jul;43(7):1192-6. https://doi.org/10.1016/j.joen.2017.03.009

39. PradeepKumar AR, Shemesh H, Chang JW, Bhowmik A, Sibi S, Gopikrishna V, et al. Preexisting Dentinal Microcracks in Nonendodontically Treated Teeth: An Ex Vivo Micro-computed Tomographic Analysis. J Endod. 2017 Jun;43(6):896-900. https://doi.org/10.1016/j.joen.2017.01.026

40. Capar ID, Gok T, Uysal B, Keles A. Comparison of microcomputed tomography, cone beam tomography, stereomicroscopy, and scanning electron microscopy techniques for detection of microcracks on root dentin and effect of different apical sizes on microcrack formation. Microsc Res Tech. 2019 Jul 16; https://doi.org/10.1002/jemt.23341

3.3 Publicação 3*

Influence of voxel size on micro-CT analysis of debris after root canal preparation

Abstract

The aim of this study was to assess the influence of micro-computed tomography (micro-CT) voxel size on the evaluation of debris accumulation after passive ultrasonic irrigation (PUI) in curved root canals prepared with rotary nickel-titanium files. Mesial root canals (n=24) of mandibular molars with curvature between 25° and 35° were prepared using ProDesign Logic 30/.05 (PDL) or HyFlex EDM 25/.08 (HEDM). PUI was performed after root canal preparation of all root canals. The specimens were scanned using high-resolution (5μm voxel size) micro-CT imaging before and after experimental procedures. The percentage of debris was analyzed in the middle and apical thirds using images with 5, 10 and 20μm voxel sizes. Data were compared using unpaired and paired Student's t-test, ANOVA and Tukey's statistical tests ($\alpha=0.05$). There were no differences among the debris analyses performed at different voxel sizes (5, 10 and 20μm) ($p>0.05$). The percentage of debris was similar between the root canals prepared by PDL and HEDM before and after PUI ($p>0.05$). In both groups, the percentage of debris decreased in the middle third after PUI ($p<0.05$). Within the limitations of this *ex vivo* study, it can be concluded that the voxel sizes evaluated did not have a significant impact on the analysis of accumulated debris. However, the results showed a tendency for detection of more debris in the analysis performed using a lower voxel size. PUI decreased the debris accumulation in the middle third of curved root canals.

Keywords: Root canal preparation; Dental pulp cavity; Instrumentation; X-Ray microtomography; Ultrasonic therapy

---

* Artigo publicado no periódico *Brazilian Oral Research.*
(https://doi.org/10.1590/1807-3107bor-2021.vol35.0008).

Introduction

The aim of root canal treatment is to prevent apical periodontitis, by eliminating microorganisms from the root canal system.[1] However, hard tissue debris is deposited on root canal walls after root canal preparation.[2] The presence of debris in the root canal makes disinfection difficult,[2,3] and decreases sealer adhesion to dentinal tubules.[4] Paqué et al.[2] developed a method to view and analyze accumulated hard tissue debris in root canals using micro-computed tomography (micro-CT). Since then, micro-CT imaging has been used to evaluate debris accumulation.[5-9]

However, micro-CT analysis can be influenced by many factors, such as different scan settings, image resolutions and ring artifacts.[10] Different micro-CT acquisition resolutions are used to analyze debris accumulation, using scanning voxel sizes of 9 µm[5, 7], 14 µm[8,11], 18µm[6,12], and up to 20 µm.[2] The different means of image acquisition and image evaluation make it difficult to discuss results and compare different studies.[10] A smaller voxel size is ideal for micro-CT analysis,[13] however, high-resolution scans require longer acquisition time, and generate large data sets.

New mechanized heat-treated nickel and titanium (NiTi) instruments have been proposed especially for centralized preparation in curved root canals.[5,14] ProDesign Logic (PDL) (Easy Equipamentos Odontológicos, Belo Horizonte, MG, Brazil) manufactures NiTi instruments submitted to a heat treatment and featuring a controlled memory (CM), with improved flexural resistance.[15] Hyflex EDM – HEDM (Coltène/Whaledent, Allstätten, Switzerland) also makes heat-treated CM instruments, and offers a surface treatment, called electro-discharge machining (EDM).[16] This manufacturing process improves the mechanical properties of HEDM files.[17] These files maintain their integrity after multiple uses, and are associated with high resistance to cyclic fatigue. [18]

However, previous studies have observed large amounts of accumulated debris in root canals after preparation with mechanized NiTi instruments.[4,5,7] Final irrigation protocols, such as passive ultrasonic irrigation (PUI), have been proposed to improve the cleaning of root canals.[4,7] Irrisonic (Helse Ultrasonic, Santa Rosa de Viterbo, SP, Brazil) is an ultrasonic tip indicated for performing PUI. It is made of stainless steel with a size 20/.01 file.[19] Ultrasonic activation with Irrisonic promoted greater reduction in microbial load within root canals.[20]

To the best of our knowledge, no studies have been performed to date that evaluate the influence of voxel size on the analysis of debris accumulation after root canal preparation. Therefore, the aim of this study was to assess the influence of voxel size in micro-CT evaluation of debris accumulation after PUI application in curved root canals prepared with PDL or HEDM. The first null hypothesis was that there would be no differences among the analyses performed at different voxel sizes (5, 10 and 20 µm). The second null hypothesis was that PUI would not promote a decrease in the percentage of debris after preparation with PDL or HEDM.

Materials and methods

All the procedures were approved by the ethics committee (CEP no. 64736116.4.0000.5416). Human mandibular first and second molars previously stored in 0.1% thymol solution at 5°C were used. The inclusion criteria consisted of the configuration of two independent mesial root canals according to the Vertucci type IV classification,[21] angle of curvature between 25° and 35°, in accordance with the Schneider method,[22] and radius of curvature smaller than 10 mm, following the Pruett method,[23] in addition to complete apical formation, and absence of root fractures, calcifications or internal resorptions. These criteria were confirmed by radiographing the specimens using a digital system (RVG 6100; Kodak Dental Systems, NY) and a micro-CT device (SkyScan 1276; Bruker-microCT, Kontich, Belgium). The first scanning was performed at low-resolution (35-µm voxel size) under the following settings: copper and aluminum filters, 87-millisecond exposure time, frame averaging of 3, 180° rotation around the vertical axis, rotational step of 0.5° at 80 kV and 300 µA.

A total of twelve roots were selected, totaling twenty-four root canals, including the mesiobuccal and mesiolingual canals of each root. The root canals were randomly divided into two experimental groups (n = 12), using stratified random sampling, considering the preoperative root canal volume. Six mesiobuccal canals and six mesiolingual canals were used in each group. The root length was standardized at 18 mm, with a tolerance of ±1 mm of discrepancy. The specimens were embedded in condensation silicone (Oranwash, Zhermack, Badia Polesine, Italy) to simulate the periodontal ligament.

Root Canal Preparation

Conventional access cavities were performed, and the root canals were explored with a size #10 K-file (Dentsply Sirona Endodontics, Ballaigues, Switzerland) up to the apical foramen. The working length (WL) was established 1 mm short of the apical foramen, and confirmed by a digital radiograph. Afterwards, a trained operator instrumented all the specimens with an operating microscope (MC-M1232, DF Vasconcellos, Valença, RJ, Brazil) at 13X magnification, using an endodontic motor (VDW Silver, VDW, Munich, Germany).

PDL Group: Instrumentation with PDL. The 30/.01 file was used in continuous rotation at 350 rpm speed and 1 Ncm torque, using in-and-out movements up to the working length. Then, the 30/.05 file was used at 600 rpm speed and 4 Ncm torque.

HEDM Group: Instrumentation with HEDM. The 10/.05 file was used in continuous rotation at 300 rpm speed and 1.8 Ncm torque, using in-and-out movements up to the working length. Then, the HEDM 25/.08 file was used at 500 rpm speed and 2.5 Ncm torque.

Root canal irrigation was performed with 5 mL of 2.5% sodium hypochlorite (NaOCl), using a 30G side-vented needle (NaviTip, Ultradent Products, South Jordan, UT) adapted to a 5 mL syringe (Ultradent Products) placed 2 mm short of the working length.

Passive Ultrasonic Irrigation (PUI)

The Irrisonic ultrasonic tip was activated in an Ultrawave XS ultrasonic device (Ultradent, South Jordan, USA) using a power of 10% and frequency of 50 Hz, according to the manufacturer's recommendation. The ultrasonic tips were positioned 2 mm short of the working length and used in in-and-out movements to avoid contact with the root canal walls. The irrigant solution was delivered into the root canals, and the ultrasonic activation was performed using three cycles of 20 seconds each, with 2.5% NaOCl in the first and third cycles, and 17% EDTA in the second cycle. A 2-mL aliquot of irrigation solution was used in each cycle, totalizing 4 mL of NaOCl and 2 mL of EDTA. The final irrigation used 5 mL of distilled water.

Micro-CT analysis

The specimens were scanned at high-resolution (5-µm voxel size) before and after instrumentation, and after PUI application, under the following settings: copper filter, 180° rotation around the vertical axis and rotational step of 0.2° at 100 kV and 100 µA. The images were reconstructed using NRecon software (V1.6.10.4; Bruker, Belgium), and superimposed by geometric alignment using DataViewer software (V.1.5.1, Bruker, Belgium). Representative images were performed with models obtained from CTVol software (v.2.3.1.0; Bruker-microCT). The quantitative analysis was performed using CTAn software (V.1.14.4, Bruker, Belgium). Original images were resized isotropically to perform comparative analyses among the different voxel sizes. Images at 10 and 20 µm were obtained and used for quantitative analysis. This was achieved by resizing the previously scanned 5-µm images by 2 and 4, respectively, using CTAn software, when loading the dataset previously superimposed in DataViewer software.[24]

The analyses were performed in the middle and apical thirds of the roots, considering 3 mm for each third. Preoperative volume, volume of the prepared canal, and volume of debris after preparation were obtained. Based on these values, the percentage of debris (% Debris) was calculated using the following formula:

$$\% \text{ Debris} = \frac{\text{Volume of debris x 100}}{\text{Volume of prepared canal}}$$

Statistical analysis

The data obtained were submitted to the Shapiro-Wilks normality test, and all the data presented normal distribution. Regarding the analyses between the groups, the no-paired t-test was used, and regarding debris quantification before and after PUI application, the paired t-test was applied. As for the analysis among images with different voxel size, ANOVA and Tukey’s tests were performed. The level of significance was set at $p < 0.05$.

Results

There were no differences among the debris analyses performed at different voxel sizes (5, 10 and 20 μm) ($p > 0.05$). The percentage of debris was similar between the two root canals prepared with PDL and the two prepared with HEDM before and after PUI application ($p > 0.05$). In both groups, the percentage of debris decreased after PUI activation in the middle third ($p < 0.05$) (Table 1). Figure 3 shows 3D models representing debris accumulation in root canals after preparation with PDL and with HEDM, before and after PUI application.

Table 1 - Means and standard deviations of percentage of debris analyzed at different voxel sizes in curved root canals prepared with ProDesign Logic 30/.05 (PDL) and HyFlex EDM 25/.08 (HEDM) before and after passive ultrasonic irrigation (PUI)

		5 μm		**10 μm**		**20 μm**	
		Before PUI	**After PUI**	**Before PUI**	**After PUI**	**Before PUI**	**After PUI**
PDL	**Middle**	3.08 ± 2.27^a	0.91 ± 0.33^b	$2.62\pm1{,}65^a$	0.84 ± 0.32^b	2.24 ± 1.47^a	0.79 ± 0.34^b
	Apical	5.07 ± 2.53^a	2.68 ± 1.23^a	4.64 ± 2.28^a	2.55 ± 1.21^a	4.39 ± 2.56^a	2.38 ± 1.17^a
HEDM	**Middle**	3.65 ± 2.03^a	1.44 ± 0.88^b	3.43 ± 0.09^a	1.32 ± 1.68^b	2.79 ± 2.32^a	1.05 ± 0.54^b
	Apical	5.77 ± 2.94^a	3.98 ± 0.98^a	5.77 ± 3.03^a	3.67 ± 0.84^a	5.25 ± 2.96^a	3.37 ± 0.91^a

Different superscript lowercase letters on the same line indicate significant differences detected among the percentages of debris before and after using PUI ($p < 0.05$).

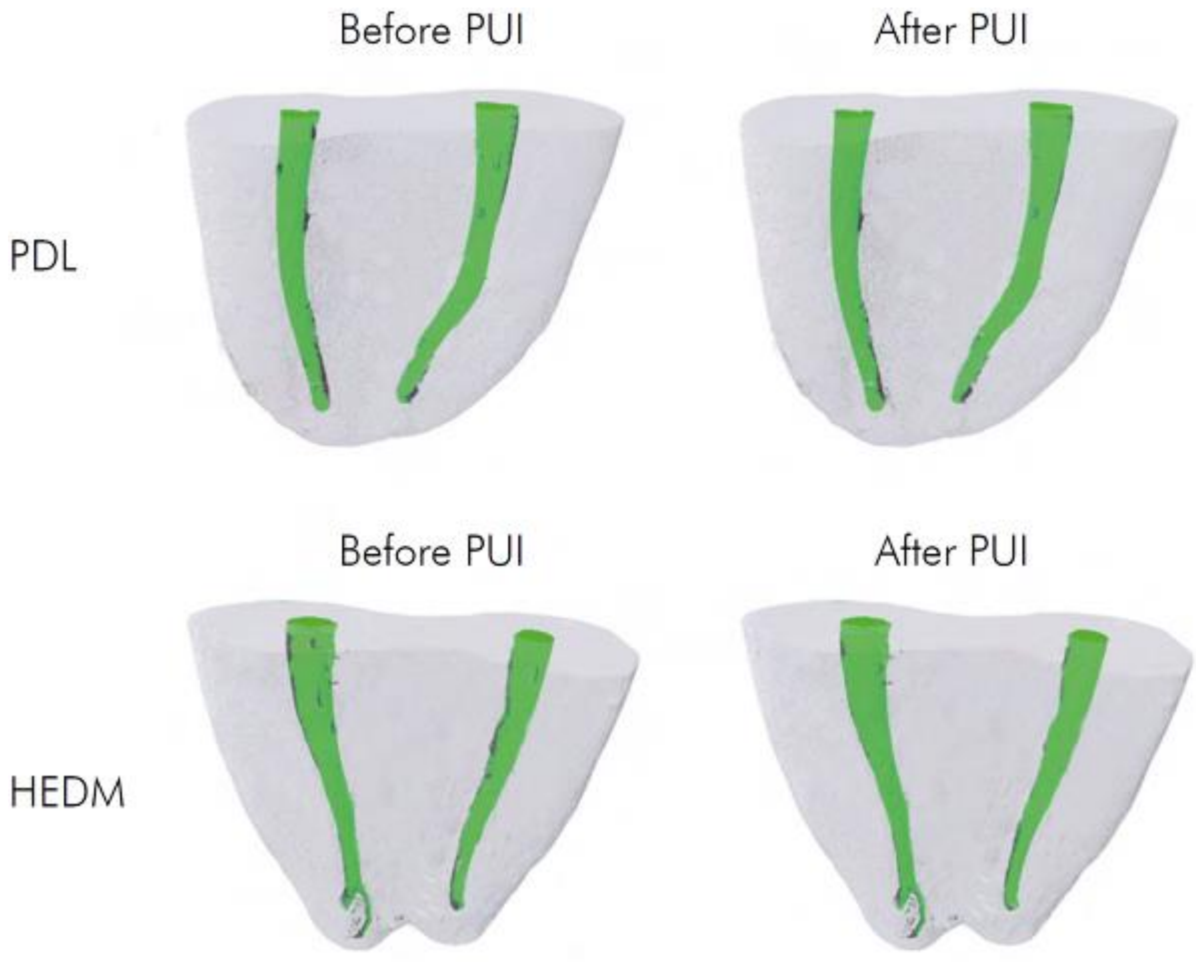

Figure 1 - 3D reconstructions of images with 5-µm voxel size of middle and apical thirds of mesial roots of mandibular molars prepared by ProDesign Logic and HyFlex EDM before and after PUI, showing debris accumulation in black

Discussion

Accumulation of debris after root canal preparation can impair disinfection of the root canal system.[25] Micro-CT has been used in recent studies to evaluate debris accumulation, owing to its high accuracy and high spatial resolution.[2,5-8] The first null hypothesis was accepted, because similar results were observed for root debris, using different voxel size analyses.

The voxel size can affect the quality of the images, and consequently that of the analyses performed.[10,26] Previous studies have observed that the analysis of trabecular bone structure[13,24,27,28] and voids in filled root canals[29] is significantly affected by micro-CT scanning voxel size. However, larger voxels do not always mean lower diagnostic accuracy.[30,31] Studies that have evaluated the influence of voxel size in diagnoses using cone beam computed tomography images of root fracture are conflicting.[31-33] Whereas a previous investigation showed significantly higher detection of vertical root fractures in images with smaller voxel size,[32] Özer et al.[33] reported that there were no significant differences in the diagnostic accuracy of root fracture among cone beam computed tomography images captured with different voxel sizes.

Higher scan resolution is a favorable feature in performing micro-CT analysis. However, scans with higher voxel size can be obtained faster and generate smaller data sets.[13] Voxel size was the only variable evaluated in the present study, as done in previous methodological models.[24,27,28] The samples were scanned at 5 µm and the reconstructed images were resized by 2 and 4 to acquire images with 10 and 20 µm voxel sizes.[24] The new values produced for the images resized to larger voxel sizes represent the average of previous voxels, leading to a decrease in the accuracy of the image.[24,27] Although this method could be considered a limitation of the current study, it actually allowed accurate comparisons among the same regions of interest[24]. In brief, by decreasing the voxel size with the software, we could save the time required to run a new micro-CT scan. Moreover, the smaller voxel size used during the scanning procedure may be considered the gold standard to determine the level of accuracy under limited resolution scenarios[27,28]. However, although the voxel size may have significant effects on the results,[13,29,34] it is not the only factor influencing spatial resolution of the micro-CT image.[10,27] The spatial resolution also depends on mean absorption of the sample, detector noise, reconstruction algorithm, X-ray focal spot size and shape, detector aperture, and scanner geometry.[10] Within the limitations of the present study, our findings suggest that a 20-µm voxel size may be used for debris evaluation, thus representing a cost reduction factor for further research.

Although the analyses of the different voxel sizes did not produce significative differences in the results, there was a tendency to have a higher percentage of debris in analyses performed at a smaller voxel size than those performed at a larger voxel size. Considering that the statistical significance is dependent on the sample variance,[35] the larger standard deviation of the results may have contributed to the statistical similarities among the analyses performed at different voxel sizes. Several studies that have evaluated debris accumulations by micro-CT have also shown a large standard deviation[2,4,7,8,11,12] or non-normal distribution of data.[5,6] Even using methods that improve the sample selection criteria, such as micro-CT analyses for tooth selection and sample randomization,[5] it is difficult to standardize the debris accumulated in each root canal after its preparation.

PUI is an irrigation protocol that uses acoustic energy-promoting hydrodynamic agitation of the liquid.[36] The reduction in root canal debris after performing PUI has been reported by several studies.[4,7,11,37] As expected, in the present study, PUI decreased the percentage of debris in the middle third after preparation with PDL and HEDM. However, PUI did not reduce the percentage of debris in the apical third. In the present investigation, Irrisonic was inserted up to 2 mm short of the WL,[4,7,11] and promoted a limited effect on the apical third of the root canal. In addition, the largest width of the cervical root canal allows it to be cleaned more effectively,[38] leading to better circulation and effect of the irrigating solution.[39,40] Moreover, a previous study showed that activation of the irrigating solution using PUI promoted less effective debris removal in the apical third than a reciprocating system for final irrigation.[38]

Conclusions

Within the limitations of the present study, it can be concluded that the voxel sizes evaluated did not have a significant impact on the analysis of accumulated debris. However, the results showed a tendency of more debris detection in analyses performed at a lower voxel size. PUI reduced the debris accumulation in the middle third of curved root canals.

Acknowledgments

This study was supported in part by the Coordenação de Aperfeiçoamento de Pessoal de Nível Superior, Brasil (CAPES), Funding Code 001, and was fully supported by the São Paulo Research Foundation – FAPESP [grant numbers 2017/19049-0 and 2018/19665-6 -0].

Conflict of interest: The authors declare that they have no conflict of interest.

References

1. Azim AA, Griggs JA, Huang GT. The Tennessee study: factors affecting treatment outcome and healing time following nonsurgical root canal treatment. Int Endod J. 2016 Jan;49(1):6-16. https://doi.org/10.1111/iej.12429

2. Paqué F, Laib A, Gautschi H, Zehnder M. Hard-tissue debris accumulation analysis by high-resolution computed tomography scans. J Endod. 2009 Jul;35(7):1044-7. https://doi.org/10.1016/j.joen.2009.04.026

3. Siqueira JF, Pérez AR, Marceliano-Alves MF, Provenzano JC, Silva SG, Pires FR, et al. What happens to unprepared root canal walls: a correlative analysis using micro-computed tomography and histology/scanning electron microscopy. Int Endod J. 2018 May;51(5):501-8. https://doi.org/10.1111/iej.12753

4. Freire LG, Iglecias EF, Cunha RS, Dos Santos M, Gavini G. Micro-Computed Tomographic Evaluation of Hard Tissue Debris Removal after Different Irrigation Methods and Its Influence on the Filling of Curved Canals. J Endod. 2015 Oct;41(10):1660-6. https://doi.org/10.1016/j.joen.2015.05.001

5. Pinto JC, Pivoto-Joao MMB, Espir CG, Ramos MLG, Guerreiro-Tanomaru JM, Tanomaru-Filho M. Micro-CT evaluation of apical enlargement of molar root canals using rotary or reciprocating heat-treated NiTi instruments. J Appl Oral Sci. 2019 Aug 12;27:e20180689. https://doi.org/10.1590/1678-7757-2018-0689

6. Espir CG, Nascimento-Mendes CA, Guerreiro-Tanomaru JM, Freire LG, Gavini G, Tanomaru-Filho M. Counterclockwise or clockwise reciprocating motion for oval root canal preparation: a micro-CT analysis. Int Endod J. 2018 May;51(5):541-8. https://doi.org/10.1111/iej.12776

7. Leoni GB, Versiani MA, Silva-Sousa YT, Bruniera JF, Pécora JD, Sousa-Neto MD. Ex vivo evaluation of four final irrigation protocols on the removal of hard-tissue debris from the mesial root canal system of mandibular first molars. Int Endod J. 2017 Apr;50(4):398-406. https://doi.org/10.1111/iej.12630

8. De-Deus G, Marins J, Silva EJ, Souza E, Belladonna FG, Reis C, et al. Accumulated hard tissue debris produced during reciprocating and rotary nickel-titanium canal preparation. J Endod. 2015 May;41(5):676-81. https://doi.org/10.1016/j.joen.2014.11.028

9. Sousa-Neto MD, Silva-Sousa YC, Mazzi-Chaves JF, Carvalho KKT, Barbosa AFS, Versiani MA, et al. Root canal preparation using micro-computed tomography analysis: a literature review. Braz Oral Res. 2018 Oct;32(suppl 1):e66. https://doi.org/10.1590/1807-3107bor-2018.vol32.0066

10. Bouxsein ML, Boyd SK, Christiansen BA, Guldberg RE, Jepsen KJ, Muller R. Guidelines for assessment of bone microstructure in rodents using micro-computed tomography. J Bone Miner Res. 2010 Jul;25(7):1468-86. https://doi.org/10.1002/jbmr.141

11. De-Deus G, Belladonna FG, de Siqueira Zuolo A, Perez R, Carvalho MS, Souza EM, et al. Micro-CT comparison of XP-endo Finisher and passive ultrasonic irrigation as final irrigation protocols on the removal of accumulated hard-tissue debris from oval shaped-canals. Clin Oral Investig. 2019 Jul;23(7):3087-93. https://doi.org/10.1007/s00784-018-2729-y

12. Espir CG, Nascimento-Mendes CA, Guerreiro-Tanomaru JM, Cavenago BC, Hungaro Duarte MA, Tanomaru-Filho M. Shaping ability of rotary or reciprocating systems for oval root canal preparation: a micro-computed tomography study. Clin Oral Investig. 2018 Dec;22(9):3189-94. https://doi.org/10.1007/s00784-018-2411-4

13. Christiansen BA. Effect of micro-computed tomography voxel size and segmentation method on trabecular bone microstructure measures in mice. Bone Rep. 2016 Dec;5:136-40. https://doi.org/10.1016/j.bonr.2016.05.006

14. Pinheiro SR, Alcalde MP, Vivacqua-Gomes N, Bramante CM, Vivan RR, Duarte MAH, et al. Evaluation of apical transportation and centring ability of five thermally treated NiTi rotary systems. Int Endod J. 2018 Jun;51(6):705-13. https://doi.org/10.1111/iej.12881

15. de Menezes SEAC, Batista SM, Lira JOP, de Melo Monteiro GQ. Cyclic Fatigue Resistance of WaveOne Gold, ProDesign R and ProDesign Logic Files in Curved Canals In Vitro. Iran Endod J. 2017 12(4):468-73. https://doi.org/10.22037/iej.v12i4.17494

16. Pedulla E, Genovesi F, Rapisarda S, La Rosa GR, Grande NM, Plotino G, et al. Effects of 6 Single-File Systems on Dentinal Crack Formation. J Endod. 2017 Mar;43(3):456-61. https://doi.org/10.1016/j.joen.2016.10.038

17. Iacono F, Pirani C, Generali L, Bolelli G, Sassatelli P, Lusvarghi L, et al. Structural analysis of HyFlex EDM instruments. Int Endod J. 2017 Mar;50(3):303-13. https://doi.org/10.1111/iej.12620

18. Pirani C, Iacono F, Generali L, Sassatelli P, Nucci C, Lusvarghi L, et al. HyFlex EDM: superficial features, metallurgical analysis and fatigue resistance of innovative electro discharge machined NiTi rotary instruments. Int Endod J. 2016 May;49(5):483-93. https://doi.org/10.1111/iej.12470

19. Dos Reis S, Cruz VM, Hungaro Duarte MA, da Silveira Bueno CE, Vivan RR, Pelegrine RA, et al. Volumetric Analysis of Irrigant Extrusion in Immature Teeth after Different Final Agitation Techniques. J Endod. 2020 May;46(5):682-7. https://doi.org/10.1016/j.joen.2020.01.014

20. Aveiro E, Chiarelli-Neto VM, de-Jesus-Soares A, Zaia AA, Ferraz CCR, Almeida JFA, et al. Efficacy of reciprocating and ultrasonic activation of 6% sodium hypochlorite in the reduction of microbial content and virulence factors in teeth with primary endodontic infection. Int Endod J. 2020 May;53(5):604-18. https://doi.org/10.1111/iej.13261

21. Vertucci FJ. Root canal anatomy of the human permanent teeth. Oral Surg Oral Med Oral Pathol. 1984 Nov;58(5):589-99. https://doi.org/10.1016/0030-4220(84)90085-9

22. Schneider SW. A comparison of canal preparations in straight and curved root canals. Oral Surg Oral Med Oral Pathol. 1971 Aug;32(2):271-5.

23. Pruett JP, Clement DJ, Carnes DL. Cyclic fatigue testing of nickel-titanium endodontic instruments. J Endod. 1997 Feb;23(2):77-85. https://doi.org/10.1016/S0099-2399(97)80250-6

24. Isaksson H, Töyräs J, Hakulinen M, Aula AS, Tamminen I, Julkunen P, et al. Structural parameters of normal and osteoporotic human trabecular bone are affected differently by microCT image resolution. Osteoporos Int. 2011 Jan;22(1):167-77. https://doi.org/10.1007/s00198-010-1219-0

25. Haapasalo M, Qian W, Portenier I, Waltimo T. Effects of dentin on the antimicrobial properties of endodontic medicaments. J Endod. 2007 Aug;33(8):917-25. https://doi.org/10.1016/j.joen.2007.04.008

26. Dalili Z, Taramsari M, Mousavi Mehr SZ, Salamat F. Diagnostic value of two modes of cone-beam computed tomography in evaluation of simulated external root resorption: an in vitro study. Imaging Sci Dent. 2012 Mar;42(1):19-24. https://doi.org/10.5624/isd.2012.42.1.19

27. Kim DG, Christopherson GT, Dong XN, Fyhrie DP, Yeni YN. The effect of microcomputed tomography scanning and reconstruction voxel size on the accuracy of stereological measurements in human cancellous bone. Bone. 2004 Dec;35(6):1375-82. https://doi.org/10.1016/j.bone.2004.09.007

28. Sode M, Burghardt AJ, Nissenson RA, Majumdar S. Resolution dependence of the non-metric trabecular structure indices. Bone. 2008 Apr;42(4):728-36. https://doi.org/10.1016/j.bone.2007.12.004

29. Orhan K, Jacobs R, Celikten B, Huang Y, de Faria Vasconcelos K, Nicolielo LFP, et al. Evaluation of Threshold Values for Root Canal Filling Voids in Micro-CT and Nano-CT Images. Scanning. 2018 Jul;2018:9437569. https://doi.org/10.1155/2018/9437569

30. Choi JW. Factors affecting modulation transfer function measurements in cone-beam computed tomographic images. Imaging Sci Dent. 2019 Jun;49(2):131-7. https://doi.org/10.5624/isd.2019.49.2.131

31. Güngör E, Doğan MS. Reliability and accuracy of cone-beam computed tomography voxel density and linear distance measurement at different voxel sizes: A study on sheep head cadaver. J Dent Sci. 2017 Jun;12(2):145-50. https://doi.org/10.1016/j.jds.2016.11.004

32. Bragatto FP, Iwaki Filho L, Kasuya AV, Chicarelli M, Queiroz AF, Takeshita WM, et al. Accuracy in the diagnosis of vertical root fractures, external root resorptions, and root perforations using cone-beam computed tomography with different voxel sizes of acquisition. J Conserv Dent. 2016 Nov-Dec;19(6):573-7. https://doi.org/10.4103/0972-0707.194029

33. Özer SY. Detection of vertical root fractures by using cone beam computed tomography with variable voxel sizes in an in vitro model. J Endod. 2011 Jan;37(1):75-9. https://doi.org/10.1016/j.joen.2010.04.021

34. Yamamoto-Silva FP, de Oliveira Siqueira CF, Silva MAGS, Fonseca RB, Santos AA, Estrela C, et al. Influence of voxel size on cone-beam computed tomography-based detection of vertical root fractures in the presence of intracanal metallic posts. Imaging Sci Dent. 2018 Sep;48(3):177-84. https://doi.org/10.5624/isd.2018.48.3.177

35. Van Calster B, Steyerberg EW, Collins GS, Smits T. Consequences of relying on statistical significance: Some illustrations. Eur J Clin Invest. 2018 May;48(5):e12912. https://doi.org/10.1111/eci.12912

36. van der Sluis LW, Versluis M, Wu MK, Wesselink PR. Passive ultrasonic irrigation of the root canal: a review of the literature. Int Endod J. 2007 Jun;40(6):415-26. https://doi.org/10.1111/j.1365-2591.2007.01243.x

37. Bueno CRE, Cury MTS, Vasques AMV, Sarmiento JL, Trizzi JQ, Jacinto RC, et al. Cleaning effectiveness of a nickel-titanium ultrasonic tip in ultrasonically activated irrigation: a SEM study. Braz Oral Res. 2019 Mar;33:e017. https://doi.org/10.1590/1807-3107bor-2019.vol33.0017

38. Kato AS, Cunha RS, da Silveira Bueno CE, Pelegrine RA, Fontana CE, de Martin AS. Investigation of the Efficacy of Passive Ultrasonic Irrigation Versus Irrigation with Reciprocating Activation: An Environmental Scanning Electron Microscopic Study. J Endod. 2016 Apr;42(4):659-63. https://doi.org/10.1016/j.joen.2016.01.016

39. Teixeira CS, Felippe MC, Felippe WT. The effect of application time of EDTA and NaOCl on intracanal smear layer removal: an SEM analysis. Int Endod J. 2005 May;38(5):285-90. https://doi.org/10.1111/j.1365-2591.2005.00930.x

40. Mendonça DH, Colucci V, Rached-Junior FJ, Miranda CE, Silva-Sousa YT, Silva SR. Effects of various irrigation/aspiration protocols on cleaning of flattened root canals. Braz Oral Res. 2015 May;29(1):1-9. https://doi.org/10.1590/1807-3107BOR-2015.vol29.0082

3.4 Publicação 4*

Evaluation of curved root canals filled with a new bioceramic sealer: a micro-computed tomographic study using images with different voxel sizes and segmentation methods

Abstract

The aim of this study was to investigate the filling ability of a new premixed bioceramic sealer in comparison with an epoxy resin-based sealer in curved root canals using different segmentation methods and voxel sizes in micro-CT images. Twelve curved mesial roots of mandibular molars with two separated canals were selected. All root canals were prepared by using HyFlex EDM files size 25/.08 and filled by the single cone technique and Bio-C Sealer or AH Plus (n = 12). The samples were scanned by micro–CT at 5 µm. The images were analyzed at 5, 10 and 20 µm for the volumetric analysis of voids in filling. Visual image segmentation was performed by two examiners, and the automatic segmentation was accomplished for comparison. Radiopacity of the sealers was evaluated by radiographic analysis. Data were submitted to the two-way ANOVA and non-paired t-tests at a significance level of 5%. AH Plus had the highest radiopacity ($p < .05$). Root canals filled with AH Plus or Bio-C had similar low percentage of voids ($p > .05$). There was no difference interobserver, which had similar results to those obtained with automatic segmentation for all voxel sizes evaluated ($p > .05$). Bio-C Sealer had appropriate filling ability. Visual and automatic segmentation can be applied to micro-CT images with voxel sizes from 5 to 20 µm to evaluate the filling of sealers with adequate radiopacity. Automatic segmentation should be used as a faster method.

KEYWORDS

calcium silicate, dental materials, physical properties, root canal filling, x-ray microtomography

---

* Artigo publicado no periódico *Microscopy Research and Technique*. (https://doi.org/10.1002/jemt.23855).

Graphical Abstract

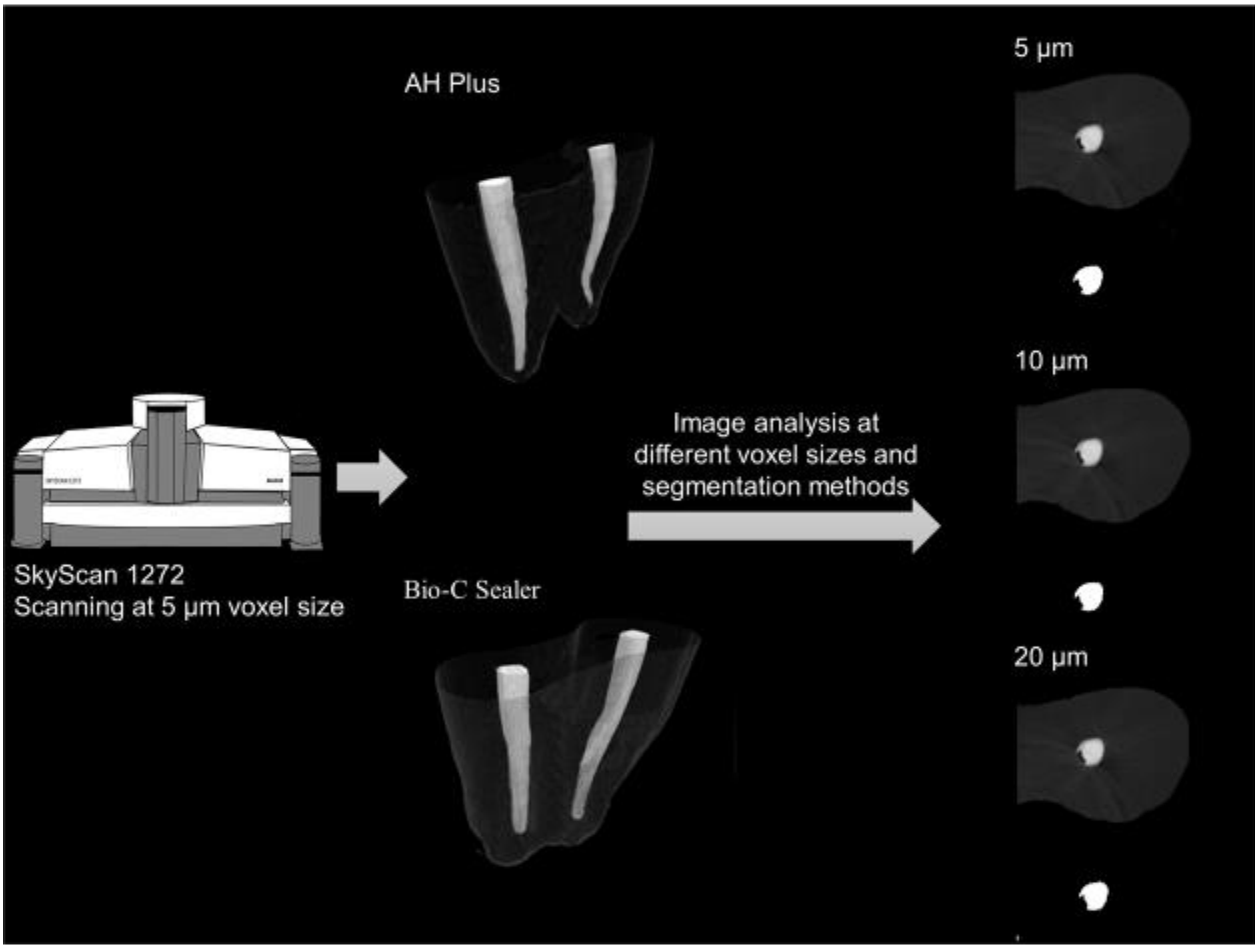

Introduction

Three-dimensional root canal filling may directly impact the endodontic treatment, since the presence of voids within filling can harbor bacteria, causing a negative impact on the long-term tooth prognosis (Aktemur Türker, Uzunoğlu Özyürek, & Tek, 2020; Ricucci, Lin, & Spångberg, 2009). X-ray micro-computed tomography (micro-CT) is a non-destructive method applied to evaluate the root canal filling quality with different materials and techniques, using images with different voxel sizes (Huang et al., 2017; Kierklo, Tabor, Pawińska, & Jaworska, 2015; Pedulla et al., 2020; Viapiana et al., 2016; Wolf, Kupper, Reimann, Bourauel, & Frentzen, 2014). Although micro-CT scanning can be considered as gold standard for measurements in endodontics (Campello et al., 2019; Celikten et al., 2019; de Oliveira et al., 2017), the high density of filling materials may hamper the image analysis (Celikten et al., 2019; Kierklo et al., 2015).

Several root canal sealers are available and their different radiopacity produce distinct artifacts in 3D images (Celikten et al., 2019). AH Plus (DentsplyDeTrey, Konstanz, Germany) is an epoxy resin-based root canal sealer with excellent physicochemical properties, including high flow and radiopacity (Silva Almeida, Moraes, Morgental, & Pappen, 2017). However, AH Plus has no bioactive properties (Viapiana, Guerreiro-Tanomaru, Hungaro-Duarte, Tanomaru-Filho, & Camilleri, 2014). Endodontic sealers based on calcium silicates have been proposed due to their cytocompatibility and mineralization ability (Alves Silva et al., 2020; Sanz et al., 2020). Bio-C Sealer (Angelus, Londrina, PR, Brazil) is a new premixed ready-to-use calcium silicate–based sealer presenting radiopacity and flow in accordance with the ISO 6876 standard (Zordan-Bronzel et al., 2019), as well as biocompatibility and bioactivity (Alves Silva et al., 2020; Sanz et al., 2020). In addition, Bio-C Sealer had similar filling ability to AH Plus in flattened root canals (Tavares et al., 2020). However, up to now, there is no study investigating the filling ability of Bio-C Sealer in curved root canals.

The different approaches to image acquisition and evaluation make difficult the interpretation and comparison of findings across studies using micro-CT (Bouxsein et al., 2010; Torres et al., 2020). The segmentation of micro-CT images may have a significant impact on all assessment (Bouxsein et al., 2010; Moinzadeh, Zerbst, Boutsioukis, Shemesh, & Zaslansky, 2015), and the current literature is divergent about which segmentation method is the most reliable (Christiansen, 2016; Galibourg et al., 2018; Michetti, Basarab, Diemer, & Kouame, 2017; Rovaris et al., 2018). Regardless of the method used, accuracy of the segmentation depends on the image quality (Michetti, Georgelin-Gurgel, Mallet, Diemer, & Boulanouar, 2015), and the voxel size was identified as one of the main factors that can affect the results of studies that evaluated the root canal filling by using micro-CT (Orhan et al., 2018).

No study has assessed the influence of the segmentation method in micro-CT images with different resolutions for root canal filling quality analysis. In addition, investigations are needed to better understand the performance of new calcium silicate-based sealers before their clinical indication (Torres et al., 2020). Therefore, the aim of this study was to investigate the percentage of voids in curved root canals filled with a new bioceramic sealer (Bio-C Sealer), in comparison with the gold standard AH Plus, using micro-CT images with different voxel sizes and methods of segmentation. The radiopacity of the root canal sealers were also evaluated. The first null hypothesis was that there would be no difference between AH Plus and Bio-C Sealer regarding their filling ability in curved root canals. The second null hypothesis was that would be no differences among analyzes performed by different segmentation methods using images with different voxel sizes.

Materials and methods

Specimen selection

In the present study, the sample calculation was performed using a specific software (G * Power 3.1.7 for Windows, Heinrich Heine, Universitat Dusseldorf). The t-test for two independent groups was used, with alpha type error of .05 and beta power of .95. The effect size (1.73) was calculated based on previous study with similar methodology (Oh et al., 2016). Nine specimens per group were indicated as the ideal size required. A sample of 12 root canals per group was used.

All experimental procedures used in this study were approved by the Faculty's Ethics Committee (protocol no. 10411219.9.0000.5416). The selected root canals were stored in a 0.1% thymol solution at 5°C. The sample used consists of human mandibular first and second molars with two independent mesial root canals according type IV Vertucci's classification (Vertucci, 1984), angle of curvature between 25° and 35° in accordance with the Schneider method (Schneider, 1971) and radius of curvature smaller than 10 mm, following the Pruett's method (Pruett, Clement, & Carnes, 1997). All selected roots had complete apical formation, absence of root fractures, calcifications or internal resorptions. The tooth size was standardized at 18 mm, considering the root and crown, with a tolerance of ±1 mm of discrepancy. The samples were measured with a millimeter ruler (Golgran. Sao Caetano do Sul, SP, Brazil) and the lengths were confirmed by radiographic analysis. A digital radiographic system (RVG 6100; Kodak Dental Systems, NY) was used to select teeth according with inclusion criteria. Image J program (National Institutes of Health, Bethesda, MD, USA) was used to assess degree and radius of curvature in the radiographic images. All teeth selected by radiographic exams were scanned using a micro-CT device (SkyScan 1276; Bruker-microCT, Kontich, Belgium) at a low-resolution (35 µm voxel size). Then, the three-dimensional images obtained were used for a more accurate selection, confirming the inclusion criteria. The micro-CT scanning was performed under the following settings: copper and aluminum filters, 87-millisecond exposure time, frame averaging of 3, 180° rotation around the vertical axis, rotational step of 0.5° at 80 kV and 300 µA. A total of twelve roots were selected, totaling twenty-four root canals, including the mesiobuccal and mesiolingual canals of each root. The specimens were embedded in condensation silicone (Oranwash, Zhermack SpA, Badia Polesine, Italy) to simulate the periodontal ligament. The root canal preparation and filling steps were performed by an experienced endodontist.

Root canal preparation

Traditional access cavities were prepared using high speed bur (n.2, KG Sorensen, São Paulo, Brazil) with complete removal of the pulp chamber roof followed by achieving straight-line access to the canal orifices, with smoothly divergent axial walls. The working length was defined at 1 mm short of the apical foramen, by using a type K#10 file (Dentsply, Maillefer, Switzerland). For preparation, HyFlex EDM (HEDM; Coltene/Whaledent, Altstätten, Switzerland) 10/.05 was operated by electric motor VDW SILVER (VDW GmbH, Munich, Germany) in rotary motion at 300 rpm and torque 1.8 Ncm, with in-and-out movements up to the WL. Then, HEDM 25/.08 was used at 500 rpm and torque 2.5 Ncm, as described above. After use of each instrument the patency was maintained using a K#10 file. Each root canal was irrigated with 5 mL of 2.5% sodium hypochlorite (NaOCl). The ultrasonic tip Irrisonic (Helse Ultrasonic, Santa Rosa de Viterbo, SP, Brazil), activated by the ultrasonic device Ultrawave XS (Ultradent, South Jordan, USA), was used to perform passive ultrasonic irrigation (PUI) in all root canals. Following the manufacturer's recommendation, a power of 10% and frequency of 50 Hz were used. Activations was performed with three cycles of 20 seconds, using the following sequence: 2 mL of 2.5% NaOCL, 2 mL of 17% EDTA and 2 mL of 2.5% of NaOC. As final irrigation, 5 mL of distilled water was used. The root canals were dried with absorbent paper points , without causing excessive dryness for Bio-C Sealer Group.

Root canal filling

A stratified random sampling statistical method was used to divide the root canals in two experimental groups, considering the post-preparation volume (n = 12). Before filling, a previous selection of the gutta-percha cones size 25/.08 (Coltene/Whaledent, Langenau, Germany) was performed using a Profilometer (Profile Projector Nikon Model 6C-2, Nikon, Tokyo, Japan) in order to ensure higher standardization of their tip size and taper. Previously to the filling stage, radiographic adaptation proof of the gutta-percha points 1 mm short of the apex was obtained. The sealers were used in accordance with the manufacturer´s instructions and their composition and proportion are described in Table 1. All the root canals were filled using the single-cone technique, as follows:

AH Plus Group: A Lentulo spiral #25 (Dentsply Maillefer) coupled to a low-speed motor (Micromotor N270 and Counter-angle, Dabi-Atlante, Ribeirão Preto, SP, Brazil) and #25 K-file was used to insert sealer in the root canal. Both instruments were used in in-and-out motions in the clockwise directions to insert the sealer into the root canal. Lentulo was used up to the 3 mm short of the WL and K-file up to the WL. This procedure was repeated three times.

Bio-C Sealer Group: A syringe and plastic needles provided by its manufacturer were used to inject the sealer into the root canal at 4 mm of the WL.

For all root canals, the coronal excesses of gutta-percha were cut with a heat plugger (Golgran, São Caetano do Sul, SP, Brazil), and then a light compaction was performed using the same plugger. Digital radiographs were taken to assess the quality of root canal fillings. For this evaluation was considerate the apical limit of obturation and the filling by endodontic sealer. The access cavities were filled with Coltosol (Vigodent, Rio de Janeiro, RJ, Brazil) and stored at 37º C and 95% relative humidity for 1 week to allow the sealers to set completely.

Table 1 - Root canal sealers, their Manufacturer, Composition, and the Proportion Used

Material	Manufacturer	Composition	Proportion
Bio-C Sealer	Angelus, Londrina, PR, Brazil	Calcium silicates, calcium aluminate, calcium oxide, zirconium oxide, iron oxide, silicon dioxide, dispersing agent.	Ready to use
AH Plus	Dentsply DeTrey GmbH, Konstanz, Germany	Bisphenol-A epoxy resin, bisphenol-F epoxy resin, calcium tungstate, zirconium oxide, silica, iron oxide pigments dibenzyldiamine, aminoadamantane, silicone oil.	1 g:1 g (paste/paste)

Micro-CT analysis

All roots were scanned before and after filling using a micro-CT device (SkyScan 1272. Bruker, Kontich, Belgium). For images acquisitions were used de following settings: 5 µm voxel size, energy of 100 kV, intensity of 100 µAP, cooper filter, 180° rotation around the vertical axis and rotational step of 0.2°. NRecon software (V1.6.10.4; Bruker, Belgium) was used for images reconstruction, and DataViewer software (V.1.5.1, Bruker, Belgium) was used to performer the geometric alignment between the images from before and after root canal filling. Representative images (3D models) were obtained in CTVox software (v.3.2; Bruker, Belgium).

For quantitative analysis, images at 5, 10 and 20 µm were segmented using the CTAn software (V.1.14.4, Bruker, Belgium) (Figure 1). For this purpose, the previously scanned 5 µm images were resized by 2 and 4, respectively (Torres et al., 2020). Initially, two independent examiners, with previous experience in micro-CT analysis, segmented the images visually using the adaptive/local method, and recorded the threshold values. Then, the global segmentation was performed through the automatic thresholding plug-in available on CTAn software. The post-preparation volume of the canal and the filling volume were quantified. To obtain the percentage of voids the following formula was used: [Percentage of voids = 100 - (filling material volume x 100 / canal volume)]. The analyzes were accomplished in the apical third of the root canals considering their last 4 mm.

Radiopacity analysis

Six specimens for each group were produced by using stainless steel rings measuring 10 mm in diameter × 1 mm thick and stored at 37º C and 95% relative humidity until setting process. Each sample was positioned on occlusal radiographic films (Insight-Kodak Comp, Rochester, NY) and exposed close to an aluminum scale with variable thickness (from 2–16 mm in 2-mm increments). An X-ray unit (Instrumentarium Dental, Tuusula, Finland) was operated according to the following parameters: 60 kV, 7 mA, 0.32 pulses per second, and a focus-film distance of 33 cm. For the film processing was used a standard automatic processor (Dent-X 9000; Dent-X, Elmsford, NY). After the radiographs digitizing, the images were imported into Image Tool 3.0 software to determine the radiopacity equivalence of the sealers in millimeters of aluminum (mm Al).

Statistical analysis

Statistical analysis was performed using GraphPad Prism 5 (GraphPad Software Inc, La Jolla, CA, USA). Shapiro-Wilk test was used to test the data normality. The comparations between the sealers regarding radiopacity and percentage of voids were performed using non-paired t-test. ANOVA test was used for comparation among different segmentation methods and voxel size. The level of significance was set at 5%.

Results

Both sealers had radiopacity values above than the minimum required by ISO 6876, 3 mm aluminum. However, AH Plus had the highest radiopacity (p < .05). For all voxel sizes evaluated there was no statistically significant difference interobserver in analyzes performed with adaptive thresholding, which had similar results to those obtained with automatic segmentation ($p > .05$). There was no difference in the percentage of voids between root canals filled with AH Plus or Bio-C Sealer in the apical third ($p > .05$). The results are represented in Table 2 and Figure 2. Representative three-dimensional reconstructions of images obtained by micro-CT of root canals filled with AH Plus and Bio-C Sealer can be visualized in Figure 3.

Table 2 - Percentage volume of voids in curved root canals (Mean ± standard deviation) after obturation by using AH Plus and Bio-C Sealer. Different segmentation methods in images with different voxel sizes were compared

	5 μm		**10 μm**		**20 μm**	
	AH Plus	**Bio-C**	**AH Plus**	**Bio-C**	**AH Plus**	**Bio-C**
Visual method: Examiner 1	8.18 ± 1.9	8.72 ± 2.1	7.78 ± 2.6	7.13 ± 2.2	7.25 ± 2.9	7.10 ± 3.0
Visual method: Examiner 2	7.93 ± 1.0	8.06 ± 1.3	8.09 ± 2.4	7.63 ± 2.7	7.14 ± 3.1	7.25 ± 2.1
Global method: Automatic thresholding	7.14 ± 1.0	8.08 ± 1.2	6.91 ± 2.9	7.12 ± 2.1	6.54 ± 3.2	6.50 ± 2.0

Note. There was not significantly different among the segmentation methods, voxel sizes and between the root canal sealers ($p > .05$).

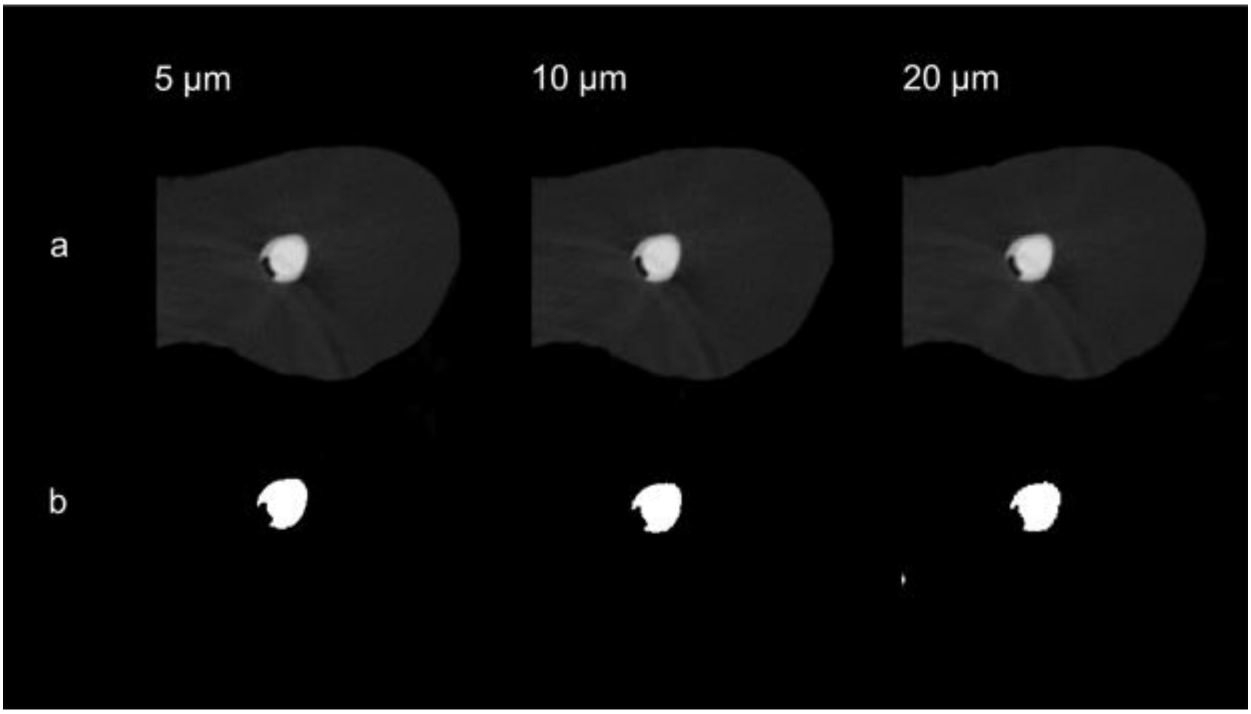

Figure 1 - Representative axial sections of image obtained by micro-CT of filled root canal. (a) original image at 5 µm and images resized by 2 and 4 at 10 and 20 µm respectively. (b) the same images after segmentation.

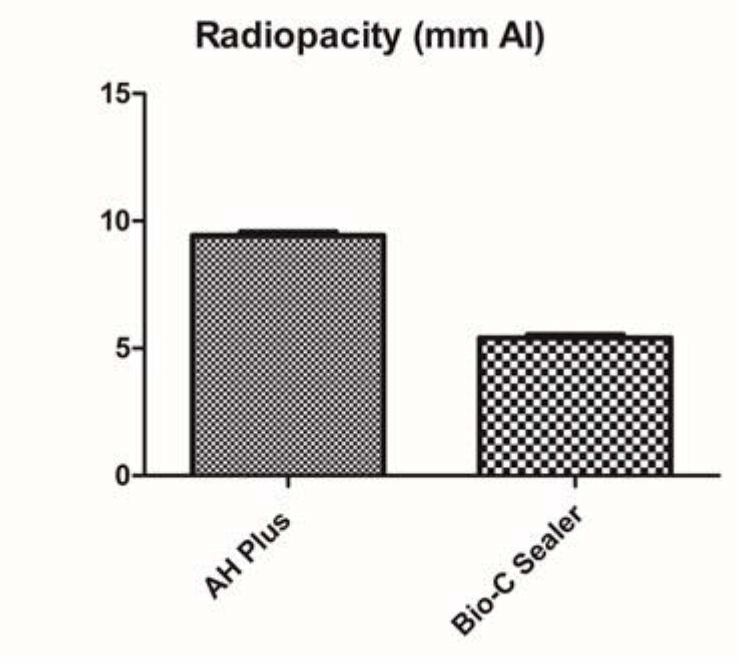

Figure 2 - Mean and standard deviation of the radiopacity of the sealers (*p* < .05).

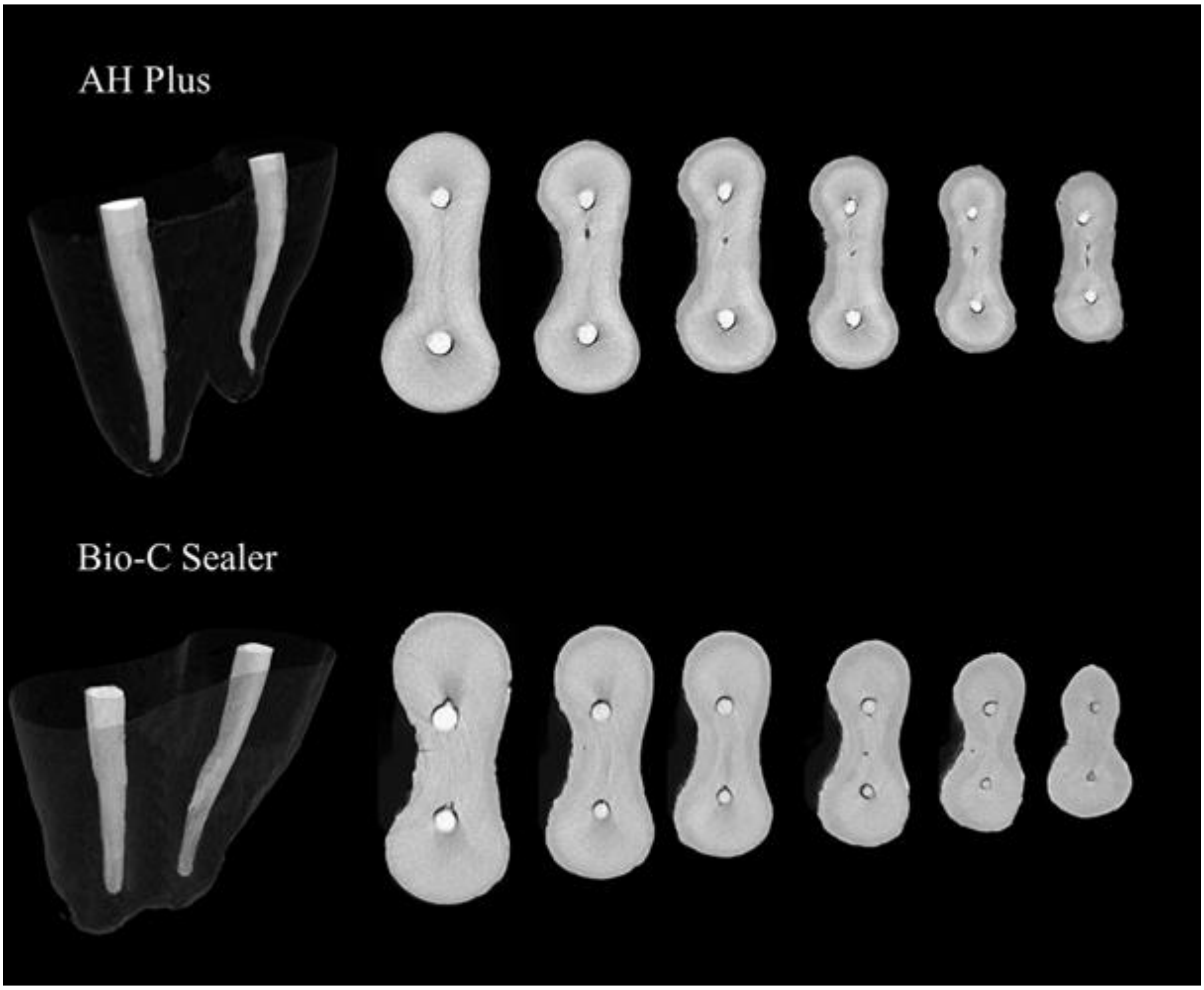

Figure 3 - Tree-dimensional reconstructions and axial sections of images obtained by micro-CT in the apical third of mesial root canals of mandibular molars filled by single cone technique with AH Plus or Bio-C Sealer.

Discussion

The current study assessed the filling ability of two endodontic sealers by micro-CT using different segmentation methods in images with different voxel sizes. Accepting our both null hypotheses, similarities were observed between root canal filling promoted by AH Plus and Bio-C Sealer as well as among the segmentation methods and voxel sizes used.

The root canal morphology may influence the voids within root fillings (Pedulla et al., 2020), and may be difficult to properly fill curved root canals (Alim & Garip Berker, 2020). The evaluation of obturation techniques in root canals with this morphology is limited (Schäfer, Nelius, & Bürklein, 2012). Additionally, the apical third is considered critical for endodontic treatment success and control of re-infection (Ricucci, Lin, & Spångberg, 2009). Therefore, the present study showed the ability of the sealers evaluated to fill the apical third of curved root canals. Our findings corroborate a previous investigation that showed similar filling ability between Bio-C Sealer and AH Plus in flattened root canal (Tavares et al., 2020). The filling ability of Bio-C Sealer can be related to the small particle size and viscosity of calcium silicate–based sealers (Huang et al., 2017). Considering that AH Plus is the gold standard regarding physical properties and no differences were observed between AH Plus and Bio-C, this new calcium silicate-based sealer has adequate ability for root canal filling.

The single cone technique was used in the present study due to its root canal filling ability (Moinzadeh et al., 2015) with less operator influence (Heran, Khalid, Albaaj, Tomson, & Camilleri, 2019; Keleş & Keskin, 2020). Micro-CT is a tool widely used to evaluate quality of root fillings and voids due to its non-destructive characteristic and spatial resolution (Celikten et al., 2019; Orhan et al., 2018; Pedulla et al., 2020). However, the approaches to image acquisition and assessment led to a lack of consistency for interpreting the results of studies using micro-CT (Bouxsein et al., 2010; Torres et al., 2020). Analysis of micro-CT images can be conducted using manual (Küçükkaya Eren, Askerbeyli Örs, & Yılmaz, 2017; Viapiana et al., 2016) or automatic segmentation (Celikten et al., 2019; Huang et al., 2017; Moinzadeh et al., 2015). Manual segmentation method generally is time-consuming, and the results achieved may vary according to the operator's skills (Barrett & Mortensen, 1997). Although automatic methods, such as global threshold, are faster and less operator-dependent (Galibourg et al., 2018; Moinzadeh et al., 2015), manual segmentation showed lower absolute error values for the assessment of 2-dimensional morphometric parameters (Camargo et al., 2020). For both methods, beam hardening, noise, and partial volume effects can considerably reduce the quality of the segmentation, influencing the choice of a grey value as the threshold to separate the object from the background (Galibourg et al., 2018; Michetti et al., 2017; Michetti et al., 2015). Hence, analyses in structures scanned in high resolution with a homogenous structure are less influenced by the segmentation method (Hangartner, 2007).

In the present study, for all voxel sizes evaluated, there was no difference interobserver in analyzes performed with adaptive thresholding, which had similar results to those obtained with automatic segmentation when evaluating the filled root canals. Our findings corroborate a previous study (Queiroz et al., 2017) that observed similar results for manual and automatic thresholding for image segmentation regarding to the human bone morphometric analysis. The authors stated that automatic segmentation should be the first choice in micro-CT studies since this technique does not have human input, in agreement with our conclusions. On the other hand, an evaluation of the presence of voids in filled root canals with different voxel sizes detected more voids with smaller voxel sizes (5.2, 8.1 and 11.2 μm) than at 16.73 μm (Orhan et al., 2018). However, the authors scanned all teeth with different voxel sizes in the micro and nano-CT devices. In the present methodology, the samples were scanned at 5 μm and, after the reconstruction, the images were resized by 2 and 4 in order to acquire images at 10 and 20 μm respectively (Torres, Jacobs, et al., 2020). Moreover, the voxel size is only one of the factors that affect the spatial resolution of the images, since mean absorption of the sample, detector noise, reconstruction algorithm, X-ray focal spot size and shape, detector aperture, and scanner geometry are fundamental factors for image quality (Bouxsein et al., 2010).

Since the root canal filling materials may influence quantitative assessment of voids along with voxel sizes (Orhan et al., 2018), our study assessed this variable. AH Plus had higher radiopacity than Bio-C Sealer, in accordance with a previous study (Zordan-Bronzel et al., 2019). However, both sealers had radiopacity above 3 mm aluminum, as recommended by the ISO 6876 standard. Although there was reported that the different radiopacity among the sealers may be a concern in micro-CT analyzes (Celikten et al., 2019; Viapiana et al., 2016), this property did not influence our findings. Since the radiodensity of the scanned structure influences artifacts formation (Bouxsein et al., 2010; Celikten et al., 2019), affecting the final quality of the images, the current investigation used high energy (100 kV) and high intensity (100 μAP) for sample scans. These scans parameters generated images with great quality, probably decreasing the influence of the sealers radiopacity, voxel sizes, and segmentation method.

The search for new experimental models has been highlighted as very useful for further studies on bioceramics root canal sealers (Silva et al., 2020). Therefore, the similarity of results using different voxel sizes and segmentation methods in the present study is important for future research, since the micro-CT scan with larger voxel sizes, and the automatic segmentation of the images enable faster methodology with less influence of the operator. In addition, it is important to point that intra and inter-examiner calibration tests can help to improve the consistency of results.

Within the limitation of the present *ex vivo* study, it may be concluded that Bio-C Sealer and AH Plus provided proper filling ability of curved root canals. In addition, visual and automatic segmentation can be applied to micro-CT images with voxel sizes from 5 to 20 µm in order to evaluate the filling quality of sealers that present radiopacity according to ISO 6876. Automatic segmentation method should be considered as the first choice to evaluate the root canal filling quality due to its fast, reliable and less operator-dependent characteristics.

Conflict of Interest

The authors deny any conflicts of interest related to this study.

References

Aktemur Türker, S., Uzunoğlu Özyürek, E., & Tek, V. (2020). The effect of different obturation methods on sealer penetration alongside apically separated rotary nickel-titanium instruments: A confocal laser scanning microscopy study. *Microscopy Research and Technique*, 83, 720-726. doi:10.1002/jemt.23461

Alim, B. A., & Garip Berker, Y. (2020). Evaluation of different root canal filling techniques in severely curved canals by micro-computed tomography. *The Saudi Dental Journal,* 32, 200-205. doi:10.1016/j.sdentj.2019.08.009

Alves Silva, E. C., Tanomaru-Filho, M., da Silva, G. F., Delfino, M. M., Cerri, P. S., & Guerreiro-Tanomaru, J. M. (2020). Biocompatibility and bioactive potential of new calcium silicate-based endodontic sealers: Bio-C Sealer and Sealer Plus BC. *Journal of Endodontics,* 46, 1470-1477. doi:10.1016/j.joen.2020.07.011

Barrett, W. A., & Mortensen, E. N. (1997). Interactive live-wire boundary extraction. *Medical Image Analysis,* 1, 331-341. doi:10.1016/s1361-8415(97)85005-0

Bouxsein, M. L., Boyd, S. K., Christiansen, B. A., Guldberg, R. E., Jepsen, K. J., & Müller, R. (2010). Guidelines for assessment of bone microstructure in rodents using micro-computed tomography. *Journal of Bone and Mineral Research,* 25, 1468-1486. doi:10.1002/jbmr.141

Camargo, R. V., Mazzi-Chaves, J. F., Leoni, G. B., Vasconcelos, K. F., Lamira, A., Jacobs, R., & Sousa-Neto, M. D. (2020). Quantitative Assessment of 2-dimensional Parameters in Tomographic Images by Using Different Segmentation Methods. *Journal of Endodontics,* 46, 694-699. doi:10.1016/j.joen.2020.01.012

Campello, A. F., Marceliano-Alves, M. F., Siqueira, J. F., Jr., Marques, F. V., Guedes, F. R., Lopes, R. T., . . . Alves, F. R. F. (2019). Determination of the Initial Apical Canal Diameter by the First File to Bind or Cone-beam Computed Tomographic Measurements Using Micro-computed Tomography as the Gold Standard: An Ex Vivo Study in Human Cadavers. *Journal of Endodontics,* 45, 619-622. doi:10.1016/j.joen.2019.01.020

Celikten, B., Jacobs, R., de Faria Vasconcelos, K., Huang, Y., Shaheen, E., Nicolielo, L. F. P., & Orhan, K. (2019). Comparative evaluation of cone beam CT and micro-CT on blooming artifacts in human teeth filled with bioceramic sealers. *Clinical Oral Investigations,* 23, 3267-3273. doi:10.1007/s00784-018-2748-8

Christiansen, B. A. (2016). Effect of micro-computed tomography voxel size and segmentation method on trabecular bone microstructure measures in mice. *Bone Reports,* 5, 136-140. doi:10.1016/j.bonr.2016.05.006

de Oliveira, B. P., Camara, A. C., Duarte, D. A., Gomes, A. S. L., Heck, R. J., Antonino, A. C. D., & Aguiar, C. M. (2017). Detection of Apical Root Cracks Using Spectral Domain and Swept-source Optical Coherence Tomography. *Journal of Endodontics,* 43, 1148-1151. doi:10.1016/j.joen.2017.01.019

Galibourg, A., Dumoncel, J., Telmon, N., Calvet, A., Michetti, J., & Maret, D. (2018). Assessment of automatic segmentation of teeth using a watershed-based method. *Dentomaxillofacial Radiology,* 47, 20170220. doi:10.1259/dmfr.20170220

Hangartner, T. N. (2007). Thresholding technique for accurate analysis of density and geometry in QCT, pQCT and microCT images. *Journal of Musculoskeletal & Neuronal Interactions,* 7, 9-16. PMID: 17396001

Heran, J., Khalid, S., Albaaj, F., Tomson, P. L., & Camilleri, J. (2019). The single cone obturation technique with a modified warm filler. *Journal of Dentistry,* 89, 103181. doi:10.1016/j.jdent.2019.103181

Huang, Y., Celikten, B., de Faria Vasconcelos, K., Ferreira Pinheiro Nicolielo, L., Lippiatt, N., Buyuksungur, A., . . . Orhan, K. (2017). Micro-CT and nano-CT analysis of filling quality of three different endodontic sealers. *Dentomaxillofacial Radiology,* 46, 20170223. doi:10.1259/dmfr.20170223

Keleş, A., & Keskin, C. (2020). Presence of voids after warm vertical compaction and single-cone obturation in band-shaped isthmuses using micro-computed tomography: A phantom study. *Microscopy Research and Technique*, *83*(4), 370-374. doi:10.1002/jemt.23423

Kierklo, A., Tabor, Z., Pawińska, M., & Jaworska, M. (2015). A microcomputed tomography-based comparison of root canal filling quality following different instrumentation and obturation techniques. *Medical Principles and Practice,* 24, 84-91. doi:10.1159/000368307

Küçükkaya Eren, S., Askerbeyli Örs, S., & Yılmaz, Z. (2017). Effect of Post Space Preparation on Apical Obturation Quality of Teeth Obturated with Different Techniques: A Micro-computed Tomographic Study. *Journal of Endodontics,* 43, 1152-1156. doi:10.1016/j.joen.2017.01.039

Michetti, J., Basarab, A., Diemer, F., & Kouame, D. (2017). Comparison of an adaptive local thresholding method on CBCT and µCT endodontic images. *Physics in Medicine and Biology,* 63, 015020. doi:10.1088/1361-6560/aa90ff

Michetti, J., Georgelin-Gurgel, M., Mallet, J. P., Diemer, F., & Boulanouar, K. (2015). Influence of CBCT parameters on the output of an automatic edge-detection-based endodontic segmentation. *Dentomaxillofacial Radiology,* 44, 20140413. doi:10.1259/dmfr.20140413

Moinzadeh, A. T., Zerbst, W., Boutsioukis, C., Shemesh, H., & Zaslansky, P. (2015). Porosity distribution in root canals filled with gutta percha and calcium silicate cement. *Dental Materials,* 31, 1100-1108. doi:10.1016/j.dental.2015.06.009

Oh, S., Perinpanayagam, H., Kum, D. J. W., Lim, S. M., Yoo, Y. J., Chang, S. W., . . . Kum, K. Y. (2016). Evaluation of three obturation techniques in the apical third of mandibular first molar mesial root canals using micro-computed tomography. *Journal of Dental Sciences,* 11, 95-102. doi:10.1016/j.jds.2015.11.002

Orhan, K., Jacobs, R., Celikten, B., Huang, Y., de Faria Vasconcelos, K., Nicolielo, L. F. P., . . . Van Dessel, J. (2018). Evaluation of Threshold Values for Root Canal Filling Voids in Micro-CT and Nano-CT Images. *Scanning,* 2018, 9437569. doi:10.1155/2018/9437569

Pedulla, E., Abiad, R. S., Conte, G., La Rosa, G. R. M., Rapisarda, E., & Neelakantan, P. (2020). Root fillings with a matched-taper single cone and two calcium silicate-based sealers: an analysis of voids using micro-computed tomography. *Clinical Oral Investig*ations, 24, 4487-4492. doi:10.1007/s00784-020-03313-5

Pruett, J. P., Clement, D. J., & Carnes, D. L. (1997). Cyclic fatigue testing of nickel-titanium endodontic instruments. *Journal of Endodontics,* 23, 77-85. doi:10.1016/S0099-2399(97)80250-6

Queiroz, P. M., Rovaris, K., Gaeta-Araujo, H., Marzola de Souza Bueno, S., Freitas, D. Q., Groppo, F. C., & Haiter-Neto, F. (2017). Influence of Artifact Reduction Tools in Micro-computed Tomography Images for Endodontic Research. *Journal of Endodontics,* 43, 2108-2111. doi:10.1016/j.joen.2017.07.024

Ricucci, D., Lin, L. M., & Spångberg, L. S. (2009). Wound healing of apical tissues after root canal therapy: a long-term clinical, radiographic, and histopathologic observation study. *Oral Surgery, Oral Medical, Oral Pathology, Oral Radiology and Endodontics,* 108, 609-621. doi:10.1016/j.tripleo.2009.05.028

Rovaris, K., Queiroz, P. M., Vasconcelos, K. F., Corpas, L. D. S., Silveira, B. M. D., & Freitas, D. Q. (2018). Segmentation Methods for Micro CT Images: A Comparative Study Using Human Bone Samples. *Brazilian Dental Journal,* 29, 150-153. doi:10.1590/0103-6440201801385

Sanz, J. L., Lopez-Garcia, S., Lozano, A., Pecci-Lloret, M. P., Llena, C., Guerrero-Girones, J., . . . Forner, L. (2020). Microstructural composition, ion release, and bioactive potential of new premixed calcium silicate-based endodontic sealers indicated for warm vertical compaction technique. *Clinical Oral Investigations*. doi:10.1007/s00784-020-03453-8

Schäfer, E., Nelius, B., & Bürklein, S. (2012). A comparative evaluation of gutta-percha filled areas in curved root canals obturated with different techniques. *Clinical Oral Investigations,* 16, 225-230. doi:10.1007/s00784-011-0509-z

Schneider, S. W. (1971). A comparison of canal preparations in straight and curved root canals. *Oral Surgery, Oral Medicine and Oral Pathology,* 32, 271-275.

Silva Almeida, L. H., Moraes, R. R., Morgental, R. D., & Pappen, F. G. (2017). Are Premixed Calcium Silicate-based Endodontic Sealers Comparable to Conventional Materials? A Systematic Review of In Vitro Studies. *Journal of Endodontics,* 43, 527-535. doi:10.1016/j.joen.2016.11.019

Silva, E., Ehrhardt, I. C., Sampaio, G. C., Cardoso, M. L., Oliveira, D. D. S., Uzeda, M. J., . . . De-Deus, G. (2020). Determining the setting of root canal sealers using an in vivo animal experimental model. *Clinical Oral Investigations*. doi:10.1007/s00784-020-03496-x

Tavares, K. I. M. C., Pinto, J. C., Santos-Junior, A. O., Torres, F. F. E., Guerreiro-Tanomaru, J. M., & Tanomaru-Filho, M. (2020). Micro-CT evaluation of filling of flattened root canals using a new premixed ready-to-use calcium silicate sealer by single-cone technique. *Microscopy Research and Technique.* doi:10.1002/jemt.23658

Torres, F. F. E., Jacobs, R., EzEldeen, M., de Faria-Vasconcelos, K., Guerreiro-Tanomaru, J. M., Dos Santos, B. C., & Tanomaru-Filho, M. (2020). How image-processing parameters can influence the assessment of dental materials using micro-CT. *Imaging Science in Dentistry,* 50, 161-168. doi:10.5624/isd.2020.50.2.161

Torres, F. F. E., Zordan-Bronzel, C. L., Guerreiro-Tanomaru, J. M., Chavez-Andrade, G. M., Pinto, J. C., & Tanomaru-Filho, M. (2020). Effect of immersion in distilled water or phosphate-buffered saline on the solubility, volumetric change and presence of voids within new calcium silicate-based root canal sealers. *International Endodontic Journal,* 53, 385-391. doi:10.1111/iej.13225

Vertucci, F. J. (1984). Root canal anatomy of the human permanent teeth. *Oral Surgery, Oral Medicine and Oral Pathology,* 58, 589-599. doi:10.1016/0030-4220(84)90085-9

Viapiana, R., Guerreiro-Tanomaru, J. M., Hungaro-Duarte, M. A., Tanomaru-Filho, M., & Camilleri, J. (2014). Chemical characterization and bioactivity of epoxy resin and Portland cement-based sealers with niobium and zirconium oxide radiopacifiers. *Dental Materials,* 30, 1005-1020. doi:10.1016/j.dental.2014.05.007

Viapiana, R., Moinzadeh, A. T., Camilleri, L., Wesselink, P. R., Tanomaru Filho, M., & Camilleri, J. (2016). Porosity and sealing ability of root fillings with gutta-percha and BioRoot RCS or AH Plus sealers. Evaluation by three ex vivo methods. *International Endodontic Journal,* 49, 774-782. doi:10.1111/iej.12513

Wolf, M., Kupper, K., Reimann, S., Bourauel, C., & Frentzen, M. (2014). 3D analyses of interface voids in root canals filled with different sealer materials in combination with warm gutta-percha technique. *Clinical Oral Investigations,* 18, 155-161. doi:10.1007/s00784-013-0970-y

Zordan-Bronzel, C. L., Esteves Torres, F. F., Tanomaru-Filho, M., Chavez-Andrade, G. M., Bosso-Martelo, R., & Guerreiro-Tanomaru, J. M. (2019). Evaluation of Physicochemical Properties of a New Calcium Silicate-based Sealer, Bio-C Sealer. *Journal of Endodontics,* 45, 1248-1252. doi:10.1016/j.joen.2019.07.006

3.5 Publicação 5*

Influence of different sealers and supplementary approaches on endodontic retreatment

Abstract

The aim of this study was to assess the influence of root canal sealers based on calcium silicate or epoxy resin on filling material removal during endodontic retreatment, as well as to compare the efficacy of XP-endo Finisher and ProDesign Logic (PDL) as supplementary retreatment protocols. Mesial root canals of extracted mandibular molars were prepared using HyFlex EDM 25/.08 and filled with Bio-C Sealer or AH Plus using the single cone technique ($n = 12$). Retreatment was performed using PDL RT and apical preparation was performed with PDL 35/.05. After retreatment, the specimens were randomly divided into two experimental groups ($n = 12$), considering a similar distribution of the sealers. A supplementary retreatment was performed with PDL 50/.01 or XP-endo Finisher. The volume of root canals, transportation, and the percentage of remaining filling material were evaluated using high-resolution (5 µm voxel size) micro-CT imaging. Statistical analysis was performed using t-tests ($\alpha = 0.05$). The root canals filled with AH Plus had the highest percentage of residual filling material ($p < 0.05$). Both systems decreased the residual volume of filling material in the apical third ($p < 0.05$). PDL 50/.01 increased the root canal volume in the apical third ($p < .05$). No differences were observed between the systems for canal transportation ($p > 0.05$). The removal of AH Plus was more difficult than in Bio-C. PDL 50/.01 and XP-endo Finisher provided greater removal of filling materials in the apical third after retreatment. Both complementary approaches did not promote apical transportation.

Keywords: Heat-Treated Nickel-Titanium Files; Retreatment; Root Canal Preparation; X-Ray Microtomography.

* Artigo em revisão no periódico *Brazilian Oral Research.*

Introduction

The removal of filling material in retreatment procedures is essential to obtain disinfection of the root canal system.[1] Endodontic sealers based on calcium silicates are used due to their biocompatibility and induction of mineralization.[2] However, the literature is controversial regarding the impact of calcium silicate-based sealers on endodontic retreatment.[3] Although previous studies showed similar filling material removal after retreatments of root canals filled with AH Plus (Dentsply DeTrey, Konstanz, Germany) or sealers based on calcium silicates,[4-6] the sealer used may influence the removal of the filling material.[7]

Bio-C Sealer (Angelus, Londrina, PR, Brazil) is a new premixed ready-to-use calcium silicate–based sealer. This sealer has shown cytocompatibility and mineralization,[8] besides radiopacity and flow in accordance with the ISO 6876 standard.[9] Bio-C Sealer has low presence of voids, similar to AH Plus,[10] providing appropriate root canal filling.[11] However, up to now, there is no study investigating the retreatment in root canals filled with Bio-C Sealer.

The apical region of the root canal represents a critical zone to maintain infection of the root canal system.[12] Apical enlargement can improve the removal of filling material.[13] However, root canal preparation using nickel-titanium (NiTi) instruments with high diameter and taper in curved root canals can promote root canal transportation due to their low flexibility.[14] ProDesign Logic 50/.01 (PDL - Easy Equipamentos Odontológicos, Belo Horizonte, MG, Brazil) is a NiTi rotary instrument with Control Memory (CM) heat-treatment, large tip size and minimum taper, which was proposed to perform apical enlargement.[15] This instrument significantly decreased the amount of filling material in the apical third of curved lateral incisors.[13] Although it has been reported that NiTi files with CM heat-treatment enables apical enlargement in curved root canals,[16] there are no studies evaluating apical transportation caused for CM instruments with tip size 50.

XP-endo Finisher (FKG Dentaire, La Chaux-de-Fonds, Switzerland) is a rotary MaxWire NiTi instrument with tip size 25 and nontapered that changes its shape according to the temperature.[17,18] This file effectively removed accumulated remaining filling material.[19, 20] XP-endo Finisher and XP-endo Finisher R files were equally effective as additional procedure in endodontic retreatment.[20] However, there is no investigation comparing filling material removal using XP-Endo Finisher or apical enlargement, besides apical transportation and volume increase after its use in curved root canals of molars.

The aim of the present study was to assess the influence of a ready-to-use calcium silicate–based root canal sealer in comparison to an epoxy resin-based sealer on filling material removal during endodontic retreatment, as well as to compare filling material removal, apical transportation and volume increase of curved mesial root canals of mandibular molar filled with AH Plus or Bio-C Sealer, after using size 50, .01 taper instrument or XP-endo Finisher. The first null hypothesis was that the obturation of the root canal with AH Plus or Bio-C Sealer would not impact the filling material removal. The second null hypothesis was that no differences would be observed in the amount of filling material, transport and root canal volume using PDL 50/.01 and XP-endo files.

Methodology

Sample size calculation

G* Power 3.1.7 for Windows program (Heinrich-Heine-Universitat Dusseldorf, Dusseldorf, Germany) was used for the sample calculation. The t-test for two dependent groups was used with an Alpha type error of 0.05 and Beta power of 0.95 for all the variables. Previous studies were used to determine the specific effect size for amount of remaining filling material, 2.348[19]; root canal volume, 1.860[16] and root canal transportation, 3.111[21]. A total of 12 specimens was indicated as being the ideal size required.

Sample selection

All procedures were approved by the Faculty's Ethics Committee (CEP no. No. 10411219.9.0000.5416). Human mandibular first and second molars previously stored in 0.1% thymol solution at 5°C were used. The inclusion criteria included two independent mesial root canals according type IV Vertucci's classification,[22] angle of curvature between 25° and 35° in accordance with the Schneider method,[23] and radius of curvature smaller than 10 mm, following the Pruett's method.[24] Complete apical formation, absence of root fractures, calcifications or internal resorptions were also included. For this purpose, a digital system (RVG 6100; Kodak Dental Systems, NY) and a micro-CT device (SkyScan 1276; Bruker-microCT, Kontich, Belgium) were used. Micro-CT was applied at a low-resolution (35 µm voxel size) under the following settings: copper and aluminum filters, 87-millisecond exposure time, frame averaging of 3, 180° rotation around the vertical axis, rotational step of 0.5° at 80 kV and 300 µA. A total of twelve roots were selected, totalizing twenty-four root canals, including mesiobuccal and mesiolingual canal of each root.

Root canal preparation

Conventional access cavities were performed, and the root canals were explored by using a size #10 K-file (Dentsply Sirona Endodontics, Ballaigues, Switzerland). The working length (WL) was established 1 mm shorter from the apical foramen. For preparation, HyFlex EDM (HEDM; Coltene/Whaledent, Altstätten, Switzerland) 10/.05 was operated by electric motor VDW SILVER (VDW GmbH, Munich, Germany) in rotary motion at 300 rpm and torque 1.8 Ncm, with in-and-out movements up to the WL. Then, HEDM 25/.08 was used at 500 rpm and torque 2.5 Ncm, as described above. Each root canal was irrigated with 5 mL of 2.5% sodium hypochlorite (NaOCl). Passive ultrasonic irrigation (PUI) was performed in all root canals with the ultrasonic tip Irrisonic (Helse Ultrasonic, Santa Rosa de Viterbo, SP, Brazil) activated in an ultrasonic device Ultrawave XS (Ultradent, South Jordan, USA) using a power of 10 % and frequency of 50 Hz, according to the manufacturer's recommendation. The ultrasonic tips were positioned 2 mm short of the WL and activated for 20 seconds, interleaving 2.5% NaOCl, and 17% EDTA. 2 mL of irrigation solution was used in each cycle. As final irrigation, 5 mL of distilled water was used.

Root canal filling

A stratified random sampling statistical method was used to divide the root canals in two experimental groups, considering the post-preparation volume (n = 12). The root canals were dried with paper points and filled by single cone technique with gutta-percha cones 25/.08 (Coltene/Whaledent, Langenau, Germany) and an epoxy resin-based sealer (AH Plus; Dentsply DeTrey, Konstanz, Germany) or a calcium silicate-based material (Bio-C Sealer; Angelus, Londrina, PR, Brazil). AH Plus was inserted into the root canal with a Lentulo spiral #25 (Dentsply Maillefer) coupled to a low speed motor (Micromotor N270 and Counter-angle, Dabi-Atlante, Ribeirão Preto, SP, Brazil). Bio-C Sealer was injected into the root canal at 4 mm of the WL, using the syringe and plastic needles provided by its manufacturer. The access cavities were filled with Coltosol (Vigodent, Rio de Janeiro, RJ, Brazil). The samples were stored at 37º C and 95% relative humidity for 1 week to allow the sealers to set completely.

Root canal retreatment

Electric motor VDW SILVER, in rotary motion at 600 rpm and torque 3 Ncm was used. The files were used with in-and-out movements up to the WL. ProDesign Logic RT (PDLRT - Easy Equipamentos Odontológicos, Belo Horizonte, MG, Brazil) 30/10 was used to remove the filling of the cervical third, PDLRT 25/.08 was used in the middle third and PDLRT 20/.06 was used to remove the filling of the apical third. The root canals were enlarged with PDL 35/.05 as described above. Each root canal was irrigated with 8 mL of 2.5% NaOCl (2 mL for each instrument). Final irrigation was performed with 2.5 ml of 17% EDTA, under agitation for 3 minutes, with a gutta-percha cone size 25, followed by 5 mL of distilled water.

Supplementary retreatment approach

The mesial root canals of the specimens were randomly divided into two experimental groups (n = 12), with stratified random sampling, considering the remaining root canal filling after retreatment and equality distribution of the sealers (AH Plus and Bio-C Sealer) between the groups.

PDL 50/.01: the instrument was operated using an electric motor VDW SILVER, in rotary motion at a speed of 350 rpm and torque 1 Ncm, with in-and-out movements up to the WL. The root canals were irrigated with 2 mL of 2.5% NaOCl. Final irrigation was performed as previously described.

XP-endo Finisher: the instrument was operated on an electric motor VDW SILVER, in rotary motion at a speed of 800 rpm and torque 1 Ncm. Each canal was filled with 1 mL of 2.5% NaOCl, and the XP-endo file was inserted without rotation. Then, rotation was initialized (800 rpm and 1 Ncm), and the instrument was activated for 30 seconds using slow and gentle 7–8 mm lengthwise movements up to the WL. This procedure was repeated two times. Final irrigation was performed as previously described.

Micro-CT analysis

The specimens were scanned at a high-resolution (5 µm voxel size) in a micro-CT device (SkyScan 1272. Bruker, Kontich, Belgium) before and after retreatment procedures under the following settings: copper filter, 180° rotation around the vertical axis and rotational step of 0.2° at 100 kV and 100 µA. The images were reconstructed using the NRecon software (V1.6.10.4; Bruker, Belgium), and superimposed with geometric alignment using the DataViewer software (V.1.5.1, Bruker, Belgium). The quantitative analysis was performed using the CTAn software (V.1.14.4, Bruker, Belgium). Representative images were performed by means of models obtained by CTVox software (v.3.2; Bruker-microCT).

Root canal volume and remaining filling material were quantified after retreatment steps. The gray scale range required to recognize each object under study was determined in a density histogram by using the global threshold method. To obtain the percentage of remaining filling material the following formula was used: [Percentage remaining filling material = (filling material after retreatment x 100 / filling material before retreatment)]. The analyzes were performed in the apical third of the root canals considering 4 mm.

The apical transportation was measured in millimeters using transverse cross sections images of the roots obtained before and after retreatments procedures (Figure 1). Ten cross sections were measured in the apical third of each root canal and determined by the arithmetical mean value. The root canal transportation was obtained by means of the following equation: $(X1-X2) – (Y1-Y2)$ [25].

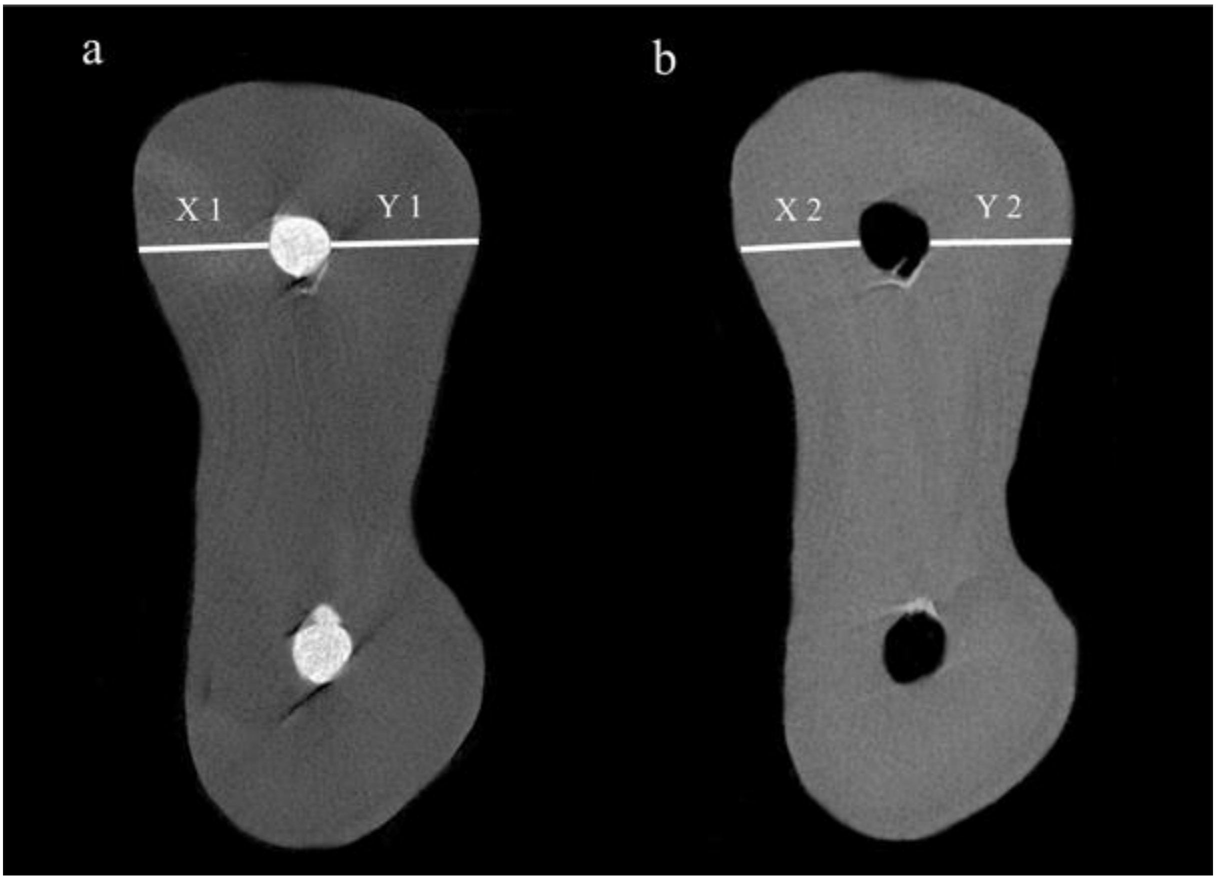

Figure 1 - Representative cross-sectional micro-CT images showing how apical transportation was calculated: (A) before and (B) after root canal retreatment.

Statistical analysis

The normality of the data was tested using the Shapiro-Wilk test. The paired t-test was used for comparison of root canals before and after supplementary cleaning approach. For comparisons between the groups non-paired t test was used. The level of significance was 5% for all the analysis.

Results

The root canals filled with AH Plus showed higher percentage of remaining filling material than Bio-C Sealer ($p < 0.05$) (Figure 2). The volume of the remaining filling material was similar between the groups before and after the supplementary cleaning approach with PDL 50/.01 or XP-endo ($p > 0.05$). Both files decreased the volume of remaining filling material in the apical third ($p < 0.05$) (Table 1, Figure 3). PDL 50/.01 increased the root canal volume in the apical third ($p < 0.05$) (Table 2). Both supplementary approaches maintained the root canal trajectory, with no differences between them ($p > 0.05$) (Table 3).

Table 1. Residual filling material (%) in the apical third of the root canals before and after the use of ProDesign Logic 50/.01 or XP-endo Finisher files and the reduction of residual filling material (%) (mean and standard deviation).

	Before additional cleaning method	After additional cleaning method	Reduction in residual filling material
PDL 50.01	13.26 ± 3.36^{a}	7.50 ± 2.13^{b}	48.55 ± 6.70
XP-endo Finisher	10.61 ± 2.33^{a}	6.33 ± 1.64^{b}	53.50 ± 9.64

Different lowercase letters on same line represent significant differences intragroup ($p < 0.05$).

There was no significant difference intergroup ($p > 0.05$).

Table 2. Root canal volume (mm^3) in the apical third of the root canals before and after the use of ProDesign Logic 50/.01 or XP-endo Finisher files, and root canal volume increase (%) (mean and standard deviation).

	Before additional cleaning method	After additional cleaning method	Increase in volume
PDL 50.01	0.81 ± 0.24^{aA}	1.04 ± 0.32^{aB}	29.36 ± 8.87^{a}
XP-endo Finisher	0.80 ± 0.24^{aA}	0.83 ± 0.25^{bB}	3.89 ± 1.93^{b}

Different lowercase letters on same column represent significant differences intergroup ($p < 0.05$).

Different capital letters on same line represent significant differences intragroup ($p < 0.05$).

Table 3. Transportation (mm) in the apical third of the root canals before and after the use of ProDesign Logic 50/.01 or XP-endo Finisher files (mean and standard deviation).

	Before additional cleaning method	After additional cleaning method
PDL 50.01	0.038 ± 0.015	0.057 ± 0.035
XP-endo Finisher	0.039 ± 0.020	0.053 ± 0.021

There were no significant differences intragroup or intergroup ($p > 0.05$).

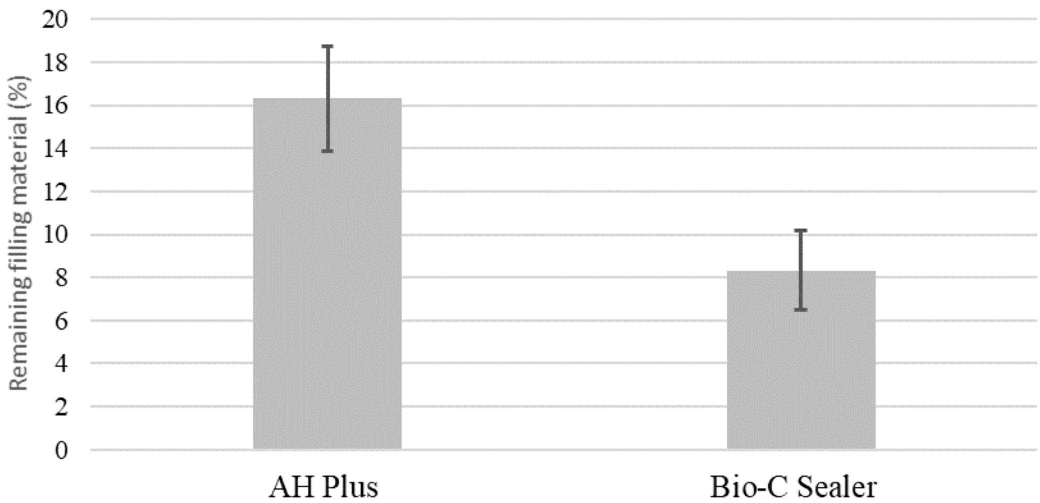

Figure 2 – Means and standard deviations of residual filling material (%) in the apical third of the root canals filled with AH Plus or Bio-C Sealer. There is a significant difference intragroup ($p < 0.05$)

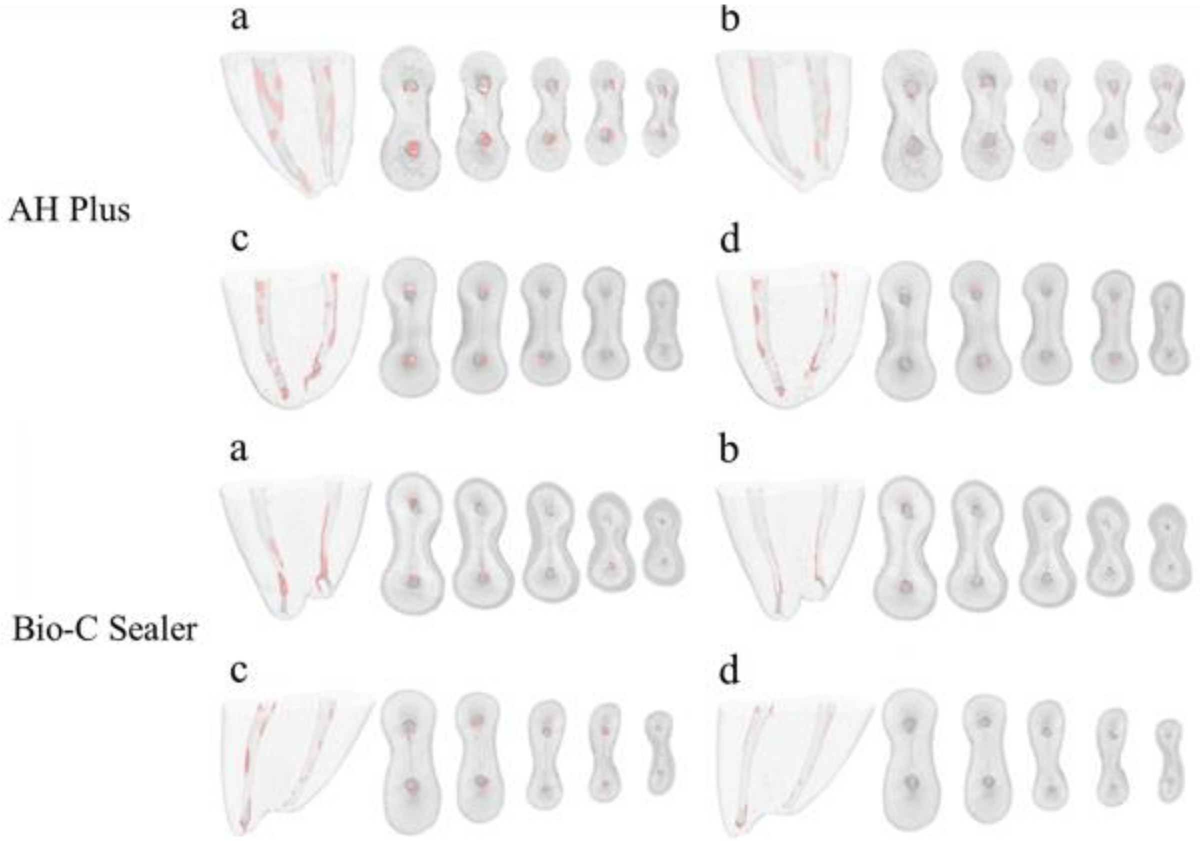

Figure 3 - Representative 3D reconstructions of images obtained by micro-CT showing in pink remain filling material in the apical third of mesial canals of mandibular molars (A) before PDL use (B) after PDL use (C) before XP-endo Finisher use and (D) after XP-endo Finisher use.

Discussion

Rejecting the first null hypothesis, the root canals obturated with Bio-C sealer showed less remaining filling material than AH Plus. The removal of calcium silicate-based sealers was greater compared to AH Plus in a previous investigation.[4] The physicochemical properties of calcium silicate-based sealers may influence their removal during retreatment procedures.[7] Bio-C Sealer has higher solubility than AH Plus,[10] which could contribute to its removal by the mechanical action of files and the physical effect of irrigation solutions. In addition, the high bond strength of AH Plus may contribute to its adhesion to the dentine walls,[26, 27] making difficult its removal.

Besides evaluation of the influence the of a ready-to-use calcium silicate–based sealer on retreatments procedures, our study also compared the efficacy of two approaches for additional retreatments. Therefore, in order to maintain an adequate sample size, after the retreatment, the root canals filled with AH Plus and Bio-C sealer were randomly divided into two experimental groups considering an equality distribution of the sealers between the groups. Therefore, after this experimental step, the influence of the sealer was not considered. Partially rejecting the second null hypothesis, PDL 50/.01 and XP-endo Finisher improved the removal of remaining filling material in the apical third of curved mesial root canals of mandibular molars, with no difference between the instruments. Our findings corroborate previous studies showing that XP-Endo Finisher files are related to removal of filling materials during retreatment.[5, 20, 28] The alloy MaxWire, used to produce the XP-endo Finisher files allows its expansion at body temperature.[29] So, the instrument tip is forced against the root canal wall, since the elliptical part of the file is compressed by the resistance imposed by canal anatomy.[30] The mechanical action of the tip in the root walls can dislodge the root filling material, which is removed during canal irrigation.

Our findings showed that PDL 50/.01 promoted higher increase in volume than XP-endo Finisher in the apical third. Large apical preparations increase the ability of the instrument to touch root canal surfaces,[31] increasing the removal of remaining filling material. In addition, apical enlargement improves physical effect of irrigating solution,[32] allowing better apical cleaning,[33] and significantly enhancing the root canal disinfection.[34] However, a concern about the preparation using files with larger tip and taper is the risk of excessive removal of dentin, which may decrease the radicular strength.[35] The root canal preparation for retreatment using the size 35/.05 taper promotes a 0.55 mm diameter at 4 mm from the apical preparation. Therefore, one may argue that PDL 50/.01 file did not promote dentinal removal in cervical and middle thirds, since this file has a 0.54 mm diameter at 4 mm from the apical preparation.

Root canal transportation, perforations or excessive wear of root canal walls can negatively affect the outcomes of endodontic treatments.[36] In the current study, retreatment with apical size 35/.05 taper and the supplementary approach using the PDL 50/.01 or XP-endo Finisher did not result in canal transportation in the critical apical area. The mean transportation observed in this study ranged from 0.038 to 0.057 mm, which is below the acceptable limit of 0.15 mm.[37] Heat-treated NiTi instruments are more flexible, and do not promote significative root canal transportation,[16, 38] even in retreatment procedures [39]. The CM-wire alloy of the instruments used in this study may have contributed to the retreatment of curved root canals due to their fatigue resistance and flexibility. Even with a large tip, the small taper of the PDL 50/.01 makes the instrument more flexible.[40] The XP-Endo Finisher has a small core tip size and zero taper resulting in high flexibility, cleaning the dentine without change the original root canal morphology [17].

Since different endodontic sealers based on calcium silicates have been introduced to the market, it is important to evaluate their impact in the retreatment procedures. The current results demonstrated the enhanced removal of filling materials with the PDL 50/.01 and XP-Endo Finisher files. Bio-C Sealer showed greater retractility. In addition, this research showed similar filling material removal of the apical third and no root canal transportation for the systems evaluated. Although PDL 50/.01 has effect only in the apical root canal third due to its taper, the apical increase can improve root canal disinfection. Both supplementary approaches tested can be indicated for cleaning the apical third of curved root canals.

Conclusions

The removal of filling material from the apical third was easier for root canals filled with Bio-C Sealer than AH Plus in all retreatment procedures. PDL 50/.01 and XP-endo Finisher provided greater removal of filling materials in the apical third after retreatment of curved root canals. Both supplementary approaches presented no apical transportation. PDL 50/.01 promoted greater volume increase of apical third than XP-endo Finisher.

Acknowledgment
This study was financed in part by the Coordenação de Aperfeiçoamento de Pessoal de Nível Superior - Brasil (CAPES) - Finance Code 001, CNPq (302206/2017-5), and was supported by São Paulo Research Foundation - FAPESP (2017/19049, 2018/19665-6 and 2019/22885-0).

Conflict of interest: The authors declare that they have no conflict of interest.

References

1. Cavenago BC, Ordinola-Zapata R, Duarte MA, et al. Efficacy of xylene and passive ultrasonic irrigation on remaining root filling material during retreatment of anatomically complex teeth. Int Endod J. 2014 Nov;47(11):1078-83. https://doi:10.1111/iej.12253
2. Camilleri J, Sorrentino F, Damidot D. Investigation of the hydration and bioactivity of radiopacified tricalcium silicate cement, Biodentine and MTA Angelus. Dent Mater. 2013 May;29(5):580-93. https://doi:10.1016/j.dental.2013.03.007
3. Donnermeyer D, Bürklein S, Dammaschke T, Schäfer E. Endodontic sealers based on calcium silicates: a systematic review. Odontology. 2019 Oct;107(4):421-436. https:// doi:10.1007/s10266-018-0400-3
4. Donnermeyer D, Bunne C, Schäfer E, Dammaschke T. Retreatability of three calcium silicate-containing sealers and one epoxy resin-based root canal sealer with four different root canal instruments. Clin Oral Investig. 2018 Mar;22(2):811-817. https://doi:10.1007/s00784-017-2156-5
5. Aksel H, Küçükkaya Eren S, Askerbeyli Örs S, Serper A, Ocak M, Çelik HH. Micro-CT evaluation of the removal of root fillings using the ProTaper Universal Retreatment system supplemented by the XP-Endo Finisher file. Int Endod J. 2019 Jul;52(7):1070-1076. https://doi:10.1111/iej.13094
6. Simsek N, Keles A, Ahmetoglu F, Ocak MS, Yologlu S. Comparison of different retreatment techniques and root canal sealers: a scanning electron microscopic study. Braz Oral Res. 2014;28doi:10.1590/1807-3107bor-2014.vol28.0006
7. Neelakantan P, Grotra D, Sharma S. Retreatability of 2 mineral trioxide aggregate-based root canal sealers: a cone-beam computed tomography analysis. J Endod. 2013 Jul;39(7):893-6. https://doi:10.1016/j.joen.2013.04.022
8. López-García S, Pecci-Lloret MR, Guerrero-Gironés J, et al. Comparative Cytocompatibility and Mineralization Potential of Bio-C Sealer and TotalFill BC Sealer. Materials (Basel). 2019 Sep;12(19) https://doi:10.3390/ma12193087
9. Zordan-Bronzel CL, Esteves Torres FF, Tanomaru-Filho M, Chávez-Andrade GM, Bosso-Martelo R, Guerreiro-Tanomaru JM. Evaluation of Physicochemical Properties of a New Calcium Silicate-based Sealer, Bio-C Sealer. J Endod. Oct 2019 45(10):1248-1252. https://doi:10.1016/j.joen.2019.07.006

10. Torres FFE, Zordan-Bronzel CL, Guerreiro-Tanomaru JM, Chávez-Andrade GM, Pinto JC, Tanomaru-Filho M. Effect of immersion in distilled water or phosphate-buffered saline on the solubility, volumetric change and presence of voids within new calcium silicate-based root canal sealers. Int Endod J. 2020 Mar;53(3):385-391. https://doi:10.1111/iej.13225

11. Santos-Junior AO, Tanomaru-Filho M, Pinto JC, Tavares KIMC, Torres FFE, Guerreiro-Tanomaru JM. Effect of obturation technique using a new bioceramic sealer on the presence of voids in flattened root canals. Braz Oral Res. 2021;35:e028. https://doi:10.1590/1807-3107bor-2021.vol35.0028

12. Siqueira JF, Rôças IN. Clinical implications and microbiology of bacterial persistence after treatment procedures. J Endod. 2008 Nov;34(11):1291-1301.e3. https://doi:10.1016/j.joen.2008.07.028

13. Rodrigues CT, Duarte MA, de Almeida MM, de Andrade FB, Bernardineli N. Efficacy of CM-Wire, M-Wire, and Nickel-Titanium Instruments for Removing Filling Material from Curved Root Canals: A Micro-Computed Tomography Study. J Endod. 2016 Nov;42(11):1651-1655. https://doi:10.1016/j.joen.2016.08.012

14. Gagliardi J, Versiani MA, de Sousa-Neto MD, Plazas-Garzon A, Basrani B. Evaluation of the Shaping Characteristics of ProTaper Gold, ProTaper NEXT, and ProTaper Universal in Curved Canals. J Endod. 2015 Oct;41(10):1718-24. https://doi:10.1016/j.joen.2015.07.009

15. Rodrigues CT, Duarte MA, de Almeida MM, de Andrade FB, Bernardineli N. Efficacy of CM-Wire, M-Wire, and Nickel-Titanium Instruments for Removing Filling Material from Curved Root Canals: A Micro-Computed Tomography Study. J Endod. 2016 Nov;42(11):1651-1655. https://doi:10.1016/j.joen.2016.08.012

16. Pinto JC, Pivoto-João MMB, Espir CG, Ramos MLG, Guerreiro-Tanomaru JM, Tanomaru-Filho M. Micro-CT evaluation of apical enlargement of molar root canals using rotary or reciprocating heat-treated NiTi instruments. J Appl Oral Sci. 2019 Aug;27:e20180689. https://doi:10.1590/1678-7757-2018-0689

17. Hamdan R, Michetti J, Pinchon D, Diemer F, Georgelin-Gurgel M. The XP-Endo Finisher for the removal of calcium hydroxide paste from root canals and from the apical third. J Clin Exp Dent. 2017Jul;9(7):e855-e860. https://doi:10.4317/jced.53962

18. Carvalho MC, Zuolo ML, Arruda-Vasconcelos R, et al. Effectiveness of XP-Endo Finisher in the reduction of bacterial load in oval-shaped root canals. Braz Oral Res. 2019;33:e021. https://doi:10.1590/1807-3107bor-2019.vol33.0021

19. Alves FR, Marceliano-Alves MF, Sousa JC, Silveira SB, Provenzano JC, Siqueira JF. Removal of Root Canal Fillings in Curved Canals Using Either Reciprocating Single- or Rotary Multi-instrument Systems and a Supplementary Step with the XP-Endo Finisher. J Endod. 2016 Jul;42(7):1114-9. https:// doi:10.1016/j.joen.2016.04.007

20. Silva EJNL, Belladonna FG, Zuolo AS, et al. Effectiveness of XP-endo Finisher and XP-endo Finisher R in removing root filling remnants: a micro-CT study. Int Endod J. 2018 51(1):86-91. https://doi:10.1111/iej.12788

21. Pedullà E, Plotino G, Grande NM, et al. Shaping ability of two nickel-titanium instruments activated by continuous rotation or adaptive motion: a micro-computed tomography study. Clin Oral Investig. 2016 Nov;20(8):2227-2233. https://doi:10.1007/s00784-016-1732-4

22. Vertucci FJ. Root canal anatomy of the human permanent teeth. Oral Surg Oral Med Oral Pathol. 1984 Nov;58(5):589-99. https://doi:10.1016/0030-4220(84)90085-9

23. Schneider SW. A comparison of canal preparations in straight and curved root canals. Oral Surg Oral Med Oral Pathol. 1971 Aug;32(2):271-5.

24. Pruett JP, Clement DJ, Carnes DL. Cyclic fatigue testing of nickel-titanium endodontic instruments. J Endod. 1997 Feb;23(2):77-85. https://doi:10.1016/S0099-2399(97)80250-6

25. Gambill JM, Alder M, del Rio CE. Comparison of nickel-titanium and stainless steel hand-file instrumentation using computed tomography. J Endod. 1996 Jul;22(7):369-75. https://doi:10.1016/S0099-2399(96)80221-4

26. Carvalho CN, Grazziotin-Soares R, de Miranda Candeiro GT, et al. Micro Push-out Bond Strength and Bioactivity Analysis of a Bioceramic Root Canal Sealer. Iran Endod J. 2017 12(3):343-348. https://doi:10.22037/iej.v12i3.16091

27. Donnermeyer D, Dornseifer P, Schäfer E, Dammaschke T. The push-out bond strength of calcium silicate-based endodontic sealers. Head Face Med. 2018 Aug;14(1):13. https://doi:10.1186/s13005-018-0170-8

28. De-Deus G, Belladonna FG, de Siqueira Zuolo A, et al. Micro-CT comparison of XP-endo Finisher and passive ultrasonic irrigation as final irrigation protocols on

the removal of accumulated hard-tissue debris from oval shaped-canals. Clin Oral Investig. 2019 Jul;23(7):3087-3093. https://doi:10.1007/s00784-018-2729-y

29. Keskin C, Sariyilmaz E, Sariyilmaz Ö. Efficacy of XP-endo Finisher File in Removing Calcium Hydroxide from Simulated Internal Resorption Cavity. J Endod. 2017 Jan;43(1):126-130. https://doi:10.1016/j.joen.2016.09.009

30. De-Deus G, Belladonna FG, Zuolo AS, et al. XP-endo Finisher R instrument optimizes the removal of root filling remnants in oval-shaped canals. Int Endod J. 2019 Jun;52(6):899-907. https://doi:10.1111/iej.13077

31. Plotino G, Grande NM, Tocci L, Testarelli L, Gambarini G. Influence of Different Apical Preparations on Root Canal Cleanliness in Human Molars: a SEM Study. J Oral Maxillofac Res. 2014 Apr;5(2):e4. https://doi:10.5037/jomr.2014.5204

32. Srikanth P, Krishna AG, Srinivas S, Reddy ES, Battu S, Aravelli S. Minimal Apical Enlargement for Penetration of Irrigants to the Apical Third of Root Canal System: A Scanning Electron Microscope Study. J Int Oral Health. 2015 Jun;7(6):92-6.

33. Falk KW, Sedgley CM. The influence of preparation size on the mechanical efficacy of root canal irrigation in vitro. J Endod. Oct 2005 31(10):742-5. https://doi:10.1097/01.don.0000158007.56170.0c

34. Rodrigues RCV, Zandi H, Kristoffersen AK, et al. Influence of the Apical Preparation Size and the Irrigant Type on Bacterial Reduction in Root Canal-treated Teeth with Apical Periodontitis. J Endod. 2017 Jul;43(7):1058-1063. https://doi:10.1016/j.joen.2017.02.004

35. Elayouti A, Dima E, Judenhofer MS, Löst C, Pichler BJ. Increased apical enlargement contributes to excessive dentin removal in curved root canals: a stepwise microcomputed tomography study. J Endod. 2011 Nov;37(11):1580-4. https://doi:10.1016/j.joen.2011.08.019

36. Peters OA, Morgental RD, Schulze KA, Paqué F, Kopper PM, Vier-Pelisser FV. Determining cutting efficiency of nickel-titanium coronal flaring instruments used in lateral action. Int Endod J. 2014 Jun;47(6):505-13. https://doi:10.1111/iej.12177

37. Peters OA. Current challenges and concepts in the preparation of root canal systems: a review. J Endod. 2014 Aug;30(8):559-67.

38. Pinheiro SR, Alcalde MP, Vivacqua-Gomes N, et al. Evaluation of apical transportation and centring ability of five thermally treated NiTi rotary systems. Int Endod J. 2018 Jun;51(6):705-713. https://doi:10.1111/iej.12881

39. Kırıcı D, Demirbuga S, Karataş E. Micro-computed Tomographic Assessment of the Residual Filling Volume, Apical Transportation, and Crack Formation after Retreatment with Reciproc and Reciproc Blue Systems in Curved Root Canals. J Endod. 2020 Feb;46(2):238-243. https://doi:10.1016/j.joen.2019.11.003

40. Capar ID, Kaval ME, Ertas H, Sen BH. Comparison of the cyclic fatigue resistance of 5 different rotary pathfinding instruments made of conventional nickel-titanium wire, M-wire, and controlled memory wire. J Endod. 2015 Apr;41(4):535-8. https://doi:10.1016/j.joen.2014.11.008

3.6 Publicação 6*

Influence of voxel size on micro-CT analyzes of remaining filling material

Abstract

The aim of this study was to investigate the influence of micro-computed tomography (micro-CT) voxel size on assessment of remaining filling material after endodontic retreatment. Twelve curved mesial roots of mandibular molars with two separated canals were selected. All root canals were prepared by using HyFlex EDM files size 25/.08 and filled by the single cone technique and Bio-C Sealer or AH Plus (n = 12). Retreatment was performed using ProDesign Logic (PDL) RT and apical preparation was performed with PDL 35/.05. The samples were scanned by micro–CT at 5 μm before and after the retreatment. Then, to analyze the influence of voxel size on the evaluation of remaining filling material, images with sub-resolution of 10 and 20 μm voxel sizes were obtained. The percentage of remaining filling material was assessed, and data were submitted to the one-way ANOVA and non-paired t-tests at a significance level of 5%. Micro-CT images using different voxel sizes did not influence the analyze of remaining filling material independently of the sealer, AH Plus or Bio-C Sealer ($p > .05$). The root canals filled with Bio-C Sealer had lower percentage of remaining filling material in comparation with AH Plus ($p < 0.05$). Within the limitations of this “ex vivo” study, it can be concluded that voxel sizes used did not influence the analyzes of residual filling material in both sealers evaluated. Bio-C sealer was removed easier than AH Plus during endodontic retreatment.

KEYWORDS

calcium silicate, dental materials, root canal filling, x-ray microtomography

---

* Artigo em revisão no periódico *Microscopy Research and Technique.*

Graphical Abstract

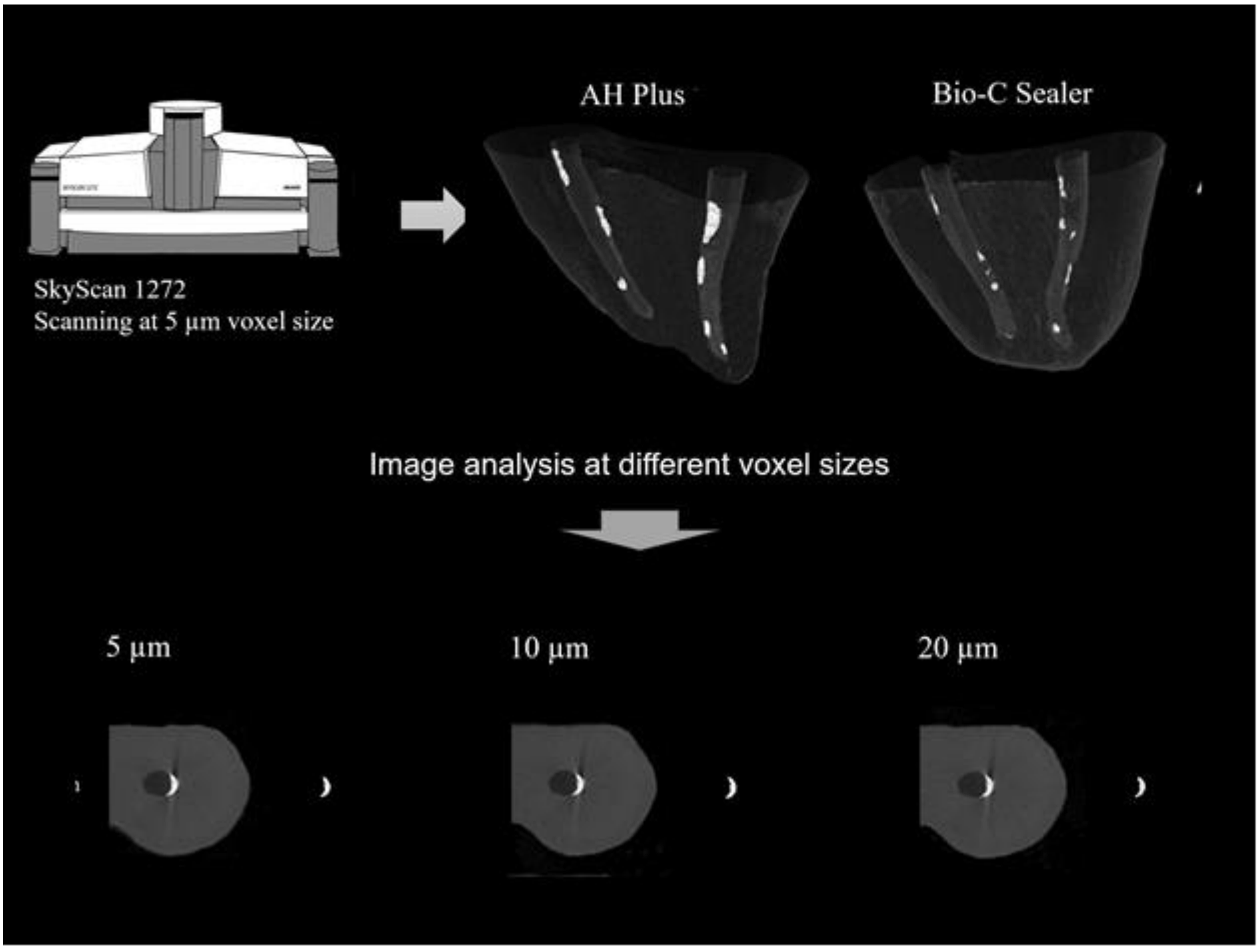

Introduction

Recontamination or bacterial permanence within the root canal system is the main reason for the failure of endodontic treatment (Torabinejad, Corr, Handysides, & Shabahang, 2009). During retreatment procedures, the filling material removal is necessary to disinfect the root canal system (Cavenago et al., 2014). However, retreatment techniques are not able to remove completely root canal filling materials (Rossi-Fedele, & Ahmed, 2017).

Micro computed tomography (micro-CT) have been wildly used for volumetric quantification of remaining filling material after endodontics retreatments (Rödig et al., 2012; Bernardes et al., 2016). However, there is no standardization regarding the scanning parameters used for micro-CT evaluations (Rödig et al., 2012; Alves et al.,2016; Bernardes et al., 2016). Although the conflicting results among studies have been attributed to the filling material, teeth anatomy and the retreatment technique (Rödig et al., 2012; Silveira, et al., 2018), the voxel size of the micro-CT images must also be taken into account. Due to the effect of partial volume, voxel size may affect the quality of micro-CT images, and consequently decreases the accuracy the analyses performed (Bouxsein et al., 2010).

Different endodontic sealers associated to gutta-percha are usually used for filling root canals (Kratchman, 2004). The analysis of remaining filling material by micro-CT may be even more difficult when different sealers are compared, since they different radiopacities makes difficult the images standardization (Viapiana, et al., 2016). AH Plus (DentsplyDeTrey, Konstanz, Germany) is an epoxy resin-based root canal sealer considered the gold standard due to its excellent physicochemical properties (Silva et al., 2017). Bio-C Sealer (Angelus, Londrina, PR, Brazil) is a premixed ready-to-use calcium silicate–based sealer. Bio-C has radiopacity and flow properties in accordance with the ISO 6876:2012, besides alkalization ability, cytocompatibility and mineralization capacity   (Candeiro et al., 2012; López-García et al., 2019).

To the best of the authors' knowledge, no study has assessed the influence of voxel size on micro-CT analysis of remaining filling material, as well the influence of the different radiopacity of endodontic sealers. Therefore, the aim of the present study was to assess the remaining filling material after retreatment of curved root canal filled with AH Plus or Bio-C Sealer using micro-CT images with different voxel size. The null hypothesis was that there would be no differences between the analyses performed using images with different voxel sizes.

Materials and methods

Sample size calculation

G* Power 3.1.7 for Windows program (Heinrich-Heine-Universitat Dusseldorf, Dusseldorf, Germany) was used for the sample calculation. The t-test for two dependent groups was used with an Alpha type error of 0.05 and Beta power of 0.95 for all the variables. Previous study was used to determine the effect size for amount of remaining filling material, 2.348 (Alves et al., 2016). A total of 10 specimens was indicated as being the ideal size required.

Sample selection

All procedures were approved by the Faculty's Ethics Committee (CEP no. No. 10411219.9.0000.5416). Human mandibular first and second molars previously stored in 0.1% thymol solution at 5°C were used. The inclusion criteria included two independent mesial root canals according type IV Vertucci's classification (Vertucci, 1984), angle of curvature between 25° and 35° in accordance with the Schneider method (Schneider, 1971), and radius of curvature smaller than 10 mm, following the Pruett's method (Pruett, Clement, & Carnes, 1997). Complete apical formation, absence of root fractures, calcifications or internal resorptions were also included. For this purpose, a digital system (RVG 6100; Kodak Dental Systems, NY) and a micro-CT device (SkyScan 1276; Bruker-microCT, Kontich, Belgium) were used. Micro-CT was applied at a low-resolution (35 µm voxel size) under the following settings: copper and aluminum filters, 87-millisecond exposure time, frame averaging of 3, 180° rotation around the vertical axis, rotational step of 0.5° at 80 kV and 300 µA. A total of twelve roots were selected, totalizing twenty-four root canals, including mesiobuccal and mesiolingual canal of each root.

Root canal preparation

Conventional access cavities were performed, and the root canals were explored by using a size #10 K-file (Dentsply Sirona Endodontics, Ballaigues, Switzerland). The working length (WL) was established 1 mm shorter from the apical foramen. For preparation, HyFlex EDM (HEDM; Coltene/Whaledent, Altstätten, Switzerland) 10/.05

was operated by electric motor VDW SILVER (VDW GmbH, Munich, Germany) in rotary motion at 300 rpm and torque 1.8 Ncm, with in-and-out movements up to the WL. Then, HEDM 25/.08 was used at 500 rpm and torque 2.5 Ncm, as described above. Each root canal was irrigated with 5 mL of 2.5% sodium hypochlorite (NaOCl). Passive ultrasonic irrigation (PUI) was performed in all root canals with the ultrasonic tip Irrisonic (Helse Ultrasonic, Santa Rosa de Viterbo, SP, Brazil) activated in an ultrasonic device Ultrawave XS (Ultradent, South Jordan, USA) using a power of 10 % and frequency of 50 Hz, according to the manufacturer's recommendation. The ultrasonic tips were positioned 2 mm short of the WL and activated for 20 seconds, interleaving 2.5% NaOCl, and 17% EDTA. 2 mL of irrigation solution was used in each cycle. As final irrigation, 5 mL of distilled water was used.

Root canal filling

A stratified random sampling statistical method was used to divide the root canals in two experimental groups, considering the post-preparation volume (n = 12). The root canals were dried with paper points and filled by single cone technique with gutta-percha cones 25/.08 (Coltene/Whaledent, Langenau, Germany) and an epoxy resin-based sealer (AH Plus; Dentsply DeTrey, Konstanz, Germany) or a calcium silicate-based material (Bio-C Sealer; Angelus, Londrina, PR, Brazil). AH Plus was inserted into the root canal with a Lentulo spiral #25 (Dentsply Maillefer) coupled to a low speed motor (Micromotor N270 and Counter-angle, Dabi-Atlante, Ribeirão Preto, SP, Brazil). Bio-C Sealer was injected into the root canal at 4 mm of the WL, using the syringe and plastic needles provided by its manufacturer. The access cavities were filled with Coltosol (Vigodent, Rio de Janeiro, RJ, Brazil). The samples were stored at 37º C and 95% relative humidity for 1 week to allow the sealers to set completely.

Root canal retreatment

Electric motor VDW SILVER, in rotary motion at 600 rpm and torque 3 Ncm was used. The files were used with in-and-out movements up to the WL. ProDesign Logic RT (PDLRT - Easy Equipamentos Odontológicos, Belo Horizonte, MG, Brazil) 30/10 was used to remove the filling of the cervical third, PDLRT 25/.08 was used in the middle third and PDLRT 20/.06 was used to remove the filling of the apical third. The root canals were enlarged with PDL 35/.05 as described above. Each root canal was irrigated with 8 mL of 2.5% NaOCl (2 mL for each instrument). Final irrigation was performed using 2.5 ml of 17% EDTA, under agitation for 3 minutes, with a gutta-percha cone size 25, followed by 5 mL of distilled water.

Micro-CT analysis

The specimens were scanned at a high-resolution (5 µm voxel size) in a micro-CT device (SkyScan 1272. Bruker, Kontich, Belgium) before and after retreatment procedures under the following settings: copper filter, 180° rotation around the vertical axis and rotational step of 0.2° at 100 kV and 100 µA. The images were reconstructed using the NRecon software (V1.6.10.4; Bruker, Belgium), and superimposed with geometric alignment using the DataViewer software (V.1.5.1, Bruker, Belgium). For quantitative analysis, images at 5, 10 and 20 µm were segmented using the CTAn software (V.1.14.4, Bruker, Belgium). For this purpose, the previously scanned 5 µm images were resized by 2 and 4, respectively (Figure 1). The quantitative analysis was performed using the CTAn software (V.1.14.4, Bruker, Belgium). Representative images were performed by means of models obtained by CTVox software (v.3.2; Bruker-microCT).

Root canal volume and remaining filling material were quantified after retreatment steps. The gray scale range required to recognize each object under study was determined in a density histogram by using the global threshold method. To obtain the percentage of remaining filling material the following formula was used: [Percentage remaining filling material = (filling material after retreatment x 100 / filling material before retreatment)]. The analyzes were performed in the apical third of the root canals considering 4 mm.

Statistical analysis

Shapiro-Wilk test was used to test the data normality. The comparations between the sealers regarding the percentage of remaining filling material was performed using non-paired t-test. ANOVA test was used for comparation among different voxel size. The level of significance was set at 5%.

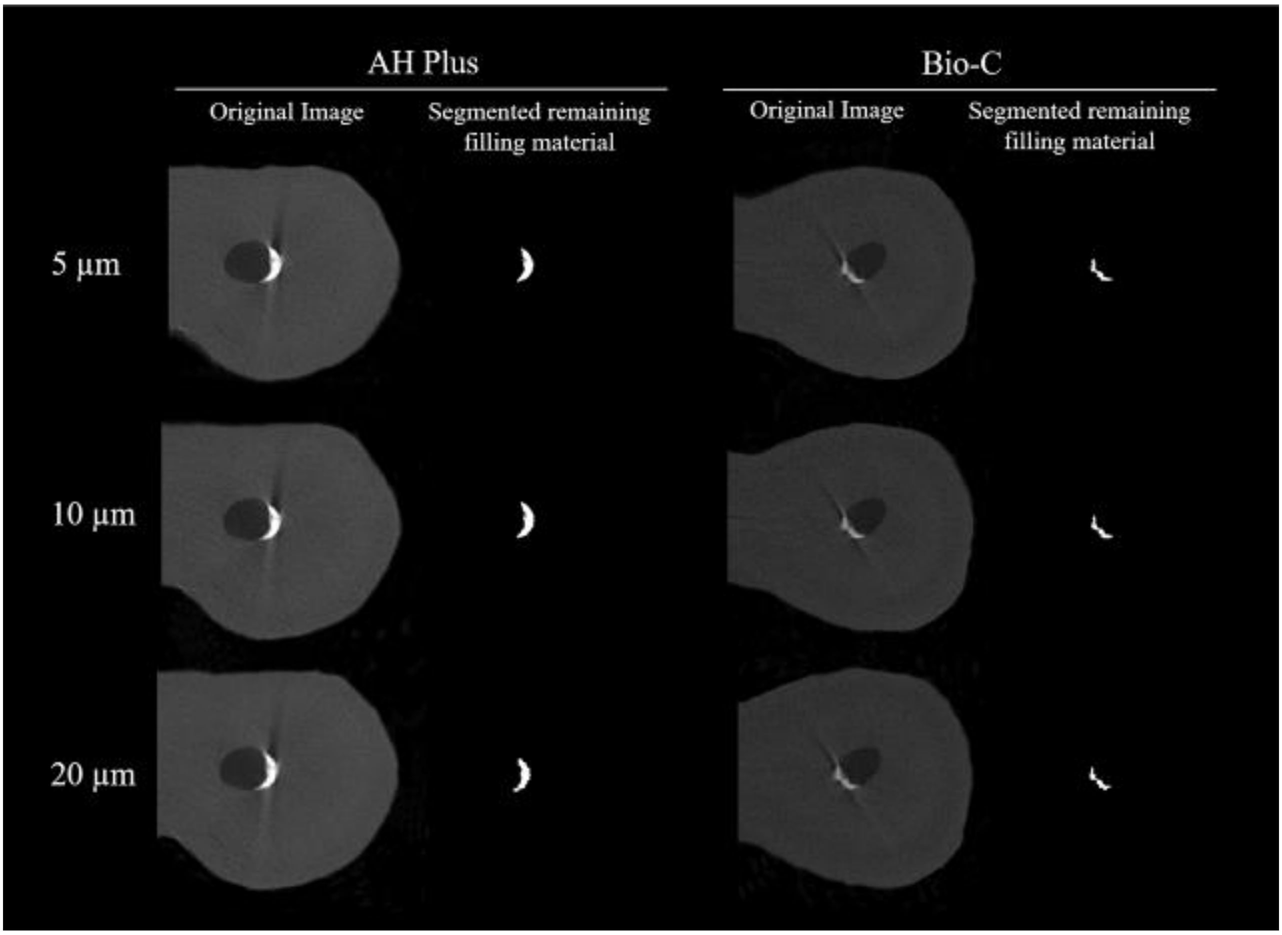

Figure 1 - Representative cross-sectional micro–CT images showing the original images and the segmentation of remaining filling material at different voxel sizes.

Results

Table 1 shows the mean and standard deviations of the percentage of remaining filing material in root canal filled with AH Plus or Bio-C Sealer after retreatment until PDL 35/.05, considering the analysis performed at the different voxel sizes (5, 10 and 20 µm). Micro-CT images using different voxel sizes did not influence the analyze of remaining filling material independently of the sealer, AH Plus or Bio-C Sealer ($p > .05$). The root canals filled with Bio-C Sealer had lower percentage of maiming filling material in comparison with AH Plus ($p < 0.05$) (Figure 2).

Table 1 - Mean and standard deviation of percentage volume of remaining filling material in the apical third of the root canals after endodontic retreatment

	5 µm	10 µm	20 µm
AH Plus	16.46 ± 3.44[a]	16.23 ± 3.51[a]	16.11 ± 3.22[a]
Bio-C	8.33 ± 2.44[b]	8.22 ± 2.41[b]	8.08 ± 2.85[b]

Note. There was not significantly different among the voxel sizes (*p* > .05). Different lowercase letters on same column represent significant differences between groups (p < .05).

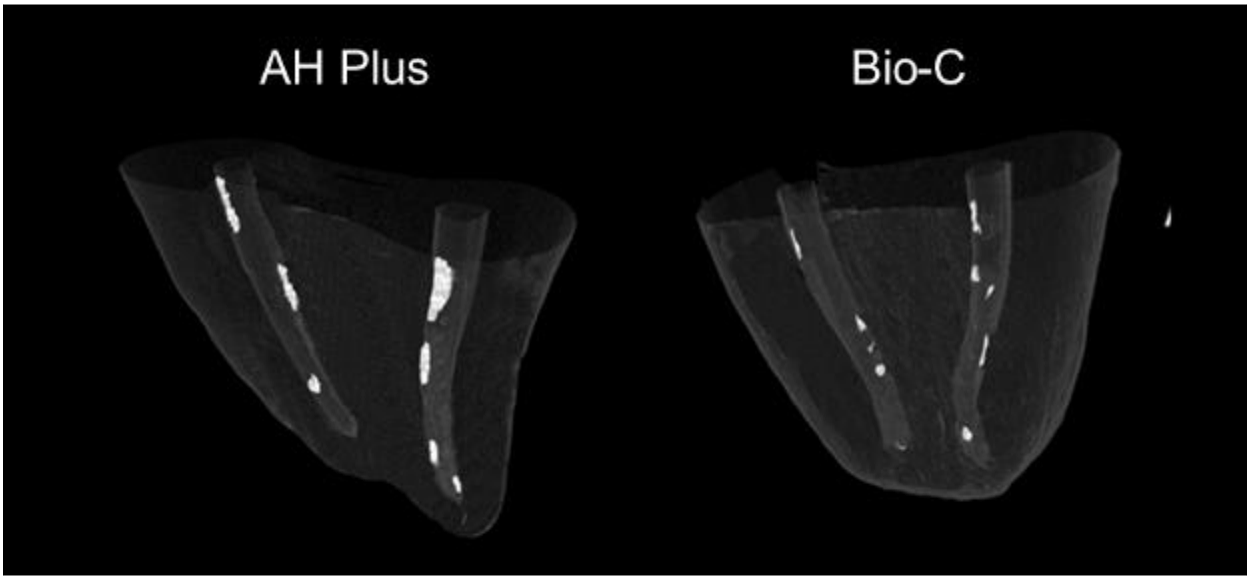

Figure 2 - Tree-dimensional reconstructions of images obtained by micro-CT showing in white remaining filling material in the apical third of mesial canals of mandibular molars.

Discussion

To the best of the authors' knowledge, this was the first study to assess the influence of micro-CT voxel size and sealer radiopacity on retreatments assessments. Previous studies have demonstrated the influence of voxel size on different kind of evaluations, such as trabecular bone structure (Kim et al., 2004; Sode et al., 2008) and voids in filled root canals (Orhan et al., 2018). However, in this study, the null hypothesis was accepted, since the voxel size did not influence the volumetric analysis of remaining filing material after endodontic retreatment independently of the sealer used in the filling, AH Plus or Bio-C sealer.

In the present study, the samples were scanned at 5 µm and subsequently, the reconstructed images were resized by 2 and 4 to acquire images with 10 and 20 µm voxel sizes. This study design allows precise evaluation of the effect of voxel size on micro-CT analysis, with accurate comparisons among the same regions (Pinto et al., 2020). However the spatial resolutions of images also depends of other acquisitions parameters, such as mean absorption of the sample, detector noise, reconstruction algorithm, X-ray focal spot size and shape, detector aperture, and scanner geometry (Bouxsein et al., 2021). Therefore, despite the fact the new values produced for the images resized to larger voxel sizes leads to a decrease in the accuracy of the image (Kim et al., 2004), because the partial effect volume (Heckel, et al., 2014). The adequate scans parameters used in the images acquisitions produced images with high quality, even with higher voxel size.

The radiodensity of the structures scanned by micro-CT influences beam hardening formation, affecting the final quality of the images (Celikten et al., 2019). Therefore, the different radiopacity among the endodontic sealers may be a concern for micro-CT analyzes (Viapiana et al., Celikten et al., 2019). AH Plus has higher radiopacity than Bio-C Sealer (Zordan-Bronzel et al. 2019), and there was reported that the radiopacifiers presented in the AH Plus composition may cause a larger extent of artifact than the calcium silicate–based sealers (Celikten et al., 2019). However, in the present study the different sealers used for root canal filling did not influence the findings. Both sealers had radiopacity above 3 mm aluminum, as recommended by the ISO 6876 standard (Zordan-Bronzel et al. 2019). In addition, the high energy (100 kV) and high intensity (100 µAP) for sample scans may have minimized the influence of the sealer on the final quality of the images.

The remaining filling material may impair root canal disinfection allowing the maintenance of periapical inflammation (Siqueira Jr., 2001). Anatomical challenges, such as curved root canals become the success of endodontic retreatment unpredictable (Kırıcı, Demirbuga, & Karataş, 2020). Therefore, in this study, Bio-C sealer was easier removal of curved root canal than AH Plus. In agreement, a previous study have shown a higher removal of calcium silicate-based sealers compared with AH Plus (Donnermeyer et al., 2018). This behavior may be explained for the higher solubility presented for the Bio-C sealer when compared with AH Plus (Torres et al., 2020). In addition, the high bond strength of AH Plus may contribute to its adhesion to the dentine walls, making difficult its removal (Carvalho et al., 2017; Donnermeyer et al., 2018).

The similar results achieved in micro-CT analyses using images with different voxel sizes is an important finding for further research. Although a smaller voxel size is ideal for micro-CT analysis (Christiansen, 2016), high-resolution scans require longer acquisition time, and generate large data sets. In addition, several endodontic sealers based on calcium silicates have been introduced to the market; therefore, it is important to evaluate their impact in the retreatment procedures.

Within the limitation of this ex vivo study, it may be concluded that the different voxel sizes used did not influences the volumetric analyses of remaining filling material. The findings were not influenced by sealers with different radiopacity, as long as there according to ISO 6876. Bio-C Sealer was easier removal from curved root canal than AH Plus.

Conflict of Interest

The authors deny any conflicts of interest related to this study.

References

.Alves, F. R., Marceliano-Alves, M. F., Sousa, J. C., Silveira, S. B., Provenzano, J. C., & Siqueira, J. F., Jr (2016). Removal of Root Canal Fillings in Curved Canals Using Either Reciprocating Single- or Rotary Multi-instrument Systems and a Supplementary Step with the XP-Endo Finisher. *Journal of Endodontics*, 42, 1114–1119. https://doi.org/10.1016/j.joen.2016.04.007

Bernardes, R.A., Duarte, M.A., Vivan, R.R., Alcalde, M.P., Vasconcelos, B.C., & Bramante, C.M. (2016) Comparison of three retreatment techniques with ultrasonic activation in flattened canals using micro-computed tomography and scanning electron microscopy. *International Endodontic Journal*, 49, 890-897. https://doi.org/10.1111/iej.12522

Bouxsein, M.L., Boyd, S.K., Christiansen, B.A., Guldberg, R.E., Jepsen, K.J., & Muller, R. (2010) Guidelines for assessment of bone microstructure in rodents using micro-computed tomography. *J Bone Miner Res*, 25, 1468-1486. https://doi.org/10.1002/jbmr.141

Candeiro, G.T., Correia, F.C., Duarte, M.A., Ribeiro-Siqueira, D.C., & Gavini, G. (2012) Evaluation of radiopacity, pH, release of calcium ions, and flow of a bioceramic root canal sealer. *Journal do Endodontics*, 38, 842-845. https://doi.org/10.1016/j.joen.2012.02.029

Carvalho, C. N., Grazziotin-Soares, R., de Miranda Candeiro, G. T., Gallego Martinez, L., de Souza, J. P., Santos Oliveira, P., Bauer, J., & Gavini, G. (2017) Micro Push-out Bond Strength and Bioactivity Analysis of a Bioceramic Root Canal Sealer. *Iranian Endodontic Journal*, 12, 343-348. https://doi.org/10.22037/iej.v12i3.16091

Cavenago, B. C., Ordinola-Zapata, R., Duarte, M. A., del Carpio-Perochena, A. E., Villas-Bôas, M. H., Marciano, M. A., Bramante, C. M., & Moraes, I. G. (2014) Efficacy of xylene and passive ultrasonic irrigation on remaining root filling material during retreatment of anatomically complex teeth. *International Endodontic Journal,* 47, 1078-1083. https://doi.org/10.1111/iej.12253

Celikten, B., Jacobs, R., de Faria Vasconcelos, K., Huang, Y., Shaheen, E., Nicolielo, L., & Orhan, K. (2019). Comparative evaluation of cone beam CT and micro-CT on blooming artifacts in human teeth filled with bioceramic sealers. *Clinical Oral Investigations,* 23, 3267-3273. https://doi.org/10.1007/s00784-018-2748-8

Christiansen B. A. (2016). Effect of micro-computed tomography voxel size and segmentation method on trabecular bone microstructure measures in mice. *Bone Reports*, 5, 136–140. https://doi.org/10.1016/j.bonr.2016.05.006

Donnermeyer, D., Bunne, C., Schäfer, E., & Dammaschke T. (2018) Retreatability of three calcium silicate-containing sealers and one epoxy resin-based root canal sealer with four different root canal instruments. *Clinical Oral Investigations*, 22, 811-817. https://doi.org/10.1007/s00784-017-2156-5

Donnermeyer, D., Dornseifer, P., Schäfer, E., & Dammaschke, T. (2018) The push-out bond strength of calcium silicate-based endodontic sealers. *Head Face Med*, 14, 13. The push-out bond strength of calcium silicate-based endodontic sealers

Heckel, F., Meine, H., Moltz, J. H., Kuhnigk, J. M., Heverhagen, J. T., Kiessling, A., Buerke, B., & Hahn, H. K (2014) Segmentation-based partial volume correction for volume estimation of solid lesions in CT. *IEEE Trans Med Imaging*, 33, 462-480. https://doi.org/10.1109/TMI.2013.2287374

Kim, D.G., Christopherson, G.T., Dong, X.N., Fyhrie, D.P., & Yeni, Y.N. (2004) The effect of microcomputed tomography scanning and reconstruction voxel size on the accuracy of stereological measurements in human cancellous bone. *Bone,* 35, 1375-1382. https://doi.org/10.1016/j.bone.2004.09.007

Kim, D.G., Christopherson, G.T., Dong, X.N., Fyhrie, D.P., & Yeni, Y.N. (2004) The effect of microcomputed tomography scanning and reconstruction voxel size on the accuracy of stereological measurements in human cancellous bone. *Bone,* 35, 1375-1382. https://doi.org/10.1016/j.bone.2004.09.007

Kırıcı, D., Demirbuga, S., & Karataş, E. (2020) Micro-computed Tomographic Assessment of the Residual Filling Volume, Apical Transportation, and Crack Formation after Retreatment with Reciproc and Reciproc Blue Systems in Curved Root Canals. Journal of Endodontic 2020;46:238-243. https://doi.org/10.1016/j.joen.2019.11.003

Kratchman, S.I. (2004) Obturation of the root canal system. *Dent Clin North Am*, 48, 203-215. https://doi.org/10.1016/j.cden.2003.12.004

López-García, S., Pecci-Lloret, M.R., Guerrero-Gironés, J., et al. (2019) Comparative Cytocompatibility and Mineralization Potential of Bio-C Sealer and TotalFill BC Sealer. *Materials (Basel)*,12. 3087. https://doi.org/10.3390/ma12193087

Orhan, K., Jacobs, R., Celikten, B., Huang, Y., de Faria Vasconcelos, K., Nicolielo, L., Buyuksungur, A., & Van Dessel, J. (2018) Evaluation of Threshold Values for Root Canal Filling Voids in Micro-CT and Nano-CT Images. *Scanning*, 9437569. https://doi.org/10.1155/2018/9437569

Pinto, J. C., Torres, F. F. E., Santos, A. O., Tavares, K. I. M. C., Guerreiro-Tanomaru, J. M., & Tanomaru-Filho, M. (2020). Influence of voxel size on micro-CT analysis of debris after root canal preparation. *Brazilian Oral Research*, 35. https://doi.org/10.1590/1807-3107bor-2021.vol35.0008

Pruett, J. P., Clement, D. J., & Carnes, D. L. (1997). Cyclic fatigue testing of nickel-titanium endodontic instruments. *Journal of Endodontics,* 23, 77-85. https://doi:10.1016/S0099-2399(97)80250-6

Rödig, T., Hausdorfer, T., Konietschke, F., et al. (2012) Efficacy of D-RaCe and ProTaper Universal Retreatment NiTi instruments and hand files in removing gutta-percha from curved root canals: a micro-computed tomography study. *International Endodic Journal,* 45, 580–589. https://doi.org/10.1111/j.1365-2591.2012.02014.x

Rossi-Fedele, G., & Ahmed, H.M. (2017) Assessment of Root Canal Filling Removal Effectiveness Using Micro-computed Tomography: A Systematic Review. *Journal of Endodontics*, 43, 520-526. https://doi.org/10.1016/j.joen.2016.12.008

Schneider, S. W. (1971). A comparison of canal preparations in straight and curved root canals. *Oral Surgery, Oral Medicine and Oral Pathology,* 32, 271-275.

Silva Almeida, L.H., Moraes, R.R., Morgental, R.D., & Pappen, F.G. (2017) Are Premixed Calcium Silicate-based Endodontic Sealers Comparable to Conventional Materials? A Systematic Review of In Vitro Studies. *Journal of Endodontics*, 43, 527-535. https://doi.org/10.1016/j.joen.2016.11.019

Silveira, S. B., Alves, F. R., Marceliano-Alves, M. F., Sousa, J. C. N., Vieira, V. T., Siqueira Jr, J. F., ... & Provenzano, J. C. (2018). Removal of root canal fillings in curved canals using either Mani GPR or HyFlex NT followed by passive ultrasonic irrigation. Journal of endodontics, 44(2), 299-303. https://doi.org/10.1016/j.joen.2017.09.012

Siqueira Jr, J.F. (2001) Aetiology of root canal treatment failure: why well-treated teeth can fail. International Endodontic Journal, 34, 1-10. https://doi.org/10.1046/j.1365-2591.2001.00396.x

Sode, M., Burghardt, A.J., Nissenson, R.A., & Majumdar, S. (2008) Resolution dependence of the non-metric trabecular structure indices. *Bone,* 42, 728-736. https://doi.org/10.1016/j.bone.2007.12.004

Torabinejad, M., Corr, R., Handysides, R., & Shabahang, S. (2009) Outcomes of nonsurgical retreatment and endodontic surgery: a systematic review. *Journal of Endodontics*, 35, 930-937. https://doi.org/10.1016/j.joen.2009.04.023

Torres, F.F.E., Zordan-Bronzel, C.L., Guerreiro-Tanomaru. J.M., Chávez-Andrade, G.M., Pinto, J.C., & Tanomaru-Filho, M. (2020) Effect of immersion in distilled water or phosphate-buffered saline on the solubility, volumetric change and presence of voids within new calcium silicate-based root canal sealers. *International Endodontic Journal*, 53, 385-391. https://doi.org/10.1111/iej.13225

Vertucci, F. J. (1984). Root canal anatomy of the human permanent teeth. *Oral Surgery, Oral Medicine and Oral Pathology,* 58, 589-599. https://doi:10.1016/0030-4220(84)90085-9

Viapiana, R., Moinzadeh, A.T., Camilleri, L., Wesselink, P.R., Tanomaru Filho, M., & Camilleri J. (2016) Porosity and sealing ability of root fillings with gutta-percha and BioRoot RCS or AH Plus sealers. Evaluation by three ex vivo methods. International Endodontic Journal, 49, 774-782. https://doi.org/10.1111/iej.12513

Zordan-Bronzel, C.L., Esteves Torres, F.F., Tanomaru-Filho, M., Chávez-Andrade, G.M., Bosso-Martelo, R., & Guerreiro-Tanomaru, J.M. (2019) Evaluation of Physicochemical Properties of a New Calcium Silicate-based Sealer, Bio-C Sealer. *Journal of Endodontic*, 45, 1248-1252. https://doi.org/10.1016/j.joen.2019.07.006

3.7 Publicação 7*

Evaluation of ten cone-beam computed tomography devices for endodontic assessment of fine anatomical structures

Abstract

Aim: To classify ten CBCT devices, by using a ranking model, according to the detection of fine endodontic structures. **Methods:** A dedicated dentate anthropomorphic phantom was scanned two times using ten CBCT devices: without any metal (metal-free condition) and with an endodontically treated tooth containing a metallic pin (metal condition). A reference image acquired on an industrial micro-CT device was used to register all CBCT images, yielding corresponding anatomic slices. Afterwards, three experienced observers assessed all acquired CBCT images for their ability to assess narrow canal, isthmus and apical delta ramification following a categorical rank from 1 (best) to 10 (worst). Fleiss Kappa statistics were used to calculate intra- and interobserver agreements for each CBCT device separately. Based on the observers` scores, general linear mixed models were applied to compare image quality among different CBCTs for performing endodontic diagnostic tasks (α = .05). **Results:** The ten CBCT devices performed differently for the evaluated endodontic tasks (P < .05), with three devices performing better for endodontic feature detection. Yet, in the presence of metal, only two devices were able to keep a high level of endodontic feature detection. C**onclusions:** The evaluated endodontic tasks were CBCT device-dependent, and its detection was influenced by the presence of metal.

Keywords: Anatomy, artifacts, cone-beam computed tomography, endodontics.

---

* Artigo publicado no periódico *Journal of Endodontics.* (https://doi.org/10.1016/j.joen.2021.02.013).

Introduction

The assessment of fine structures, such as narrow canal, isthmus and ramifications may directly impact endodontic treatment planning and outcomes(1-3). Cone-beam computed tomography (CBCT) may be an auxiliary tool for detecting and locating such structures (1, 2, 4, 5). However, CBCT-based diagnosis is hampered by artifacts arising from high-density materials such as gutta percha, sealers, and metallic posts/pins (6-9). Therefore, an accurate CBCT performance remains challenging.

Another challenge is the difficulty of comparing performances from different devices, as results found for one CBCT cannot simply be applied to another (10, 11). Thus, caution is needed when interpreting CBCT-based reports on endodontic purposes (2,12-18). Although previous studies have shown high sensitivity and specificity for CBCT images (2, 13), other studies showed no significant difference between this image modality and 2D images for performing different tasks (15, 17, 18). This variability may be explained due to the wide diversity of CBCT devices available on the market, with distinct technical characteristics and consequently different clinical performance (19, 20). Additionally, the diagnostic tasks must also be taken into account, since the size of the structures may directly affect their visualization (14).

In clinical scenarios, image quality provided by several CBCT devices may differ significantly, especially in the presence of artifacts generated by high-density objects (21). Therefore, our study aimed to classify ten CBCT devices, by using a ranking model, according to the detection of fine endodontic structures in the presence and absence of a metallic pin. For such purpose, CBCT images of narrow canals, isthmus, and apical delta were evaluated. The null hypothesis was that all CBCTs performed similarly for all tasks.

Material and Methods

This experimental study was designed according to the local institutional research ethics committee (protocol number S55619/ML9535). An anthropomorphic phantom composed of a dry human skull and a mandible with all teeth was covered with Mix-D. A mixture of paraffin wax and other chemicals prepared according to Oenning et al 2019 to simulate soft tissue attenuation (22). A mix-D tongue model was positioned in the corresponding space of the phantom (Figure 1A). Two set-ups were created: 1) Metal-free condition: without any metal (Figure 1B); 2) Metal condition: the same model with the second lower premolars endodontically treated and the right premolar containing a gold alloy metallic pin made in-house (Figure 1C). The root canals were prepared with Reciproc R25 file (VDW, Munich, Germany) and filled by lateral compaction using AH Plus sealer (Dentsply DeTrey GmbH, Konstanz, Germany). Additionally, silicone guides made with Zetaplus silicone (Zhermack SpA, Badia Polesine, Italy) were used to reproduce the positioning of the teeth for image acquisition.

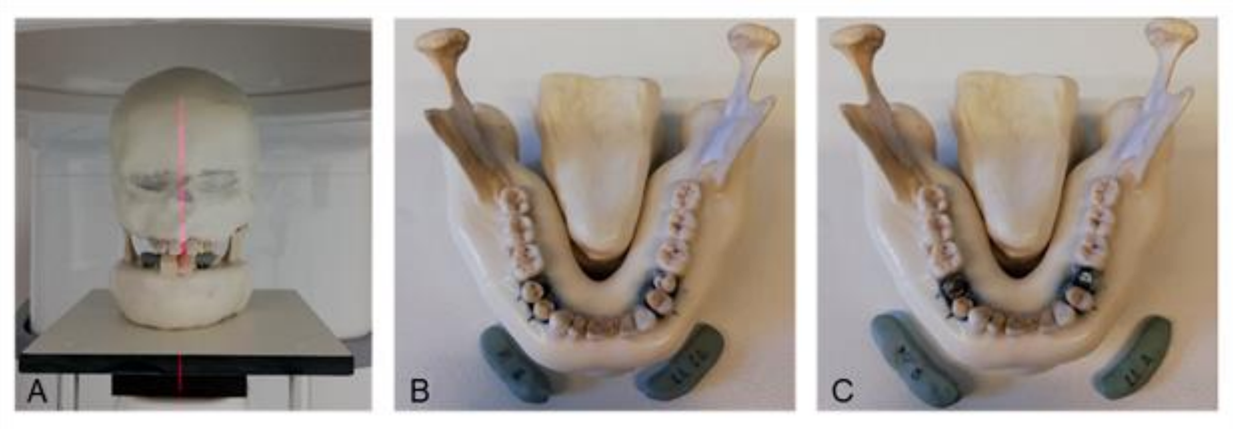

Figure 1 - A) Phantom of a dry human skull with mandible covered in mix-D; B) set-up 1 - mandible without metal; C) set-up 2 - mandible with endodontic treated premolars with metallic pin and amalgam restoration.

Reference image acquisition

In order to acquire a reference image, the mandible was scanned in an industrial micro-CT scanner Nikon XT H 225 (Nikon Metrology Inc, Brighton, MI, USA) using 200 kVp, 350 µA, 2.5 mm Cu filtration, and 40 µm voxel size. This industrial CT reference image was used by one independent examiner to initially evaluate the presence of the fine anatomical structures and mainly to register all CBCT images. Accordingly, this ensured CBCT evaluation of each endodontic task at the same anatomical level by other three experienced observers (Figure 2).

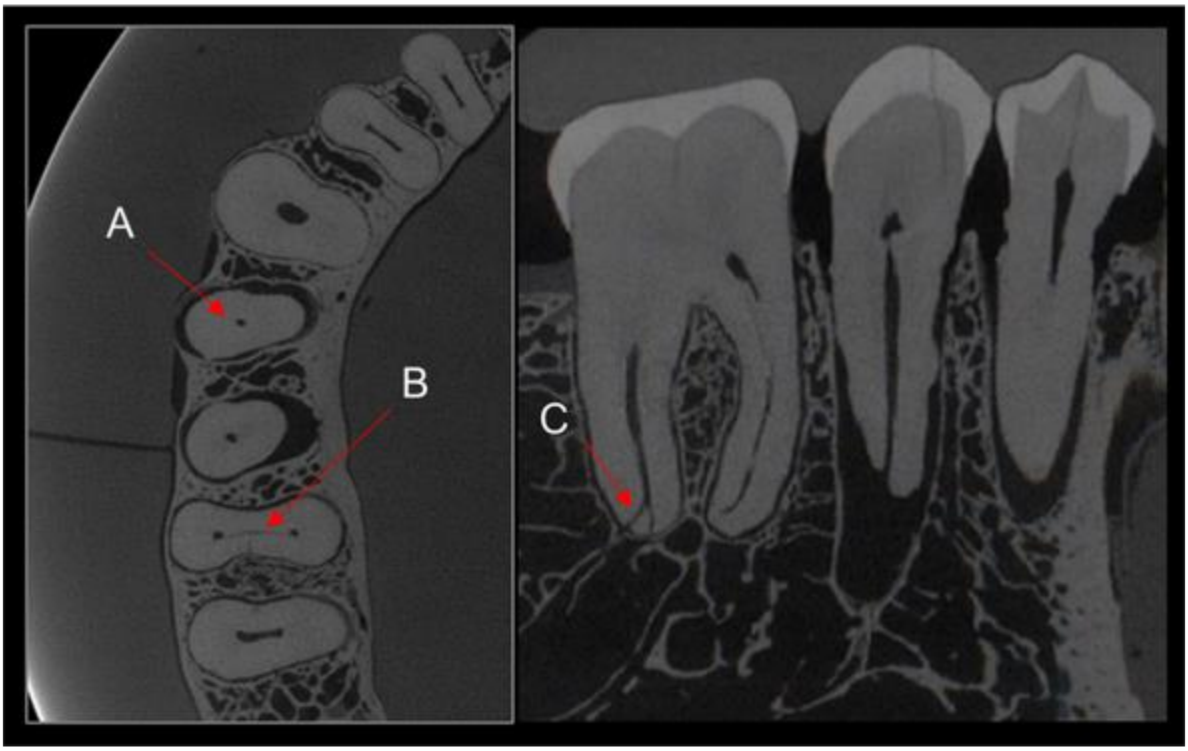

Figure 2 - Reference images (axial and sagittal views) from industrial micro-CT showing all evaluated endodontic diagnostic tasks. A – narrow canal, B – isthmus, C – delta.

CBCT imaging acquisitions

The two aforementioned set-ups were scanned using ten each CBCT devices. Clinical high-resolution exposure parameters were selected in each CBCT device and coded using letters (A to J). Table 1 shows all CBCT devices, manufacturers, codes, and exposure parameters.

Table 1 - CBCT devices, manufacture, codes and comparable scanning parameters

CBCT devices	Manufactures	Code	FOV (mm)	kVp	mA	Voxel (mm)
3D Accuitomo 170	J. Morita, Tokyo, Japan	A	4 X 4	90	5	0.08
Veraview X800	J. Morita, Tokyo, Japan	B	4 X 4	100	7.9	0.08
3Shape X1	3Shape, Copenhagen, Denmark	C	4 X 4	90	12	0.1
NewTom VGi evo	Cefla Dental Group, Imola, Italy	D	5 X 5	110	3	0.1
OP 3D Pro	Instrumentarium, Helsinki, Finland	E	5 X 5	90	8.6	0.085
OP 3D	Instrumentarium, Helsinki, Finland	F	5 X 5	95	4	0.08
CS 9300	Carestream, Rochester, USA	G	5 X 5	90	4	0.09
ProMax 3D Max	Planmeca, Helsinki, Finland	H	6 X 6	96	12	0.075
Orthophos SL 3D	Dentsply Sirona, Charlotte, USA	I	5 X 5	85	6	0.079
Spectral Dental UEG	UEG Medical, Shangai, China	J	6 X 6	110	8	0.075

Image registration

Subsequently, mutual information-based registration was performed using Amira 2019 software (Thermo Fisher Scientific, Waltham, USA / Zuse Institute Berlin, Germany) considering the industrial micro-CT scan as reference image. This method measures the statistical dependence or information redundancy between image intensities of corresponding voxels in both images, which is assumed to be maximal if images are geometrically aligned (23). Therefore, reference image (micro-CT) was used to initially detect the presence of the fine anatomical structures and mainly to register CBCT images, ensuring CBCT evaluation of each endodontic structure at the same anatomical level by the three observers.

Subjective image quality assessment

After image registration a set of CBCT images containing each anatomical structure separately was shown to three experienced observers (Figure 2). These observers have been previously trained and calibrated. Images were randomly displayed on the same screen without showing the reference image and the observers were blinded to the CBCT device. Brightness, contrast, and magnification of the image could not be modified and adjusted by the observers. All images were ranked from 1 (best) to 10 (worst) for their ability to detect the fine anatomical structures. Calibration and evaluation sessions were performed in a low-light environment using a 24.1-inch flat-screen monitor (Barco, Kortrijk, Belgium). After 30 days, 25% of the images were re-evaluated to assess intra-observer reproducibility.

Statistical analysis

Statistical modeling and analysis were performed using S-Plus for Linux 8.0 (Tibco Software, Palo Alto, CA, USA). Fleiss Kappa statistics were used to calculate intra- and interobserver agreements for each CBCT device separately. This analysis was based on the observers` scores transformed into a binary variable. The cumulative percentage that each device was ranked among the best five devices were compared between the first and second observations (for intra-observer agreement) and between observers (for inter-observer agreement). Cases in which a specific device was always classified among the best five were considered as perfect agreement.

General linear mixed (GLM) models were applied to compare different CBCT devices in the accomplishment of diagnostic tasks. The models were fit with observers and questions related to the tasks as the random variables and CBCT devices as fixed variables to perform the ranking. This analysis intended to choose the best devices. In the evaluation of challenging endodontic structures using two different clinical conditions (metal-free and with metal). Differences between CBCT images for each purpose were calculated using the fixed effects from the GLM models and their variance-covariance matrix. A correction for simultaneous hypothesis testing according to Tukey was applied. Differences among devices were assessed by first considering the empirical cumulative function of the scores by dividing each score rank by (1+number of scores). These empirical cumulative function values were then subject to probit transformation, in which the corresponding quantiles of a standard normal distribution were taken. Subsequently, a multiple comparison with the hypothetical best and worst device for each task and condition (higher and lower score) was performed at 95% confidence interval. Residual analysis of the GLM models via a normal quantile plot showed that the assumptions of normality of residuals was achieved when using the probit transformed values.

Results

A perfect intra-observer agreement was found in four CBCT devices (A to D). For CBCT devices E to J, kappa values ranged between 0.33 and 0.99. Regarding inter-observer agreement, a perfect agreement was found only for device A.

Table 2 shows the mean ranks and range of scores achieved by each CBCT device for evaluating delta, narrow canal apical, narrow canal middle, and isthmus, respectively, in two different conditions (metal-free and with metal). The table also indicates the multiple comparison of each CBCT position with the best and worst ranked device for each diagnostic task and condition. For such purpose, a three-grade level classification was created by using shades of greys. Lighter shades of grey were used to display the best ranked CBCT devices. Conversely, darker grey represents devices with similar worst ranking.

In metal-free condition, device B scored best for all diagnostic tasks. Devices F and J had a similar worst compared to the others. In the presence of metal, a higher score was achieved by device A, but the difference was not statistically significant with device D. Contrarily, the ranking of device J was significantly worse than the others, as also shown in Table 2.

Table 2 - Comparison of mean scores (range) among all studied CBCT devices for evaluating narrow canal, delta ramifications and isthmus in two different conditions (metal free and with metal)

Narrow canal middle				Narrow canal apical				Delta				Isthmus			
Metal free		With metal		Metal free		With metal		Metal free		With metal		Metal free		With metal	
CBCT Device	**Mean Score (Range)**	**CBCT Device**	**Mean Score (Range)**	**CBCT Device**	**Mean Score (Range)**	**CBCT Device**	**Mean Score (Range)**	**CBCT Device**	**Mean Score (Range)**	**CBCT Device**	**Mean Score (Range)**	**CBCT Device**	**Mean Score (Range)**	**CBCT Device**	**Mean Score (Range)**
C	1.1 (1-1)	I	1.7 (1-2)	B	1.0 (1-1)	A	1.0 (1-1)	A	1.1 (1-1)	A	1.1 (1-1)	A	2.7 (1-6)	G	1.3 (1-2)
A	2.3 (2-3)	A	2.0 (1-4)	A	2.7 (2-4)	B	2.7 (2-4)	B	2.0 (2-2)	D	2.3 (2-3)	C	2.7 (1-5)	E	3.0 (1-5)
B	2.7 (3-7)	D	3.0 (2-4)	C	3.0 (2-4)	D	3.0 (3-3)	G	4.3 (3-6)	E	3.7 (3-4)	G	3.0 (2-4)	A	3.7 (2-6)
D	4.0 (4-4)	C	3.3 (3-4)	D	4.0 (3-5)	G	3.3 (2-4)	C	4.7 (4-5)	C	4.3 (3-5)	B	4.0 (2-6)	B	4.3 (2-7)
I	5.3 (6-6)	G	5.0 (5-5)	G	4.3 (3-5)	F	5.7 (5-7)	E	5.0 (3-6)	B	5.0 (2-8)	E	4.3 (3-7)	D	5.0 (3-6)
G	6.3 (6-7)	H	6.3 (6-7)	I	6.0 (6-6)	E	6.3 (5-8)	I	5.3 (4-7)	I	6.3 (6-7)	I	4.7 (4-5)	F	6.0 (4-7)
H	7.7 (5-10)	E	6.7 (6-7)	H	7.3 (7-8)	H	6.7 (6-7)	D	5.7 (3-7)	G	6.7 (6-7)	D	7.3 (6-9)	I	6.0 (5-8)
E	8.0 (7-9)	B	8.7 (8-9)	E	7.7 (7-8)	C	8.3 (6-10)	J	8.3 (8-9)	F	7.0 (4-9)	J	8.3 (7-10)	C	7.0 (4-9)
F	8.0 (7-9)	J	8.7 (8-10)	F	9.0 (9-9)	J	8.7 (8-9)	H	8.7 (8-9)	H	9.0 (8-10)	F	8.7 (8-10)	H	8.7 (8-9)
J	9.7 (9-10)	F	9.7 (9-10)	J	10.0 (10-10)	I	9.3 (9-10	F	10.0 (10-10)	J	9.7 (9-10)	H	9.2 (9-10)	J	10.0 (10-10)

The light grey highlighted the devices with best performance and the contrary was illustrated by dark grey. The CBCT codes are represented in the table 1.

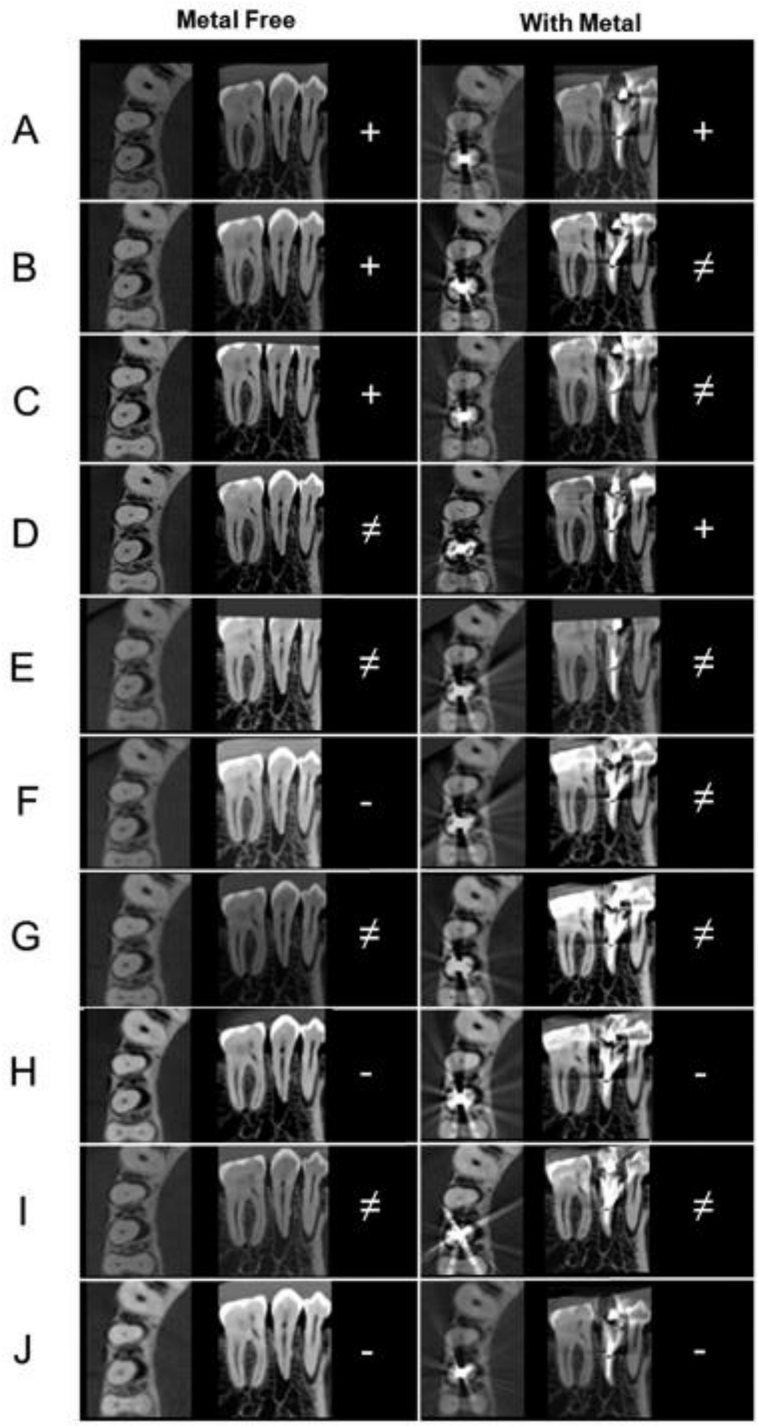

Figure 3 - Comparison of CBCT images with the hypothetical best and worst device in two conditions (metal-free and with metal). The CBCT devices marked with + did not differ from the best (95% confidence interval) for all diagnostic tasks, the ones marked with - did not differ from the worst (lower score) and the ones marked with ≠ differed from the best and the worst.

Discussion

In the present study, the null hypothesis was rejected since endodontic assessment of fine anatomical structures differed significantly among CBCT devices for different endodontic tasks in metal-free condition and in the presence of metal. When a CBCT examination is required, optimized exposure settings should be used to account for the diagnostic task (22) The differences found can be explained by the different technical characteristics of each CBCT device (19, 20). Although all CBCT protocols were selected in ‘high resolution’ mode, the actual spatial resolution is influenced by several device-specific factors such as focal spot size, detector pixel size, magnification factor, number of projections, and reconstruction filter (19). Nowadays, there is a wide variability concerning physical and technical features; therefore, different machines have varying performance for specific diagnostic tasks (19, 24-26). This variability may be even more evident when metallic materials are present in the scanned volume.

The endodontic tasks were CBCT device-dependent, with three devices allowing for better endodontic feature detection in absence of metal artifacts. In the presence of metal, two devices performed better than the others. Only one CBCT device (A) presented a consistently high rank for all tasks and set-ups. An opposite behavior was observed for another device (J). High-dense materials commonly used in endodontic treatments may cause device-specific artifacts, deteriorating image quality to different extents for each CBCT device (6-8, 27).

Regarding narrow canal, the presence of metallic pin in the middle third might have influenced its detectability. In the apical third only gutta percha was present. Previous investigations found that artifacts from metallic objects have a higher impact on image quality, making diagnosis more difficult (28-30). On the other hand, the influence of artifacts from gutta-percha and sealer varies in the current literature (7, 27, 28). For isthmus evaluation, more CBCT devices obtained statistically similar scores compared to the best ranked, irrespective of the presence of metal. This result is in line with the high specificity and sensitivity for isthmus detection founded in the literature (13). On the other hand, for delta ramification, in the presence of metal, only three CBCT devices received the best scores, in agreement with a previous study that found low accuracy of CBCT for detecting ramifications (3, 5).

One of the main advantages of the present study was its reproducibility and clinically realistic comparative set-up. The use of an anthropomorphic phantom with modular teeth having specific endodontic challenges allowed to evaluate the same structure in ten different CBCT devices. Subsequently, image registration standardized the regions of interest (21). Additionally, a dry human skull covered with mix-D material provided similar attenuation as clinical scans (22). Moreover, the present study did not work with simulated tasks. Therefore, all evaluated diagnostic tasks were naturally pre-existing. On the other hand, our study was not able to consider patient movement, which is a factor inherent to a clinical scan that influence image quality (31, 32).

It should be said that our study did not aim to compare diagnostic accuracy or efficacy of CBCT devices. Therefore, although significant variations could be noticed concerning image quality among different machines, further investigation is still necessary to analyze the impact of these dissimilarities for performing a challenging detection of fine endodontic structures. One must bear in mind that a CBCT device should provide an image of sufficient image quality for a specific diagnostic task. Following the ALADAIP (as low as diagnostically acceptable being indication-oriented and patient-specific) principle, the exposure parameters of a CBCT device should be adjusted for each patient and clinical situation in order to provide an image with enough quality for diagnosis with the lowest possible radiation dose (33).

Our results highlighted the diversity regarding the quality and ranking of several CBCT devices for the same endodontic diagnostic task. Thus, differences between CBCT devices should be considered when referring a patient for an endodontic evaluation, especially when the patient has prior metallic restorations or implants. One may opt to use specific devices when a proper detection of narrow canal, isthmus, and apical delta ramification are needed. In case the patient has high-dense materials present, referral to CBCT may be even more restrictive, as only few devices are showing a good detection of these subtle anatomic structures when metallic objects are present. It is evident that even with the best possible selection of CBCT device and protocol, effective endodontic diagnosis can only be obtained when CBCT reading is combined with a comprehensive dental history and clinical findings (34, 35).

Conclusion

The evaluated endodontic tasks were CBCT device-dependent, and its detection was influenced by the presence of metal.

Acknowledgments

This study was supported by the following funding sources: Coordenação de Aperfeiçoamento de Pessoal de Nível Superior (CAPES) - Finance Code 001, São Paulo Research Foundation - FAPESP (2019/22885-0), European Union Horizon 2020 Research and Innovation Programme under the Marie Skłodowska-Curie Grant agreement number 754513 and Aarhus University Research Foundation (AIAS-COFUND), and Fundação de Apoio à Pesquisa do Distrito Federal (protocol 23106.013588/2019-5).

The authors deny any conflicts of interest related to this study

References

1. Patel S, Dawood A, Ford TP, Whaites E. The potential applications of cone beam computed tomography in the management of endodontic problems. Int Endod J. 2007;40(10):818-30.
2. Vizzotto MB, Silveira PF, Arús NA, Montagner F, Gomes BP, da Silveira HE. CBCT for the assessment of second mesiobuccal (MB2) canals in maxillary molar teeth: effect of voxel size and presence of root filling. Int Endod J. 2013;46(9):870-6.
3. Sousa TO, Hassan B, Mirmohammadi H, Shemesh H, Haiter-Neto F. Feasibility of Cone-beam Computed Tomography in Detecting Lateral Canals before and after Root Canal Treatment: An Ex Vivo Study. J Endod. 2017;43(6):1014-7.
4. Cotton TP, Geisler TM, Holden DT, Schwartz SA, Schindler WG. Endodontic applications of cone-beam volumetric tomography. J Endod. 2007;33(9):1121-32.
5. Nascimento EHL, Abrahão Elias MR, Vasconcelos VHF, Haiter-Neto F, Mendonça EF, Sousa TO. Ex Vivo Detection of Apical Delta in Premolars: A Comparative Study Using Periapical Radiography, Cone-beam Computed Tomography, and Micro-computed Tomography. J Endod. 2019;45(5):549-53.

6. Hassan B, Metska ME, Ozok AR, van der Stelt P, Wesselink PR. Comparison of five cone beam computed tomography systems for the detection of vertical root fractures. J Endod. 2010;36(1):126-9.

7. Khedmat S, Rouhi N, Drage N, Shokouhinejad N, Nekoofar MH. Evaluation of three imaging techniques for the detection of vertical root fractures in the absence and presence of gutta-percha root fillings. Int Endod J. 2012;45(11):1004-9.

8. Melo SL, Bortoluzzi EA, Abreu M, Corrêa LR, Corrêa M. Diagnostic ability of a cone-beam computed tomography scan to assess longitudinal root fractures in prosthetically treated teeth. J Endod. 2010;36(11):1879-82.

9. Codari M, de Faria Vasconcelos K, Ferreira Pinheiro Nicolielo L, Haiter Neto F, Jacobs R. Quantitative evaluation of metal artifacts using different CBCT devices, high-density materials and field of views. Clin Oral Implants Res. 2017;28(12):1509-14.

10. Jacobs R. Dental cone beam CT and its justified use in oral health care. JBR-BTR. 2011;94(5):254-65.

11. Jacobs R, Salmon B, Codari M, Hassan B, Bornstein MM. Cone beam computed tomography in implant dentistry: recommendations for clinical use. BMC Oral Health. 2018;18(1):88.

12. Srivastava S, Alrogaibah NA, Aljarbou G. Cone-beam computed tomographic analysis of middle mesial canals and isthmus in mesial roots of mandibular first molars-prevalence and related factors. J Conserv Dent. 2018;21(5):526-30.

13. Rashed B, Iino Y, Komatsu K, Nishijo M, Hanada T, Ebihara A, et al. Evaluation of Root Canal Anatomy of Maxillary Premolars Using Swept-Source Optical Coherence Tomography in Comparison with Dental Operating Microscope and Cone Beam Computed Tomography. Photomed Laser Surg. 2018;36(9):487-92.

14. Guo XL, Li G, Zheng JQ, Ma RH, Liu FC, Yuan FS, et al. Accuracy of detecting vertical root fractures in non-root filled teeth using cone beam computed tomography: effect of voxel size and fracture width. Int Endod J. 2019;52(6):887-98.

15. Ma RH, Ge ZP, Li G. Detection accuracy of root fractures in cone-beam computed tomography images: a systematic review and meta-analysis. Int Endod J. 2016;49(7):646-54.

16. Corbella S, Del Fabbro M, Tamse A, Rosen E, Tsesis I, Taschieri S. Cone beam computed tomography for the diagnosis of vertical root fractures: a systematic review of the literature and meta-analysis. Oral Surg Oral Med Oral Pathol Oral Radiol. 2014;118(5):593-602.

17. Kambungton J, Janhom A, Prapayasatok S, Pongsiriwet S. Assessment of vertical root fractures using three imaging modalities: cone beam CT, intraoral digital radiography and film. Dentomaxillofac Radiol. 2012;41(2):91-5.

18. Patel S, Brady E, Wilson R, Brown J, Mannocci F. The detection of vertical root fractures in root filled teeth with periapical radiographs and CBCT scans. Int Endod J. 2013;46(12):1140-52.

19. Gaêta-Araujo H, Alzoubi T, Vasconcelos KF, Orhan K, Pauwels R, Casselman JW, et al. Cone beam computed tomography in dentomaxillofacial radiology: a two-decade overview. Dentomaxillofac Radiol. 2020:20200145.

20. Pauwels R, Stamatakis H, Bosmans H, Bogaerts R, Jacobs R, Horner K, et al. Quantification of metal artifacts on cone beam computed tomography images. Clin Oral Implants Res. 2013;24 Suppl A100:94-9.

21. Vasconcelos KF, Nicolielo LF, Nascimento MC, Haiter-Neto F, Bóscolo FN, Van Dessel J, et al. Artefact expression associated with several cone-beam computed tomographic machines when imaging root filled teeth. Int Endod J. 2015;48(10):994-1000.

22. Oenning AC, Pauwels R, Stratis A, De Faria Vasconcelos K, Tijskens E, De Grauwe A, et al. Halve the dose while maintaining image quality in paediatric Cone Beam CT. Sci Rep. 2019;9(1):5521.

23. Maes F, Collignon A, Vandermeulen D, Marchal G, Suetens P. Multimodality image registration by maximization of mutual information. IEEE Trans Med Imaging. 1997;16(2):187-98.

24. Pauwels R, Beinsberger J, Collaert B, Theodorakou C, Rogers J, Walker A, et al. Effective dose range for dental cone beam computed tomography scanners. Eur J Radiol. 2012;81(2):267-71.

25. Kiljunen T, Kaasalainen T, Suomalainen A, Kortesniemi M. Dental cone beam CT: A review. Phys Med. 2015;31(8):844-60.

26. Dawood A, Patel S, Brown J. Cone beam CT in dental practice. Br Dent J. 2009;207(1):23-8.

27. Decurcio DA, Bueno MR, de Alencar AH, Porto OC, Azevedo BC, Estrela C. Effect of root canal filling materials on dimensions of cone-beam computed tomography images. J Appl Oral Sci. 2012;20(2):260-7.
28. Dutra KL, Pachêco-Pereira C, Bortoluzzi EA, Flores-Mir C, Lagravère MO, Corrêa M. Influence of Intracanal Materials in Vertical Root Fracture Pathway Detection with Cone-beam Computed Tomography. J Endod. 2017;43(7):1170-5.
29. Costa FF, Gaia BF, Umetsubo OS, Cavalcanti MG. Detection of horizontal root fracture with small-volume cone-beam computed tomography in the presence and absence of intracanal metallic post. J Endod. 2011;37(10):1456-9.
30. Costa FF, Gaia BF, Umetsubo OS, Pinheiro LR, Tortamano IP, Cavalcanti MG. Use of large-volume cone-beam computed tomography in identification and localization of horizontal root fracture in the presence and absence of intracanal metallic post. J Endod. 2012;38(6):856-9.
31. Nardi C, Molteni R, Lorini C, Taliani GG, Matteuzzi B, Mazzoni E, et al. Motion artefacts in cone beam CT: an in vitro study about the effects on the images. Br J Radiol. 2016;89(1058):20150687.
32. Spin-Neto R, Matzen LH, Schropp LW, Sørensen TS, Wenzel A. An ex vivo study of automated motion artefact correction and the impact on cone beam CT image quality and interpretability. Dentomaxillofac Radiol. 2018;47(5):20180013.
33. Oenning AC, Jacobs R, Pauwels R, Stratis A, Hedesiu M, Salmon B, et al. Cone-beam CT in paediatric dentistry: DIMITRA project position statement. Pediatr Radiol. 2018;48(3):308-16.
34. Parker J, Mol A, Rivera EM, Tawil P. CBCT uses in clinical endodontics: the effect of CBCT on the ability to locate MB2 canals in maxillary molars. Int Endod J. 2017;50(12):1109-15.
35. Edlund M, Nair MK, Nair UP. Detection of vertical root fractures by using cone-beam computed tomography: a clinical study. J Endod. 2011;37(6):768-72.

3.8 Publicação 8*

Assessment of CBCT devices for visualizing root cracks and fine anatomic structures: influence of scanning protocols and metallic materials.

Abstract

Objectives. To assess the influence of cone-beam computed tomography (CBCT) scanning protocols and the presence of metal on the visualization of root cracks and fine endodontic anatomical structures.

Study Design. An anthropomorphic phantom containing teeth with cracks, isthmus, narrow canal, and apical delta was scanned using ten CBCT devices. A reference industrial CT image was used to detect and measure all structures. Three conditions were created: 1. metal-free, 2. 'endo' and 3.'implant' with metallic objects placed next to those teeth. For each condition, three protocols were selected: medium field of view (FOV) standard resolution, small FOV standard, and high resolution. Fleiss Kappa statistics were used for intra-observer agreement for each CBCT device. Kruskal-Wallis and Dunn's test (α = 0.05) were used, for comparisons among conditions and protocols, within CBCT device.

Results. only small FOV high-resolution metal-free images from two devices (A and H) were appropriate to visualize cracks. For fine structures, the best result was observed for small FOV high resolution. However, the visualization significantly worsened in the presence of a metallic post.

Conclusions. The capacity of CBCT images for visualizing cracks is highly limited and restricted to certain devices and protocols in the absence of metal. The other structures were better visualized with a small FOV high-resolution protocol as long as there were no high-density objects in the region of interest.

Keywords: Anatomy. Artifacts. Cone-beam computed tomography. Endodontics.

---

* Artigo em revisão no periódico *Oral Surg Oral Med Oral Pathol Oral Radiol.nhyry.*

INTRODUCTION

Knowledge of root anatomy is important for diagnosis, treatment, and prognosis of endodontic diseases. The initial visualization of challenging anatomical structures, as well as the accurate early diagnosis of cracked teeth using cone-beam computed tomography (CBCT) images is of paramount importance for long-term tooth prognosis, due to its direct influence on the endodontic treatment[1].

The literature is conflicting regarding the sensitivity and specificity of CBCT images for performing endodontic tasks (such as the detection of root fracture and extra canals[2-6]. The selection of high-resolution protocols on CBCT devices with small field of view (FOV) and voxel sizes has been strongly recommended for visualizing the intricacies of the root canal system and periodontium[7,8]. Conversely, a systematic review did not find any correlation between smaller voxel sizes and better diagnostic accuracy of root fractures in non-endodontically treated teeth5. Furthermore, the effect of voxel size may be device-dependent due to other limiting factors for spatial resolution, such as the type of the detector and the reconstruction process[8]. Technical characteristics vary widely among commercially available CBCT devices[10,11], which makes it difficult to generalize diagnostic capability for all devices and acquisitions protocols8. Moreover, high-density materials, such as endodontic fillings and or posts and dental implants within or outside the FOV may image quality on CBCT[12,13]. Therefore, the influence of such materials on visualization of fine anatomical structures requires further investigation.

Optimized acquisition protocols should be selected when a CBCT examination is warranted[8,14,15]. In an ideal scenario, visualization of endodontic structures on CBCT should be performed on images acquired by high-resolution scanning protocols without the presence of metal near to the region of interest8. However, in clinical practice, this is not a common condition. Therefore, the present study evaluated the influence of different scanning protocols on 10 CBCT devices and the presence of metal for the visualization of root cracks and fine anatomic structures such as narrow canals, isthmus, and apical delta. The null hypothesis was that imaging scanning protocols and the presence of metal would not influence the visualization of root cracks and fine endodontics structures.

MATERIAL AND METHODS

This experimental study was designed according to the local institutional research ethics committee (protocol number NH019 2019-09-03). An anthropomorphic phantom composed of a dry human skull and a mandible was covered with mix-D material to simulate soft tissue attenuation[14]. Additionally, a mix-D tongue was positioned in the corresponding space of the phantom. A reference industrial image confirmed the presence of a narrow canal in the right mandibular first premolar, and cracks, isthmus, and apical delta in the mandibular first molar (Fig. 1). To assess the influence of metal on the visualization of the aforementioned structures and cracks, three clinical conditions were created: 1. Metal-free (Fig. 2b); 2. 'Endo': with an endodontically treated second mandibular premolar containing a gold alloy metallic post made in-house. The root canals were prepared with Reciproc R25 file (VDW, Munich, Germany) and filled by lateral compaction using AH Plus sealer (Dentsply DeTrey GmbH, Konstanz, Germany) (Fig. 2c); and 3. Implant: the same phantom with a titanium implant with 10 mm length and a platform with 3.5 mm diameter, model Tapered PMC NP (Nobel Biocare, Zurich, Switzerland) placed in the right mandibular premolar region (Fig. 2d). Moreover, silicone guides made with Zetaplus silicone (Zhermack SpA, Badia Polesine, Italy) were used to reproduce the positioning of the teeth for image acquisition.

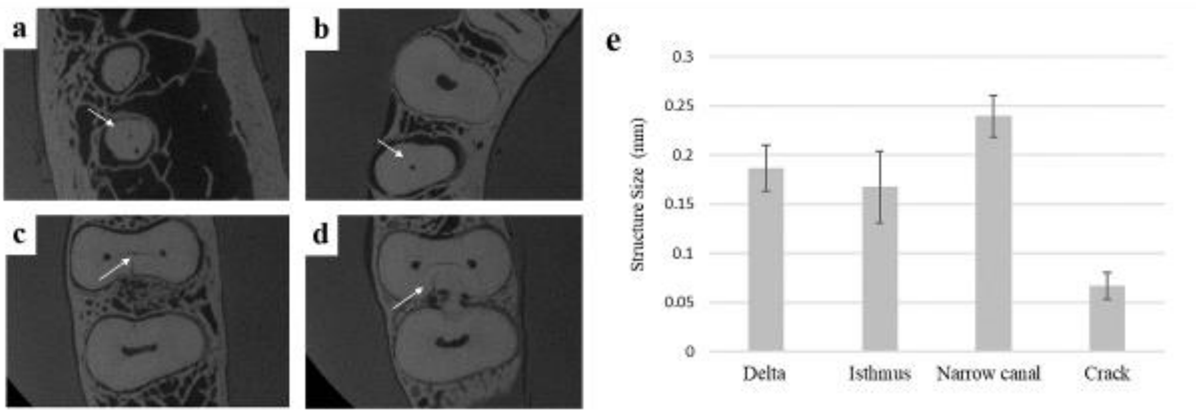

Figure 1 Representative images obtained from industrial CT showing a) delta ramifications, b) narrow canal, c) isthmus and d) crack used as reference images, and e) bar chart showing the means and standard deviations of the size of these structures.

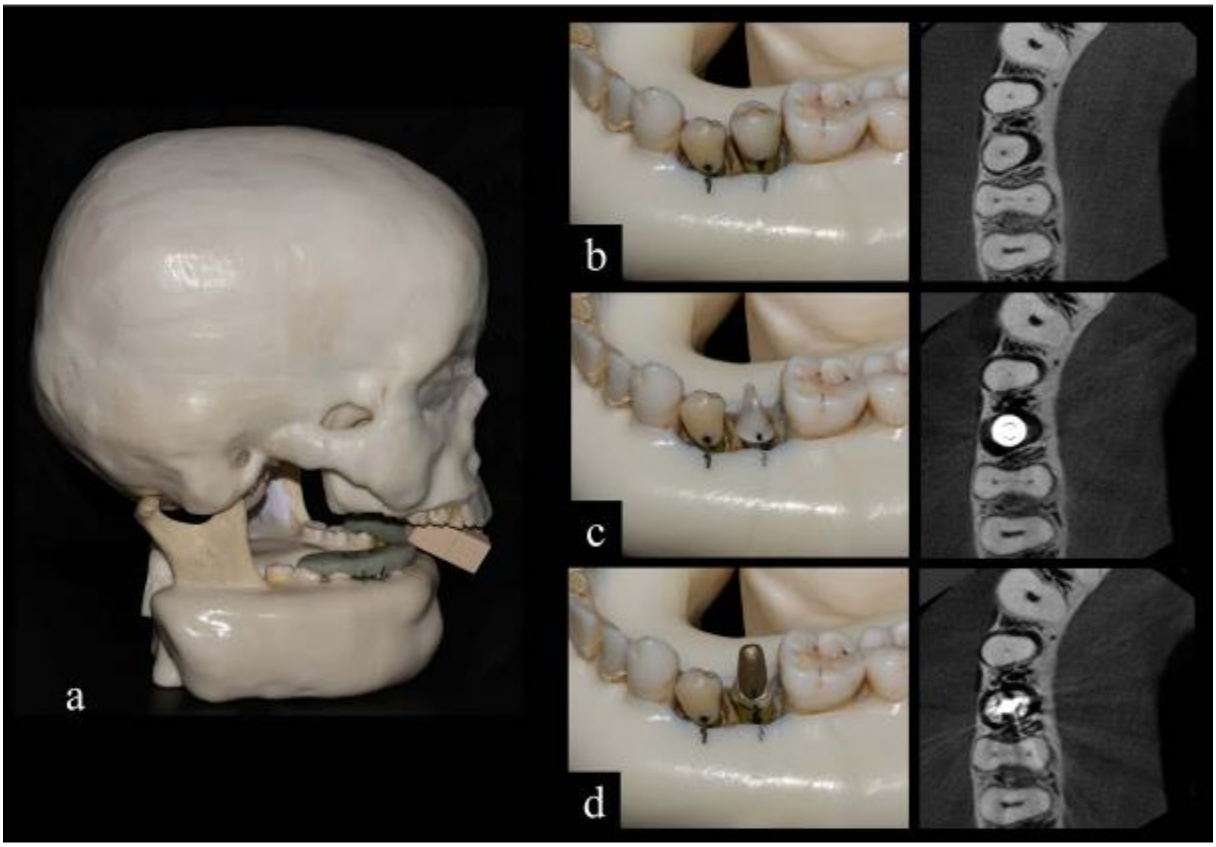

Figure 2 Anthropomorphic phantom of a dry human skull with mandible covered with mix-D (a) and representation of the region of interest considering the three conditions evaluated: metal-free (b), implant (c) and endo (d).

CBCT imaging acquisitions

Initially, ten CBCT devices were selected based on their potential use for endodontic diagnosis, besides their widespread availability worldwide. Subsequently, in order to compare the influence of scanning protocols, all conditions were scanned by selecting three different protocols (medium FOV standard resolution, small FOV standard resolution and small FOV high resolution) on each of the devices. Table 1 shows all CBCT devices, codes (A to J), exposure parameters and their corresponding dose-area product provided by the manufacturers. The study criteria for the protocols selection were based on the comparison of high-resolution protocols, suggested by the current literature for endodontic assessment, with two others protocols: medium FOV standard resolution, selected in the daily practice for complete mandibular assessment, and a small FOV standard resolution. The last one was selected in order to assess the influence of FOV while keeping the other variables constant. Although some of the devices tested allow the selection of a specific algorithm for metal artifact reduction, this tool was not used in the present study, to avoid confounding variables.

Reference image acquisition

The mandible was scanned on a Nikon XT H 225 industrial computed tomography (CT) scanner (Nikon Metrology Inc, Brighton, MI, USA) using the following parameters: 200 kV, 350 µA, 2.5 mm Cu filtration, 8x8 cm FOV and 40 µm voxel size. In addition to being used to accurately detect and measure the size of the structures and cracks evaluated, the industrial CT scan was used as a reference to register all CBCT images. For each investigated structure, five different representative slices were selected. For narrow canals and apical delta, the diameter of the canals was measured and for root cracks and isthmus, the width was determined by the arithmetic mean value of five measurements along their length (Fig. 1). All measurements were made by an independent examiner using CTAn software (v.1.14.4; Bruker-micro-CT, Kontich, Belgium). Figure 1e shows the average size for each structure: 0.23mm for narrow canals, 0.18mm for apical delta, 0.06mm for root cracks, and 0.16mm for isthmus.

Image registration

The evaluations in the present study were based on comparisons between a set of images within each CBCT device and their respective industrial CT reference image, considering all the different conditions and protocols. Therefore, mutual information-based registration16 was performed in Amira 2019 software (Thermo Fisher Scientific, Waltham, MA, USA) using the industrial CT scan as a reference image. The aforementioned registration method allowed the selection of the same slice and consequently ensured the assessment of the same region of interest on all CBCT devices. One hundred and eighty slices per CBCT device were selected to evaluate all diagnostic tasks, considering five slices for each task (20 slices in total) in the three different protocols and three different conditions.

Subjective image quality assessment

A set of unique images containing fine endodontic structures in other regions of the phantom was used to calibrate two oral radiologists to the study method. After the calibration process the radiologists evaluated each diagnostic task separately. For each device and diagnostic task, there were a set of nine unseen images containing all scanning protocols and clinical conditions randomly displayed on the same computer screen along with the correspondent reference image (Fig. 3). Observers were aware of the appearance and location of the structures of interest and cracks in the reference image, but blinded to the respective CBCT device, protocols and presence of metal. Due to the difference in histogram distribution of each CBCT device, the brightness and contrast of the images were pre-adjusted by an experienced operator to provide images suitable for evaluation of each device. Afterwards, the image brightness, contrast and magnification could not be adjusted by the observers. They evaluated each image in comparison to the reference image, and classified it into one of three categories by consensus: 1 - appropriate for visualization of the specific structure; 2 - acceptable for visualization of the specific structure (the observer could distinguish the structure, however, it was not as clear as in the reference image); 3 - inappropriate for visualization of the specific structure (the observer could not distinguish the structure of interest). Calibration and evaluation sessions were performed in a low-light environment using a 61.2 cm flat-screen monitor MD Barco MDRC-2221 (Barco, Kortrijk, Belgium). After 30 days, 20% of the images were re-evaluated to assess intra-observer agreement.

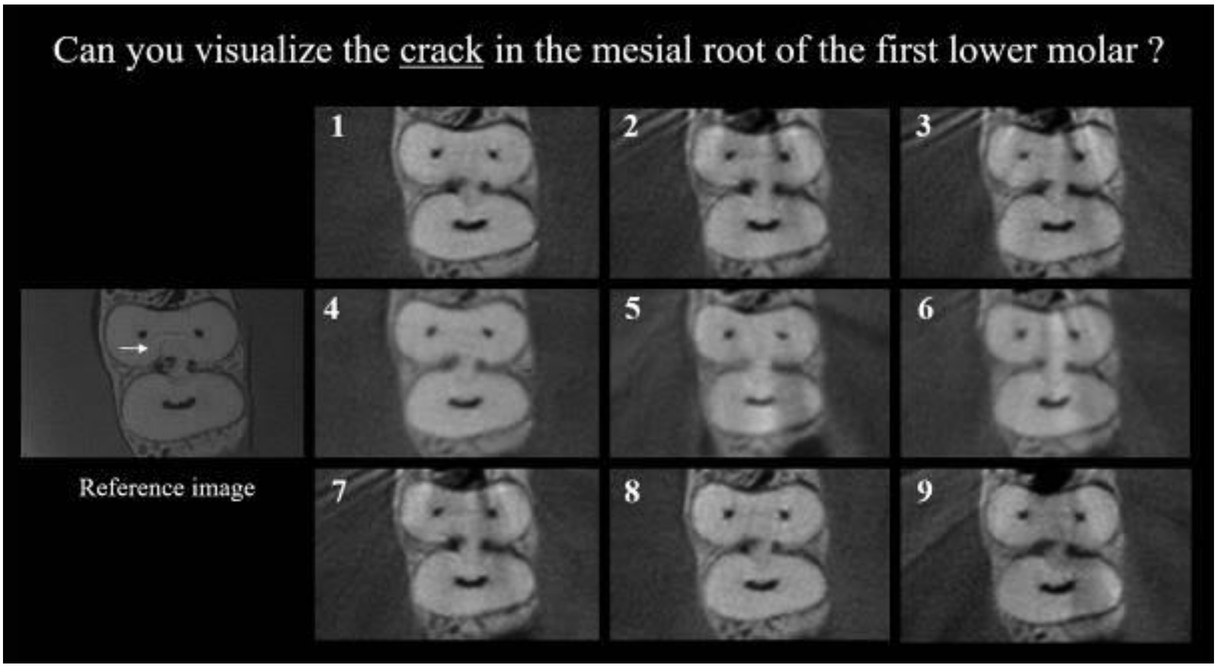

Figure 3 Set of images used for crack assessment containing a reference image from industrial CT and numbered images of a specific CBCT device for all conditions and scanning protocols.

Statistical analysis

Statistical modeling and analysis were performed using GraphPad Prism 5 (GraphPad Software Inc, La Jolla, CA, USA). Fleiss kappa statistics was used to calculate intra-observer agreement for each CBCT device separately. Kruskal-Wallis and Dunn`s tests were used to compare the different conditions and scanning protocols of each CBCT device with the reference image. A significance level of 0.05 was used for the analysis.

RESULTS

Kappa values indicate high intra-observer agreement (> 0.81 for all CBCT devices). Figure 1 shows representative industrial CT images of the accessed endodontic tasks used as reference in the present study.

This figure also contains a bar chart indicating mean values and standard deviations of the size of narrow canal, isthmus, apical delta, and root cracks. A significantly lower size was observed for root cracks when compared to the other evaluated structures ($P < 0.05$). Figure 4 shows the percentage of images classified as appropriate, acceptable, or inappropriate for each CBCT device, considering all scanning protocols and the presence/absence of metal. Additionally, figure 4 shows a set of images from device A which yielded better results (highest percentage of images classified as appropriate) and device J which performed worst (lowest percentage of images classified as appropriate).

Tables 2 and 3 show the mean classifications achieved by each scanning protocols (small FOV standard and high resolution and medium FOV standard resolution) and conditions (metal-free, implant and endo) of all CBCT devices and tasks. Moreover, they also demonstrate multiple comparison tests of each scanning protocol and condition with the reference images.

Table 2 shows that only devices A and H presented similar performance to the reference for visualizing root cracks, but only in metal-free condition scanned with a small-FOV high-resolution protocol.

Scanning protocols influenced the visualization of endodontics structures (narrow canal, delta apical and isthmus), with small-FOV high-resolution protocols performing better than the others ($P < 0.05$), as seen in Table 3. The presence of a metallic post decreased the ability to visualize the structures even for high resolution protocols ($P < 0.05$). However, similar behavior was not observed when the implant was present ($P > 0.05$). In the absence of metal, the small FOVs standard resolution from the devices A, B, C, E, and G displayed similar visualization to the reference image. In the presence of implants, only device C remained similar to the reference ($P>0.05$). For medium FOV standard resolution, only device A did not differ from the reference in the presence of metallic structures. Device J was not able to perform similarly to the reference image for any of the protocols and conditions ($P < 0.05$).

Table 1 Detailed description of the CBCT devices, manufacturers, codes, and scanning protocols used in the present study

CBCT devices	Codes	Manufacturer	Small FOV High Resolution					Small FOV Standard Resolution					Medium FOV Standard Resolution				
			FOV (cm)	kV	mA	Voxel size (mm)	DAP (mGY cm2)	FOV (cm)	kV	mA	Voxel size (mm)	DAP (mGY cm2)	FOV (cm)	kV	mA	Voxel size (mm)	DAP (mGY cm2)
3D Accuitomo 170	A	J. Morita, Kyoto, Japan	4 X 4	90	5	0.08	706	4 X 4	90	5	0.125	402	8 X 8	90	5	0.125	2310
OP 3D Pro	B	Instrumentarium, Tuusula, Finland	5 X 5	90	8.6	0.085	755	5 X 5	90	7.1	0.125	452	8 X 8	90	7.1	0.2	899
Veraview X800	C	J. Morita, Kyoto, Japan	4 X 4	100	7.9	0.08	589	4 X 4	101	8	0.125	596	8 X 8	100	8	0.125	2112
X1	D	3Shape, Copenhagen, Denmark	4 X 4	90	12	0.1	309	4 X 4	90	12	0.15	231	8 X 8	90	12	0.15	773
CS 9300	E	Carestream, Rochester, NY, USA	5 X 5	90	4	0.09	572	5 X 5	90	4	0.2	572	7.7 X 7.7	90	4	0.18	455
NewTom VGi evo	F	Cefla Dental Group, Imola, Italy	5 X 5	110	3	0.1	148	5 X 5	110	3	0.125	148	8.2 X 8.2	110	3	0.125	329
Veraviewepocs 3DR100	G	J. Morita, Kyoto, Japan	-	-	-	-	-	4 X 4	90	8	0.125	525	8 X 8	90	8	0.125	1780
Orthophos SL 3D	H	Dentsply Sirona, Charlotte, NC, USA	5 X 5	85	6	0.079	421	5 X 5	85	10	0.16	214	8.2 X 8.2	85	6	0.16	657
OP 3D	I	Instrumentarium, Tuusula, Finland	5 X 5	95	4	0.08	1165	5 X 5	90	4	0.125	582	8 X 8	94	2.8	0.2	940
ProMax 3D Max	J	Planmeca, Helsinki, Finland	6 X 6	96	12	0.075	1155	6 X 6	96	7.1	0.15	657	10 X 10	96	7.1	0.15	668

Table 2 Mean values of visualization assessment of root cracks (1- appropriate, 2 – acceptable and 3- inappropriate) considering scanning protocols and conditions

CBCT devices	Control	Small FOV High Resolution			Small FOV Standard Resolution			Medium FOV Standard Resolution		
		Metal-Free	Implant	Post	Metal-Free	Implant	Post	Metal-Free	Implant	Post
A	1.0*	2.2*	2.8	2.8	2.8	3.0	3.0	3.0	3.0	3.0
B	1.0	2.8	3.0	3.0	2.8	3.0	3.0	2.6	3.0	3.0
C	1.0	2.8	2.6	3.0	2.8	3.0	3.0	3.0	3.0	3.0
D	1.0	2.8	3.0	3.0	3.0	3.0	3.0	3.0	3.0	3.0
E	1.0	2.8	2.8	3.0	3.0	3.0	3.0	3.0	3.0	3.0
F	1.0	3.0	3.0	3.0	3.0	3.0	3.0	3.0	3.0	3.0
G	1.0				2.8	3.0	3.0	3.0	3.0	3.0
H	1.0*	2.4*	3.0	3.0	3.0	3.0	2.8	2.8	3.0	3.0
I	1.0	2.8	3.0	2.8	3.0	3.0	3.0	3.0	3.0	3.0
J	1.0	3.0	3.0	3.0	3.0	3.0	3.0	3.0	3.0	3.0

* indicates statistical similarity with the reference industrial CT scan, which is shown as ‘Control’ (1.0 – appropriate for visualizing the anatomical structures).

Table 3 Mean values of visualization assessment (1- appropriate, 2 – acceptable and 3- inappropriate) of anatomical endodontic structures considering scanning protocols and conditions

CBCT devices	Control	Small FOV High Resolution			Small FOV Standard Resolution			Medium FOV Standard Resolution		
		Metal-Free	Implant	Endo	Metal-Free	Implant	Endo	Metal-Free	Implant	Endo
A	1.0*	1.1*	1.3*	1.5*	1.6*	1.9	2.0	1.8*	1.7*	1.9
B	1.0*	1.6*	1.7*	1.9	1.8*	2.1	1.9	2.2	2.3	2.3
C	1.0*	1.5*	1.6*	2.1	1.8	1.8*	2.1	2.3	2.4	2.5
D	1.0*	1.6*	1.6*	1.6*	2.2	1.9	2.3	2.3	2.5	2.6
E	1.0*	1.3*	1.3*	1.5*	1.5*	2.0	2.2	2.7	2.8	2.7
F	1.0*	1.6*	1.8*	2.1*	2.3*	2.5	2.3	2.3	2.4	2.4
G	1.0*				1.6*	2.3	1.9	2.3	2.6	2.0
H	1.0*	1.5*	1.5*	1.6*	2.5	2.7	2.7	2.3	2.4	2.4
I	1.0*	1.9*	1.9*	2.3	2.9	2.2	2.1	2.9	2.8	2.8
J	1.0	2.1	2.3	2.1	2.9	2.9	2.5	2.3	2.5	2.8

* indicates statistical similarity with the reference industrial CT scan, which is shown as 'Control' (1.0 – appropriate for visualizing the anatomical structures).

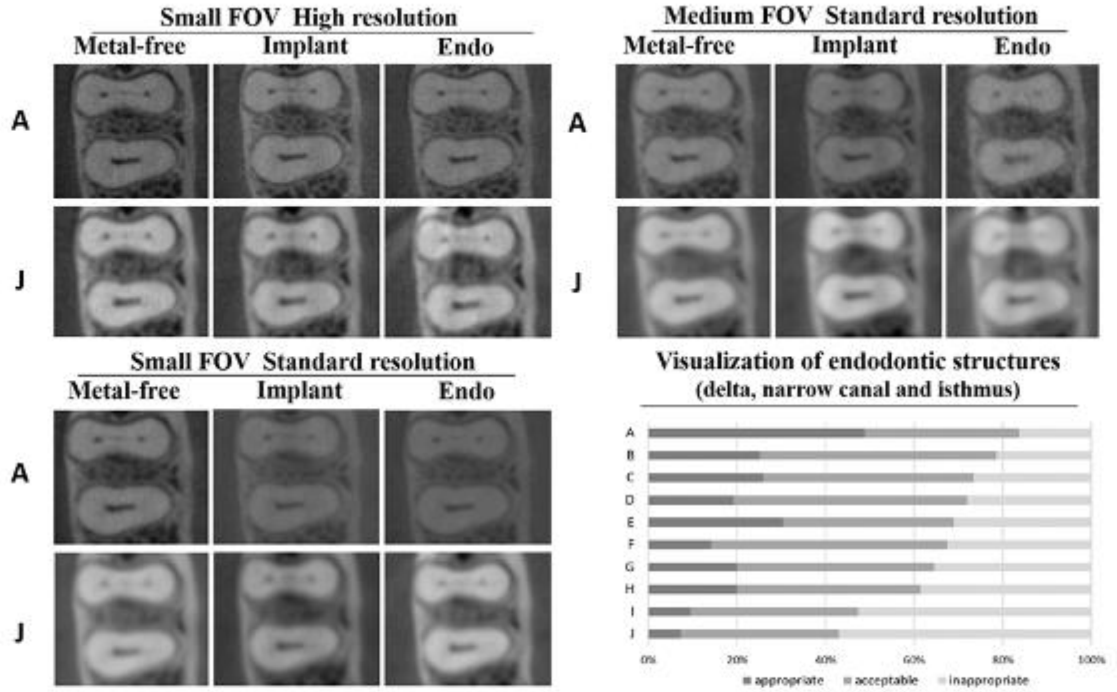

Figure 4 Representative images of isthmus from the devices with the most (A) and least (J) appropriate images for visualization of fine endodontic structures; and stacked bar graph showing the percentage of appropriate, acceptable or inappropriate grades achieved for each CBCT device, taking into account all conditions and the scanning protocol.

DISCUSSION

To the best of our knowledge, this was the first study to assess the influence of scanning protocols and metallic materials on the visualization of root cracks and fine endodontic anatomical structures on ten different CBCT devices. These devices were selected considering their widespread availability worldwide and their common use for endodontic diagnoses and treatment planning. Furthermore, out of all available CBCT devices[11] the selected devices represent the large variability in terms of CBCT technology currently available on the market.

The null hypothesis was rejected, as all tasks were influenced by scanning protocols and presence of metallic materials. The small-FOV high-resolution protocols provided images with appropriate or acceptable visualization capability of endodontics structures (narrow canal, delta apical and isthmus) for all devices evaluated, except for device J. This result confirmed that most CBCT images acquired with limited FOV and high-resolution protocols are preferable for fine endodontic structures visualization[17]. However, it is noteworthy that some devices have provided images similar to the reference even when small FOV standard resolution was selected, and that device A presented such capability regardless the protocol. Despite that, an increased exposure to ionizing radiation should be considered. These findings may be explained by differences in terms of other technical features amongst CBCT devices, such as focal spot size, detector pixel size, number of projections, and reconstruction filters[18].

High-density materials such as filling materials, gutta-percha and metallic posts may cause device-specific artifacts, reducing CBCT image quality[19-21]. The present results highlighted a decrease in the ability to visualize small endodontic structures in images with metallic posts within the FOV. Previous investigations found that artifacts generated from metallic posts have high impact on image quality[22,23]. Interestingly, the presence of an implant did not influence the behavior of most devices and scanning protocols. These results may be explained by differences in terms of atomic number of the gold metallic post (Z=79) and titanium implant (Z=22), since materials with higher atomic numbers are associated with more artifact expression in CBCT24. Although several studies have shown the impact of artifacts in regions adjacent to dental implants on CBCT images[12,25,26], few of them evaluated their influence on the visualization of structures in adjacent teeth, and certainly none of them in a series of CBCT with a standardized condition as the present study.

Concerning crack visualization, only two devices performed similar to the reference image, and only for a specific condition and scanning protocol. Considering its lowest average diameter of 0.07mm, cracks could be considered the most challenging to be identified compared to the other evaluated structures. The partial volume effect may explain the difficulty of detecting structures which are smaller than the voxel size[27]. This effect occurs when a single voxel represents two or more structures, precluding their proper identification[28]. In addition to this limitation, the presence of high-density materials generates artifacts that mimic or overlap fracture lines[22,29] . Other previous studies have also discussed the aforementioned limitations for detecting cracks on CBCT images and their size is undoubtedly one of the most crucial factors[9,30]. However, when diagnosing root cracks and fractures, other factors should be taken into consideration, such as clinical signs and symptoms, and the pattern of bone loss on images[13]. Furthermore, the exposure parameters, detector technology, and reconstruction algorithms should also be considered for diagnostic purposes5. It is important to keep track of the constant evolution of technology and investigate how this may lead to improve diagnostic efficacy.

Due to the inherent limitation related to an ex-vivo investigation, the present study was not able to consider patient motion and its effect on the final image quality[31,32]. On the other hand, the use of an anthropomorphic phantom was the only way to evaluate the same scanned structure by selecting various protocols on ten CBCT devices. Image registration using a reference image allowed standardizing the regions of interest, consequently improving the reproducibility of the study[33]. The anthropomorphic phantom was composed of a complete dried human skull and a mandible covered with a soft tissue substitute material[14]. This dedicated material, called mix-D, provided similar attenuation to soft tissues. In addition, the endodontic challenging tasks evaluated were naturally pre-existing, avoiding the limitation related to its artificial creation.

The present study highlighted the influence of different scanning protocols and the presence of metal structures within the FOV on the visualization of root cracks and challenging endodontic tasks. Furthermore, the results showed that this influence is device-dependent. As long as there are no high-density objects in the scanned region, several CBCT machines may be suitable. Yet, once high-density materials are present, fine endodontic diagnosis may be compromised in many CBCT machines, with only a limited number of machines still having some diagnostic value. For small root cracks (average diameter of 0.07 mm), CBCT diagnosis in the presence of metallic structures becomes extremely challenging, even though a comprehensive dental history and specific clinical findings might guide the diagnostic process[17,34].

CONCLUSIONS

Considering this study design, the capacity of CBCT images for visualizing small cracks was highly limited and restricted to certain devices and protocols in the absence of metal. The visualization of fine endodontic structures was CBCT-device dependent with a better capacity observed for small-FOV high-resolution protocols as long as there were no high-density objects adjacent to the region of interest

Acknowledgements

This study was supported by the following funding sources: Coordenação de Aperfeiçoamento de Pessoal de Nível Superior (CAPES) - Finance Code 001, São Paulo Research Foundation - FAPESP (2019/22885-0), and Fundação de Apoio à Pesquisa do Distrito Federal (protocol 23106.013588/2019-5).

R. Pauwels is supported by the European Union Horizon 2020 Research and Innovation Programme under the Marie Skłodowska-Curie Grant agreement number 754513 and Aarhus University Research Foundation (AIAS-COFUND).

The authors would like to acknowledge Jozef Ludovic Beckers for the provision of a gold alloy metallic post and Wouter Mollemans and Wouter Reybrouck for enabling part of the data collection investigated in this research.

References

1. Bhatt M, Coil J, Chehroudi B, Esteves A, Aleksejuniene J, MacDonald D. Clinical decision-making and importance of the AAE/AAOMR position statement for CBCT examination in endodontic cases. *Int Endod J*. 2021;54:26-37.

2. Kambungton J, Janhom A, Prapayasatok S, Pongsiriwet S. Assessment of vertical root fractures using three imaging modalities: cone beam CT, intraoral digital radiography and film. *Dentomaxillofac Radiol*. 2012;41:91-95..

3. Patel S, Brady E, Wilson R, Brown J, Mannocci F. The detection of vertical root fractures in root filled teeth with periapical radiographs and CBCT scans. *Int Endod J*. 2013;46(12):1140-1152.

4. Vizzotto MB, Silveira PF, Arús NA, Montagner F, Gomes BP, da Silveira HE. CBCT for the assessment of second mesiobuccal (MB2) canals in maxillary molar teeth: effect of voxel size and presence of root filling. *Int Endod J*. 2013;46:870-876.

5. Ma RH, Ge ZP, Li G. Detection accuracy of root fractures in cone-beam computed tomography images: a systematic review and meta-analysis. *Int Endod J*. 2016;49:646-654

6. Rashed B, Iino Y, Komatsu K, et al. Evaluation of Root Canal Anatomy of Maxillary Premolars Using Swept-Source Optical Coherence Tomography in Comparison with Dental Operating Microscope and Cone Beam Computed Tomography. *Photomed Laser Surg*. 2018;36:487-492.

7. Patel S, Brown J, Pimentel T, Kelly RD, Abella F, Durack C. Cone beam computed tomography in Endodontics - a review of the literature. *Int Endod J*. 2019;52:1138-1152.

8. Patel S, Brown J, Semper M, Abella F, Mannocci F. European Society of Endodontology position statement: Use of cone beam computed tomography in Endodontics: European Society of Endodontology (ESE) developed by. *Int Endod J*. 2019;52:1675-1678.

9. Guo XL, Li G, Zheng JQ, et al. Accuracy of detecting vertical root fractures in non-root filled teeth using cone beam computed tomography: effect of voxel size and fracture width. *Int Endod J*. 2019;52:887-898

10. Pauwels R, Stamatakis H, Bosmans H, et al. Quantification of metal artifacts on cone beam computed tomography images. *Clin Oral Implants Res*. 2013;24 Suppl A100:94-99.

11. Gaêta-Araujo H, Alzoubi T, Vasconcelos KF, et al. Cone beam computed tomography in dentomaxillofacial radiology: a two-decade overview. *Dentomaxillofac Radiol*. 2020;49:20200145.

12. Demirturk Kocasarac H, Ustaoglu G, Bayrak S, et al. Evaluation of artifacts generated by titanium, zirconium, and titanium-zirconium alloy dental implants on MRI, CT, and CBCT images: A phantom study. *Oral Surg Oral Med Oral Pathol Oral Radiol*. 2019;127:535-544.

13. Zhang L, Wang T, Cao Y, et al. In Vivo Detection of Subtle Vertical Root Fracture in Endodontically Treated Teeth by Cone-beam Computed Tomography. J Endod. 2019;45: 856-862.

14. Oenning AC, Pauwels R, Stratis A, et al. Halve the dose while maintaining image quality in paediatric Cone Beam CT [published correction appears in Sci Rep. 2020 Feb 7;10(1):2474]. *Sci Rep*. 2019;9:5521.

15. da Silva Moura W, Chiqueto K, Pithon GM, Neves LS, Castro R, Henriques JFC. Factors influencing the effective dose associated with CBCT: a systematic review. *Clin Oral Investig*. 2019;23:1319-1330.

16. Maes F, Collignon A, Vandermeulen D, Marchal G, Suetens P. Multimodality image registration by maximization of mutual information. *IEEE Trans Med Imaging*. 1997;16:187-198.

17. Edlund M, Nair MK, Nair UP. Detection of vertical root fractures by using cone-beam computed tomography: a clinical study. *J Endod*. 2011;37:768-772.

18 Min CK, Kim KA. Quantitative analysis of metal artefacts of dental implant in CBCT image by correlation analysis to micro-CT: A microstructural study. *Dentomaxillofac Radiol*. 2021;50:20200365.

19. Melo SL, Bortoluzzi EA, Abreu M Jr, Corrêa LR, Corrêa M. Diagnostic ability of a cone-beam computed tomography scan to assess longitudinal root fractures in prosthetically treated teeth. *J Endod*. 2010;36:1879-1882.

20. Decurcio DA, Bueno MR, de Alencar AH, Porto OC, Azevedo BC, Estrela C. Effect of root canal filling materials on dimensions of cone-beam computed tomography images. *J Appl Oral Sci*. 2012;20:260-267.

21. Khedmat S, Rouhi N, Drage N, Shokouhinejad N, Nekoofar MH. Evaluation of three imaging techniques for the detection of vertical root fractures in the absence and presence of gutta-percha root fillings. *Int Endod J*. 2012;45:1004-1009.

22. Costa FF, Gaia BF, Umetsubo OS, Cavalcanti MG. Detection of horizontal root fracture with small-volume cone-beam computed tomography in the presence and absence of intracanal metallic post. *J Endod*. 2011;37:1456-1459.

23. Dutra KL, Pachêco-Pereira C, Bortoluzzi EA, Flores-Mir C, Lagravère MO, Corrêa M. Influence of Intracanal Materials in Vertical Root Fracture Pathway Detection with Cone-beam Computed Tomography. *J Endod*. 2017;43:1170-1175.

24. Schulze RK, Berndt D, d'Hoedt B. On cone-beam computed tomography artifacts induced by titanium implants. *Clin Oral Implants Res*. 2010;21:100-107. doi:10.1111/j.1600-0501.2009.01817.x

25. Sancho-Puchades M, Hämmerle CH, Benic GI. In vitro assessment of artifacts induced by titanium, titanium-zirconium and zirconium dioxide implants in cone-beam computed tomography. *Clin Oral Implants Res*. 2015;26:1222-1228. doi:10.1111/clr.12438

26. Machado AH, Fardim KAC, de Souza CF, Sotto-Maior BS, Assis NMSP, Devito KL. Effect of anatomical region on the formation of metal artefacts produced by dental implants in cone beam computed tomographic images. *Dentomaxillofac Radiol*. 2018;47:20170281.

27. Huang CC, Chang YC, Chuang MC, et al. Analysis of the width of vertical root fracture in endodontically treated teeth by 2 micro-computed tomography systems. *J Endod*. 2014;40:698-702.

28. Heckel F, Meine H, Moltz JH, et al. Segmentation-based partial volume correction for volume estimation of solid lesions in CT. *IEEE Trans Med Imaging*. 2014;33:462-480.

29. Freitas DQ, Vasconcelos TV, Noujeim M. Diagnosis of vertical root fracture in teeth close and distant to implant: an in vitro study to assess the influence of artifacts produced in cone beam computed tomography. *Clin Oral Investig*. 2019;23:1263-1270.

30. Guo XL, Li G, Yin S, Ma RH, Guo YJ, Bornstein MM. Effect of fracture orientation on detection accuracy of vertical root fractures in non-endodontically treated teeth using cone beam computed tomography. *Clin Oral Investig*. 2019;23:4433-4439.

31. Nardi C, Molteni R, Lorini C, et al. Motion artefacts in cone beam CT: an in vitro study about the effects on the images. *Br J Radiol*. 2016;89(1058):20150687.

32. Spin-Neto R, Matzen LH, Schropp LW, Sørensen TS, Wenzel A. An ex vivo study of automated motion artefact correction and the impact on cone beam CT image quality and interpretability. *Dentomaxillofac Radiol*. 2018;47:20180013.

33. Vasconcelos KF, Nicolielo LF, Nascimento MC, et al. Artefact expression associated with several cone-beam computed tomographic machines when imaging root filled teeth. *Int Endod J*. 2015;48:994-1000.

34. Parker J, Mol A, Rivera EM, Tawil P. CBCT uses in clinical endodontics: the effect of CBCT on the ability to locate MB2 canals in maxillary molars. *Int Endod J*. 2017;50:1109-1115.

3.9 Publicação 9*

Effect of foraminal enlargement on microcrack formation and apical transportation: A Nano-CT assessment

Abstract

Purpose: To evaluate the foraminal enlargement and its influence on microcrack formation and apical transportation in root canals with apical curvature. **Methods:** Eighteen maxillary lateral incisors with apical curvature were selected by using micro-CT images. Root canals were randomly divided in two groups (n=9) according to root canal preparation using two working lengths: 1 mm short of the apical foramen (control group) and 1 mm beyond the apical foramen (foraminal enlargement). For both groups Reciproc Blue R40 was used for root canal instrumentation. Specimens were scanned by nano-CT (UniTOM HR) before and after root canal preparation. Percentage, length, and width of microcracks, and apical transportation were assessed. Kappa, chi-square and McNemar tests were used for qualitative analyses while paired and unpaired t-test were used for quantitative analyses ($\alpha=0.05$). **Results:** For both groups, rather similar and low percentages of microcracks were observed before root canal preparation ($P>0.05$). The foraminal enlargement promoted new microcracks, not observed in the control group. An increase in microcrack length was observed when the foraminal enlargement was performed ($P<0.05$). Higher apical transportation was observed when foraminal enlargement was performed ($P< 0.05$). **Conclusions:** Foraminal enlargement using a heat-treated reciprocating file size 40 promoted microcracks and higher apical transportation than root canal preparation up to 1 mm short of apical foramen.

Keywords: Dentinal microcrack. Root canal preparation. Dental Pulp Cavity. NiTi instruments. X-Ray Microtomography

---

* Artigo em revisão no periódico *Odontology*.

Introduction

Root canal instrumentation directly influences long-term endodontic prognosis [1]. However, the apical limit of the root canal instrumentation is still a controversial topic in endodontics [1,2]. Although the most accepted working length is 1 mm short of the apical foramen [1], the foraminal enlargement technique has also been proposed by some authors [2-4]. This procedure aims to clean the apical foramen [4] in order to improve the root canal disinfection [2,4]. However, it is still not well defined if foraminal enlargement can promote microcracks and increase transportation of the apical foramen [5-8].

The presence of dentinal microcracks may influence long-term survival of the tooth [9], since microorganisms may proliferate in crack lines, leading to the establishment of biofilm on the root surface [10]. In addition, microcracks could potentially promote a vertical root fracture [11], especially in roots with reduced dentin thickness [12]. Apical transportation may also negatively affect cleaning and filling of the apical root portion, resulting in failure to control infection and to promote root canal sealing [13].

Micro-computed tomography (micro-CT) has been used to evaluate dentin microcracks, since it is a high precision tool that enables the location of such defects [14]. However, this method has limitations especially for visualizing small microcracks, with lower accuracy than operating microscope with transillumination [15]. Accordingly, to detect small structures or to perform high accuracy measurements, a higher precision tool is required [14]. Nano-computed tomography (nano-CT) devices have small focal spot and increased signal-to-noise ratio, making possible to achieve a maximum spatial resolution in the submicrometer range [16].

Therefore, the aim of the present study was to evaluate the influence of foraminal enlargement on microcrack formation and apical transportation in maxillary lateral incisors with apical curvature by using nano-CT. The null hypothesis was that the enlargement of apical foramen would not cause microcracks and/or apical transportation.

Materials and methods

Specimen Selection

All procedures were approved by the Faculty's Ethics Committee (CEP no. 29320820.8.0000.5416). Human maxillary lateral incisors with apical curvature (25°-35°) [17] previously stored in 0.1% thymol solution were used. The inclusion criteria comprised teeth with complete apical formation, absence of root fractures, calcifications or internal resorptions. Roots were inspected under a stereomicroscope at ×12 magnification to exclude those with any external dentinal defect and roots with immature apices. A digital radiographic system (RVG 6100; Kodak Dental Systems, NY) was used to select teeth according to inclusion criteria. Image J program (National Institutes of Health, Bethesda, MD, USA) was used to assess the degree of curvature in radiographic images. All selected teeth were scanned using a micro-CT device (SkyScan 1276; Bruker-micro-CT, Kontich, Belgium) at a low-resolution (35 µm voxel size). The three-dimensional images allowed a more accurate selection, and the inclusion criteria confirmation. After exclusion of teeth that did not reach the inclusion criteria, 18–maxillary lateral incisors with apical curvature were selected. Specimens were stored individually in numbered Eppendorf tubes at 100% humidity throughout the execution of the research.

Root Canal Instrumentation

Conventional access cavities were performed, and root canals were explored using a size #10 K-file (Dentsply Sirona, Ballaigues, Switzerland). When the tip of the instrument was visible through the main foramen, the working length (WL) was determined. In order to simulate the periodontal ligament, the specimens were assembled in an apparatus with acrylic resin and each tooth was embedded in condensation silicone (Oranwash, Zhermack SpA, Badia Polesine, Italy). The apparatus was immersed in distilled water during the operative steps to prevent dehydration of the specimens. The same dentist, specialist in endodontics, prepared all the teeth.

Lateral incisors were randomly divided into two experimental groups (n = 9), by using a stratified random sampling method, considering the preoperative volume of the root canals. For the control group, a conventional preparation was used, meaning that the WL was defined as 1mm short of the apical foramen. For the foramen enlargement group, the WL was defined as 1 mm beyond the apical foramen. For both groups, Reciproc Blue R40 (VDW GmbH, Munich, Germany) files were operated by an electric motor VDW SILVER (VDW GmbH) set in the "RECIPROC ALL" function. Each instrument was gradually inserted into the canal using in-and-out movements, at the three levels (cervical, middle and apical) up to WL. Root canal irrigation was performed with 5 mL of 2.5% sodium hypochlorite (NaOCl), using a 30G side-vented needle (NaviTip, Ultradent Products, South Jordan, UT) adapted to a 5 mL syringe (Ultradent Products). As final irrigation, 2 mL of 17% EDTA followed by 5 mL of distilled water were used.

Nano-CT Analysis

For nano-CT image acquisition, a high-resolution protocol (2µm voxel size) was used to scan all teeth before and after instrumentation by using UniTOM HR device (Tescan, Brno, Czech Republic). A tungsten target was employed, and the voltage and current applied were 65 kV and 123 µA, respectively, with an exposure time of 310 ms, 0.5 mm Al filter and 360° rotation around the vertical axis. Images were reconstructed using Acquila reconstruction software (Acquila v.2900), and superimposed with geometric alignment by DataViewer software program (Data Viewer v.1.5.1, Bruker). Quantitative and qualitative analyzes were performed using a CTAn software program (CTAn v.1.14.4, Bruker). Three-dimensional images were made with a CTVox software program (CTVox v.3.2; Bruker).

Analyses were performed in the 2-mm apical region of the roots. For qualitative analyses of microcracks, cross-sectional images before and after instrumentation were simultaneously assessed. Then, these were compared by two blinded examiners at two different time points. Microcracks were defined as lines or defects extending from inside the root canal to the dentin or from the outer root surface into the dentin. The distribution of microcracks was expressed as a percentage of the total cross-sectional images. The qualitative analyses of microcracks were based on their length and width. For length measurement, the extension of slices containing the microcrack was recorded, knowing that each slice represents exactly 0.002 mm, the number of slices was multiplicated for this value, and the result was considered as the microcrack length in mm. For width measurement, the extension of the microcracks was measured in each 10 cross-sectional slices, corresponding to 0.020 mm.

Measurement of the apical transportation were obtained before and after instrumentation on cross-sectional images of the roots. As proposed by Gambill et al. [18], the following formula was used to calculate the root canal transportation: (X1-X2) – (Y1-Y2). X1 represented the shortest distance from the outside of the curved root to the periphery of the canal before instrumentation, Y1 represented the shortest distance from the inside of the curved root to the periphery of the canal before instrumentation, X2 represented the shortest distance from the outside of the curved root to the periphery of the instrumented canal, and Y2 represented the shortest distance from the inside of the curved root to the periphery of the instrumented canal. Ten cross-sectional images, determined by the arithmetical mean value, were measured in the last 2 mm of apex of each root.

Statistical Analysis

For sample calculation, G* Power 3.1.7 for Windows program (Heinrich-Heine-Universität Dusseldorf, Dusseldorf, Germany) was used. Chi-square and t test were used with an Alpha type error of 0.05 and Beta power of 0.95. Previous studies were used to determine the specific effect size for percentage of microcracks, 0.93 [19]; and root canal transportation, 3.11 [20]. A total of 8 specimens was indicated as being the ideal size required.

All outcome data were analyzed with the GraphPad Prism 7.00 statistical software package (GraphPad Software, La Jolla, CA, USA).

For qualitative analyses of microcracks, results were expressed as the percentage for each group. Kappa statistics was used for intra- and inter-examiner agreement. McNemar test was used to determine significant differences before and after instrumentation and chi-square test was used for comparations between groups. For the qualitative analysis of microcracks and transportation, the normality of the data was tested using the Shapiro-Wilk test. The paired t-test was used for comparisons between before and after instrumentation. For comparisons between the groups non-paired t test was used. The level of significance was 5% for all the analysis.

Results

High intra and inter -examiner agreement was found with Kappa values higher than 0.91 for all evaluations.

Table 1 shows the mean of slices presenting microcracks, taking into account all evaluated samples. These results indicate a low percentage of microcracks before preparation, being similar between groups (P>0.05). The enlargement of apical foramina caused new microcracks with a higher percentage when compared to the preparation 1 mm short of apical foramen (P<0.05). New microcracks were not found in the control group (P>0.05). Figure 1 shows the appearance of new microcracks only after foraminal enlargement, as this finding was not detected in the control group.

Table 2 indicates the mean values and standard deviations of the length and width of microcracks observed before and after instrumentation. An increase in the microcracks length could be observed after foraminal enlargement (P<0.05), while in the control group the length values were similar before and after instrumentation (P>0.05). The width of cracks was similar between groups and before and after instrumentation for both groups (P>0.05).

Figure 2 indicates significant higher apical transportation after foramen enlargement in comparison with the control group (P <0.05). Figure 3 shows the presence of microcracks and apical deformations in 3D reconstructed images of nano-CT.

Table 1 Percentage of dentinal microcracks before and after preparation

	Before Preparation	**After Preparation**
Control Group	3.83^{aA}	4.40^{aA}
Foraminal enlargement	3.73^{aA}	12.87^{bB}

Different lowercase letters overlapped on the same line indicate statistical difference between before and after preparation in same group. Different capital letters overlapped on the same column indicate statistical difference between groups.

Table 2 Mean and standard deviation of the length and width (mm) of the microcracks found before and after preparation

		Before Preparation	After Preparation
length	Control Group	0.23 ± 0.06	0.23 ± 0.08
	Foraminal enlargement	0.22 ± 0.04*	0.33 ± 0.07*
width	Control Group	0.23 ± 0.07	0.27 ± 0.08
	Foraminal enlargement	0.26 ± 0.04	0.27 ± 0.05

* represents statistical difference between before and after preparation.

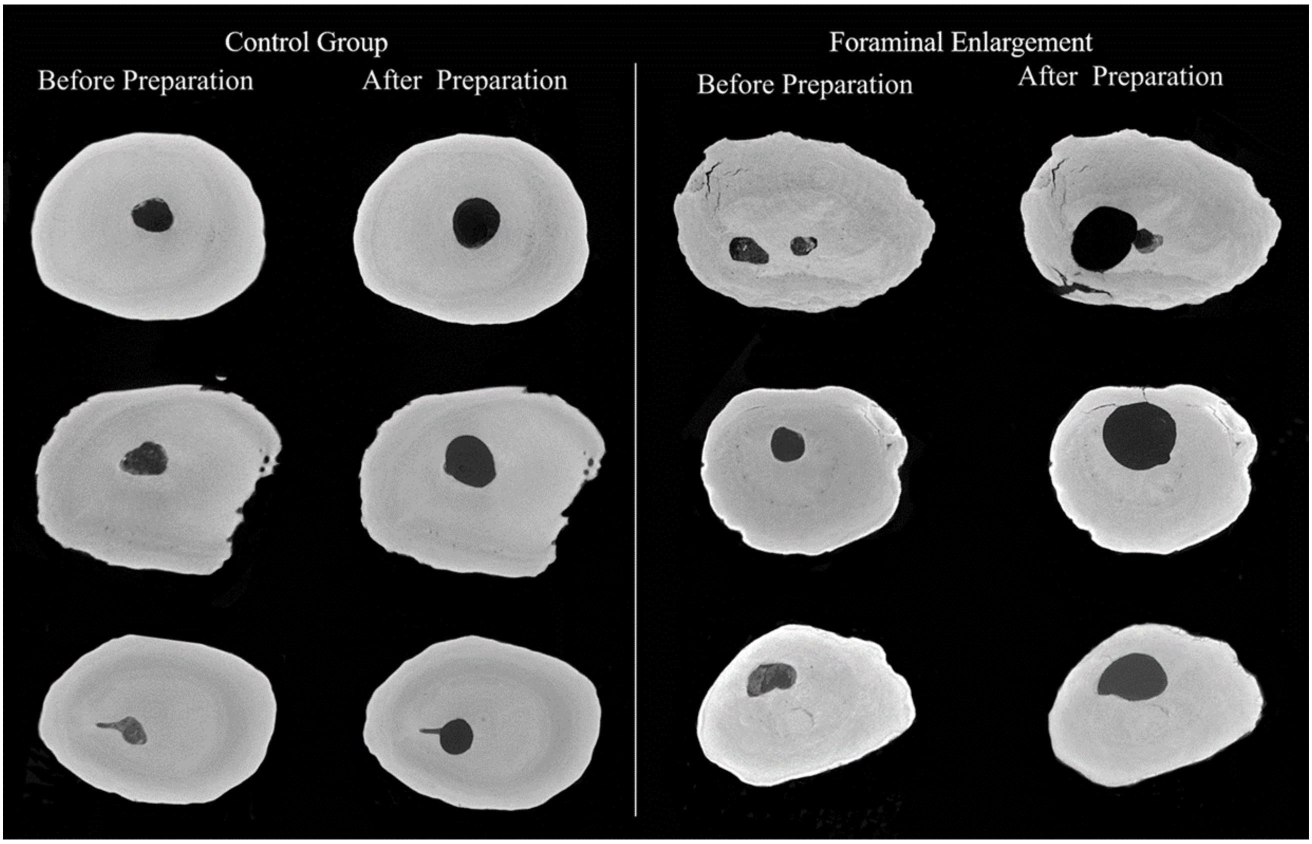

Figure 1 Representative cross-sectional nano–CT images showing the formation of microcracks after instrumentation for apical enlargement group.

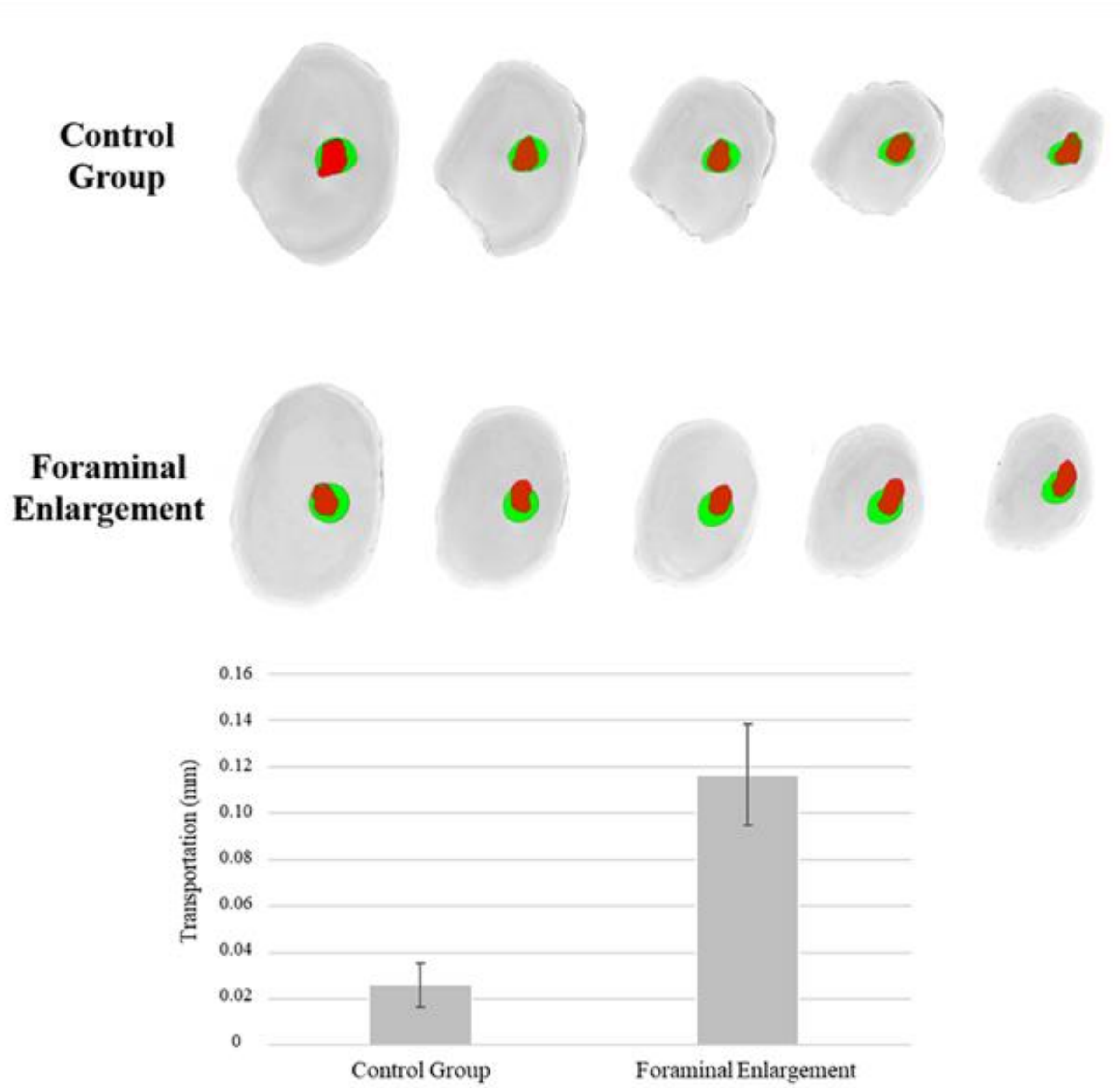

Figure 2 Representative cross-sectional of 3D reconstructions showing superposition of the root canal before instrumentation (red) with after instrumentation (green) and bar chart showing mean and standard deviation of the transportation (mm) caused in the root canals after preparation.

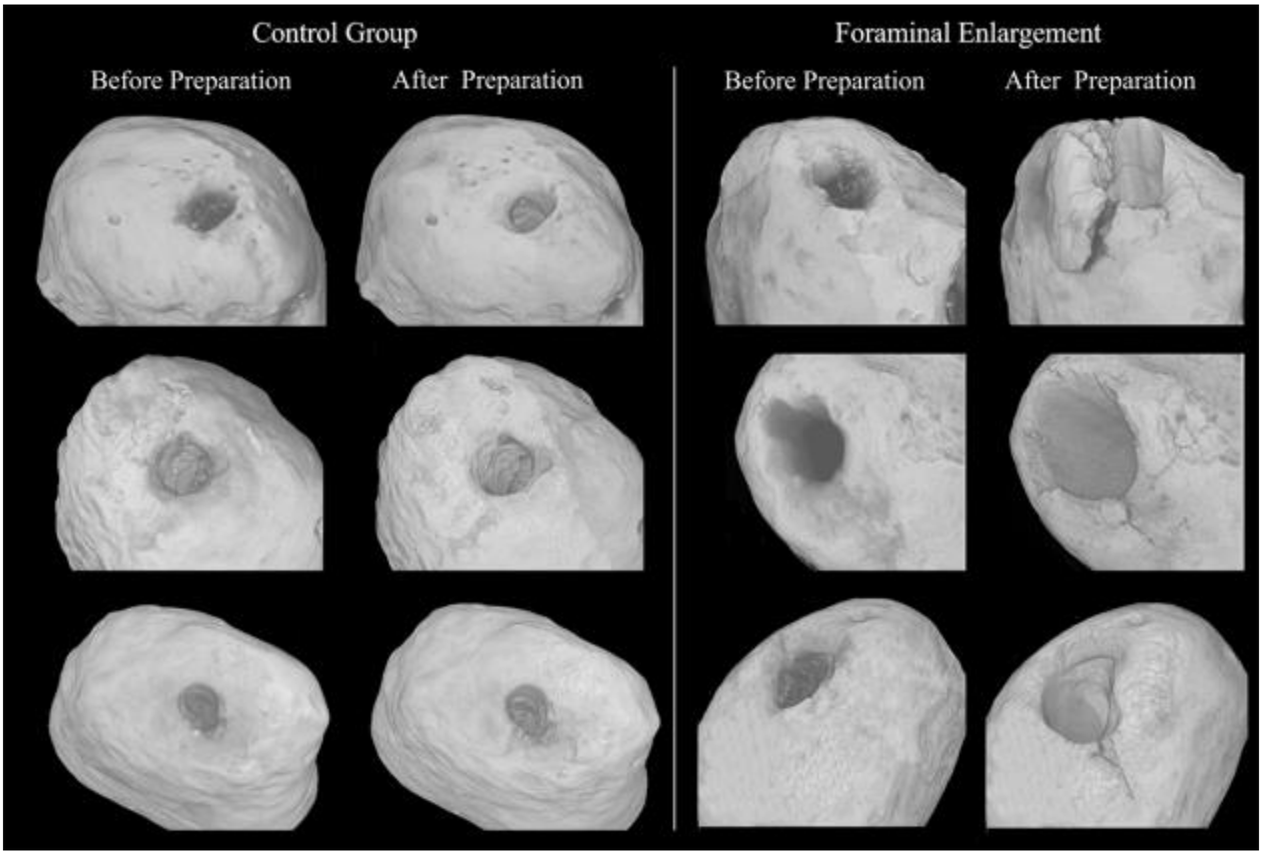

Figure 3 3D reconstruction of nano-CT showing the presence of microcracks and apical deformations after foraminal enlargement.

Discussion

The results of this *ex-vivo* study suggest that the enlargement of apical foramen using a heat-treated reciprocating file size #40 promoted the formation of microcracks and apical transportation. Therefore, the null hypothesis was rejected.

The current literature is still controversial regarding whether the limit of root canal preparation affect treatment prognosis [1, 2]. Moreover, a lack of consistency is observed in relation to the association between the working length and the presence of microcracks [5-8]. These conflicting results may be attributed to the use of different methodological designs, teeth morphology and analytical methods [15]. Therefore, this is the first study to assess the influence of working length on microcrack formation and on root foramen transportation by using nano-CT system.

A recent study did not find any correlation between the working length and the formation of new dentinal microcracks after preparation, however with a different methodological approach, especially regarding the size of apical preparation [8]. In this previous study, a lower apical preparation was performed until the size 0.25 mm by using Reciproc Blue R25. Nevertheless, the use of larger apical preparation has been recommended to improve the effect of irrigating solution [21], and to enhance root canal disinfection [22]. In addition, the current state-of-art of the heat-treated NiTi instruments, transversal sections and tapers results in safer root canal preparation of curved root canals [23]. The aforementioned statements justify the use of a larger apical preparation with the reciprocating NiTi file Reciproc Blue R40 in the present study. On the other hand, the higher size of preparation may have influenced microcrack formation after foraminal enlargement.

The high-resolution nano-CT images allowed accurate location of the microcracks before and after root canal preparation. In both groups, the microcracks presented small size, achieving an average length of 0.22 mm and an average width of 0.27 mm. When the foraminal enlargement was performed, microcracks were longer after preparation, while in the control group, preoperative microcracks remained unchanged. These microcracks can be a potential site for bacterial infection (6), significantly decreasing the long-term prognosis of the teeth.

In both groups, a small percentage of microcracks were observed before root canal instrumentation, as also observed in previous studies [24-27]. These microcracks can be attributed to the forces during extraction and excessive occlusal functional loads or even tooth age [28]. Dentin dehydration during experimental steps also have been referred as a risk factor for microcracks appearance [29]. However, to prevent the dentin dehydration the teeth were stored in 0.1% thymol and during nano-CT scans the specimens were covered with parafilm paper. Additionally, besides the facts that each specimen has acted as its own control, in the control group no new microcracks were found after instrumentation.

The foraminal enlargement caused more transportation in the root apex than the instrumentation performed 1 mm short of apical foramen. Reciproc Blue files are submitted to a heat treatment that improves their flexibility [30], making them suitable for instrumentation of curved root canal [31]. However, previous studies have shown some transportation, even using instruments with heat treatment [8, 32]. Some authors have also pointed out that this transportation can occur more frequently in preparations 1 mm beyond the foramen [8, 33]. Root canal transportation may negatively affect the outcomes of endodontic treatments [34], especially in the apical region that represents a critical zone to maintain infection of the root canal system [35]. In addition, as can been observed in figure 3, the transportation is still associated with deformations of the apical foramen [8]. In agreement, a previous study also observed higher apical foramen deformations after foraminal enlargement [33]. Moreover, it should be emphasized that such deformations may affect the sealing of the root canal filling.

Even with the inherent limitations related to an *ex-vivo* investigation, our results support the concept of restricting the root canal instrumentation procedures to the root canal limit, especially when larger files are used. Although some authors have recommended the enlargement of apical foramen to improve the apical cleaning [36], this might increase microcrack formation and canal transportation. Further studies are necessary to verify the influence of foraminal enlargement on filling adaption as well on the root canal cleaning.

Conclusion

In this *ex-vivo* study, the evaluation of ultra-resolution images showed a higher number of microcracks and apical transportation with the foraminal enlargement technique using heat-treated reciprocating files when compared to conventional preparation until 1mm short of apical foramen.

Compliance with ethical standards

Conflict of Interest The authors declare that they have no conflict of interest.

Funding

This study was entire supported by São Paulo Research Foundation - FAPESP (2019/22885-0).

Ethical approval All applicable guidelines were followed. The study was approved by the Institutional Ethics Committee (CEP no. 29320820.8.0000.5416).

Informed consent For this type of study, formal consent is not required.

Reference

1. Ricucci D (2021) Apical limit of root canal instrumentation and obturation, part 1. Literature review. Int Endod J 31:384-393. https://doi.org/10.1046/j.1365-2591.1998.00184.x
2. Yaylali IE, Teke A, Tunca YM 9(2017) The Effect of Foraminal Enlargement of Necrotic Teeth with a Continuous Rotary System on Postoperative Pain: A Randomized Controlled Trial. J Endod 43:359-363. https://doi.org/10.1016/j.joen.2016.11.009
3. Borlina SC, de Souza V, Holland R, et al (2010) Influence of apical foramen widening and sealer on the healing of chronic periapical lesions induced in dogs' teeth. Oral Surg Oral Med Oral Pathol Oral Radiol Endod 109:932-940. https://doi.org/10.1016/j.tripleo.2010.01.028
4. de Souza Filho FJ, Benatti O, de Almeida OP (1987) Influence of the enlargement of the apical foramen in periapical repair of contaminated teeth of dog. Oral Surg Oral Med Oral Pathol 64:480-484. https://doi.org/10.1016/0030-4220(87)90157-5
5. Adorno CG, Yoshioka T, Suda H (2010) The effect of working length and root canal preparation technique on crack development in the apical root canal wall. Int Endod J 43:321-327. https://doi.org/10.1111/j.1365-2591.2010.01684.x
6. Adorno CG, Yoshioka T, Suda H (2011) Crack initiation on the apical root surface caused by three different nickel-titanium rotary files at different working lengths. J Endod 37:522-525. https://doi.org/10.1016/j.joen.2010.12.002
7. de Oliveira BP, Câmara AC, Duarte DA, Heck RJ, Antonino ACD, Aguiar CM (2017) Micro-computed Tomographic Analysis of Apical Microcracks before and after Root Canal Preparation by Hand, Rotary, and Reciprocating Instruments at Different Working Lengths. J Endod 43:1143-1147. https://doi.org/10.1016/j.joen.2017.01.017
8. Vieira MLO, Dantas HV, de Sousa FB, et al (2020) Morphologic Changes of Apical Foramen and Microcrack Formation after Foraminal Enlargement: A Scanning Electron Microscopic and Micro-computed Tomographic Analysis. J Endod 46:1726-1732. https://doi.org/10.1016/j.joen.2020.07.017

9. Sim IG, Lim TS, Krishnaswamy G, Chen NN (2016) Decision Making for Retention of Endodontically Treated Posterior Cracked Teeth: A 5-year Follow-up Study. J Endod 42:225-229. https://doi.org/10.1016/j.joen.2015.11.011

10. Shen Y, Stojicic S, Haapasalo M (2011) Antimicrobial efficacy of chlorhexidine against bacteria in biofilms at different stages of development. J Endod 37:657-661. https://doi.org/10.1016/j.joen.2011.02.007

11. Wilcox LR, Roskelley C, Sutton T (1997) The relationship of root canal enlargement to finger-spreader induced vertical root fracture. J Endod 23:533-534. https://doi.org/10.1016/S0099-2399(97)80316-0

12. Lertchirakarn V, Palamara JE, Messer HH (2003) Patterns of vertical root fracture: factors affecting stress distribution in the root canal. J Endod 29:523-528. https://doi.org/10.1097/00004770-200308000-00008

13. Vaudt J, Bitter K, Neumann K, Kielbassa AM (2009) Ex vivo study on root canal instrumentation of two rotary nickel-titanium systems in comparison to stainless steel hand instruments. Int Endod J 42:22-33. https://doi.org/10.1111/j.1365-2591.2008.01489.x

14. Aksoy C, Keris EY, Yaman SD, Ocak M, Geneci F, Celik HH (2019) Evaluation of XP-endo Shaper, Reciproc Blue, and ProTaper Universal NiTi Systems on Dentinal Microcrack Formation Using Micro-Computed Tomography. J Endod 45:338-342. https://doi.org/10.1016/j.joen.2018.12.005

15. Andrea F, Campello MFM-A, José C, et al (2021) Accuracy of Microcomputed Tomography in Detecting DentinalCracks: A Correlative Study with Scanning Electron andOperative Microscopy. Scanning 2021. https://doi.org/10.1155/2021/5571123

16. Kampschulte M, Langheinirch AC, Sender J, et al (2016) Nano-Computed Tomography: Technique and Applications. Rofo 188:146-154. https://doi.org/10.1055/s-0041-106541

17. Schneider SW (1971) A comparison of canal preparations in straight and curved root canals. Oral Surg Oral Med Oral Pathol 32:271-175. https://doi.org/10.1016/0030-4220(71)90230-1

18. Gambill JM, Alder M, del Rio CE (1996) Comparison of nickel-titanium and stainless steel hand-file instrumentation using computed tomography. J Endod 22:369-375. https://doi.org/10.1016/S0099-2399(96)80221-4

19. Rödig T, Krämer J, Müller C, Wiegand A, Haupt F, Rizk M (2019) Incidence of microcracks after preparation of straight and curved root canals with three different NiTi instrumentation techniques assessed by micro-CT. Aust Endod J 45:394-399. https://doi.org/10.1111/aej.12339

20. Pedullà E, Plotino G, Grande NM, et al (2016) Shaping ability of two nickel-titanium instruments activated by continuous rotation or adaptive motion: a micro-computed tomography study. Clin Oral Investig 20:2227-2233. https://doi.org/10.1007/s00784-016-1732-4

21. Srikanth P, Krishna AG, Srinivas S, Reddy ES, Battu S, Aravelli S (2015) Minimal Apical Enlargement for Penetration of Irrigants to the Apical Third of Root Canal System: A Scanning Electron Microscope Study. J Int Oral Health 7:92-96.

22. Rodrigues RCV, Zandi H, Kristoffersen AK, et al (2017) Influence of the Apical Preparation Size and the Irrigant Type on Bacterial Reduction in Root Canal-treated Teeth with Apical Periodontitis. J Endod 43:1058-1063. https://doi.org/10.1016/j.joen.2017.02.004

23. Pivoto-João MMB, Tanomaru-Filho M, Pinto JC, Espir CG, Guerreiro-Tanomaru JM (2020) Root Canal Preparation and Enlargement Using Thermally Treated Nickel-Titanium Rotary Systems in Curved Canals. J Endod 46:1758-1765. https://doi.org/10.1016/j.joen.2020.08.007

24. Ceyhanlı KT, Erdilek N, Tatar I, Çelik D (2016) Response to comments on to our published article entitled: 'Comparison of ProTaper, RaCe and Safesider instruments in the induction of dentinal microcracks: a micro-CT study'. Int Endod J 49:212-215. https://doi.org/10.1111/iej.12497

25. De-Deus G, Belladonna FG, Souza EM, et al (2015) Micro-computed Tomographic Assessment on the Effect of ProTaper Next and Twisted File Adaptive Systems on Dentinal Cracks. J Endod 41:1116-1119. https://doi.org/10.1016/j.joen.2015.02.012

26. Bayram HM, Bayram E, Ocak M, Uzuner MB, Geneci F, Celik HH (2017) Micro-computed Tomographic Evaluation of Dentinal Microcrack Formation after Using New Heat-treated Nickel-titanium Systems. J Endod 43:1736-1739. https://doi.org/10.1016/j.joen.2017.05.02

27 Pop I, Manoharan A, Zanini F, Tromba G, Patel S, Foschi F (2015). Synchrotron light-based μCT to analyse the presence of dentinal microcracks post-

rotary and reciprocating NiTi instrumentation. Clin Oral Investig 19:11-16. https://doi.org/10.1007/s00784-014-1206-5

28. PradeepKumar AR, Shemesh H, Chang JW, et al (2017) Preexisting Dentinal Microcracks in Nonendodontically Treated Teeth: An Ex Vivo Micro-computed Tomographic Analysis. J Endod 43:896-900. https://doi.org/10.1016/j.joen.2017.01.026

29. De-Deus G, Cesar de Azevedo Carvalhal J, et al (2017) Dentinal Microcrack Development after Canal Preparation: A Longitudinal in Situ Micro-computed Tomography Study Using a Cadaver Model. J Endod 43:1553-1558. https://doi.org/10.1016/j.joen.2017.04.027

30. De-Deus G, Silva EJ, Vieira VT, et al (2017) Blue Thermomechanical Treatment Optimizes Fatigue Resistance and Flexibility of the Reciproc Files. J Endod 43:462-466. https://doi.org/10.1016/j.joen.2016.10.039

31. Belladonna FG, Carvalho MS, Cavalcante DM, et al (2018) Micro-computed Tomography Shaping Ability Assessment of the New Blue Thermal Treated Reciproc Instrument. J Endod 44:1146-1150. https://doi.org/10.1016/j.joen.2018.03.008

32. Hu W, Whitten B, Sedgley C, Svec T (2014) Effect of three NiTi files on transportation of the apical foramen. Int Endod J 47:1064-1071. https://doi.org/10.1111/iej.12249

33. Silva Santos AM, Portela FMSF, Coelho MS, Fontana CE, De Martin AS (2018) Foraminal Deformation after Foraminal Enlargement with Rotary and Reciprocating Kinematics: A Scanning Electronic Microscopy Study. J Endod. 2018;44:145-8. https://doi.org/10.1016/j.joen.2017.08.013

34. Peters OA, Morgental RD, Schulze KA, Paqué F, Kopper PM, Vier-Pelisser FV (2014) Determining cutting efficiency of nickel-titanium coronal flaring instruments used in lateral action. Int Endod J 47:505-513. https://doi.org/10.1111/iej.12177

35. Siqueira JF, Rôças IN (2008) Clinical implications and microbiology of bacterial persistence after treatment procedures. J Endod 34:1291-301.e3. https://doi.org/10.1016/j.joen.2008.07.028ui..iou

36. Brandão PM, de Figueiredo JAP, Morgental RD, et al (2019) Correction to: Influence of foraminal enlargement on the healing of periapical lesions in rat molars. Clin Oral Investig 23:2001-2003. https://doi.org/10.1007/s00784-018-2628-2.

4 DISCUSSÃO

Micro-CT é utilizado para avaliação do preparo de canais radiculares com diferentes instrumentos endodônticos mecanizados[1,5,6]. Os resultados do presente estudo revelaram que a influência do tamanho do voxel nas análises de preparo por micro-CT é dependente da estrutura avaliada. As publicações 1 e 3 mostraram não haver diferença significativa nas análises de volume do canal e acumulo de debris após o preparo entre as análises realizadas nos diferentes tamanhos de voxel, 5, 10 e 20 µm. Porém um desfecho diferente foi obtido nas comparações de superfície não instrumentada quando as análises foram realizadas a 5 µm. Ainda, a publicação 2 mostra a maior precisão para avaliações qualitativas de microtrincas dentinárias em imagens de micro-CT com tamanho de voxel de 5 µm. A influência do tamanho pode ser explicada pelo efeito de volume parcial que ocorre quando um único voxel representa duas ou mais estruturas, dificultando sua visualização correta[91].

Tendo em vista a importância da instrumentação radicular para o prognóstico do tratamento endodôntico[24,25], a publicação 1 mostra que PDL e HFEDM tiveram capacidade de preparo semelhante com relação ao volume, debris e superfície não tocada. No entanto, na publicação 2, pode ser observada uma associação do instrumento HFEDM com maior formação de microtrincas dentinárias no terço médio, que não foi observada para o instrumento PDL. Este comportamento pode estar relacionado a diversos fatores como conicidades, desenho da ponta e secções transversais distintas entre os instrumentos[92-94]. Além disso o instrumento HFEDM apresenta superfície mais dura devido tratamento de superfície EDM[95,96].

Com relação a publicação 3, especial atenção dever ser dada para o fato de que o PUI só foi eficaz para remoção de debris no terço médio. Levando em conta a importância da limpeza do terço apical para o prognostico do tratamento endodôntico, sendo que esta região representa a zona crítica para manutenção da infecção periradicular[97]. Ampliações maiores do batente apical devem ser encorajadas, principalmente em dentes com periodontite apical. Apesar do presente estudo ter utilizado preparos até o tamanho 30/.05 para PDL e 25/.08 para HFEDM, ampliações apicais maiores chegando 35 ou 40 foram recomendados para canais curvos, sendo associadas a maior remoção de debris sem ocasionar transporte do canal[98,99]. Além disso, maior diâmetro do preparo pode levar a melhor circulação da substancia irrigadora durante o PUI[100,101].

A significativa maior precisão na detecção de microtrincas dentinárias para imagens com menor tamanho de voxel, destacada na publicação 2, motivou a escolha do nano-CT para avaliação de microtrincas dentinárias na publicação 9. As imagens de nano-TC com alta resolução permitiram a localização precisa das microtrincas, além de mensurações com grande acurácia. Apesar de alguns autores sugerirem a ampliação do forame apical[102-104], alegando maior limpeza e deinfeção[105]. Nosso estudo mostrou uma associação da ampliação do forame apical com a formação de microtrincas dentinárias e transporte apical. As microtrincas dentinárias no ápice podem abrigar biofilme bacteriano[106] e o transporte apical é relacionado a deformações no forame apical[107] que pode afetar negativamente o selamento da obturação endodôntica. Desta forma, deve ser encorajado o preparo dos canais radiculares até 1 mm aquém do forame apical, respeitando os limites do canal radicular.

O preenchimento adequado do sistema de canais radiculares é fundamental para um prognostico favorável a longo prazo dos dentes submetidos a tratamento endodôntico[108]. Desta forma a capacidade de preenchimento é uma das propriedades necessárias ao cimento endodôntico. Todavia, em alguns tratamentos endodônticos, devido à persistência bacteriana já existente ou contaminação do canal radicular posterior ao tratamento, o retratamento endodôntico é indicado[37]. Neste caso, a fácil remoção do material do interior do canal radicular é uma característica desejável ao cimento endodôntico. A publicação 4 reporta que o cimento a base de silicato de cálcio Bio-C Sealer teve capacidade de preenchimento similar ao AH Plus, e as publicações 5 e 6 mostraram que este cimento é removido mais facilmente dos canais radiculares curvos que o AH Plus em caso de retratamento. Tendo em vista que cimento AH Plus é considerado padrão ouro devido suas excelentes propriedades físico-químicas[41] e que os resultados foram favoráveis para cimento Bio-C Sealer, que é biocompatível e bioativo[109,110] além de apresentar bons resultados nos testes físico-químicos[111], podemos considerar o cimento Bio-C Sealer como alternativa na obturação de canais radiculares.

As dificuldades na escolha dos parâmetros de escaneamento por micro-CT relatadas nas análises do preparo do canal radicular[112], se tornam ainda mais desafiadoras quando o objeto de análise é a obturação ou retratamento. Os artefatos provenientes de materiais com alto peso atômico, como os radipacificadores dos cimentos endodônticos prejudicam a qualidade final das imagens dificultando as análises volumétricas[113]. No entanto, as publicações 4 e 6 mostraram que independente do cimento obturador utilizado os diferentes tamanhos de voxel não influenciaram os resultados das avaliações de obturação e retratamento endodôntico. Porém, deve-se ter em mente que apesar das radiopacidades distintas entre si, tanto AH Plus quanto Bio-C Sealer apresentam radioapacidade em acordo com a norma ISO[111]. Ainda, a escolha correta dos parâmetros de aquisição propiciou imagens com boa qualidade, mesmo nos maiores tamanhos de voxel. É importante enfatizar que a resolução da imagem além do tamanho do voxel, depende de outras variáveis como absorção média da amostra, ruído do detector, algoritmo de reconstrução, tamanho e forma do ponto focal de raios-X, abertura do detector e geometria do scanner[114].

Atualmente o uso de TCFC tem sido cada vez mais difundido na endodontia. Imagens tridimensionais auxiliam no diagnostico, plano de tratamento e prognóstico endodôntico[66-68]. As Publicações 7 e 8 mostram que existe uma heterogeneidade com relação ao desempenho dos aparelhos de TCFC para visualização de estruturas endodônticas pequenas como canais estreitos, istmos e delta apicais. Esses achados podem ser explicados pela variabilidade de dimensões físicas, características, modalidades de imagem disponíveis e parâmetros essenciais, como especificações da fonte de raios-X e parâmetros de exposição, campo de visão entre os dispositivos de CBCT[86]. A influência negativa da presença de metal no campo de visão para visualização das estruturas também foi observada. Sendo ainda ressaltada na publicação 8 a maior influência do pino metálico em relação o implante dentário de titânio. O maior peso atômico do pino metálico de ouro (Z=79) em reação ao implante de titânio (Z=22) provavelmente causou maior formação de artefatos nas imagens de TCFC, uma vez que existe uma associação direta entre a presença de materiais com levado número atômico e maior formação de artefatos[115].

A publicação 8 ressalta ainda a importância de protocolos de alta de resolução e o uso de campos de visão pequenos para realização das tarefas diagnosticas endodônticas. Além disso, foi evidenciada a grande limitação da visualização de pequenas trincas usando imagens de TCFC. Sendo assim, no diagnóstico de trincas radiculares, outros fatores devem ser levados em consideração, como sinais e sintomas clínicos e o padrão de perda óssea nas imagens[116].

De forma geral, com relação às análises de preparo podemos concluir que a influência do tamanho de voxel é dependente da variável a ser avaliada. Os instrumentos PDL e HFEDM tem capacidade de preparo semelhante, sendo que HFEDM é mais propício a formação de microtrincas dentinárias. Os preparos radiculares preferencialmente devem ser realizados 1 mm aquém do forame apical. A respeito das análises de obturação e retratamento, O cimento Bio-Sealer tem adequada capacidade de preenchimento, além disso este material pode ser removido mais facilmente que o AH Plus em caso de retratamento. Os diferentes tamanhos de voxel, bem como, cimentos com diferentes radiopacidades não influenciaram as análises volumétricas.

Com relação as avaliações de TCFC foi observado resultados distintos entre os aparelhos para realização de tarefas diagnosticas endodônticas, sendo que os protocolos de alta resolução com campo de visão pequenos são preferíveis para visualização de pequenas estruturas. A presença de metal piorou significativamente a qualidade das imagens de TCFC, principalmente o pino metálico de ouro.

5 CONCLUSÃO

De acordo com os resultados do presente estudo, pode-se concluir:

O tamanho de voxel não teve impacto significativo na análise do volume dos canais radiculares e de debris. Porém, o tamanho do voxel deve ser considerado como um fator potencial para superfície não instrumentada, uma vez que foram observados resultados diferentes para imagens a 5 µm, em comparação com imagens de tamanhos de voxel de 10 e 20 µm. PDL e HFEDM tiveram capacidade de preparo semelhantes.

Os diferentes tamanhos de voxel influenciaram a análise de microtrincas por micro-CT, sendo a maior precisão observada para análises realizadas com tamanho de voxel de 5 µm. HyFlex EDM causou ainda mais microtrincas no terço médio, detectáveis apenas pela visualização de imagens feitas em tamanho de voxel de 5 µm.

Os tamanhos dos voxels avaliados não tiveram impacto significativo na análise de debris. No entanto, os resultados mostraram uma tendência de detecção de mais debris em análises realizadas com um tamanho de voxel menor. O PUI reduziu o acúmulo de debris no terço médio dos canais radiculares curvos.

Bio-C Sealer e AH Plus forneceram capacidade de preenchimento adequada em canais radiculares curvos. Além disso, a segmentação visual e automática pode ser aplicada a imagens de micro-TC com tamanhos de voxel de 5 a 20 µm para avaliar a qualidade do preenchimento endodôntico. O método de segmentação automática deve ser considerado como primeira escolha para avaliar a qualidade da obturação do canal radicular devido às suas características rápidas, confiáveis e menos dependentes do operador.

A remoção do material obturador do terço apical foi mais fácil para os canais obturados com Bio-C Sealer do que com AH Plus. PDL 50/.01 e XP-endo Finisher proporcionaram maior remoção de materiais obturadores no terço apical após retratamento de canais radiculares curvos. Ambas as abordagens suplementares não apresentaram transporte apical. PDL 50/.01 promoveu maior aumento de volume do terço apical que o XP-endo Finisher.

Imagens de micro-CT usando diferentes tamanhos de voxel não influenciaram na análise do material de preenchimento remanescente independentemente do cimento endodôntico, AH Plus ou Bio-C Sealer.

A visualização de estruturas endodônticas pequenas foi dependente do dispositivo de TCFCT e sua detecção foi influenciada pela presença de metal.

A capacidade de visualização de pequenas trincas em imagens de TCFC é altamente limitada e restrita a determinados dispositivos e protocolos na ausência de metal. A visualização de estruturas endodônticas pequenas foi dependente do dispositivo TCFC com uma melhor capacidade observada para protocolo de alta resolução com FOV pequeno, desde que não houvesse objetos de alta densidade adjacentes à região de interesse

O alargamento do forame apical pode aumentar a formação de microtrincas e o transporte do canal, especialmente quando limas maiores são utilizadas, reforçando o conceito de restringir os procedimentos de instrumentação do canal radicular ao limite do canal radicular.

REFERÊNCIAS*

1. Freire LG, Iglecias EF, Cunha RS, Dos Santos M, Gavini G. Micro-computed tomographic evaluation of hard tissue debris removal after different irrigation methods and its influence on the filling of curved canals. J Endod. 2015; 41(10): 1660-6.
2. Huang Y, Orhan K, Celikten B, ORHAN A, Tufenkci P, Sevimay S. Evaluation of the sealing ability of different root canal sealers: a combined SEM and micro-CT study. J Appl Oral Sci. 2018; 26. doi: 10.1590/1678-7757- 2016-0584.
3. Rödig T, Hausdörfer T, Konietschke F, Dullin C, Hahn W, Hülsmann M. Efficacy of D-RaCe and ProTaper Universal Retreatment NiTi instruments and hand files in removing gutta-percha from curved root canals: a micro-computed tomography study. Int Endod J. 2012; 45(6): 580–9.
4. Christiansen BA. Effect of micro-computed tomography voxel size and segmentation method on trabecular bone microstructure measures in mice. Bone Re. 2016; 5:136-40.
5. Versiani MA, De-Deus G, Vera J, Souza E, Steier L, Pécora JD, Sousa-Neto MD. 3D mapping of the irrigated areas of the root canal space using micro-computed tomography. Clin Oral Investig. 2015; 19(4): 859-66.
6. Gergi R, Osta N, Bourbouze G, Zgheib C, Arbab-Chirani R, Naaman A. Effects of three nickel titanium instrument systems on root canal geometry assessed by micro-computed tomography. Int Endod J. 2015; 48(2): 162-70.
7. Stavileci M, Hoxha V, Görduysus Ö, Tatar I, Laperre K, Hostens J, Küçükkaya S, Muhaxheri E. Evaluation of root canal preparation using rotary system and hand instruments assessed by micro-computed tomography. Med Sci Monit Basic Res. 2015; 21: 123-30.
8. Ahmetoglu F, Keles A, Simsek N, Ocak MS, Yologlu S. Comparative evaluation of root canal preparations of maxillary first molars with self-adjusting file, reciproc single file, and revo-s rotary file: a micro-computed tomography study. Scanning. 2015; 37(3): 218-25
9. Pasqualini D, Alovisi M, Cemenasco A, Mancini L, Paolino DS, Bianchi CC, Roggia A, Scotti N, Berutti E. Micro-computed tomography evaluation of Protaper Next and Biorace Shaping outcomes in maxillary first molar curved canals. J Endod 2015; 41(10): 1706-10.

* De acordo com o Guia de Trabalhos Acadêmicos da FOAr, adaptado das Normas Vancouver. Disponível no site da Biblioteca: http://www.foar.unesp.br/Home/Biblioteca/guia-de-normalizacao-atualizado.pdf

10. Leoni GB, Versiani MA, Silva-Sousa YT, Bruniera JF, Pécora JD, Sousa-Neto MD. Ex vivo evaluation of four final irrigation protocols on the removal of hard-tissue debris from the mesial root canal system of mandibular first molars. Int Endod J. 2017; 50(4): 398-406.

11. Li D, Jiang S, Yin X, Chang JW, Ke J, Zhang C. Efficacy of needle, ultrasonic, and endoactivator irrigation and photon-induced photoacoustic streaming in removing calcium hydroxide from the main canal and isthmus: an in vitro micro-computed tomography and scanning electron microscopy study. Photomed Laser Surg. 2015; 33(6): 330-7.

12. Paqué F, Laib A, Gautschi H, Zehnder M. Hard-tissue debris accumulation analysis by high-resolution computed tomography scans. J Endod. 2009; 35(7): 1044–7.

13. Robinson JP, Lumley PJ, Claridge E, Cooper PR, Grover LM, Williams RL, Walmsley AD. An analytical Micro CT methodology for quantifying inorganic dentine debris following internal tooth preparation. J Dent. 2012; 40(11): 999-1005.

14. Robinson JP, Lumley PJ, Cooper PR, Grover LM, Walmsley AD. Reciprocating root canal technique induces greater debris accumulation than a continuous rotary technique as assessed by 3-dimensional micro-computed tomography. J Endod. 2013; 39(8): 1067-1070.

15. Campello AF, Marceliano-Alves MF, Provenzano JC, Loyola SC, Siqueira JF Jr, Machado AG, et al. Accuracy of microcomputed tomography in detecting dentinalcracks: a correlative study with scanning electron and operative microscopy. Scanning 2021. https://doi.org/10.1155/2021/5571123

16. Jamleh A, Komabayashi T, Ebihara A, Nassar M, Watanabe S, Yoshioka T, Miyara K, Suda H. Root surface strain during canal shaping and its influence on apical microcrack development: a preliminary investigation. Int Endod J. 2015; 48(12): 1103-11.

17. De-Deus G, Belladonna FG, Souza EM, Silva EJ, Neves Ade A, Alves H, et al. Micro-computed Tomographic Assessment on the Effect of ProTaper Next and Twisted File Adaptive Systems on Dentinal Cracks. J Endod 2015; 41(7): 1116-9.

18. De-Deus G, Belladonna FG, Souza EM, Silva EJ, Neves Ade A, Alves H, Lopes RT, Versiani MA. Micro-computed Tomographic Assessment on the Effect of ProTaper Next and Twisted File adaptive systems on dentinal cracks. J Endod. 2015; 41(7):1116-9.

19. Cassimiro M, Romeiro K, Gominho L, de Almeida A, Costa L, Albuquerque D. Occurence of dentinal defects after root canal preparation with R-phase, M-Wire and Gold Wire instruments: a micro-CT analysis. BMC Oral Health. 2017; 17(11): 1-6

20. Ceyhanli KT, Erdilek N, Tatar I, Celik D. Comparison of ProTaper, RaCe and Safesider instruments in the induction of dentinal microcracks: a micro-CT study. Int Endod J 2016; 49(7): 684-9.

21. Aksoy C, Keris EY, Yaman SD, Ocak M, Geneci F, Celik HH. Evaluation of XP-endo Shaper, Reciproc Blue, and ProTaper Universal NiTi systems on dentinal microcrack formation using Micro-Computed Tomography. J Endod. 2019; 45(3): 338-42.

22. Kampschulte M, Langheinirch AC, Sender J, Litzlbauer HD, Althöhn U, Schwab JD, et al. Nano-Computed Tomography: Technique and Applications. Rofo. 2016; 188(2): 146-54.

23. Seibert JA. Flat-panel detectors: how much better are they? Pediatr Radiol 2006;36:173-81.

24. Schilder H. Cleaning and shaping the root canal. Dent Clin North Am. 1974; 18(2): 269-96.

25. Wu MK, Dummer PM, Wesselink PR. Consequences of and strategies to deal with residual post-treatment root canal infection. Int Endod J. 2006; 39(5): 343-56.

26. Hieawy A, Haapasalo M, Zhou H, Wang Z, Shen Y. Phase transformation behavior and resistance to bending and cyclic fatigue of ProTaper Gold and ProTaper Universal instruments. J Endod. 2015; 41(7): 1134-8.

27. Elnaghy AM, Elsaka E. Mechanical properties of ProTaper Gold Nickel Titanium rotary instruments. Int Endod J. 2016; 49(11): 1073-8.

28. Saber SEDM, Nagy MM, Schafer E. Comparative evaluation of the shaping ability of ProTaper Next, RaCe and Hyflex CM Rotary NITI files in severely curved root canals. Int. Endod. J. 2015; 48(2): 131-6.

29. Marceliano-Alves MF, Sousa-Neto MD, Fidel SR, Steier L, Robinson JP, Pécora JD, et al.Shaping ability of single-file reciprocating and heat-treated multifile rotary systems: a micro-CT study. Int Endod J.2015; 48(12): 1129-36.

30. Pinheiro SR, Alcalde MP, Vivacqua-Gomes N, Bramante CM, Vivan RR, Duarte MAH, et al. Evaluation of apical transportation and centring ability of five thermally treated NiTi rotary systems. Int Endod J. 2017; 22(6): 1-9.

31. Pedullà E, Savio FL, Boninelli S, Plotino G, Grande NM, La Rosa G, et al. Torsional and cyclic fatigue resistance of a new nickel-titanium instrument manufactured by electrical discharge machining. J Endod. 2016; 42(1): 156-9.

32. Pirani C, Iacono F, Generali L, Sassatelli P, Nucci C, Lusvarghi L, et al. Hyflex EDM: superficial features, metallurgical analysis and fatigue resistance of innovative electro discharge machined NiTi Rotary instruments. Int Endod J. 2016; 49(5): 483–93.

33. Iacono F, Pirani C, Generali L, Bolelli G, Sassatelli P, Lusvarghi L, et al. Structural analysis of HyFlex EDM instruments. Int Endod J. 2017; 50(3): 303-13.

34. De Menezes SEAC, Batista SM, Lira JOP, de Melo Monteiro GQ. Cyclic fatigue resistance of WaveOne Gold, ProDesign R and ProDesign logic files in curved canals in vitro. Iran Endod J. 2017; 12(4): 468-43.

35. De-Deus G, Silva EJ, Vieira VT, Belladonna FG, Elias CN, Plotino G et al. Blue thermomechanical treatment optimizes fatigue resistance and flexibility of the reciproc files. J Endod. 2017; 43(3): 462-6.

36. Leonardo M, Leonardo RT. Tratamento de canais radiculares: avanços tecnológicos de uma endodontia minimamente invasiva e reparadora. São Paulo: Artes Médicas 2012.

37. Lopes HP, Siqueira JR. JF. Endodontia biologia e técnica. 3° ed. Rio de Janeiro: Guanabara Koogan 2013.

38. Taşdemir T, Er K, Yildirim T, Buruk K, Çelik D, Cora S, Serper A. Comparison of the sealing ability of three filling techniques in canals shaped with two different rotary systems: a bacterial leakage study. Oral Surgery, Oral Medicine, Oral Pathology, Oral Radiology, and Endodontology. 2009; 108(3): e129-e134.

39. Cavenago BC, Duarte MAH, Ordinola-Zapata R, Marciano MA, Carpio-Perochena AED, Bramante CM. Interfacial adaptation of an epoxy-resin sealer and a self-etch sealer to root canal dentin using the System B or the single cone technique. Braz Dent J. 2012; 23: 205-11.

40. Qu W, Bai W, Liang YH, Gao XJ. Influence of warm vertical compaction technique on physical properties of root canal sealers. J Endod. 2016; 42(12): 1829-33.

41. Almeida LHS, Moraes RR, Morgental RD, Pappen FG. Are Premixed Calcium Silicate–based Endodontic Sealers Comparable to Conventional Materials? A Systematic Review of In Vitro Studies. J Endod. 2017; 43(4): 527-35.

42. Peng L, Ye L, Tan H, Zhou X. Outcome of root canal obturation by warm gutta-percha versus cold lateral condensation: a meta-analysis. J Endod. 2007; 33(2): 106-9.

43. Camilleri J. Staining potential of Neo MTA Plus, MTA Plus and Biodentine used for pulpotomy procedures. J Endod. 2015; 41(7): 1139-45.

44. Tanomaru-Filho M, Andrade AS, Rodrigues EM, Viola KS, Faria G, Camilleri J, et al. Biocompatibility and mineralized nodule formation of Neo MTA Plus and an experimental tricalcium silicate cement containing tantalum oxide. Int Endod J 2017; 50: 31-9.

45. Zordan-Bronzel CL, Esteves Torres FF, Tanomaru-Filho M, Chávez-Andrade GM, Bosso-Martelo R, Guerreiro-Tanomaru JM. Evaluation of physicochemical properties of a new calcium silicate-based sealer, Bio-c Sealer. J Endod. 2019; 45(10): 1248-52.

46. Torres FFE, Zordan-Bronzel CL, Guerreiro-Tanomaru JM, Chávez-Andrade GM, Pinto JC, Tanomaru-Filho M. Effect of immersion in distilled water or phosphate-buffered saline on the solubility, volumetric change and presence of voids within new calcium silicate-based root canal sealers. Int Endod J. 2020 ; 53(3): 38-391.

47. Ho ES, Chang JW, Cheung GS. Quality of root canal fillings using three gutta-percha obturation techniques. Restorative Dentistry & Endodontics. 2016; 41(10): 22-8.

48. Iglecias EF, Freire LG, de Miranda Candeiro GT. Dos Santos M, Antoniazzi JH, Gavini G. Presence of voids after continuous wave of condensation and single-cone obturation in mandibular molars: A micro-computed tomography analysis. J Endod. 2017; 43(4), 638-42.

49. Oh S, Perinpanayagam H, Kum DJ, Lim SM, Yoo YJ, Chang SW, et al. Evaluation of three obturation techniques in the apical third of mandibular first molar mesial root canals using micro-computed tomography. Journal of Dental Sciences. 2016; 11(1): 95-102.

50. Keleş A, Alcin H, Kamalak A, Versiani MA. Micro-CT evaluation of root filling quality in oval-shaped canals. Int Endod J. 2014; 47(12):1177-84.

51. Zogheib C, Naaman A, Sigurdsson A, Medioni E, Bourbouze G, Arbab-Chirani R. Comparative micro-computed tomographic evaluation of two carrier-based obturation systems. Clin Oral Investig. 2013; 17(8): 1879-83.

52. Zaslansky P, Fratzl P, Rack A, Wu MK, Wesselink PR, Shemesh H. Identification of root filling interfaces by microscopy and tomography methods. Int Endod J. 2011; 44(5): 395-401.

53. Kierklo A, Tabor Z, Pawińska M, Jaworska M. A microcomputed tomography-based comparison of root canal filling quality following different instrumentation and obturation techniques. Med princ pract. 2015; 24(1) :84-91.

54. Torabinejad M, Walton RE. Endodontia: Princípios e Prática. 4° Ed., Rio de Janeiro: Elsevier, 2010, 474 p. 1 v. p. 203-211 e 334-335, ISNB 978-85-352-34444-2.

55. Zuolo AS, Mello JE Jr, Cunha RS, Zuolo ML, Bueno CE. Efficacy of reciprocating and rotary techniques for removing filling material during root canal retreatment. Int Endod J. 2013; 46(10): 947–53.

56. Rios M de A, Villela AM, Cunha RS, Velasco RC, De Martin AS, Kato AS, et al. Efficacy of 2 reciprocating systems compared with a rotary retreatment system for gutta-percha removal. J Endod. 2014; 40(4): 543–6.

57. Elnaghy AM, Mandorah A, Elsaka SE. Effectiveness of XP-endo Finisher, EndoActivator, and File agitation on debris and smear layer removal in curved root canals: a comparative study. Odontology. 2017; 105(2):

58. Alves FR, Marceliano-Alves MF, Sousa JCN, Silveira B, Provenzano JC, Siqueira Jr JF. Removal of root canal fillings in curved canals using either reciprocating single-or rotary multi-instrument systems and a supplementary step with the XP-Endo Finisher. J Endod. 2016; 42(7): 1114-9.

59. Rödig T, Hausdorfer T, Konietschke F, Dullin C, Hahn W, Hülsmann M. Efficacy of D-RaCe and ProTaper Universal Retreatment NiTi instruments and hand files in removing gutta-percha from curved root canals: a micro-computed tomography study. Int Endod J. 2012; 45(6): 580–9.

60. Bernardes RA, Duarte MA, Vivan RR, Alcalde MP, Vasconcelos BC, Bramante CM. Comparison of three retreatment techniques with ultrasonic activation in flattened canals using micro-computed tomography and scanning electron microscopy. Int Endod J. 2016; 49(9): 890-7.

61. Rodrigues CT, Duarte MAH, de Almeida MM, de Andrade FB, Bernardineli N. Efficacy of CM-Wire, M-Wire, and Nickel-Titanium Instruments for Removing Filling Material from Curved Root Canals: A Micro–Computed Tomography Study. J Endod. 2016; 42(11): 1651-5.

62. Silveira SB, Alves FR, Marceliano-Alves MF, Sousa JCN, Vieira VT, Siqueira Jr JF, et al. Removal of root canal fillings in curved canals using either Mani GPR or HyFlex NT followed by passive ultrasonic irrigation. J Endod. 2018; 44(2), 299-303.

63. Djomehri SI, Candell S, Case T, Browning A, Marshall GW, Yun W, Lau SH, Webb S, Ho SP. Mineral density volume gradients in normal and diseased human tissues. PLoS One. 2019; 10(4): e0121611.

64. Jung M, Lommel D, Klimek J. The imaging of root canal obturation using micro-CT. Int Endod J. 2005; 38(9): 617-26.

65. Patel S, Dawood A, Ford TP, Whaites E. The potential applications of cone beam computed tomography in the management of endodontic problems. Int Endod J. 2007; 40(10): 818-30.

66. Cotton TP, Geisler TM, Holden DT, Schwartz SA, Schindler WG. Endodontic applications of cone-beam volumetric tomography. J Endod. 2007; 33(9): 1121-32.

67. Vizzotto MB, Silveira PF, Arús NA, Montagner F, Gomes BP, da Silveira HE. CBCT for the assessment of second mesiobuccal (MB2) canals in maxillary molar teeth: effect of voxel size and presence of root filling. Int Endod J. 2013; 46(9): 870-6.

68. Nascimento EHL, Abrahão Elias MR, Vasconcelos VHF, Haiter-Neto F, Mendonça EF, Sousa TO. Ex Vivo Detection of Apical Delta in Premolars: A Comparative Study Using Periapical Radiography, Cone-beam Computed Tomography, and Micro-computed Tomography. J Endod. 2019; 45(5): 549-53.

69. Sousa TO, Hassan B, Mirmohammadi H, Shemesh H, Haiter-Neto F. Feasibility of cone-beam computed tomography in detecting lateral canals before and after root canal treatment: an ex vivo study. J Endod. 2017; 43(6): 1014-7.

70. Hassan B, Metska ME, Ozok AR, van der Stelt P, Wesselink PR. Comparison of five cone beam computed tomography systems for the detection of vertical root fractures. J Endod. 2010; 36(1): 126-9.

71. Khedmat S, Rouhi N, Drage N, Shokouhinejad N, Nekoofar MH. Evaluation of three imaging techniques for the detection of vertical root fractures in the absence and presence of gutta-percha root fillings. Int Endod J. 2012; 45(11): 1004-9.

72. Melo SL, Bortoluzzi EA, Abreu M, Corrêa LR, Corrêa M. Diagnostic ability of a cone-beam computed tomography scan to assess longitudinal root fractures in prosthetically treated teeth. J Endod. 2010; 36(11): 1879-82.

73. Codari M, de Faria Vasconcelos K, Ferreira Pinheiro Nicolielo L, Haiter Neto F, Jacobs R. Quantitative evaluation of metal artifacts using different CBCT devices, high-density materials and field of views. Clin Oral Implants Res. 2017; 28(12): 1509-14.

74. Srivastava S, Alrogaibah NA, Aljarbou G. Cone-beam computed tomographic analysis of middle mesial canals and isthmus in mesial roots of mandibular first molars-prevalence and related factors. J Conserv Dent. 2018; 21(5): 526-30.

75. Rashed B, Iino Y, Komatsu K, Nishijo M, Hanada T, Ebihara A, et al. Evaluation of root canal anatomy of maxillary premolars using swept-source optical coherence tomography in comparison with dental operating microscope and cone beam computed tomography. Photomed Laser Surg. 2018; 36(9): 487-92.

76. Guo XL, Li G, Zheng JQ, Ma RH, Liu FC, Yuan FS, et al. Accuracy of detecting vertical root fractures in non-root filled teeth using cone beam computed tomography: effect of voxel size and fracture width. Int Endod J. 2019; 52(6): 887-98.

77. Ma RH, Ge ZP, Li G. Detection accuracy of root fractures in cone-beam computed tomography images: a systematic review and meta-analysis. Int Endod J. 2016; 49(7): 646-54.

78. Corbella S, Del Fabbro M, Tamse A, Rosen E, Tsesis I, Taschieri S. Cone beam computed tomography for the diagnosis of vertical root fractures: a systematic review of the literature and meta-analysis. Oral Surg Oral Med Oral Pathol Oral Radiol. 2014; 118(5): 593-602.

79. Kambungton J, Janhom A, Prapayasatok S, Pongsiriwet S. Assessment of vertical root fractures using three imaging modalities: cone beam CT, intraoral digital radiography and film. Dentomaxillofac Radiol. 2012; 41(2): 91-5.

80. Patel S, Brady E, Wilson R, Brown J, Mannocci F. The detection of vertical root fractures in root filled teeth with periapical radiographs and CBCT scans. Int Endod J. 2013; 46(12): 1140-52.

81. Jacobs R. Dental cone beam CT and its justified use in oral health care. JBR-BTR. 2011; 94(5): 254-65.

82. Jacobs R, Salmon B, Codari M, Hassan B, Bornstein MM. Cone beam computed tomography in implant dentistry: recommendations for clinical use. BMC Oral Health. 2018; 18(1): 88.

83. Ma RH, Ge ZP, Li G. Detection accuracy of root fractures in cone-beam computed tomography images: a systematic review and meta-analysis. Int Endod J. 2016; 49(7): 646-54.

84. Kambungton J, Janhom A, Prapayasatok S, Pongsiriwet S. Assessment of vertical root fractures using three imaging modalities: cone beam CT, intraoral digital radiography and film. Dentomaxillofac Radiol. 2012; 41(2): 91-5.

85. Patel S, Brady E, Wilson R, Brown J, Mannocci F. The detection of vertical root fractures in root filled teeth with periapical radiographs and CBCT scans. Int Endod J. 2013; 46(12):1140-52.

86. Gaêta-Araujo H, Alzoubi T, Vasconcelos KF, Orhan K, Pauwels R, Casselman JW, et al. Cone beam computed tomography in dentomaxillofacial radiology: a two-decade overview. Dentomaxillofac Radiol. 2020; 49(8): 20200145.

87. Pauwels R, Stamatakis H, Bosmans H, Bogaerts R, Jacobs R, Horner K, et al. Quantification of metal artifacts on cone beam computed tomography images. Clin Oral Implants Res. 2013; 24: 94-9.

88. Patel S, Brown J, Pimentel T, Kelly RD, Abella F, Durack C. Cone beam computed tomography in Endodontics - a review of the literature. Int Endod J. 2019; 52(8): 1138-52.

89. Patel S, Brown J, Semper M, Abella F, Mannocci F. European Society of Endodontology position statement: Use of cone beam computed tomography in Endodontics: European Society of Endodontology (ESE) developed by. Int Endod J. 2019; 52(12): 1675-8.

90. Guo XL, Li G, Zheng JQ, Ma RH, Liu FC, Yuan FS, et al. Accuracy of detecting vertical root fractures in non-root filled teeth using cone beam computed tomography: effect of voxel size and fracture width. Int Endod J. 2019; 52(6): 887-98.

91. Heckel F, Meine H, Moltz JH, Kuhnigk JM, Heverhagen JT, Kießling A, et al. Segmentation-based partial volume correction for volume estimation of solid lesions in CT. Trans Med Imaging. 2013; 33(2): 462-80

92. Elashiry MM, Saber SE, Elashry SH. Comparison of shaping ability of different single-file systems using microcomputed tomography. Eur J Dent. 2010; 14(1): 70-6.

93. Sousa-Neto MD, Silva-Sousa YC, Mazzi-Chaves JF, Carvalho KKT, Barbosa AFS, Versiani MA, et al. Root canal preparation using micro-computed tomography analysis: a literature review. Braz Oral Res.2018; 32(1): e66.

94. Aksoy C, Keris EY, Yaman SD, Ocak M, Geneci F, Celik HH. Evaluation of XP-Endo Shaper, Reciproc Blue, and Protaper Universal NiTi systems on dentinal microcrack formation using micro-computed tomography. J Endod. 2019; 45(3): 338-42.

95. Pirani C, Iacono F, Generali L, Sassatelli P, Nucci C, Lusvarghi L, et al. HyFlex EDM: superficial features, metallurgical analysis and fatigue resistance of innovative electro discharge machined NiTi rotary instruments. Int Endod J. 2016; 49(5): 483-93.

96. Iacono F, Pirani C, Generali L, Bolelli G, Sassatelli P, Lusvarghi L, et al. Structural analysis of HyFlex EDM instruments. Int Endod J. 2017; 50(3): 303-13.

97. Siqueira JF, Rôças IN. Clinical implications and microbiology of bacterial persistence after treatment procedures. J Endod. 2018; 34(11): 1291-301.

98. Pinto JC, Pivoto-João MMB, Espir CG, Ramos MLG, Guerreiro-Tanomaru JM, Tanomaru-Filho M. Micro-CT evaluation of apical enlargement of molar root canals using rotary or reciprocating heat-treated NiTi instruments. J Appl Oral Sci. 2019; 27.

99. Pivoto-João MMB, Tanomaru-Filho M, Pinto JC, Espir CG, Guerreiro-Tanomaru JM. Root canal preparation and enlargement using thermally treated nickel-titanium rotary systems in curved canals. J Endod. 2020; 46(11): 1758-65.

100. Teixeira CS, Felippe MC, Felippe WT. The effect of application time of EDTA and NaOCl on intracanal smear layer removal: an SEM analysis. Int Endod J. 2005; 38(5): 285-90

101. Mendonça DH, Colucci V, Rached-Junior FJ, Miranda CE, Silva-Sousa YT, Silva SR. Effects of various irrigation/aspiration protocols on cleaning of flattened root canals. Braz Oral Res. 2015; 29(1): 1-9.

102. Yaylali IE, Teke A, Tunca YM. The effect of foraminal enlargement of necrotic teeth with a continuous rotary system on postoperative pain: a randomized controlled trial. J Endod. 2017; 43(3): 359-63.

103. Borlina SC, de Souza V, Holland R, Murata SS, Gomes-Filho JE, Junior ED, et al. Influence of apical foramen widening and sealer on the healing of chronic periapical lesions induced in dogs' teeth. Oral Surg Oral Med Oral Pathol Oral Radiol Endod. 2010; 109(60): 932-40.

104. de Souza Filho FJ, Benatti O, de Almeida OP. Influence of the enlargement of the apical foramen in periapical repair of contaminated teeth of dog. Oral Surg Oral Med Oral Pathol. 1987; 64(4): 480-4.

105. Brandão PM, de Figueiredo JAP, Morgental RD, Scarparo RK, Hartmann RC, Waltrick SBG, et al. Correction to: Influence of foraminal enlargement on the healing of periapical lesions in rat molars. Clin Oral Investig. 2019; 23(4): 2001-3.

106. Shen Y, Stojicic S, Haapasalo M. Antimicrobial efficacy of chlorhexidine against bacteria in biofilms at different stages of development. J Endod. 2011; 37(5): 657-661.

107. Vieira MLO, Dantas HV, de Sousa FB, Salazar-Silva JR, Silva EJN L, Batista AUD, et al. Morphologic changes of apical foramen and microcrack formation after foraminal enlargement: a scanning electron microscopic and micro-computed tomographic analysis. J Endod. 2020; 46(11): 1726-32.

108. Aktemur Türker S, Uzunoğlu Özyürek E, Tek V. The effect of different obturation methods on sealer penetration alongside apically separated rotary nickel-titanium instruments: A confocal laser scanning microscopy study. Microscopy Research and Technique. 2020; 83(6): 720-6.

109. Alves Silva EC, Tanomaru-Filho, M, da Silva GF, Delfino MM, Cerri, PS, Guerreiro-Tanomaru JM. Biocompatibility and bioactive potential of new calcium silicate-based endodontic sealers: Bio-C Sealer and Sealer Plus BC. J Endod. 2020: 46(10): 1470-7.

110. Sanz JL, Lopez-Garcia S, Lozano A, Pecci-Lloret MP, Llena C, Guerrero-Girones J, Forner L. Microstructural composition, ion release, and bioactive potential of new premixed calcium silicate-based endodontic sealers indicated for warm vertical compaction technique. J Endod. 2020; 46(10): 1470-7.

111. Zordan-Bronzel CL, Esteves Torres FF, Tanomaru-Filho M, Chávez-Andrade GM, Bosso-Martelo R, Guerreiro-Tanomaru JM. Evaluation of Physicochemical Properties of a New Calcium Silicate-based Sealer, Bio-C Sealer. J Endod. 2019; 45(10): 1248-52.

112. Pinto JC, Torres FFE, Santos Junior AO, Tavares KIMC, Guerreiro-Tanomaru JM, Tanomaru-Filho M. Influence of voxel size on micro-CT analysis of debris after root canal preparation. Braz Oral Res. 2020; 35: e008.

113. Orhan K, Jacobs R, Celikten B, Huang Y, de Faria Vasconcelos K, Nicolielo LFP, Buyuksungur A, Van Dessel J. Evaluation of threshold values for root canal filling voids in micro-ct and nano-ct images. Scanning. 2018 16; 2018:9437569.

114. Bouxsein ML, Boyd SK, Christiansen BA, Guldberg RE, Jepsen KJ, Muller R. Guidelines for assessment of bone microstructure in rodents using micro-computed tomography. J Bone Miner Res. 2010; 25(7): 1468-86.

115. Schulze RK, Berndt D, d'Hoedt B. On cone-beam computed tomography artifacts induced by titanium implants. Clin Oral Implants Res. 2010; 21(1): 100-7.

116. Zhang L, Wang T, Cao Y, Wang C, Tan B, Tang X, Tan R, Lin Z. In Vivo Detection of Subtle Vertical Root Fracture in Endodontically Treated Teeth by Cone-beam Computed Tomography. J Endod. 2019; 45(7): 856-62.

APÊNDICE A – METODOLOGIA EXPANDIDA

***Micro-CT**

Análise em microtomografia computadorizada

Os parâmetros para escaneamento foram baseados na variação da resolução, sendo o foco principal do projeto proposto. As amotras foram escaneadas usando aparelho de micro-CT (SkyScan 1272. Bruker, Kontich, Belgium) antes após todas as etapas experimentais. Os escamentos foram realizados com 5 µm de tamanho de voxel com os seguintes parâmetros: filtro de cobre, rotação de 180°, passo de rotação de 0.2, com 100 kV e 100 µA. Todas as imagens obtidas foram reconstruídas usando o *software* NRecon (NRecon v.1.6.3; Bruker). A sobreposição das imagens foi feita no *software* DataViewer (Data Viewer v.1.5.1, Bruker). Todas as análises foram realizadas usando o *software* CTAn (CTAn v.1.14.4, Bruker). As imagens originais foram redimensionadas isotropicamente para realizar análises com diferentes tamanhos de voxels. Imagens de 10 e 20 µm foram obtidas para as análises quantitativas e qualitativas. Isso foi conseguido redimensionando as imagens de 5 µm digitalizadas anteriormente em 2 e 4, respectivamente, usando um programa de software CTAn.

Seleção dos dentes

Foram selecionados doze primeiros e segundos molares inferiores com câmara pulpar intacta, raízes mesiais com ápice completamente formado e curvatura de 25° - 35° a partir de análises radiografias (Schneider 1971). Para a seleção dos espécimes, além da utilização do sistema de radiografia digital, foi realizado escaneamento inicial a 35 µm utilizando o microtomógrafo SkyScan 1176 (Skyscan 1176, Bruker-microCT, Konttich, Bélgica). Nesta etapa, por meio de estudos pilotos, foram definidos parâmetros de escaneamento: filtro Cu + Al, tempo de 87 ms de exposição, frame 3, rotação de 360°, 80 kV e 300 uA. Após reconstrução e análise inicial das imagens obtidas, foram selecionadas 12 raízes mesiais de molares inferiores, apresentando canais MV e ML distintos, completa formação apical, ausência de fraturas radiculares e reabsorções.

Após lavagem dos dentes em água por 48 horas, foi realizado o acesso aos canais utilizando uma broca diamantada de alta velocidade tamanho 2 (FG1012 KG, Sorensen, Sao Paulo,Brasil) sob refrigeração. Para a exploração inicial dos canais radiculares, foram utilizadas limas tipo Kerr #08 e #10 (Dentsply, Maillefer, Suíça) introduzidas no canal radicular até o forame apical. O comprimento de trabalho foi definido a 1 mm desta extensão. A solução irrigadora utilizada foi hipoclorito de sódio a 2,5%, em seringa com agulha 29 G Navip (Endo Eze NaviTip, Ultradent, Brasil). Visando simular o ligamento periodontal para a execução das técnicas, os espécimes foram montados em aparatos com resina acrílica. Cada dente foi moldado com silicone de condensação (Oranwash, Zhermack SpA, Badia Polesine, Itália) para simulação do ligamento periodontal (Figura 1).

Figura 1 – Imagem representativa das raízes mesiais de molares inferiores incluídas em silicone de condensação, nas fases experimentais de preparo e obturação

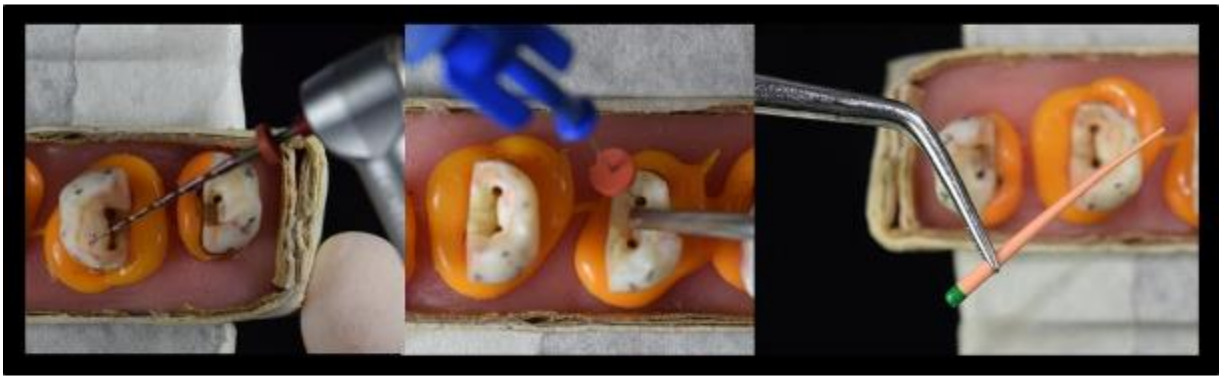

Fonte: Arquivo pessoal do autor.

Concluída a seleção das amostras, os espécimes foram submetidos ao escaneamento por micro-CT, com resolução de 5 µm com os parametros ja descritos anteriormente. Antes da divisão dos grupos, foram realizadas análises volumétricas dos canais radiculares, nas imagens obtidas pelo escaneamento inicial com intuito de realizar um sorteio para distribuição dos grupos de forma homogênea e ao mesmo tempo randomizada (Figura 2).

Figura 2- Imagem representativa das análises volumétricas das imagens, após escaneamento inicial

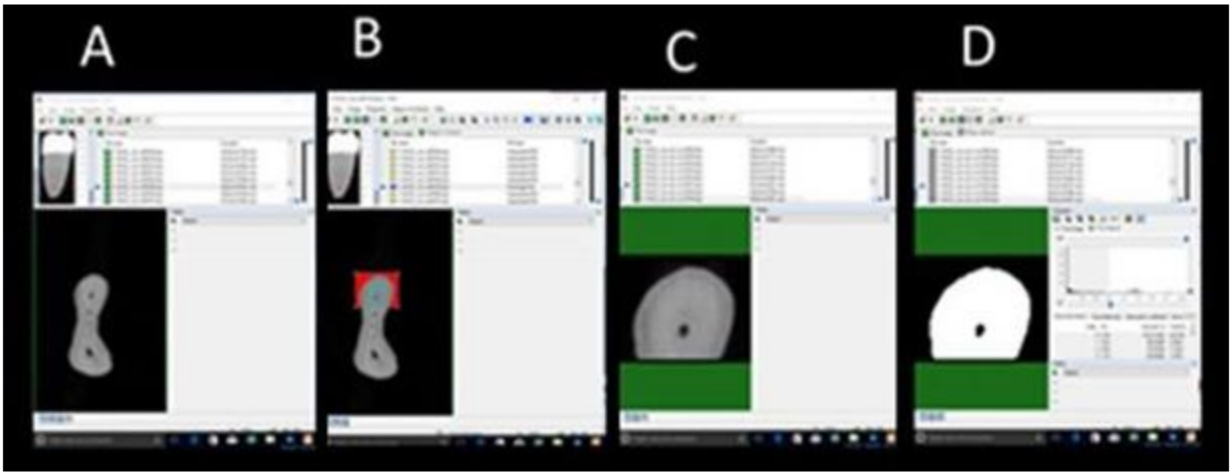

A, Espécime antes da fase experimental. B, definição do Roi, área de interesse. C, Voi, área de interesse salva para análises volumétricas. D, binarização das imagens para análise.

Fonte: Arquivo pessoal do autor.

Preparo do canal radicular com ProDesign Logic (n=12)

Instrumento ProDesign Logic tamanho 30 taper .01 foi acionado em motor elétrico (VDW.SILVER, VDW GmbH, Munique, Alemanha) em movimento rotatório a 350 rpm de acordo com as especificações do fabricante, com suaves movimentos de entrada e retirada até o comprimento de trabalho. Em seguida, instrumento ProDesign Logic tamanho 30, taper .05 foi empregado a 600 rpm com suaves movimentos em direção apical até o comprimento de trabalho. O pincelamento foi realizado na zona de segurança (parede mesial), com amplitude média de 3 mm, totalizando três movimentos: mesial, mesio-vestibular e mesio-lingual. Após cada etapa de uso, os instrumentos foram limpos com gaze estéril umedecida com água destilada

O canal foi irrigado com 6 ml de NaOcl a 2,5% (3 ml para ProDesign Logic 30.01 e 3 ml para ProDesign Logic 30.05) usando uma seringa Ultradent com agulha Navitip 30G a 2 mm aquém do CT com movimentos de entrada e saída com fluxo continuo e aspiração. Foi realizada irrigação final com 5 ml de NaOcl 2,5%, 2.5 ml de EDTA 17%, sob agitação, por 3 minutos e posteriormente 5 ml de solução fisiológica.

Preparo do canal radicular HyFlex EDM (n=12)

Instrumento HyFlex EDM tamanho 10, taper .05 foi empregado a 300 rpm com suaves movimentos de entrada e retirada até o comprimento de trabalho. Finalizando o preparo, foi utilizado o instrumento HyFlex EDM 25 com taper variado em movimento rotatório a 500 rpm com movimentos de entrada e retirada até o comprimento de trabalho. O pincelamento foi realizado na zona de segurança (parede mesial), com amplitude média de 3 mm, totalizando três movimentos: mesial, mesio-vestibular e mesio-lingual. Após cada etapa de uso, os instrumentos foram limpos com gaze estéril umedecida com água destilada.

O canal foi irrigado com 6 ml de NaOcl a 2,5% (3 ml HyFlex EDM 15.05 e 3 ml para HyFlex EDM 25.08) usando uma seringa Ultradent com agulha Navitip 30G a 2 mm aquém do CT com movimentos de entrada e saída com fluxo continuo e aspiração. Foi realizada irrigação final com 5 ml de NaOcl 2,5%, 2.5 ml de EDTA 17%, sob agitação, por 3 minutos e posteriormente 5 ml de solução fisiológica.

Concluído o preparo inicial dos canais radiculares, os espécimes foram submetidos ao escaneamento por micro- CT, com resolução de 5 µm, para comparações das imagens pré e pós-operatórias. Foram avaliados o transporte e a centralização do canal, o percentual de aumento volumétrico, as superfícies não tocadas e debris para cada sistema utilizado (Figuras 3, 4, 5 e 6).

Figura 3 - Imagens representativas da sobreposição das imagens obtidas antes e após cada procedimento experimental

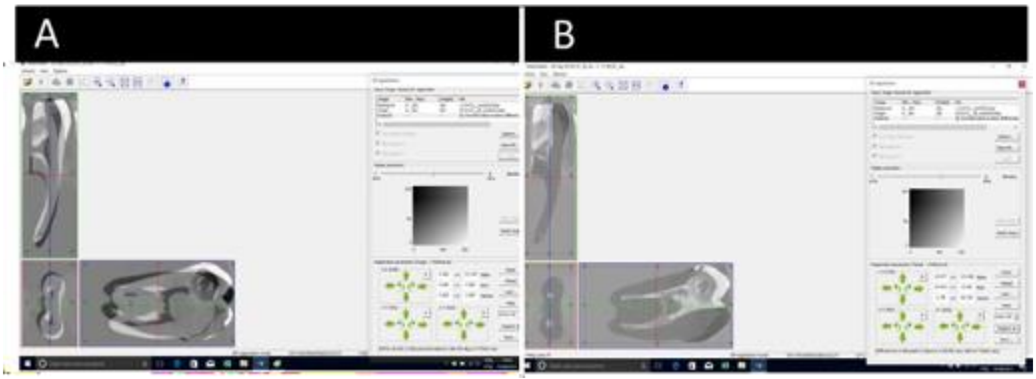

A, antes dos ajustes de sobreposição e B, após os ajustes de sobreposição.

Fonte: Arquivo pessoal do autor.

Figura 4 - Imagem representativa das análises volumétricas das imagens, antes e após cada fase experimental, no software CTAnA, Reference e target mostrando o espécime antes e após a fase experimental

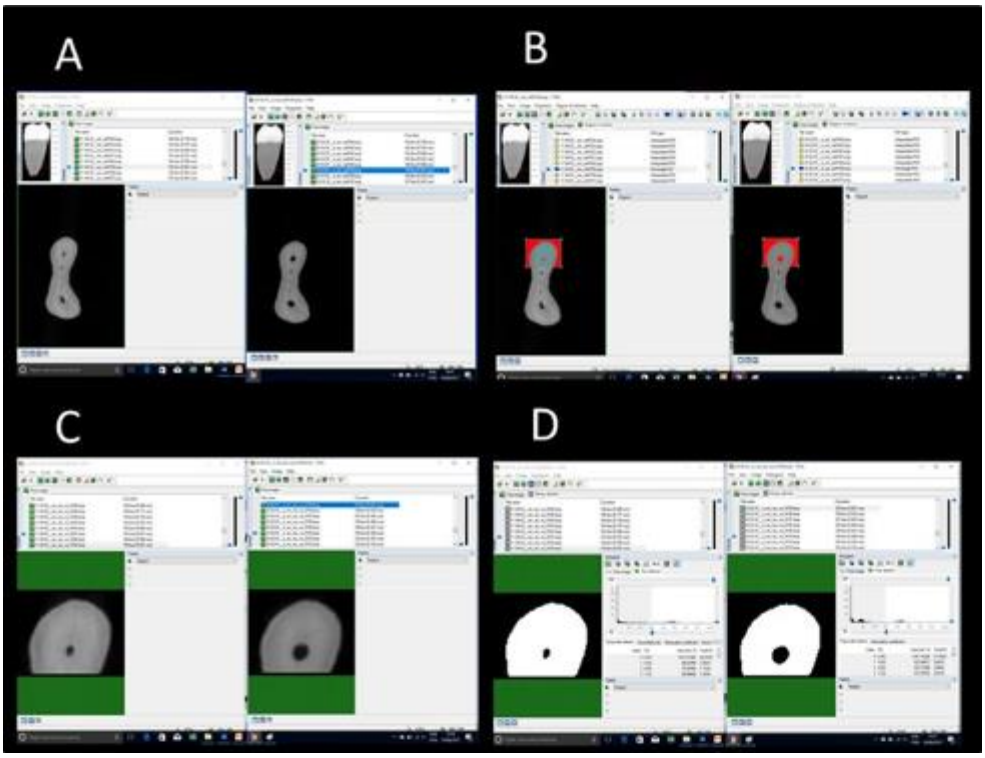

B, definição do Roi, área de interesse. C, Voi, área de interesse salva para análises volumétricas. D, binarização das imagens para análise volumétrica.

Fonte: Arquivo pessoal do autor.

Figura 5 - Imagem representativa da utilização do task lists, no software CTAn para realização de análises volumétricas

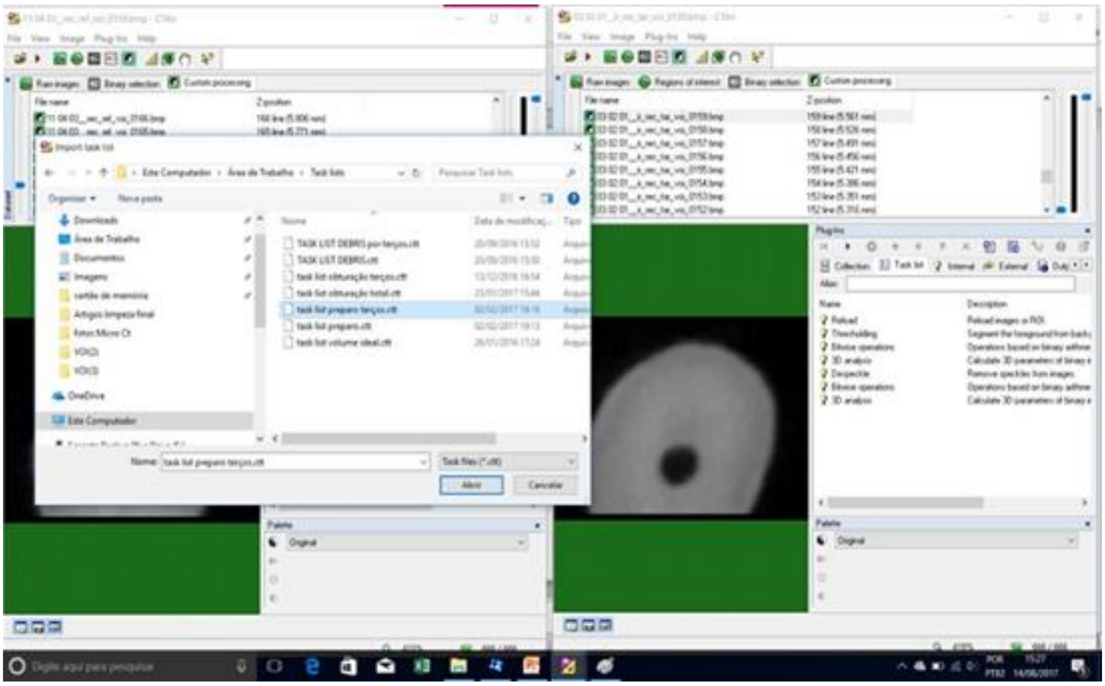

Fonte: Arquivo pessoal do autor.

Figura 8 - Imagem representativa do software CTAn, mostrado o reference e target para mensuração do limite do canal, antes do preparo e preparado, até a borda mais próxima da raiz

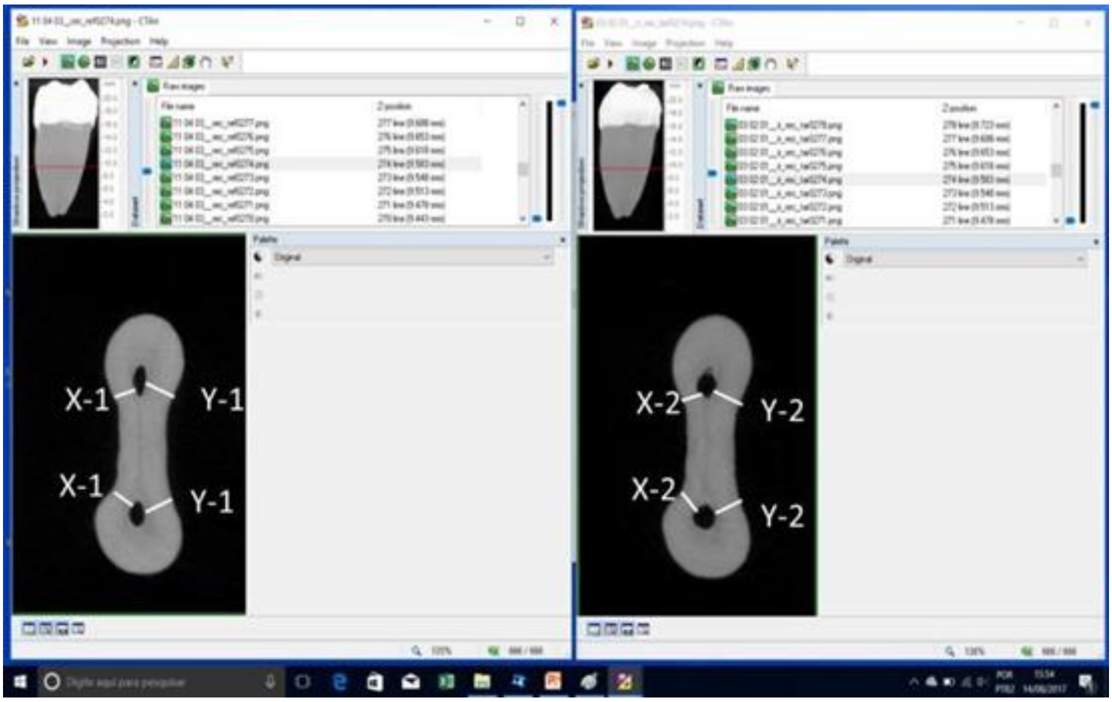

Fonte: Arquivo pessoal do autor.

Limpeza adicional (n=24)

Foi utilizada irrigação ultrassônica Passiva (PUI). Os canais foram irrigados com 5 ml de hipoclorito de sódio a 2,5 %, os insertos ultrassônicos Irrissonic (Helse, São Paulo, SP, Brasil) foram ativados pelo aparelho ultrassônico Newtron® Booster (ACTEON North America, NJ, Estados Unidos) em frequência 50/60 Hz, potência 10% a 2 mm aquém do comprimento de trabalho (20 segundos), irrigação com 5 ml de EDTA a 17%. + Irrissonic como descrito anteriormente. O canal foi novamente irrigado com 5 ml de hipoclorito a 2,5% e novamente será empregada a ativação do hipoclorito.

Concluído o protocolo de limpeza adicional, os espécimes foram submetidos à escaneamento em micro-CT, com resolução de 5 µm. Foi analisado o percentual de debris.

Obturação

Após as etapas de preparo e limpeza adicional foi realizada redistribuição das amostras de forma randomizada por meio de sorteio. No entanto, foi levado em conta na redistribuição o volume dos canais apos o prreparo, assim como a distribuição equitativa dos canais preparados pelos instrumentos Logic 30.05 e HyFlex EDM 25/~. Os canais foram obturados pela técnica do cone único com os cimentos AH Plus (Dentsply, GmbH, Ballaigues, Alemanha) ou Bio-C Sealer (Angelus, Londrina, PR, Brazil).

Após a randomização das amostras os dois grupos tiveram canais que foram preparados por ProDesign logic e HyFlex EDM. Os canais que foram preparados por ProDesign Logic 30.05, foram secos com cones de papel absorvente estéril 30 (Tanari Indústria Ltda., São Paulo, Brasil) e foram obturados com cones de guta percha 30.05 (Tanari Indústria Ltda., São Paulo, Brasil), selecionados segundo tamanho da ponta e conicidade por meio de mensurações em aparelho Perfilômetro (Profile Projector Nikon modelo 6C-2). Os canais que foram preparados por HyFlex EDM25.~ foram secos com cones de papel absorvente estéril 25 (Tanari Indústria Ltda., São Paulo, Brasil) e foram obturados cones de guta percha compatíveis com o sistema HyFlex EDM 25.~ (Coltene, Altstatten, Suíça), selecionados segundo tamanho da ponta e conicidade por meio de mensurações em aparelho Perfilômetro (Profile Projector Nikon modelo 6C-2).

O cimento AH-Plus foi manipulado de acordo com as especificações do fabricante e foi levado ao canal radicular com auxílio do instrumento Lentulo, em sentido horário em motor de baixa rotação (Micromotor N270 e Contra-ângulo , Dabi-Atlante, Brasil) a 2 mm do comprimento de trabalho e lima manual tipo Kerr girando pré-curvada no comprimento de trabalho. Para os canais que foram obturados por Bio-C Sealer, o cimento foi injetado no canal radicular, a cerca de 4 mm do comprimento de trabalho, usando a seringa e a agulha plástica fornecidas pelo fabricante.

Após a preenchimento de cimento no interior do canal radicular, o cone de guta percha envolto em cimento endodôntico foi levado ao interior do canal. Em seguida, foi realizado o corte do cone a nível cervical e o material restante foi levemente compactado no sentido vertical. Após o procedimento foi realizada uma radiografia comprobatória da qualidade da obturação.

Após a obturação dos canais radiculares, foi realizado o selamento coronário com material restaurador provisório Coltosol (Vigodent, Rio de Janeiro, Brasil) e as raízes foram mantidas em estufa a temperatura de 37° C e umidade 95%, por três dias para a presa final do cimento obturador.

Novo escaneamento em micro-CT foi realizado de acordo com os parâmetros já definidos. Nesta etapa, as análises da qualidade de obturação, bem como a presença de falhas foram realizadas.

Avaliação da eficácia do retratamento

Após manutenção dos espécimes em estufa a temperatura de 37° C, em umidade a 95%, por uma semana, foi realizado o retratamento endodôntico. Após remoção do selamento provisórios, todos os canais (n=48), foram retratados com o sistema ProDesing Logic RT (Easy Equipamentos Odontológicos, Brasil). Foi utilizado um contra ângulo acoplado a um motor elétrico WDW Silver (VDW, Munich, Germany) na sequência:

- *Desobstrução do terço cervical* - Foi realizado com o instrumento 30.10 do sistema ProDesing Logic RT a 900 rpm.

- *Desobstrução do terço cervical médio* - Foi realizado com o instrumento 25.08 do sistema ProDesing Logic RT a 900rpm.

- *Desobstrução do terço apical* - Foi realizado com instrumento ProDesing RT 20.06 a 600 rpm.

- Preparo dos terços cervical e médio e apical- Foi realizado com instrumento ProDesing Logic 35.05 a 600 rpm

O canal foi irrigado com 8 ml de NaOcl a 2,5% (2 ml para PDL RT 30.10, 2 ml para PDL RT 25.08, 2 ml para PDL RT 20.06 e 2 ml para PDL 35.05), usando uma seringa Ultradent com agulha Navitip 30G a 2 mm aquém do CT com movimentos de entrada e saída com fluxo contínuo e aspiração. Foi realizada irrigação final com 5 ml de NaOcl 2,5%, 2.5 ml de EDTA 17%, sob agitação, por 3 minutos e posteriormente 5 ml de soro fisiológico.

Os espécimes foram novamente escaneados em micro-CT de acordo com os parâmetros já definidos e padronizados. Nesta etapa, as análises de percentual de material obturador remanescente foi realizado com o intuito de averiguar a influência do cimento obturador (AH Plus ou Bio-C Sealer) empregados na técnica do cone único na capacidade de remoção do material obturador de instrumentos rotatórios de Níquel e Titânio.

Avaliação da eficácia da limpeza adicional

Após a etapa do retratamento foi realizada redistribuição das amostras de forma randomizada. No entanto, foi levado em conta na redistribuição a distribuição equitativa dos canais obturados pelo cimento AH Plus e Cimento Biocerâmico (Bio-C Sealer). Neta etapa, todos os canais que foram retratados, foram submetidos a protocolo de limpeza adicional, com XP-endo Finisher (n=12) ou alargamento apical apical com PDL 50.01.

a) XP-endo Finisher (n=12)

XP-endo Finisher foi acionado em motor elétrico (VDW.SILVER, VDW GmbH, Munique, Alemanha) em movimento rotatório a 800 rpm por 30 segundos com movimentos de entrada e retirada até a comprimento de trabalho, pressionando o instrumento contra as paredes do canal. Foi realizada nova irrigação como descrito anteriormente e novamente foi empregado o XP-endo Finisher também como descrito anteriormente. Foi realizada irrigação final com 5 ml de NaOcl 2,5%, 2.5 ml de EDTA 17%, sob agitação, por 3 minutos e posteriormente 5 ml de soro fisiológico.

b) Ampliação apical apical com PDL 50/.01 (n=12)

O instrumento PDL 50/.01 foi operado com motor elétrico VDW SILVER, em movimento rotatório à velocidade de 350 rpm e torque de 1 Ncm, com movimentos para dentro e para fora até o comprimento de trabalho. Os canais radiculares foram irrigados com 2 mL de NaOCl 2,5%. A irrigação final foi realizada conforme descrito anteriormente.

Os espécimes foram novamente escaneados em micro-CT de acordo com os parâmetros já definidos e padronizados. Nesta etapa, as análises de percentual de material obturador remanescente foram realizadas.

***Cone Bean-CT**

Um Fantoma antropomórfico composto de um crânio humano seco e uma mandíbula foi coberto com material mix-D para simular a atenuação dos tecidos moles (Oenning et al., 2019) (Figura 9).

Figura 9 - Imagem representativa de mandibula huma seca sendo recoberta por Mix-D

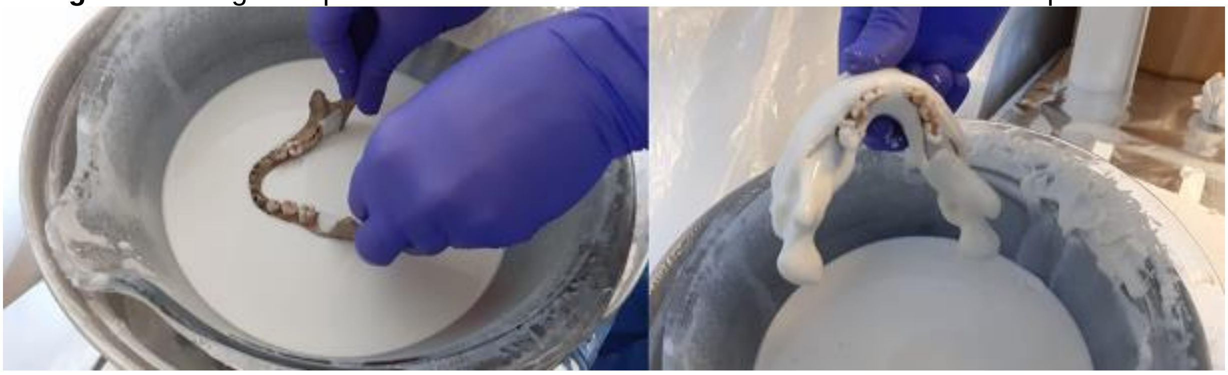

Fonte: Arquivo pessoal do autor.

Esta mandíbula apresenta um canal estreito no primeiro pré-molar inferior direito e trincas, istmo e delta apical no primeiro molar inferior, detectados por uma imagem de alta resolução obtida por meio de um aparelho de micro-CT industrial (Nikon Metrology Inc, Brighton, MI, USA) usando os seguintes parametros de escaneamento: 200 kV, 350 µA, 2.5 mm de filtro de cobre, 8x8 cm FOV and 40 µm de tamanho de voxel.

Foram criadas três condições clínicas: 1. Livre de metal (Figura 10b); 2. ‘Endo’: com um segundo pré-molar inferior tratado endodonticamente contendo um pino metálico de liga de ouro feito internamente. (Figura 10c); e 3. Implante: o mesmo modelo com um implante de titânio com 10 mm de comprimento e uma plataforma com 3,5 mm de diâmetro, modelo Tapered PMC NP (Nobel Biocare, Zurique, Suíça) colocado na região do pré-molar mandibular direito (Figura 10d).

Figura 10 - Fantoma antropomórfico de crânio humano seco com mandíbula recoberta com mix-D (a) e representação da região de interesse considerando as três condições avaliadas: isento de metal (b), implante (c) e endo (d)

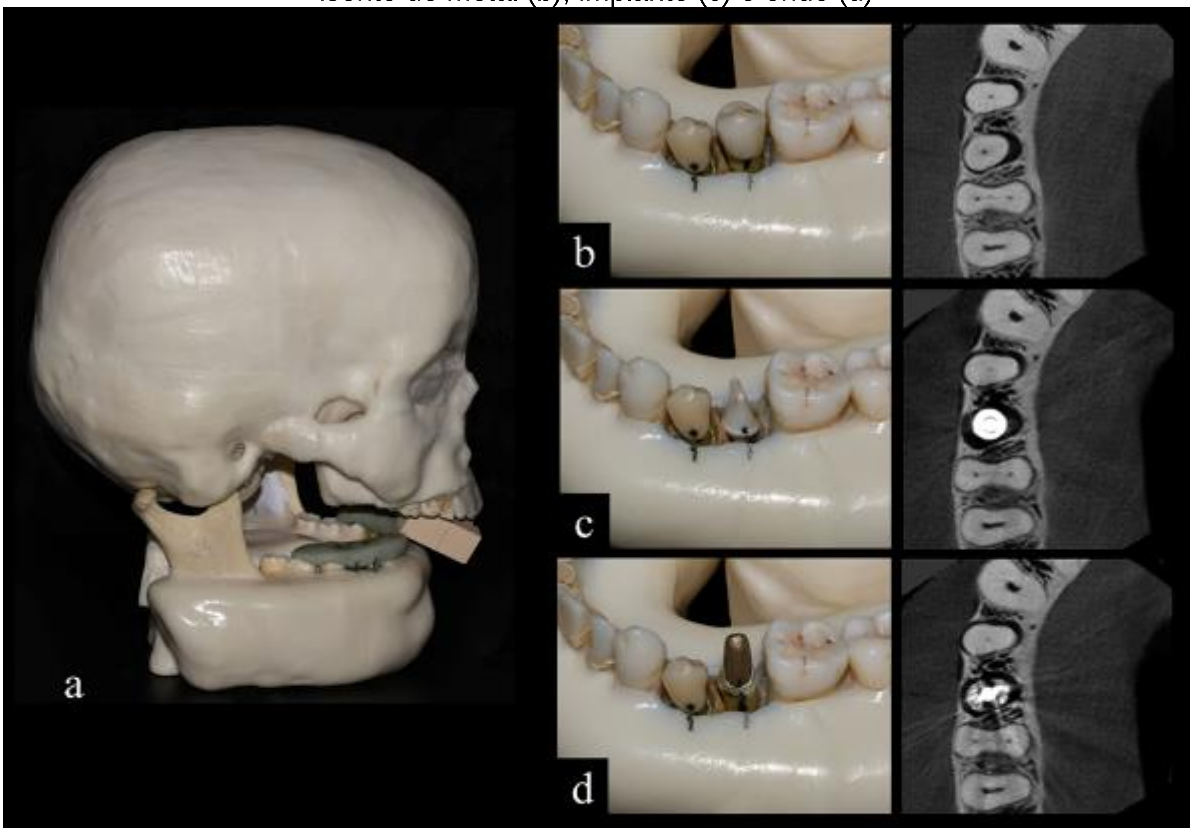

Fonte: Arquivo pessoal do autor.

As três condições foram examinadas selecionando três protocolos de aquisição diferentes (resolução padrão de FOV médio, resolução padrão de FOV pequeno e FOV pequeno em alta resolução) em cada um dos dez dispositivos de CBCT. A Tabela 1 mostra todos os dispositivos CBCT, códigos (A a J), parâmetros de exposição usados para a avaliação 1 e a tabela 2 mostra essas informações sobre a avaliação 2. A mandíbula foi digitalizada em um Nikon XT Scanner industrial de tomografia computadorizada (TC) H 225 (Nikon Metrology Inc, Brighton, MI, EUA) usando os seguintes parâmetros: 200 kV, 350 µA, filtração de cobre de 2,5 mm, FOV de 8x8 cm e tamanho de voxel de 40 µm. Além de ser usado como uma varredura de referência para registrar todas as imagens de CBCT, a tomografia computadorizada industrial foi usada para detectar e medir com precisão o tamanho das estruturas. O registro baseado em informações mútuas foi realizado no software Amira 2019 (Thermo Fisher Scientific, Waltham, MA, EUA) usando a tomografia computadorizada industrial como imagem de referência.

Tabela 1 - Dispositivos TCGC, fabricantes, códigos e parâmetros de digitalização comparáveis

CBCT devices	**Manufaturer**	**Code**	**FOV (cm)**	**kV**	**mA**	**Voxel size (mm)**
3D Accuitomo 170	J. Morita, Kyoto, Japan	A	4 X 4	90	5	0.08
Veraview X800	J. Morita, Tokyo, Japan	B	4 X 4	100	7.9	0.08
X1	3Shape, Copenhagen, Denmark	C	4 X 4	90	12	0.1
NewTom VGi evo	Cefla Dental Group, Imola, Italy	D	5 X 5	110	3	0.1
OP 3D Pro	Instrumentarium, Tuusula, Finland	E	5 X 5	90	8.6	0.085
OP 3D	Instrumentarium, Tuusula, Finland	F	5 X 5	95	4	0.08
CS 9300	Carestream, Rochester, NY, USA	G	5 X 5	90	4	0.09
ProMax 3D Max	Planmeca, Helsinki, Finland	H	6 X 6	96	12	0.075
Orthophos SL 3D	Dentsply Sirona, Charlotte, USA	I	5 X 5	85	6	0.079
Spectral Dental UEG	UEG Medical, Shangai, China	J	6 X 6	110	8	0.075

Fonte: Elaboração própria.

Tabela 2 -Descrição detalhada dos dispositivos TCFC, fabricantes, códigos e protocolos de digitalização usados no presente estudo

			Small FOV High Resolution					**Small FOV Standard Resolution**					**Medium FOV Standard Resolution**				
CBCT devices	**Codes**	**Manufacturer**	**FOV (cm)**	**kV**	**mA**	**Voxel size (mm)**	**DAP (mGY cm2)**	**FOV (cm)**	**kV**	**mA**	**Voxel size (mm)**	**DAP (mGY cm2)**	**FOV (cm)**	**kV**	**mA**	**Voxel size (mm)**	**DAP (mGY cm2)**
3D Accuitomo 170	A	J. Morita, Kyoto, Japan	4 X 4	90	5	0.08	706	4 X 4	90	5	0.125	402	8 X 8	90	5	0.125	2310
OP 3D Pro	B	Instrumentarium, Tuusula, Finland	5 X 5	90	8.6	0.085	755	5 X 5	90	7.1	0.125	452	8 X 8	90	7.1	0.2	899
Veraview X800	C	J. Morita, Kyoto, Japan	4 X 4	100	7.9	0.08	589	4 X 4	101	8	0.125	596	8 X 8	100	8	0.125	2112
X1	D	3Shape, Copenhagen, Denmark	4 X 4	90	12	0.1	309	4 X 4	90	12	0.15	231	8 X 8	90	12	0.15	773
CS 9300	E	Carestream, Rochester, NY, USA	5 X 5	90	4	0.09	572	5 X 5	90	4	0.2	572	7.7 X 7.7	90	4	0.18	455
NewTom VGi evo	F	Cefla Dental Group, Imola, Italy	5 X 5	110	3	0.1	148	5 X 5	110	3	0.125	148	8.2 X 8.2	110	3	0.125	329
Veraviewepocs 3DR100	G	J. Morita, Kyoto, Japan	-	-	-	-	-	4 X 4	90	8	0.125	525	8 X 8	90	8	0.125	1780
Orthophos SL 3D	H	Dentsply Sirona, Charlotte, NC, USA	5 X 5	85	6	0.079	421	5 X 5	85	10	0.16	214	8.2 X 8.2	85	6	0.16	657
OP 3D	I	Instrumentarium, Tuusula, Finland	5 X 5	95	4	0.08	1165	5 X 5	90	4	0.125	582	8 X 8	94	2.8	0.2	940
ProMax 3D Max	J	Planmeca, Helsinki, Finland	6 X 6	96	12	0.075	1155	6 X 6	96	7.1	0.15	657	10 X 10	96	7.1	0.15	668

Fonte: Elaboração própria.

Avaliação 1

Para esta avaliação apenas canal estreito, istmo e delta apical (Figura 11) foram usados, bem como apenas o protocolo de alta resolução do aparelho de TCFC descrito na tabela 1. Três observadores experientes foram treinados e calibrados antes da avaliação das imagens. Posteriormente, eles classificaram todas as imagens de CBCT de 1 (melhor) a 10 (pior) quanto à sua capacidade de detectar as três tarefas de diagnóstico. Com base na referência de imagem selecionada, foram obtidas fatias individuais padronizadas das máquinas. As imagens foram exibidas aleatoriamente na mesma tela sem mostrar a imagem de referência e os observadores foram cegados para o dispositivo de CBCT. As sessões de treinamento, calibração e avaliação foram realizadas em um ambiente com pouca luz usando um monitor de tela plana de 24,1 polegadas (Barco, Kortrijk, Bélgica). Após 30 dias, 25% das imagens foram reavaliadas para avaliar a reprodutibilidade intra-observador.

Figura 11 – representação das tarefas endodônticas avaliadas (a –canal estreito, b – istmo e c – delta apical) nas imagens de referências e em todos os aparelhos de TCFC avaliados

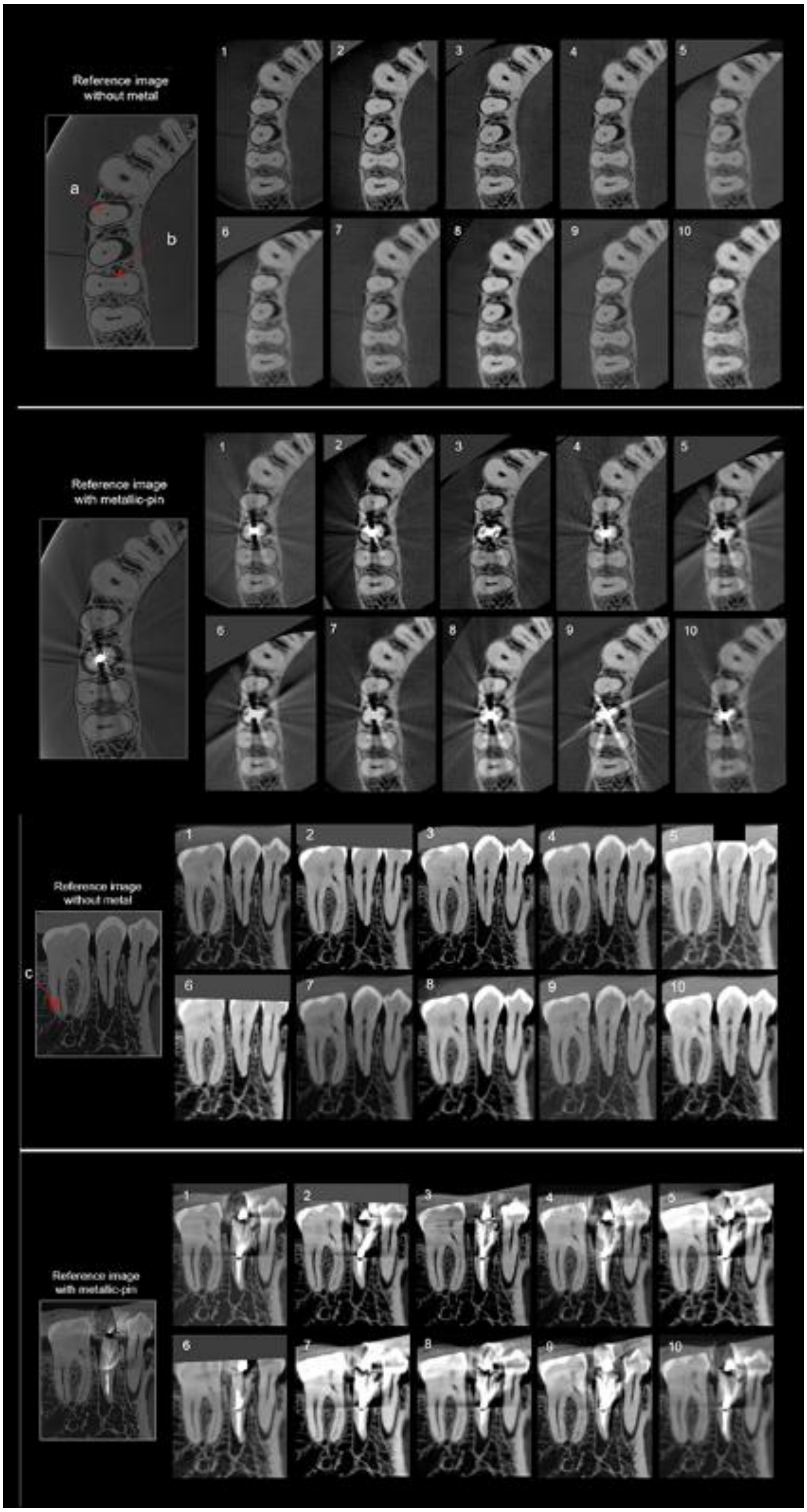

Fonte: Arquivo pessoal do autor.

Avaliação 2

Trincas radiculares, istmo e delta apical foram considerados durante esta avaliação, e foram utilizados os aparelhos de TCFC descritos na tabela 2. Um conjunto de imagens foi utilizado para calibração de dois radiologistas orais para o método de estudo. Depois disso, as imagens dos diferentes dispositivos de TCFC foram exibidas aleatoriamente na mesma tela junto com a imagem de referência correspondente.

Cada tarefa diagnóstica foi avaliada separadamente, por meio de um conjunto de nove imagens contendo todos os protocolos de varredura e condições clínicas de um dispositivo específico (Figura 12). Os observadores estavam cientes da aparência e localização da tarefa diagnóstica na imagem de referência, mas cegos para o respectivo dispositivo de CBCT. Como cada dispositivo CBCT tem uma distribuição de histograma diferente, o brilho e o contraste das imagens foram ajustados antes da observação por um operador experiente independente para fornecer imagens apropriadas para cada dispositivo. Posteriormente, o brilho, contraste e ampliação da imagem não puderam ser ajustados pelos observadores. Os observadores avaliaram cada imagem, comparada com a imagem de referência, e a classificaram em uma das três categorias por consenso: 1 - adequada para a visualização da estrutura específica comparada com a imagem de referência); 2 - aceitável para a visualização da estrutura específica (o observador conseguiu distinguir a estrutura, porém não ficou tão clara quanto na imagem de referência); 3 - impróprio para a visualização da estrutura específica (o observador não conseguiu distinguir a estrutura de interesse). As sessões de calibração e avaliação foram realizadas em um ambiente com pouca luz usando um monitor de tela plana de 61,2 cm MD Barco MDRC-2221 (Barco, Kortrijk, Bélgica). Após 30 dias, 20% das imagens foram reavaliadas para avaliar a concordância intra-observador.

Figura 12- Conjunto de imagens usado para avaliação de trinca contendo uma imagem de referência de TC industrial e imagens numeradas de um dispositivo CBCT específico para todas as condições e protocolos de varredura

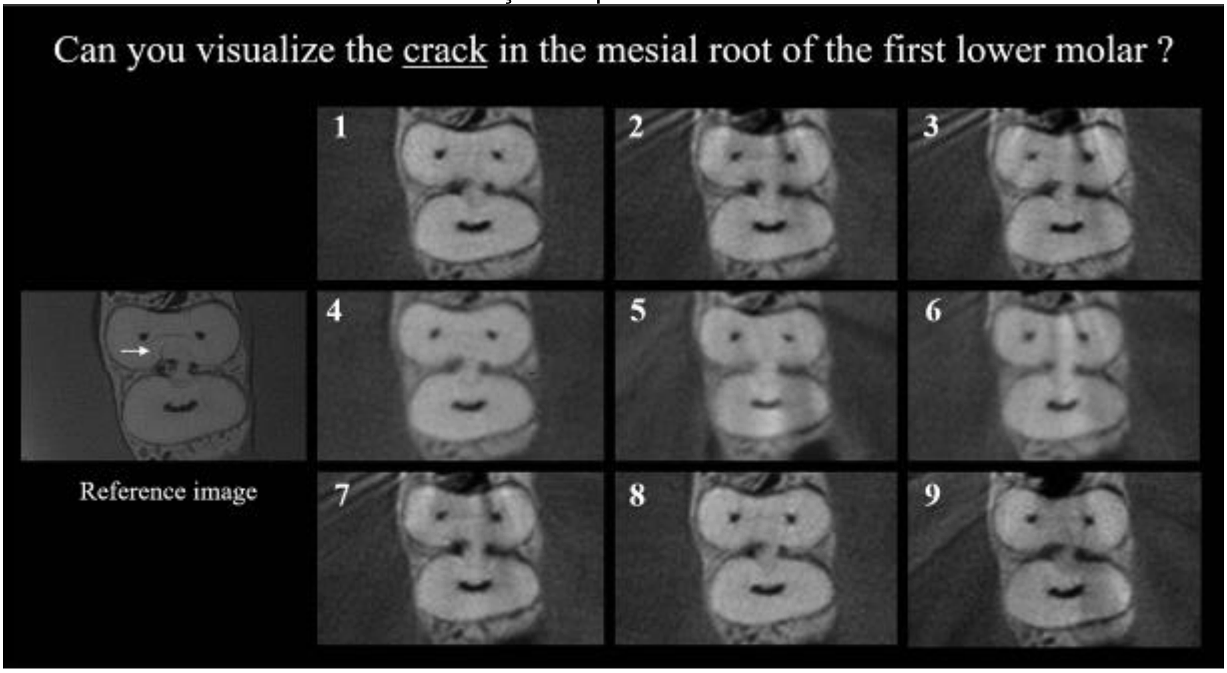

Fonte: Arquivo pessoal do autor.

***Nano-CT**

Seleção de amostra

Foram utilizados incisivos laterais superiores humanos com curvatura apical (25 ° - 35 °) previamente armazenados em solução de timol 0,1%. Os critérios de inclusão foram dentes com formação apical completa, ausência de fraturas radiculares, calcificações ou reabsorções internas. As raízes foram inspecionadas em um estereomicroscópio com aumento de 12 × para excluir aquelas com qualquer defeito dentinário externo e raízes com ápices imaturos. Um sistema radiográfico digital (RVG 6100; Kodak Dental Systems, NY) foi usado para selecionar os dentes de acordo com os critérios de inclusão. O programa Image J (National Institutes of Health, Bethesda, MD, EUA) foi usado para avaliar o grau de curvatura em imagens radiográficas. Todos os dentes selecionados foram escaneados usando um dispositivo de micro-CT (SkyScan 1276; Bruker-micro-CT, Kontich, Bélgica) em baixa resolução (tamanho de voxel de 35 µm). As imagens tridimensionais permitiram uma seleção mais precisa e a confirmação dos critérios de inclusão (Figura 13).

Figura 13 – Imagens tridimensionais de micro-CT a 35 µm de tamanho de voxel usadas para seleção da amostra

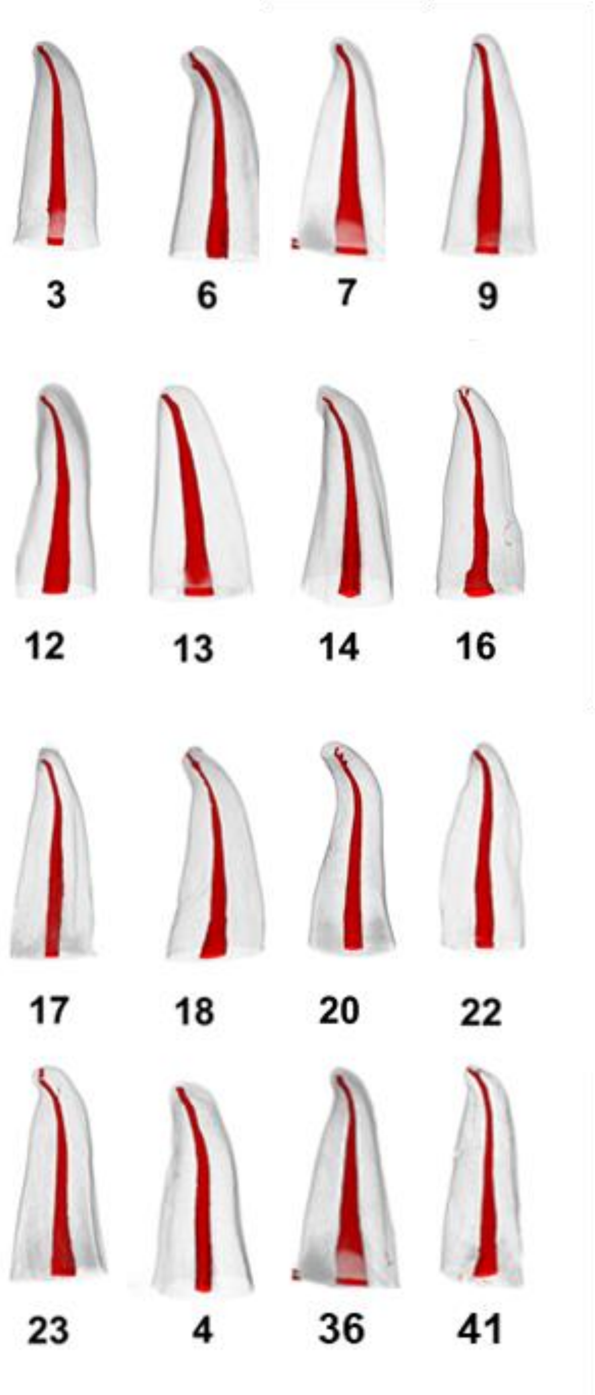

Fonte: Arquivo pessoal do autor.

Após exclusão dos dentes que não atenderam aos critérios de inclusão, foram selecionados 18 incisivos laterais superiores com curvatura apical. Os espécimes foram armazenados individualmente em tubos Eppendorf numerados e com umidade de 100% durante a execução da pesquisa (Figura 14).

Figura 14 – Dentes mantido em 100 % de humidade entre todas a etapas experimentais

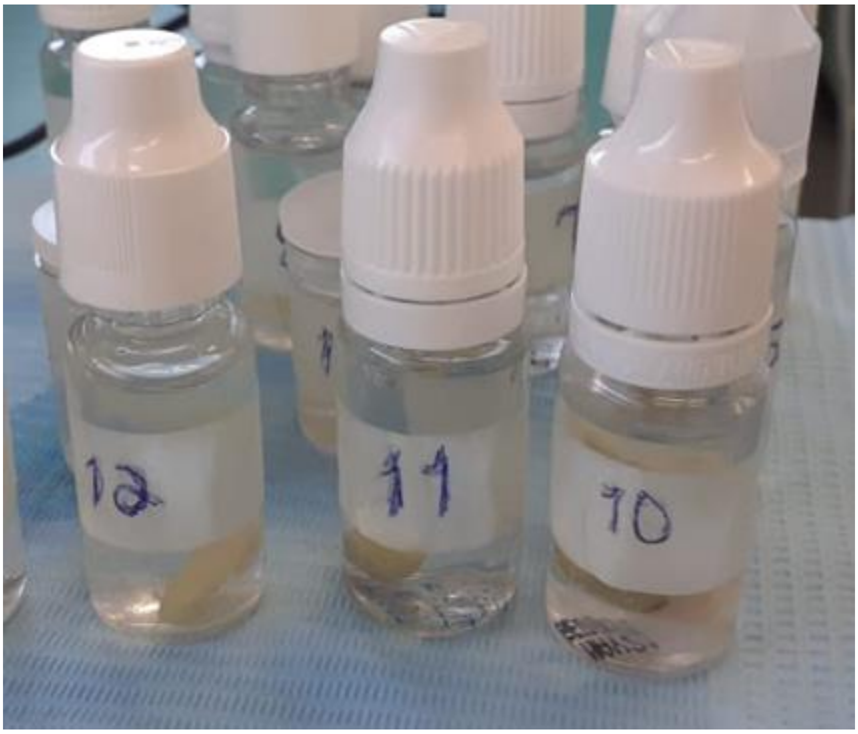

Fonte: Arquivo pessoal do autor.

Preparo do canal radicular

Cavidades de acesso convencionais foram realizadas e os canais radiculares foram explorados usando uma lima K tamanho # 10 (Dentsply Sirona, Ballaigues, Suíça). Quando a ponta do instrumento era visível através do forame principal, o comprimento de trabalho (CT) foi determinado. Para simular o ligamento periodontal, os espécimes foram montados em um aparelho com resina acrílica e cada dente foi incluído em silicone de condensação (Oranwash, Zhermack SpA, Badia Polesine, Itália). O aparelho foi imerso em água destilada durante as etapas operatórias para evitar a desidratação das amostras. O mesmo dentista, especialista em endodontia, preparou todos os dentes. Os incisivos laterais foram divididos aleatoriamente em dois grupos experimentais (n = 9), utilizando-se o método de amostragem aleatória estratificada, considerando o volume pré-operatório dos canais radiculares. Para o grupo controle, foi utilizado um preparo convencional, ou seja, o comprimento de trabalho (CT) foi definido como 1mm abaixo do forame apical. Para o grupo de ampliação do forame, o CT foi definido como 1 mm além do forame apical. Para ambos os grupos, os instrumentos Reciproc Blue R40 (VDW GmbH, Munique, Alemanha) foram operados por um motor elétrico VDW SILVER (VDW GmbH) configurado na função “RECIPROC ALL”. Cada instrumento foi inserido gradativamente no canal por meio de movimentos de entrada e saída, nos três níveis (cervical, médio e apical) até o CT. A irrigação do canal radicular foi realizada com 5 mL de hipoclorito de sódio 2,5% (NaOCl), utilizando-se agulha 30G com ventilação lateral (NaviTip, Ultradent Products, South Jordan, UT) adaptada a uma seringa de 5 mL (Ultradent Products). Como irrigação final, foram utilizados 2 mL de EDTA 17% seguidos de 5 mL de água destilada.

Análise Nano-CT

Para aquisição de imagens de nano-TC, um protocolo de alta resolução (tamanho de voxel de 2 µm) foi usado para escanear todos os dentes antes e depois da instrumentação usando o dispositivo UniTOM HR (Tescan, Brno, República Tcheca). Um *“target”* de tungstênio foi empregado, e a tensão e a corrente aplicadas foram de 65 kV e 123 µA, respectivamente, com um tempo de exposição de 310 ms, filtro de Al de 0,5 mm e rotação de 360 ° em torno do eixo vertical. As imagens foram reconstruídas usando o *software* de reconstrução Acquila (Acquila v.2900) e sobrepostas com alinhamento geométrico pelo programa de software DataViewer (Data Viewer v.1.5.1, Bruker). As análises quantitativas e qualitativas foram realizadas usando um programa de *software* CTAn (CTAn v.1.14.4, Bruker). Imagens tridimensionais foram feitas com um programa de *software* CTVox (CTVox v.3.2; Bruker).

As análises foram realizadas na região apical de 2 mm das raízes. Para análises qualitativas de microfissuras, imagens transversais antes e depois da instrumentação foram avaliadas simultaneamente. Em seguida, eles foram comparados por dois examinadores cegos em dois momentos diferentes. Microtrincas foram definidas como linhas ou defeitos que se estendem de dentro do canal radicular até a dentina ou da superfície externa da raiz até a dentina. A distribuição das microtrincas foi expressa como uma porcentagem do total das imagens transversais. As análises qualitativas das microtrincas foram baseadas em seu comprimento e largura. Para a mensuração do comprimento, foi registrada a extensão dos cortes contendo a microtrinca, sabendo-se que cada corte representa exatamente 0,002 mm, o número de cortes foi multiplicado por esse valor, e o resultado foi considerado como o comprimento da microtrinca em mm. Para a medida da largura, a extensão das microtrincas foi medida a cada 10 cortes transversais, correspondendo a 0,020 mm (Figura 15).

Figura 15 – Avaliação da presença de microtrincas e medição de sua largura antes e após o preparo

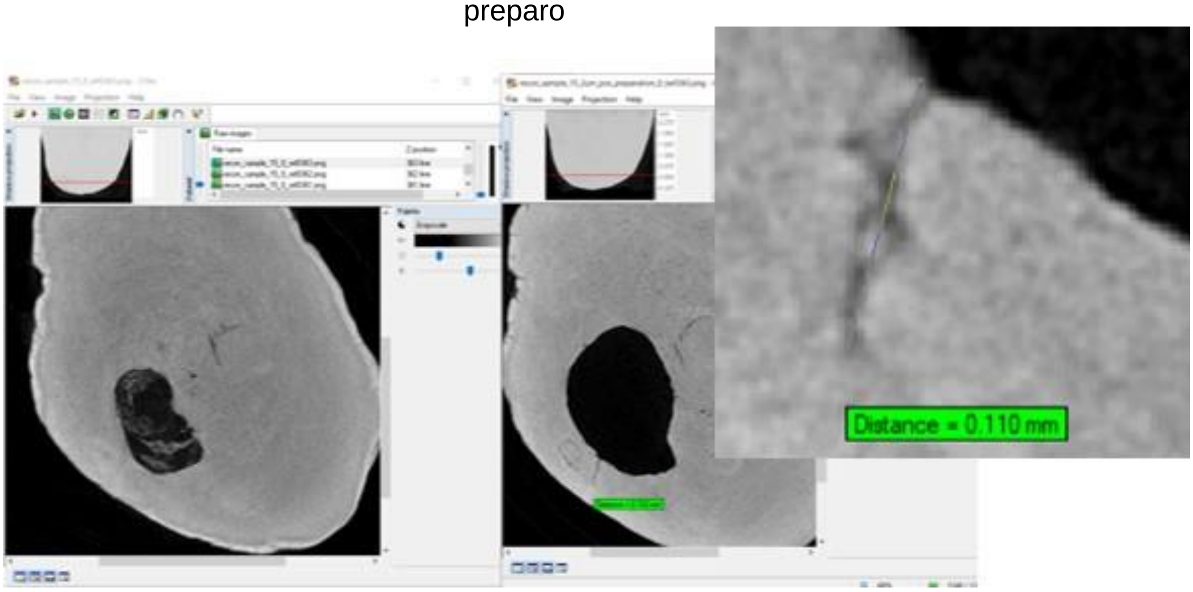

Fonte: Arquivo pessoal do autor.

As medidas do transporte apical foram obtidas antes e após o preparo do canal radicular em imagens transversais das raízes. Conforme proposto por Gambill et al. (20), a seguinte fórmula foi utilizada para calcular o transporte do canal radicular: (X1-X2) - (Y1-Y2) (Figura 15).

Figura 15 – Medição das distancias entre as bordas do canal e da raiz para avaliação do transporte

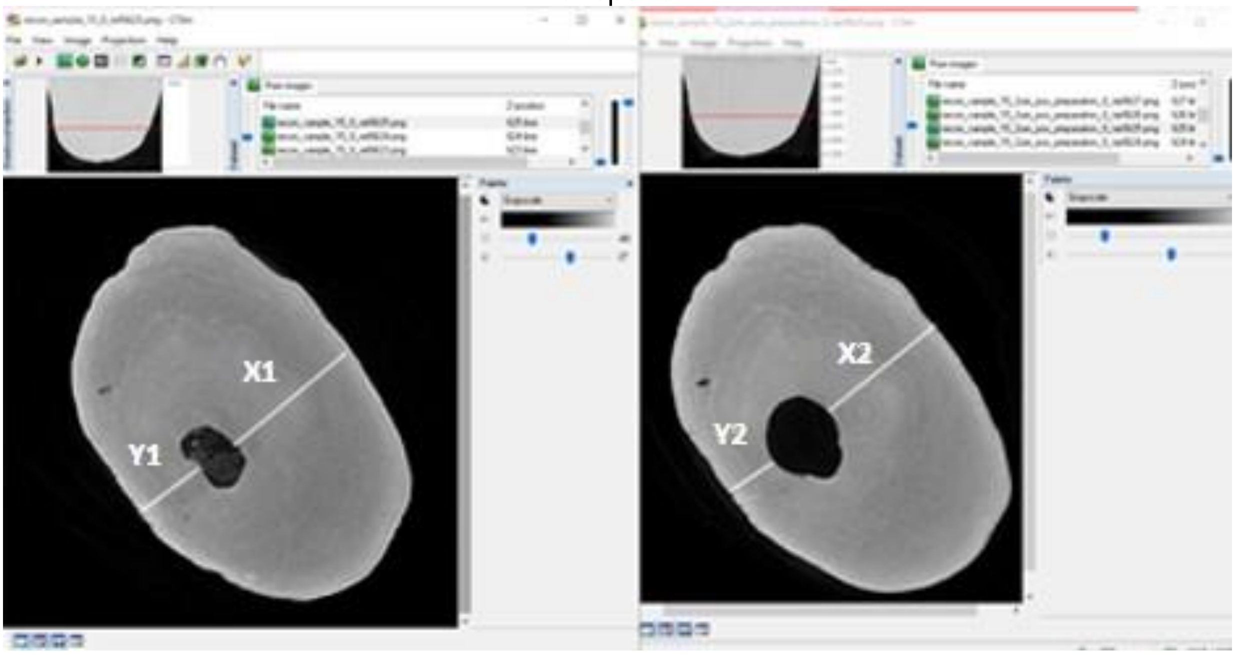

Fonte: Arquivo pessoal do autor.

ANEXO A – CERTIFICADO DO COMITÊ DE ÉTICA

Projeto de pesquisa aprovado pelo Comitê de ética em pesquisa em seres humanos - CEP da Faculdade de Odontologia de Araraquara – FOAr, UNESP. (Publicações 1 a 6)

CAAE: 10411219.0000.5416

UNESP - FACULDADE DE ODONTOLOGIA - CAMPUS ARARAQUARA

PARECER CONSUBSTANCIADO DO CEP

DADOS DO PROJETO DE PESQUISA

Título da Pesquisa: Efeito da aquisição e análise das imagens em micro-CT na avaliação das diferentes etapas do tratamento endodôntico em molares inferiores

Pesquisador: Mario Tanomaru Filho

Área Temática:

Versão: 2

CAAE: 10411219.9.0000.5416

Instituição Proponente: Faculdade de Odontologia de Araraquara - UNESP

Patrocinador Principal: FUND COORD DE APERFEICOAMENTO DE PESSOAL DE NIVEL SUP

DADOS DA NOTIFICAÇÃO

Tipo de Notificação: Envio de Relatório Parcial

Detalhe:

Justificativa:

Data do Envio: 24/10/2020

Situação da Notificação: Parecer Consubstanciado Emitido

DADOS DO PARECER

Número do Parecer: 4.402.805

Apresentação da Notificação:

Trata-se da apresentação do relatório parcial da pesquisa cujo resumo inicial constava: "O objetivo deste estudo será avaliar a influência de parâmetros para aquisição e análise das imagens em micro-CT na avaliação de etapas do tratamento endodôntico. Serão selecionadas raízes mesiais de molares inferiores com grau de curvatura entre 25° e 35° e com dois canais separados (N=24 canais),provenientes do Banco de Dentes da Faculdade de Odontologia de Araraquara-UNESP, após análise radiográfica e escaneamento em micro-CT na resolução de 35m. Os canais serão preparados por ProDesign Logic (PDL) 30.01 e 30.05 ou HyFlex EDM 10.05 e 25.08 (n=12). Será realizada uma etapa de limpeza adicional com Irrigação Ultrasônica Passiva (Irrisonic). Os canais radiculares preparados serão redistribuídos após avaliação do preparo e serão obturados por cone único e AH Plus ou Bio-C Sealer (n=12). Os canais obturados serão redistribuídos (n=12) e serão retratados pelo sistema ProDesign Logic RT com ampliação apical até PDL 35.05 (n=24). Será

Endereço: HUMAITA 1680
Bairro: CENTRO **CEP:** 14.801-903
UF: SP **Município:** ARARAQUARA
Telefone: (16)3301-6459 **E-mail:** cep@foar.unesp.br

avaliada a limpeza adicional após emprego do instrumento HyFlex EDM 40.04 associado ao XP-Endo Finisher R ou Reciproc Blue R40 associado ao ultrassom (Flatsonic). Serão realizadas 6 etapas de escaneamentos: inicial, após preparo, após limpeza adicional, após obturação, após retratamento e após limpeza adicional ao retratamento. Os escaneamentos serão realizados com resolução de 5 m (SkyScan 1272, Bruker-microCT, Kontich, Bélgica). Imagens serão salvas para obtenção de datasets com resoluções de 10 m e 20 m, e as análises serão realizadas inicialmente por softwares (NRecon, Data Viewer, CTan e CTVol), além da avaliação da possibilidade de uso de outros (Amira, Mevslab e 3-Matic). Assim, serão estabelecidos parâmetros mínimos para aquisição e análise de imagens que possibilitem a melhor avaliação de estruturas específicas: debris, superfície não instrumentada, trincas, percentual de falhas, interface obturação – paredes dentinárias e capacidade de preenchimento do material em túbulos dentinários. Os resultados obtidos serão submetidos aos testes estatísticos adequados."

Objetivo da Notificação:

Avaliar empregando microtomografia computadorizada, preparo, limpeza, obturação e retratamento dos canais com diferentes técnicas e materiais.

Definir a influência de diferentes resoluções no escaneamento de canais radiculares antes e após preparo, limpeza, obturação e retratamento, visando verificar a necessidade de escaneamentos com diferentes resoluções para análise precisa de debris, trincas, percentual de falhas, interface obturação/paredes dentinárias e capacidade de preenchimento.- Observar possíveis variações nos dados obtidos por análises realizadas utilizando diferentes softwares.

Avaliação dos Riscos e Benefícios:

Não houve ocorrência de dano decorrente dos riscos previstos.

Os benefícios obtidos estão relacionados às observações com relação as técnicas nas diferentes etapas do tratamento endodôntico, buscando a melhor forma de realizá-las e obter sucesso.

Comentários e Considerações sobre a Notificação:

Estudo nacional e unicêntrico, utilizando dentes provenientes do Banco de Dentes.

Patrocinador: Fapesp

Número de dentes: 12

Caráter acadêmico realizado para obtenção de título

Não haverá armazenamento de amostras em banco de material biológico no Brasil e fora

Previsão de encerramento do estudo: 30/09/2021

Apresentou resultados parciais e comentou que o projeto está dento do prazo e maioria das análises já foram realizadas, então até o momento não existe fator negativo a ser relatado.

Considerações sobre os Termos de apresentação obrigatória:

Foi apresentado o relatório parcial.

Recomendações:

Vide campo conclusões ou pendências e lista de inadequações

Conclusões ou Pendências e Lista de Inadequações:

Sem pendências.

Considerações Finais a critério do CEP:

Relatório Parcial APROVADO em reunião de 13 de novembro de 2020.

Este parecer foi elaborado baseado nos documentos abaixo relacionados:

Tipo Documento	Arquivo	Postagem	Autor	Situação
Envio de Relatório Parcial	relatorio_parcial_CEP_Jader.pdf	24/10/2020 17:43:10	Mario Tanomaru Filho	Postado

Situação do Parecer:
Aprovado

Necessita Apreciação da CONEP:
Não

ARARAQUARA, 17 de Novembro de 2020

Assinado por:
Andréa Gonçalves
(Coordenador(a))

ANEXO B – CERTIFICADO DO COMITÊ DE ÉTICA

Projeto de pesquisa aprovado pelo Comitê de ética em pesquisa em seres humanos da Universidade Católica de Leuven – KU Leuven (Publicações 7 e 8)

Number: NHO10 2019-09-03

Universitaire
Ziekenhuizen
Leuven

Ethische Commissie Zorg

To Dr. Pieter-Jan Verhelst

Leuven, 07-10-2019.

Study: : *Humane kadaverstudie voor beeldvorming van de onderkaak binnen OMFS-IMPATH*

Dear Dr Verhelst,

On its meeting of 24-09-2019, the ethical review board of the faculty of medicine of the KU Leuven and the Leuven University Hospitals (Ethical Committee –Care) , has given a positive advise for this study, under the condition that the cadaveric tissue is obtained from people who donated their dead body for scientific research.
Transport of cadaveric material should be carried out according to official requirements.

This study was registered at the Belgian National Council for Bioethics
(number *NH019 2019-09-03*).

Professor Martin Hiele
President of the Ethical Review Board

UZ Gasthuisberg
Herestraat 49 - B- 3000 Leuven België

Tel 016/34 42 25- 016/34 42 18
Fax 016/34 44 19

ANEXO C – CERTIFICADO DO COMITÊ DE ÉTICA

Projeto de pesquisa aprovado pelo Comitê de ética em pesquisa em seres humanos - CEP da Faculdade de Odontologia de Araraquara – FOAr, UNESP. (Publicação 9).

CAAE: 29320820.8.0000.5416

UNESP - FACULDADE DE ODONTOLOGIA - CAMPUS ARARAQUARA

PARECER CONSUBSTANCIADO DO CEP

DADOS DO PROJETO DE PESQUISA

Título da Pesquisa: Avaliação de microtrincas dentinárias por nano-CT
Pesquisador: Mario Tanomaru Filho
Área Temática:
Versão: 3
CAAE: 29320820.8.0000.5416
Instituição Proponente: Faculdade de Odontologia de Araraquara - UNESP
Patrocinador Principal: FUNDACAO DE AMPARO A PESQUISA DO ESTADO DE SAO PAULO

DADOS DA NOTIFICAÇÃO

Tipo de Notificação: Envio de Relatório Final
Detalhe:
Justificativa:
Data do Envio: 04/07/2021
Situação da Notificação: Parecer Consubstanciado Emitido

DADOS DO PARECER

Número do Parecer: 4.912.590

Apresentação da Notificação:
Trata-se da apresentação do relatório final cujo resumo inicial constava:
"A formação de microtrincas dentinárias pode propiciar a formação de fratura vertical da raiz. O presente estudo visa avaliar a presença de microtrincas dentinárias após o preparo com instrumentos de níquel e titânico (NiTi) reciprocantes 1 mm além ou 1 mm aquém do forame apical usando nanotecnologia. Incisivos laterais superiores com saída foraminal para lateral serão selecionados após a varredura por micro-TC na resolução de 35 m. Os canais radiculares serão preparados por Reciproc Blue R 40 1 mm a menos do forame apical ou 1 mm além do forame apical (n=8). Será realizado escaneamento por nano-CT, com 3 m de tamanho de voxel, antes do preparo e após o preparo. A presença de microtrincas será avaliada no terço apical (4 mm) após o registro da imagem (antes e depois) usando o software Amira. Todas as etapas deste projeto serão realizadas em parceria proposta com a Faculdade de Medicina, KU Leuven, Bélgica. Os resultados

Endereço: HUMAITA 1680, SALA 512
Bairro: CENTRO **CEP:** 14.801-903
UF: SP **Município:** ARARAQUARA
Telefone: (16)3301-6459 **E-mail:** cep@foar.unesp.br

obtidos serão submetidos ao teste estatístico adequado."

Objetivo da Notificação:

O objetivo do estudo foi comparar por nano-CT a formação de microtrincas em canais radiculares preparados com instrumentos reciprocantees de NiTi a 1 mm aquém do forame apical ou 1 mm além do forame apical.

Avaliação dos Riscos e Benefícios:

O pesquisador relatou inicialmente os seguintes ricos e benefícios:

Riscos: Os riscos envolvem os pesquisadores que serão submetidos à radiação uma vez que durante a seleção dos dentes será necessário realizar tomadas radiográficas para padronizar os espécimes, dessa maneira, será utilizado um sistema radiográfico

digital (menor tempo de exposição) com utilização de uma caixa de chumbo que evitará a propagação da radiação e protegerá o operador. Em todas as etapas experimentais do projeto, serão asseguradas as normas da Biossegurança da Faculdade de Odontologia de Araraquara – UNESP.

Benefícios: Os benefícios obtidos estão relacionados a determinação da influência do limite apical durante o preparo na propagação de microtrincas dentináras.

Comentários e Considerações sobre a Notificação:

Estudo laboratorial no qual foram utilizados 18 incisivos laterais superiores extraídos, com curvatura apical, obtidos por meio do Banco de Dentes Humanos da Faculdade de Odontologia de Araraquara Foar/Unesp. Os dentes foram divididos em dois grupos (n=9). A princípio, 16 dentes foram solicitados, tendo sido utilizado 1 dente a mais para cada grupo proposto.

O pesquisador relata ainda que, devido ao projeto bem delineado e cronograma de execução bem planejado foi possível obter as executar o experimento no tempo esperado e obter as conclusões do trabalho. Todas as etapas do projeto foram concluídas conforme esperado e fatores negativos não foram reportados.

O artigo científico “Effect of foraminal enlargement on microcrack formation and apical transportation: A Nano-CT assessment” está em fase final de redação e será enviado para o periódico Journal of Endodontics.

Considerações sobre os Termos de apresentação obrigatória:

Relatório final apresentado adequadamente.

UNESP - FACULDADE DE ODONTOLOGIA - CAMPUS ARARAQUARA

Continuação do Parecer: 4.912.590

Recomendações:

Vide campo Conclusões ou Pendências e Lista de Inadequações.

Conclusões ou Pendências e Lista de Inadequações:

Sugere-se aprovação do relatório final.

Considerações Finais a critério do CEP:

Relatório Final APROVADO em reunião de 13 de agosto de 2021.

Este parecer foi elaborado baseado nos documentos abaixo relacionados:

Tipo Documento	Arquivo	Postagem	Autor	Situação
Envio de Relatório Final	relatorio_final.pdf	04/07/2021 15:47:47	Mario Tanomaru Filho	Postado

Situação do Parecer:
Aprovado

Necessita Apreciação da CONEP:
Não

ARARAQUARA, 17 de Agosto de 2021

Assinado por:
Andréa Gonçalves
(Coordenador(a))

Endereço: HUMAITA 1680, SALA 512
Bairro: CENTRO **CEP:** 14.801-903
UF: SP **Município:** ARARAQUARA
Telefone: (16)3301-6459 **E-mail:** cep@foar.unesp.br

Araraquara, 21 de março de 2022

Jáder Camilo Pinto